CURRENT PROTOCOLS
in Stem Cell Biology
A Wiley Brand

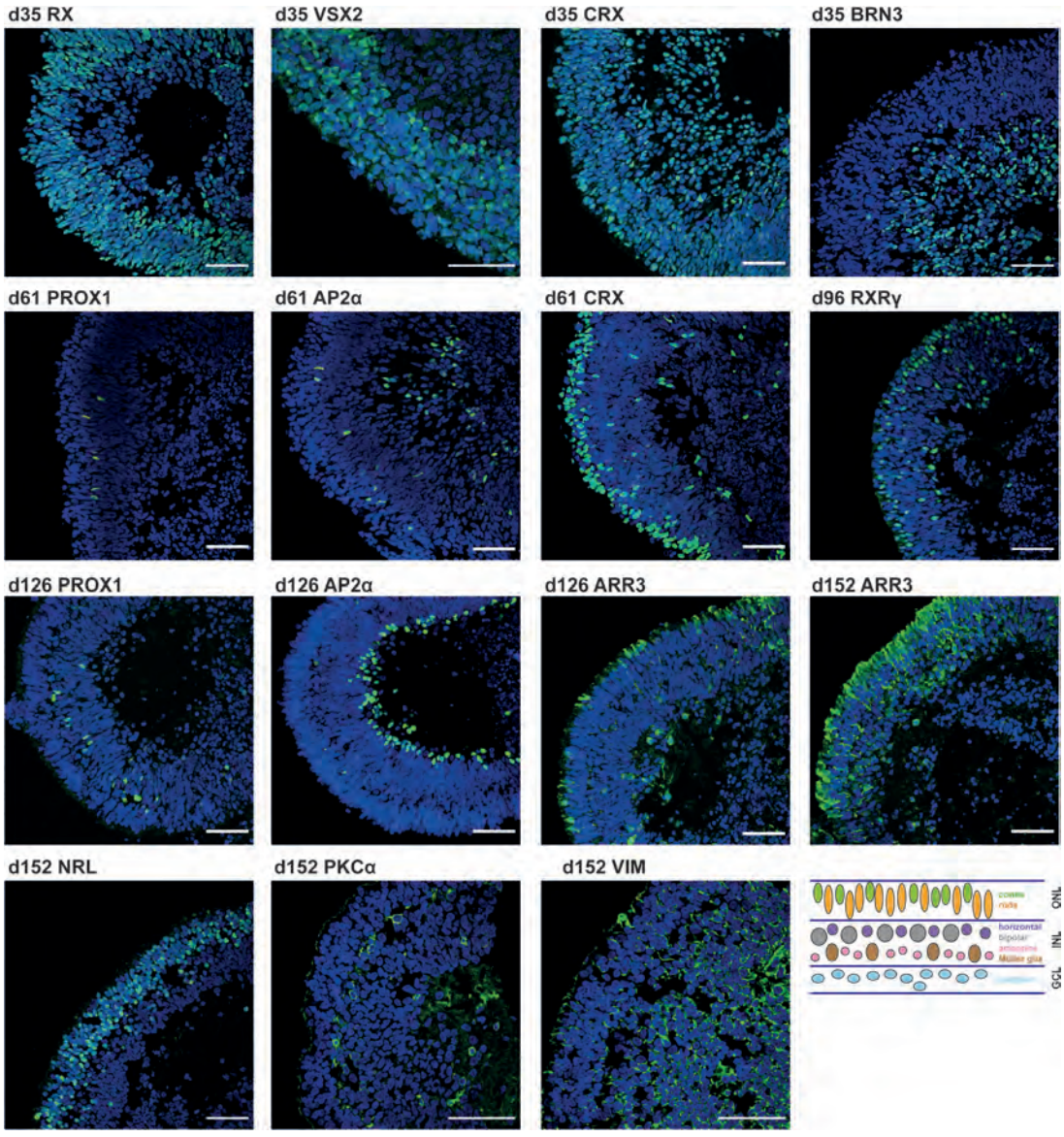

Volume 55, Issue 1
December 2020

WILEY

CURRENT PROTOCOLS in Stem Cell Biology
A Wiley Brand

Aims and Scope.
Sound and reproducible laboratory methods are the foundation of scientific discovery. Yet, all too often, nuances that are critical for an experiment's success are not captured in the primary literature but exist only as part of a lab's oral tradition. The aim of each *Current Protocols* title is to provide the clearest, most detailed and reliable step-by-step instructions for all protocols relevant to a given subject area. Written by experts in the field and extensively edited to our exacting standards, the protocols include all of the information necessary to complete an experiment in the laboratory—introduction, materials lists with supplier information, detailed step-by-step procedures with helpful annotations, recipes for reagents and solutions, illustrative figures and information-packed tables. Each article also provides invaluable discussions of background information, applications of the methods, important assumptions, key parameters, time considerations, and tips to help avoid common pitfalls and troubleshoot experiments. Furthermore, *Current Protocols* content is thoughtfully organized by topic for optimal usage and to maximize contextual knowledge. Quarterly issues allow *Current Protocols in Stem Cell Biology* to constantly evolve to keep pace with the newest discoveries and developments.

Stem cell biology is a relatively new field; it shares a foundation with developmental biology and interests with cell biology, genetics, and medicine. Stem cells have enormous and as yet untapped potential for developing therapeutic agents for a wide variety of human health concerns. In addition, study of stem cell biology can lead to major advancements in our understanding of the basic developmental process. *Current Protocols in Stem Cell Biology* is a comprehensive source for protocols in the rapidly growing field of stem cell biology, providing protocols for:

- Embryonic and Extraembryonic Stem Cells
- Somatic Stem Cells
- Mesenchymal Stem Cells
- Hematopoietic Stem Cells
- Neural Stem Cells
- Adult Stem Cells
- Multipotent Adult Progenitors
- Induced Pluripotent Stem Cells (iPSCs)
- Cancer Stem Cells
- Manipulation of Potency
- Genetic Manipulation of Stem Cells
- Tissue Engineering and Regenerative Medicine
- Regulatory Procedures, Safety, and Guidelines

Novice and experienced researchers involved in basic, clinical, or translational stem cell research constitutes the target audience for *Current Protocols in Stem Cell Biology* and contributions include protocols by Nobel Laureates, leading international investigators, and ISSCR members. Sufficient detail is provided to permit duplication of the protocols in any laboratory, whatever the disciplinary background and level of sophistication.

Current Protocols techniques are indexed in PubMed.

***Current Protocols* Editorial Support.**

For assistance with preparing your contribution, submitted manuscripts, file specifications, or CP publication policy please contact the Developmental Editor, Nidhi Bansal, Ph.D. at nbansal@wiley.com.

For submission instructions, including the style guide, sample articles, reference management software styles, and access to ScholarOne Manuscripts, visit: https://currentprotocols.onlinelibrary.wiley.com/hub/forauthors

Contributions to *Current Protocols* are generally invited by the editorial board. If you have a suggestion for a topic, or would like to submit a protocol, please contact the Developmental Editor (Nidhi Bansal).

The journal to which you are submitting your manuscript employs a plagiarism detection system. By submitting your manuscript to this journal, you accept that your manuscript may be screened for plagiarism against previously published works.

Subscriptions. *Current Protocols* offers a variety of ways to access thousands of authoritative, peer-reviewed, easy-to-follow, and frequently updated protocols. Information on library and institutional licenses for *Current Protocols*.

- For Libraries & Institutions
- Catalog for Libraries & Institutions

Information on purchasing and subscribing to *Current Protocols* for laboratories and individual users.

- For Laboratories & Individuals
- Catalog for Labs & Individuals

Publisher. *Current Protocols in Stem Cell Biology* is published by Wiley Inc., 111 River St., Hoboken, NJ, 07030-5774, +1 201 748 6000.

Journal Production. For assistance with post-acceptance articles and other production issues please contact cpprod@wiley.com.

Journal Customer Services. CP Customer Service can be reached at protocol@wiley.com

View this journal online at https://currentprotocols.onlinelibrary.wiley.com/journal/19388969/

Cover: In Döpper et al. (http://doi.org/10.1002/cpsc.120), the image shows immunostaining for early retinal markers and all retinal cell types. At d35, the outer layer stains positive for the early eye field marker RX. Moreover, in the outer part, retinal progenitor cells (VSX2), and in the inner part, ganglion cells are present (BRN3). CRX, a marker for retinal progenitors and immature photoreceptors, is present at d35, and a shift to the outer layer can be detected at d61. Horizontal cells (PROX1) and amacrine cells (AP2α) are present in the inner nuclear layer (d61, d126). Cone photoreceptors (RXRγ, ARR3; d96, d126, d152) and rod photoreceptors (NRL; d152) are present in the outer nuclear layer. Bipolar cells (PKCα) and Muller glia cells (VIM) are present in the inner nuclear layer (d152). A schematic overview of the retina with the seven different cell types organized in specific layers is given. Secondary antibodies were labeled in green (AlexaFluor 488), and nuclei were stained with DAPI (blue). Scale bar: 50 µm.

Advancing Stem Cell Technologies and Applications: A Special Collection from the PluriCore Network in the German Stem Cell Network (GSCN)

Daniel Besser[1,2]

[1]German Stem Cell Network (GSCN), Berlin, Germany
[2]Corresponding author: *d.besser@mdc-berlin.de*

Current Protocols in Stem Cell Biology is publishing a special collection of eight articles from members of the PluriCore Network in the German Stem Cell Network.

Keywords: PluriCore Network • German Stem Cell Network (GSCN) • stem cells • iPSC • hiPSC

How to cite this article:
Besser, D. (2020). Advancing stem cell technologies and applications: A special collection from the pluricore network in the german stem cell network (GSCN). *Current Protocols in Stem Cell Biology*, *55,* e129. doi: 10.1002/cpsc.129

INTRODUCTION

Stem cell research is a fast-moving field with many new findings being published every month. New technologies like formation of organoids from different cell types derived from stem cells, single cell sequencing, and methods to change the genetic information of cells using novel designer nucleases have revolutionized basic research on different stem cell types. While our understanding of the basic biology of stem cells has significantly increased over recent years, the translation of these findings into application in humans is still trailing behind. This is to be expected, given the difficulties in integrating cell types generated in cell culture into an existing environment in vivo in a patient. Nevertheless, time is of the essence, as many patients with hitherto incurable illnesses are desperately in need of new therapies and new ways of treatment.

Clinical application of cell types derived from stem cells has been a major topic for the German Stem Cell Network (GSCN) from its start in 2013 (Mahler & Besser, 2019). Many institutes and universities have created core facilities that support their researchers in the generation of stem cells and their differentiation into relevant cell types. The GSCN has created a specific network for these core facilities in Germany called the PluriCore Network. The laboratories and researchers in this network meet at least once a year and exchange novel approaches, protocols, and technologies in stem cell research. The exchange of reliable protocols that allow different laboratories worldwide to follow similar processes with the same outcome is one important prerequisite for successful progress in the science around stem cells—and ultimately for developing new approaches in the treatment of many incurable diseases.

In this issue of *Current Protocols in Stem Cell Biology* (CPSC), we have collected eight articles on protocols from the GSCN PluriCore Network. The authors of all articles, with the exception of one, are located at research institutes and universities in Germany, and all are involved with PluriCore. One contribution comes from the stem cell facility at Leiden University in the Netherlands, which is also affiliated with the German PluriCore Network. Two articles provide novel information on technologies to reprogram

CURRENT PROTOCOLS
A Wiley Brand

Current Protocols in Stem Cell Biology e129, Volume 55
Published in Wiley Online Library (wileyonlinelibrary.com).
doi: 10.1002/cpsc.129

cells to induced pluripotent stem cells (iPSC). The starting material in one of these articles, by Klingenstein and colleagues (Klingenstein, Klingenstein, Kleger, & Liebau, 2020), are keratinocytes from hair samples. These cells have the advantage of being easily accessible, and can even be acquired from different areas in the world without special transport requirements. Another material with easy access is urine; cells can be easily derived from this bodily fluid. Bouma and colleagues describe a method to reprogram cells from this source with a self-replicative RNA (Bouma, Arendzen, Mummery, Mikkers, & Freund, 2020). Once iPSCs have been derived or pluripotent cells from other sources like embryonic stem cells have been established, the further isolation of single cells and sub-cloning thereof becomes an issue. To overcome the challenges associated with manual methods, Vallone and colleagues describe application of three different automated cell isolation and dispensing devices which can enhance the single cell cloning process of hPSCs (Vallone et al., 2020). Quality control and low batch-to-batch variation of cryopreserved hiPSCs is absolutely critical for consistency and reproducibility in stem cell research. This important topic is covered by Shibamiya and colleagues, in an article where they provide cost-efficient protocols and quality-control assays for expansion and banking of hiPSCs (Shibamiya et al., 2020).

However, pluripotent stem cells (PSC) will never be the final product used in clinical settings. These cells have to be processed further to create cell types that can integrate into an organ system. Reproducible protocols describing the derivation of differentiated cell types from PSCs are of special importance for the development of clinical applications. This special collection brings together three articles on cellular differentiation and complex tissue models. Miller and colleagues report on the derivation of cardiomyocytes from pluripotent stem cells (Miller, Genehr, Telugu, Kurths, & Diecke, 2020), and Döpper and colleagues describe generation of retinal organoids that contain all seven retinal cell types (Döpper et al., 2020). Next, Applet-Menzel and coworkers review human iPSC−derived blood-brain barrier models as tools for preclinical drug discovery and development (Appelt-Menzel et al., 2020). Finally, in the field of mesenchymal stem/stromal cells (MCS), a great deal of data have been generated and discussed using these cells to support endogenous regeneration of tissues and organs, as well as modulation of immune responses and inflammation. Some of the functions of MSCs can be elicited by extracellular vesicles derived from MSC, and an article about their isolation completes this issue (Börger, Staubach, Dittrich, Stambouli, & Giebel, 2020).

The publication of reliable protocols from the work with stem cells, especially pluripotent stem cells, will be of utmost importance in the development of new therapeutic concepts. These novel therapies will ultimately improve the outcome for patients suffering from diseases that are incurable, or only insufficiently treatable to date.

AUTHOR CONTRIBUTIONS

Daniel Besser: Conceptualization; supervision; writing-original draft; writing-review & editing.

LITERATURE CITED

Appelt-Menzel, A., Oerter, S., Mathew, S., Haferkamp, U., Hartmann, C., Jung, M., … Pless, O. (2020). Human iPSC-derived blood-brain barrier models: Valuable tools for preclinical drug discovery and development? *Current Protocols in Stem Cell Biology*, *55*, e122. doi: 10.1002/cpsc.122.

Börger, V., Staubach, S., Dittrich, R., Stambouli, O., & Giebel, B. (2020). Scaled isolation of mesenchymal stem/stromal cell derived extracellular vesicles: Translation of research protocols into clinical settings. *Current Protocols in Stem Cell Biology*, *55*, e128. doi: 10.1002/cpsc.128.

Bouma, M. J., Arendzen, C. H., Mummery, C. L., Mikkers, H., & Freund, C. (2020). Reprogramming urine-derived cells using commercially available self-replicative RNA and a single electroporation. *Current Protocols in Stem Cell Biology*, *55*, e124. doi: 10.1002/cpsc.124.

Döpper, H., Menges, J., Bozet, M., Brenzel, A., Lohmann, D., Steenpass, L., & Kanber, D. (2020). Differentiation protocol for 3D retinal organoids, immunostaining and signal quantitation. *Current Protocols in Stem Cell Biology*, *55*, e120. doi: 10.1002/cpsc.120.

Klingenstein, S., Klingenstein, M., Kleger, A., & Liebau, S. (2020). From hair to iPSCs—A guide on how to reprogram keratinocytes and why. *Current Protocols in Stem Cell Biology*, *55*, e121. doi: 10.1002/cpsc.121.

Mahler, S., & Besser, D. (2019). The German stem cell network GSCN: A nationwide network with many tasks. *Stem Cell Research*, *42*, 101672. doi: 10.1016/j.scr.2019.101672.

Miller, D. C., Genehr, C., Telugu, N. S., Kurths, S., & Diecke, S. (2020). Simple workflow and comparison of media for hPSC-cardiomyocyte cryopreservation and recovery. *Current Protocols in Stem Cell Biology*, *55*, e125. doi: 10.1002/cpsc.125.

Shibamiya, A., Schulze, E., Krauß, D., Augustin, C., Reinsch, M., Schulze, M. L., … Ulmer, B. M. (2020). Cell banking of hiPSCs: A practical guide to cryopreservation and quality control in basic research. *Current Protocols in Stem Cell Biology*, *55*, e127. doi: 10.1002/cpsc.127.

Vallone, V. F., Telugu, N. S., Fischer, I., Miller, D., Schommer, S., Diecke, S., & Stachelscheid, H. (2020). Methods for automated single cell isolation and sub-cloning of human pluripotent stem cells. *Current Protocols in Stem Cell Biology*, *55*, e123. doi: 10.1002/cpsc.123.

From Hair to iPSCs—A Guide on How to Reprogram Keratinocytes and Why

Stefanie Klingenstein,[1] Moritz Klingenstein,[1] Alexander Kleger,[2,3] and Stefan Liebau[1,3,4]

[1]Institute of Neuroanatomy & Developmental Biology, Eberhard-Karls University Tübingen, Tübingen, Germany
[2]Department of Internal Medicine I, Ulm University Hospital, Ulm, Germany
[3]These authors contributed equally to this work.
[4]Corresponding author: *Stefan.Liebau@uni-tuebingen.de*

Keratinocytes, as a primary somatic cell source, offer exceptional advantages compared to fibroblasts, which are commonly used for reprogramming. Keratinocytes can beat fibroblasts in reprogramming efficiency and reprogramming time and, in addition, can be easily and non-invasively harvested from human hair roots. However, there is still much to know about acquiring keratinocytes and maintaining them in cell culture. In this article, we want to offer readers the profound knowledge that we have gained since our initial use of keratinocytes for reprogramming more than 10 years ago. Here, all hints and tricks, from plucking the hair roots to growing and maintaining keratinocytes, are described in detail. Additionally, an overview of the currently used reprogramming methods, viral and non-viral, is included, with a special focus on their applicability to keratinocytes. This overview is intended to provide a brief but comprehensive insight into the field of keratinocytes and their use for reprogramming into induced pluripotent stem cells (iPSCs). © 2020 The Authors.

Keywords: hair • induced pluripotent stem cells (iPSCs) • keratinocytes • outer root sheath • reprogramming

How to cite this article:
Klingenstein, S., Klingenstein, M., Kleger, A., & Liebau, S. (2020). From hair to iPSCs—A guide on how to reprogram keratinocytes and why. *Current Protocols in Stem Cell Biology*, *55,* e121. doi: 10.1002/cpsc.121

INTRODUCTION

Reprogramming somatic cells into induced pluripotent stem cells (iPSCs) is a widely used technique in molecular biology labs. This approach has opened up a huge field of research with unlimited application possibilities. For the successful generation of iPSCs, the selection of the proper primary cell source is a crucial task. Since the first publication (Takahashi et al., 2007) reporting the preparation of iPSCs from human skin fibroblasts in 2006 by means of the transduction of four reprogramming factors (Oct3/4, Sox2, Klf4, c-Myc) in the Yamanaka lab (rewarded with the Nobel prize for Yamanaka and Takahashi), countless publications have arisen using primary cell sources other than fibroblasts. These have included peripheral blood−derived mononuclear cells and sheared cells from urine, as well as more exotic primary cell sources like third molar teeth, milk teeth, umbilical

CURRENT PROTOCOLS
A Wiley Brand

Current Protocols in Stem Cell Biology e121, Volume 55
Published in Wiley Online Library (wileyonlinelibrary.com).
doi: 10.1002/cpsc.121

cord blood, and even post-mitotic primary neurons, all of which have been reprogrammed to human iPSCs. This article will highlight keratinocytes as a primary cell line.

Human hair−derived keratinocytes could be of major interest in the field of starting material for reprogramming in view of their numerous advantages in comparison to other cell types. Plucking hair is non-invasive, no medical personnel are needed, and hair samples can be obtained from almost any volunteer or patient. Moreover, plucked hair can be shipped at room temperature in simple media in which it can be kept for days. Although several publications are available applying keratinocytes for reprogramming (Aasen et al., 2008; Re et al., 2018), this cell source is still uncommon.

This article will describe the technique of plucking and transporting hair in detail. In addition, we provide an overview of the commercially available culture media and coatings specifically developed for keratinocytes, and explain how to deal with keratinocytes in routine laboratory work. Furthermore, the currently used reprogramming techniques are compared, and their advantages and disadvantages when using keratinocytes are discussed. For more insight into successfully carrying out procedures like transportation, cultivation, and reprogramming, tips and tricks are added to the protocols. With this guidance, it should be possible to immediately enter into the field of reprogramming human hair−derived keratinocytes successfully into iPSCs.

WHY USE HAIR?

Before we go into every step of the procedure in depth, we should discuss why to use hair in the first place. There are many advantages, but also some obstacles to overcome.

Not all available reprogramming methods can be applied to primary keratinocytes. Most of the media commonly used to dilute viruses or vectors to be transferred to somatic cells are incompatible with the requirements of keratinocytes. Here, the high calcium sensitivity of keratinocytes plays an important and crucial role. Keratinocytes should be cultivated in a low-calcium medium because they do not tolerate high concentrations of $CaCl_2$, which will cause them to differentiate and no longer be reprogrammable. In addition, reprogramming with mRNA remains difficult, as the mRNA has to be present for several passages and keratinocytes are likely to go into senescence before the pluripotent state is reached. However, knowing these drawbacks, there are many ways to reprogram keratinocytes successfully.

The most convincing advantages are the availability of hair (from people of all ages) and the non-invasive and nearly painless harvesting procedure that involves no long-term consequences. Additionally, for the action of plucking hair, no medical personnel are needed, and this can therefore be done anywhere (Raab, Klingenstein, Liebau, & Linta, 2014).

Furthermore, the choice of keratinocytes over fibroblasts results in an impressively high reprogramming efficiency. Reprogramming of primary keratinocytes from children has shown 100-fold higher efficiency compared to fibroblasts (Aasen et al., 2008; Linta et al., 2012). A possible mechanism may involve the high level of hypermethylated CpG islands, which are not found in fibroblasts; in this respect keratinocyte-derived iPSCs are more similar to ESCs than fibroblast-derived iPSCs (Barrero et al., 2012). The reprogramming time is also faster in comparison to fibroblasts (Piao, Hung, Lim, Wong, & Ko, 2014).

These advantages show that keratinocytes as a primary cell line offer a very simple and easy-to-use technique even for scientists who are new to this field.

ACQUISITION OF HAIR SAMPLES

Plucking hair

One of the huge advantages of using keratinocytes for reprogramming is the simple acquisition of hair from donors. The plucking of hair is relatively easy, and by far not as painful and invasive compared to other methods such as skin biopsies used to obtain fibroblasts. Even though the method is quite simple, there are still some aspects requiring attention.

Before plucking hair from volunteers or patients, gloves and sterilized tweezers are mandatory to minimize the contamination risk. Although it is possible to use hair from almost any region of the body, scalp hair from the top and back of the subject's head works best. Nevertheless, beard hair has showed good outcomes in our hands, but plucking from this region is much more painful for the person. The most important aspect is the awareness of "good" and "bad" hair roots (see Supporting Information video). Perfect roots are in the anagen phase of growing and have a visible white outer root sheath (ORS) (Raab et al., 2014). Catagen or telogen hair roots should not be used, as the hair is in an inactive state and does not grow; thus, no keratinocytes can be isolated (Hung, Pebay, & Wong, 2015) (Fig. 1).

Troubleshooting Tip 1: Pull fast. One should not be too cautious when extracting hair roots; otherwise, the outer root sheath may remain in the skin or be partially destroyed.

Transport of plucked hair

Work quickly to put the hair root into the medium. If the hair is exposed to the air for too long, it can wither to the degree of uselessness. Be sure to completely cover the hair

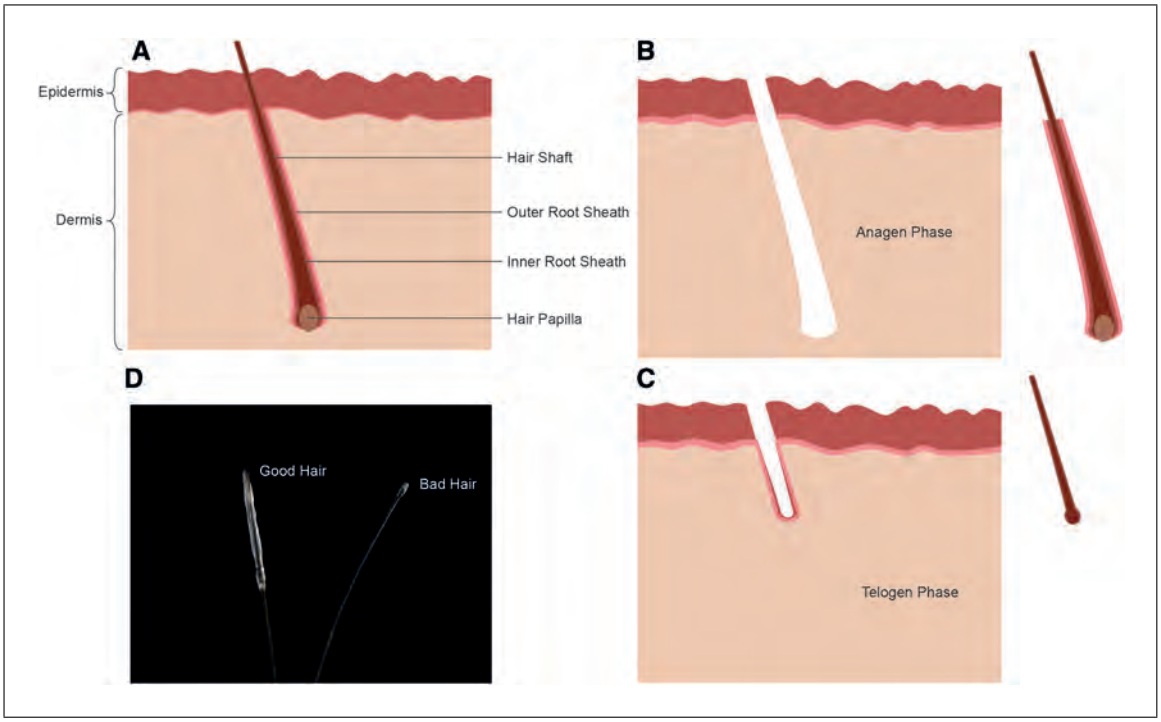

Figure 1 Comparison of "good" versus "bad" hair roots. (**A**) The human hair follicle consists of two root sheaths. The inner root sheath directly encloses the hair shaft and is surrounded by the outer epithelial root sheath (ORS). The papilla is extremely rich in vessels and guarantees the blood supply. (**B**) Anagen hair is in an active state of length growth and is characterized by a pronounced ORS. When plucking anagen hair, the ORS remains with the hair. (**C**) The telogen hair is in a resting state. When plucking telogen hair, only the hair papilla will be plucked; the ORS remains in the dermis. (**D**) Close up of good and bad hair.

with medium. It is advisable that the chosen transport vessel (e.g., 50-ml Falcon tube) be completely filled with medium (see Supporting Information video). Use of antibiotics and antimycotics in the medium is not obligatory, but can minimize contamination. The vessels can be stored and shipped with the hair over time periods up to 48 hr (best timeframe) or even longer at room temperature. Best results can be achieved when the hair roots are plated in the cell culture as quickly as possible.

Troubleshooting Tip 2: DMEM with or without serum is mostly used as a transport medium.

KERATINOCYTES IN CULTURE

Cultivation media and supplements

A high calcium concentration is necessary for physiological keratinocyte differentiation (Bikle, Xie, & Tu, 2012). In healthy skin development, keratinocytes arise from the stratum basale, a basal layer in the epidermis of the skin. In this microenvironment, a very low calcium concentration is present, which allows the keratinocytes to proliferate. Due to the ongoing differentiation, the cells migrate through increasing ion concentrations toward the outer epidermal barrier, where a very high calcium concentration is present (Elsholz, Harteneck, Muller, & Friedland, 2014). This leads directly to the most important piece of information about the cultivation of keratinocytes in vitro: that a low-$CaCl_2$ medium should be used.

Several companies offer special media for cultivation of keratinocytes. What most media have in common is a defined concentration of 0.06 mM $CaCl_2$ in the prepared medium. In addition to the calcium-reduced basal medium, keratinocytes also require supplements that, depending on the manufacturer, have already been added to the basic medium or must be added separately by the user. Manufacturers of the basal media provide corresponding supplements at standardized concentrations, but be aware of possible variations in the concentrations between different companies.

One such supplement is bovine pituitary extract (BPE). Some special formulations, for more defined media, are available without BPE. BPE is derived from the bovine pituitary gland and comprises different types of growth hormones and mitogens, such as TSH, FSH, ACTH, and GH. These hormones are responsible for growth and for the maintenance of various body functions, like the development of sex hormones (Kent & Bomser, 2003). In addition to BPE, glucocorticoids like hydrocortisone and growth factors are added. Together with insulin and transferrin, they regulate various signaling pathways, e.g., stress response, energy mobilization, and regulation of cell proliferation and differentiation (Keenan, Pearson, O'Driscoll, Gammell, & Clynes, 2006; Shen et al., 2001). The addition of antibiotics to primary cell lines is not necessary, and in some cases even inhibits the outgrowth of keratinocytes (Nygaard et al., 2015).

Plating human plucked hair

To cultivate the plucked hair roots, a crucial preparation step needs to be followed thoroughly. For this purpose, the hair shaft is cut, slightly above the visible ORS. Only the part with the ORS will be used. This reduces the shear forces when changing medium; the hair stays anchored in its position in the coating medium and the keratinocytes can grow out more easily. Subsequently, the cut hair is placed directly on coating medium (see Supporting Information video). Commonly, Matrigel or collagen I is used for coating (Ernst et al., 2013).

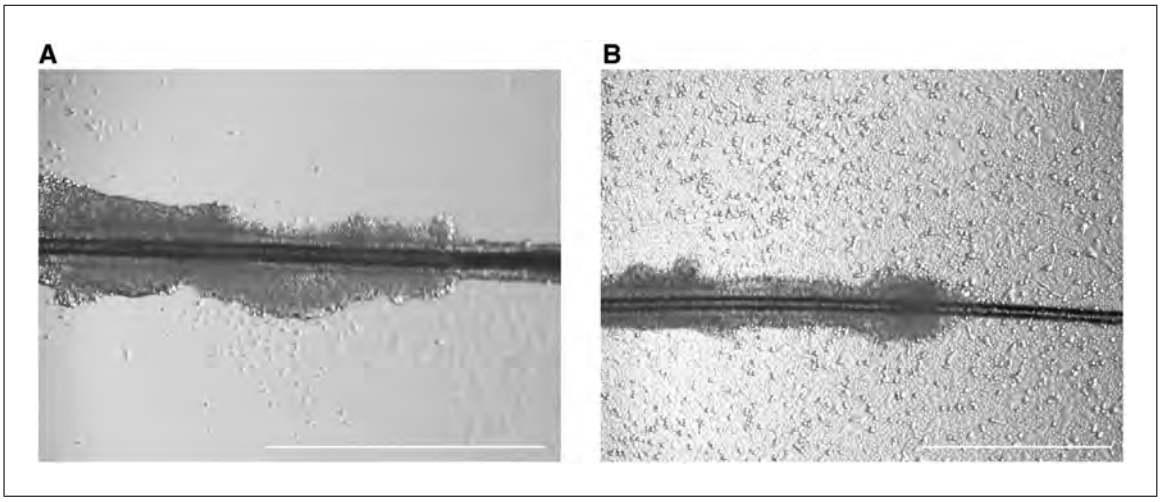

Figure 2 (**A**) Keratinocytes appearing after 2 days of culture. (**B**) Dense culture surface after 1 week of cultivation. Scale bar: 1000 µm.

Troubleshooting Tip 3: In order to improve the attachment of the hair to the coating, it is advisable to place a drop of the coating medium directly onto the hair root. This has the additional benefit that the hair roots do not dry out and that they stay in place.

Troubleshooting Tip 4: If this method is unsuccessful, the cells of the outer root sheath can be removed by an enzymatic digestion step prior to the plating step. For this purpose, the hair is predigested with enzymes, usually dispase, collagenase, or trypsin-EDTA (for more detail on digestion of outer hair roots, see Chan, Fan, Wang, Mu, & Lin, 2015; *Ernst et al., 2013*; *Re et al., 2018*; *Wagner et al., 2018). The isolated cells are plated onto the coated surface.*

As already mentioned, the next step would be carefully adding a low-calcium medium with the appropriate supplementation for the keratinocytes.

Troubleshooting Tip 5: Do not add the medium until the hair roots are firmly fixed to the coating material (approximately after 1-2 hr); otherwise, the roots will detach after adding medium.

Depending on the hair donor, the first keratinocytes will grow out after 1-2 days. However, it is also possible that the first cells will appear after 1 week or later (Fig. 2).

Troubleshooting Tip 6: For enhanced outgrowth stimulation, the freshly plated hair roots may be initially cultivated in conditioned MEF medium. This conditioned medium contains cytokines and growth factors that are secreted into the culture medium by mouse embryonic fibroblast (MEF) cells. As soon as the first keratinocytes are fully grown out, switch to a keratinocyte-specific defined medium.

Troubleshooting Tip 7: The hair roots are usually cultivated in well format, but cultivation in T-25 flasks offers a big advantage, because flasks undergo much lower evaporation compared to well format. As a positive effect, the hair roots will not dry out as easily. Use three to five hair roots per T-25 flask to achieve the best results

Passaging and cryopreservation

If the culture has reached around 70% confluence, cells must be passaged. For this purpose, they are detached enzymatically from the coating surface using TrypLE Express and passaged onto new coated wells in the appropriate culture medium. Since the primary keratinocytes mature directly from the hair roots, they only have a short passaging capacity until they fully differentiate and are no longer able to proliferate. They

usually reach this stage after four to five passages. Of note, most primary cells should not be passaged repeatedly (meaning not more than four to five passages for keratinocytes; may differ for other primary cells), as chromosomal aberrations can occur!

Troubleshooting Tip 8: A very early passage should be used for the subsequent reprogramming, since at this early stage the keratinocytes still proliferate and are easy to infect. It is recommended to start the reprogramming process with passage 1, but it is possible to achieve results with passage-2 or -3 keratinocytes. After that, most keratinocytes are fully differentiated and will no longer proliferate properly.

If the cells are to be used at a later time point, they can be easily cryopreserved. For this purpose, the keratinocytes are detached enzymatically from the coating surface using TrypLE Express and taken up in a freezing medium specially produced for keratinocytes. The cells can easily be stored in liquid nitrogen and thawed again when required. Keratinocyte-specific culture medium with 20% DMSO can also be used for cryopreservation.

REPROGRAMMING

Reprogramming is the molecular technique to restore nearly any fully differentiated cell to the state of pluripotency. Pluripotent cells have the capability to differentiate into all cells of the three germ layers: ectoderm, mesoderm, and endoderm.

To achieve this state of pluripotency, reprogramming factors, e.g., Oct4, Sox2, and Klf4, among others, have to be transferred into the primary, somatic cell lines. After several days of reprogramming, the molecular composition of the nucleus rearranges and the cells return to an embryonic, initial state. There are several techniques, viral and non-viral, to induce pluripotency in somatic cells. In the following chapter, these methods are described briefly, and pros and cons are listed.

Which virus to choose for reprogramming?

Retrovirus

In the first publication describing the successful reprogramming of human foreskin fibroblasts (HFF) to iPSCs, retrovirus particles were used (Takahashi et al., 2007). Retroviruses are single-stranded RNA viruses, and infect only dividing cells (Hotta & Ellis, 2008). The major advantage of retroviral transfection is the high reprogramming efficiency. However, retroviruses have the ability to integrate permanently into the genome of the host cell. Uncontrolled viral genome integration can cause mutagenesis and genome instability (Nakagawa et al., 2008), reducing the applicability of retroviruses for, e.g., potential transplant attempts, and they are therefore not the first choice in the current field of research.

Advantages (+) and disadvantages (−) of retrovirus:

+ High reprogramming efficiency
+ Cloning of large DNA sequences
− Stable integration into host genome
− No transplantation approaches possible

Lentivirus

Lentiviruses belong, together with adenoviruses, to the first generation of reprogramming viruses. They are single-stranded RNA viruses, which make up a genus among the retrovirus family. This kind of virus can stay lifelong in the host genome due to the ability to bypass the defense mechanisms of the immune system. They transduce dividing

and non-dividing eukaryotic cells (Fleury et al., 2003). Lentiviral infection is commonly performed with a commercially available single constitutive polycistronic vector containing all four reprogramming factors (e.g., STEMCCA-OKSM; Sommer et al., 2009). Here, the advantage is the use of one lentiviral vector, which improves the reprogramming efficiency, instead of using a pool of multiple retroviruses. The integrated virus RNA can be eliminated by Cre-enzymatic treatment.

Advantages (+) and disadvantages (−) of lentivirus:

+ High reprogramming efficiency
+ Only one virus is needed
− Stable integration into host genome, but excisable
− No transplantation approaches possible; not safe enough

Sendaivirus

After further optimization steps, negative-sense, non-integrating RNA viruses are currently being used. Sendaiviruses (SeV) show a high reprogramming efficiency and do not (or should not) integrate into the host genome by entering the nucleus (Bernloehr et al., 2004). During passaging of the generated iPSCs, the virus will be diluted out of the cells at around 10-20 passages after infection (Fusaki, Ban, Nishiyama, Saeki, & Hasegawa, 2009).

Advantages (+) and disadvantages (−) of sendaivirus:

+ High reprogramming efficiency
+ No integration into host genome (or at very low chance)
+ Little technical effort
− Expensive

Non-viral reprogramming methods

mRNA

A virus-independent method is the use of modified mRNA. However, a time-consuming approach, with multiple successive infections of the primary cell line, is necessary for successful reprogramming. This entails a high level of personnel effort and expense. However, the generated iPSCs are transgene-free and have no obvious risk of mutation (Badieyan & Evans, 2019). One publication describing the use of mRNA for the reprogramming of keratinocytes observed high dose-dependent cytotoxicity in their experimental setup, which was a serious complication for achieving a stable status of pluripotency. In addition, the use of feeder cells was crucial to this procedure (Warren et al., 2010). For other cell types, this method has been optimized with regard to reducing the number of infections needed, eliminating feeder culture, and shortening the timeframe for the whole procedure. Even if this method is not recommended for keratinocytes at this time, it can become a possible alternative after further improvements and adjustments.

Advantages (+) and disadvantages (−) of mRNA:

+ Applicable in clinical research
+ Rapid elimination of residual mRNA
− Low reprogramming efficiency
− Daily transfections of four different mRNAs, 14 days
− Currently not recommended for keratinocytes

Episomal DNA

In the second generation of reprogramming techniques, viruses are replaced by small circular DNA to introduce the reprogramming factors. Non-integrating (or partially integrating) episomal DNA plasmids encode the reprogramming factors. In this case, episomal means that the DNA is present in the cytoplasm and, in principle, is not built into the host genome. Since the genetic information for reprogramming also remains in the cytoplasm with this approach, it disappears from the iPSCs over the course of cell division. However, studies have shown that fragments of the episomal vectors are recognized as part of the cell's own DNA and incorporated into the genome (Okita, Nakagawa, Hyenjong, Ichisaka, &Yamanaka 2008; Yu et al., 2009; Schlaeger et al., 2015).

Advantages (+) and disadvantages (−) of episomal DNA plasmid:

+ No need for virus
+ Applicable in clinical research
+ Not expensive
+ Little technical effort
− Partial integration into host genome

Synthetic self-replicating RNA

Synthetic self-replicating RNA molecules offer further possibilities for optimization in reprogramming techniques. The commercially available single-stranded RNA possesses the four reprogramming factors and leads to a very high reprogramming efficiency with only one transfection. It is a virus-free, polycistronic RNA replicon that combines all four factors in one RNA strand (Steinle et al., 2019). In addition, the RNA molecules show no integration into the host genome and the remaining molecules can be removed from the cell culture medium simply by removing the interferon γ (IFN-γ) inhibitor, B18R (Kim et al., 2017). Applicability for keratinocytes is currently tested in our lab.

Advantages (+) and disadvantages (−) of RNA replicon:

+ 1 day of infection
+ High reprogramming efficiency
+ No integration into host genome
− Established for only few primary cell lines
− Not possible?/not yet published for keratinocytes

Reprogramming methods for keratinocytes

Since the discovery of the reprogramming mechanism, several approaches have appeared for restoring primary cell lines to the status of pluripotent stem cells. The first experiments to transfer the pluripotency factors into adult primary cell lines were performed using retroviral transduction. The results showed a high reprogramming efficiency; however, the virus genome remained in the host cell, rendering the generated cells unusable for possible clinical applications such as transplantation attempts. In the following generations of virus-based reprogramming methods, more secure systems such as the use of Sendai viruses were established. Additionally, non-virus-based systems were developed to reprogram the somatic cells. Use of episomal DNA and of self-replicating RNA are currently the most promising methods, and also enable possible use of the generated pluripotent cells and their differentiation products in clinical studies.

Troubleshooting Tip 8: Not all methods can be used for reprogramming keratinocytes due to the calcium sensitivity and the short passaging ability of these cells. Table 1 lists

Table 1 Currently Used Reprogramming Methods for Keratinocytes

Reprogramming method	Publication
Retrovirus	Lim et al. (2016)
Lentivirus	Raab et al. (2017)
Sendai virus	Re et al. (2018)
Episomal DNA plasmid	Hung et al. (2015)

the reprogramming methods currently suitable for keratinocytes, together with example publications.

KERATINOCYTE CULTURE AND REPROGRAMMING TECHNIQUE USED IN OUR LAB

Materials

Cell culture media:

- Transport medium for plucked hair
  - DMEM (Thermo Fisher # 41965-029)
  - 1% Antibiotic-Antimycotic (Thermo Fisher # 15240-062)
- Medium for keratinocyte preparation
  - 1:10 diluted Matrigel (Corning, cat. no. 354234) in EpiLife (Thermo Fisher, cat. no. M-EPI-500-CA) for coating
  - 1:5 diluted Matrigel (Corning, cat. no. 354234) in EpiLife (Thermo Fisher, cat. no. M-EPI-500-CA) for single droplets
- Keratinocyte medium
  - EpiLife (Thermo Fisher, cat. no. M-EPI-500-CA)
  - 1% Human Keratinocyte Growth Supplement (Thermo Fisher, cat. no. S-001-5)
  - 10 nM Y-27632 2HCl (Selleckchem, cat. no. S1049)
- Keratinocyte freezing medium
  - Cryostem (Biological Industries, cat. no. 05-710-1E)
- Mouse fibroblast medium
  - DMEM (Thermo Fisher, cat. no. 41965-039)
  - 10% fetal bovine serum (FBS; Thermo Fisher, cat. no. 10500-064)
  - 1% Antibiotic-Antimycotic (Thermo Fisher, cat. no. 15240-062)
  - 1% GlutaMAX^{TM} (Thermo Fisher, cat. no. 35050-038)
  - 1% Non-essential amino acids solution (Thermo Fisher, cat. no. 11140-050)
- Reprogramming medium
  - Knockout DMEM (Thermo Fisher, cat. no. 10829-018)
  - 20% Knockout Serum Replacement (Thermo Fisher, cat. no. 10828-028)
  - 1% GlutaMAX (Thermo Fisher, cat. no. 35050-038)
  - 1% Non-essential amino acids solution (Thermo Fisher, cat. no. 11140-050)
  - 1% Antibiotic-Antimycotic (Thermo Fisher, cat. no. 15240-062)
  - 50 mM β-mercaptoethanol (Thermo Fisher, cat. no. 31350-010)
  - 50 μg/ml ascorbic acid (Carl Roth, cat. no. 3525.1)
  - 10 nM Y-27632-2HCl (Selleckchem, cat. no. S1049)
  - 10 ng/ml FGF2 (Cell Guidance Systems, cat. no. GFH146)
- iPSC Medium
  - PeproGrowth hESC medium (PeproTech, cat. no. BM-HESC-500)
  - 1:100 Antibiotic-Antimycotic (Thermo Fisher, cat. no. 15240-062)

Chemicals:

- Dispase 5 U/ml (Stem Cell technologies, cat. no. 07913)
- TrypLE Express (Thermo Fisher, cat. no. 12604039)
- Collagen IV (Sigma, cat. no. 9007-34-5)

- iPSC Matrigel (Corning, cat. no. 354277)
- Hexadimethrine bromide (Merck, cat. no. H9268-5G)
- Polyethylenimine, 25 kDa (Merck, cat. no. 9002-98-6)
- Lenti-X Concentrator (Takara Clontech, cat. no. 631232)

Plasticware, cells and specific equipment:

- Cell culture dish, 10 cm
- Cell culture flask, 25 cm^2
- Cell culture 6-well plates
- Lenti-X 293T (Takara, cat. no. 632180)
- CD1 E14.5 (Stem cell Technologies, cat. no. 00322)
- Tweezers (F.S.T., cat. no. 11000-16)
- Scissors (F.S.T., cat. no. 15100-09)

Vectors used for viral production and reprogramming:

- psPAX2 (Addgene, Cambridge, USA)
- pMD2.6 (Addgene, Cambridge, USA)
- pRRL.PPT.SF.hOKSMco.idTom.pre FRT (Warlich et al., 2011)

Methods

Preparation and cultivation of keratinocytes

As previously described (see "Plucking hair" under Acquisition of Hair Samples and the Supporting Information video), human hair is plucked from top or back of the subject's head with large tweezers. Visible hair roots are transferred quickly into a 50-ml Falcon conical tube completely filled with DMEM, preferably containing antibiotics, and transported at room temperature into the lab. The transport time should not exceed 3 days. In the lab, the hair follicles are placed in a petri dish with DMEM, and the roots are cut with small scissors directly above the visible white outer root sheath while holding the hair shaft with tweezers. The short hair roots remain in DMEM until the T-25 flasks are prepared. The T-25 flask is coated for 1 hr with 1:10 diluted Matrigel. After that, a drop of 1:5 diluted Matrigel is added on top of the prior coating and the hair root is inserted into this drop for 1-2 hr in a humidified incubator. 1 ml of conditioned MEF medium has to be added, and changed every day until first keratinocytes appear. From now on, 2 ml of the keratinocyte medium EpiLife is added every second day. Keratinocytes can either be frozen or directly used for further reprogramming (Fig. 3).

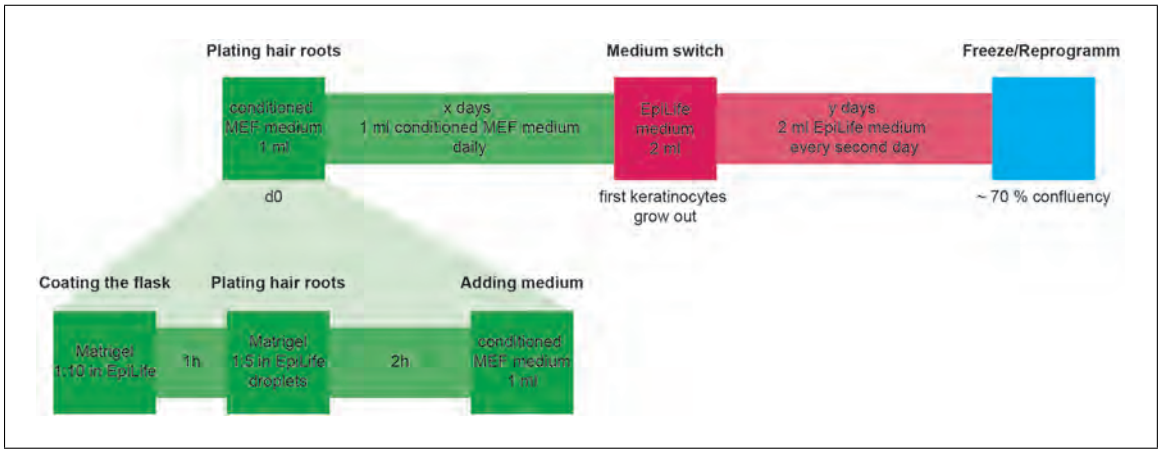

Figure 3 Timeline of plating and culturing plucked hair roots and keratinocytes. At day 0, a T-25 flask is coated for 1 hr with Matrigel diluted 1:10 in EpiLife. One drop of Matrigel diluted 1:5 in EpiLife is added before inserting the hair roots into the drop. After 2 hr, 1 ml conditioned MEF medium is added. The medium has to be changed with 1 ml conditioned MEF medium daily. When the first keratinocytes grow out, the medium is switched to 2 ml EpiLife medium, and has to be changed every second day until the keratinocytes reach around 70% confluency. From here, the keratinocytes can be frozen or directly used for reprogramming.

Preparation of conditioned MEF medium

CD1 E14.5 mouse fibroblast cells are cultivated in mouse fibroblast medium under humidified conditions. At 2 and 4 days after passaging the cells, the spent medium will be collected and filtered. The freshly prepared medium has to be enriched with 5 ng/ml FGF2, 10 nM Y-27632-2HCl, and 50 μg/ml ascorbic acid.

Production of viral particles

Viral particles can be obtained from Lenti-X 293T cells. Therefore, the cells are transfected for 4 hr in serum-free MEF medium with 8 μg lentiviral pRRL.PPT.SF.hOKSMco.idTom.pre FRT plasmid (Warlich et al., 2011) together with 5.5 μg psPAX2 and 2 μg pMD2.6 plasmid using polyethylenimine. After changing to serum-containing MEF medium, the supernatant can be collected 2 and 4 days after transfection. To concentrate the viral particles, a viral concentrator must be used according to the manufacturer's protocol. The viral particles can be suspended in EpiLife and stored for further reprogramming in –80°C.

Reprogramming of keratinocytes

Keratinocytes grow on collagen IV−coated culture plates. On 2 successive days, viral particles together with 8 μg/ml hexadimethrine bromide are added directly to the keratinocytes. Infected cells are plated on inactivated feeder cells and kept in reprogramming medium (for more details on inactivation of feeder cells, see Linta et al., 2012). After 3-4 weeks, the first stem cell colonies appear. Colonies can be picked mechanically using a pipet and transferred onto iPSC Matrigel−coated culture plates (6-well-plates) in 1.5 ml iPSC medium. The medium has to be changed every day with 1.5 ml of fresh iPSC medium.

Verification of iPSCs

To confirm the pluripotency of the generated iPSCs, differentiation into all three germ layers must be verified, and pluripotency assays and alkaline phosphate staining have to be performed (for more detail on iPSC characterization, see Klingenstein et al., 2016).

CONCLUSION

In summary, the use of keratinocytes has obvious advantages over the commonly used fibroblasts. In addition, almost all established reprogramming methods can be applied to keratinocytes. In the future, use of keratinocytes as a primary somatic cell line may increase.

ACKNOWLEDGMENTS

Open access funding enabled and organized by Projekt DEAL.

LITERATURE CITED

Aasen, T., Raya, A., Barrero, M. J., Garreta, E., Consiglio, A., Gonzalez, F., … Izpisua Belmonte, J. C. (2008). Efficient and rapid generation of induced pluripotent stem cells from human keratinocytes. *Nature Biotechnology*, *26*(11), 1276–1284. doi: 10.1038/nbt.1503.

Badieyan, Z. S., & Evans, T. (2019). Concise review: Application of chemically modified mRNA in cell fate conversion and tissue engineering. *Stem Cells Translational Medicine*, *8*(8), 833–843. doi: 10.1002/sctm.18-0259.

Barrero, M. J., Berdasco, M., Paramonov, I., Bilic, J., Vitaloni, M., Esteller, M., & Izpisua Belmonte, J. C. (2012). DNA hypermethylation in somatic cells correlates with higher reprogramming efficiency. *Stem Cells*, *30*(8), 1696–1702. doi: 10.1002/stem.1138.

Bernloehr, C., Bossow, S., Ungerechts, G., Armeanu, S., Neubert, W. J., Lauer, U. M., & Bitzer, M. (2004). Efficient propagation of single gene deleted recombinant Sendai virus vectors. *Virus Research*, *99*(2), 193–197. doi: 10.1016/j.virusres.2003.11.005.

Bikle, D. D., Xie, Z., & Tu, C. L. (2012). Calcium regulation of keratinocyte differentiation. *Expert Review of Endocrinology & Metabolism*, *7*(4), 461–472. doi: 10.1586/eem.12.34.

Chan, C. C., Fan, S. M., Wang, W. H., Mu, Y. F., & Lin, S. J. (2015). A two-stepped culture method for efficient production of trichogenic keratinocytes. *Tissue Engineering. Part C, Methods*, *21*(10), 1070–1079. doi: 10.1089/ten.TEC.2015.0033.

Elsholz, F., Harteneck, C., Muller, W., & Friedland, K. (2014). Calcium—a central regulator of keratinocyte differentiation in health and disease. *European Journal of Dermatology*, *24*(6), 650–661. doi: 10.1684/ejd.2014.2452.

Ernst, N., Yay, A., Biro, T., Tiede, S., Humphries, M., Paus, R., & Kloepper, J. E. (2013). Beta1 integrin signaling maintains human epithelial progenitor cell survival in situ and controls proliferation, apoptosis and migration of their progeny. *PloS One*, *8*(12), e84356. doi: 10.1371/journal.pone.0084356.

Fleury, S., Simeoni, E., Zuppinger, C., Deglon, N., von Segesser, L. K., Kappenberger, L., & Vassalli, G. (2003). Multiply attenuated, self-inactivating lentiviral vectors efficiently deliver and express genes for extended periods of time in adult rat cardiomyocytes in vivo. *Circulation*, *107*(18), 2375–2382. doi: 10.1161/01.CIR.0000065598.46411.EF.

Fusaki, N., Ban, H., Nishiyama, A., Saeki, K., & Hasegawa, M. (2009). Efficient induction of transgene-free human pluripotent stem cells using a vector based on Sendai virus, an RNA virus that does not integrate into the host genome. *Proceedings of the Japan Academy. Series B, Physical and Biological Sciences*, *85*(8), 348–362. doi: 10.2183/pjab.85.348.

Hotta, A., & Ellis, J. (2008). Retroviral vector silencing during iPS cell induction: An epigenetic beacon that signals distinct pluripotent states. *Journal of Cellular Biochemistry*, *105*(4), 940–948. doi: 10.1002/jcb.21912.

Hung, S. S., Pebay, A., & Wong, R. C. (2015). Generation of integration-free human induced pluripotent stem cells using hair-derived keratinocytes. *Journal of Visualized Experiments*, *102*, e53174. doi: 10.3791/53174.

Keenan, J., Pearson, D., O'Driscoll, L., Gammell, P., & Clynes, M. (2006). Evaluation of recombinant human transferrin (DeltaFerrin^{TM}) as an iron chelator in serum-free media for mammalian cell culture. *Cytotechnology*, *51*(1), 29–37. doi: 10.1007/s10616-006-9011-x.

Kent, K. D., & Bomser, J. A. (2003). Bovine pituitary extract provides remarkable protection against oxidative stress in human prostate epithelial cells. *In Vitro Cellular & Developmental Biology Animal*, *39*(8-9), 388–394. doi: 10.1290/1543-706X(2003)039⟨0388:BPEPRP⟩2.0.CO;2.

Kim, Y. G., Baltabekova, A. Z., Zhiyenbay, E. E., Aksambayeva, A. S., Shagyrova, Z. S., Khannanov, R., … Shustov, A. V. (2017). Recombinant Vaccinia virus−coded interferon inhibitor B18R: Expression, refolding and a use in a mammalian expression system with a RNA-vector. *PloS One*, *12*(12), e0189308. doi: 10.1371/journal.pone.0189308.

Klingenstein, M., Raab, S., Achberger, K., Kleger, A., Liebau, S., & Linta, L. (2016). TBX3 knockdown decreases reprogramming efficiency of human cells. *Stem Cells International*, *2016*, 6759343. doi: 10.1155/2016/6759343.

Lim, S. J., Ho, S. C., Mok, P. L., Tan, K. L., Ong, A. H., & Gan, S. C. (2016). Induced pluripotent stem cells from human hair follicle keratinocytes as a potential source for in vitro hair follicle cloning. *PeerJ*, *4*, e2695. doi: 10.7717/peerj.2695.

Linta, L., Stockmann, M., Kleinhans, K. N., Bockers, A., Storch, A., Zaehres, H., … Liebau, S. (2012). Rat embryonic fibroblasts improve reprogramming of human keratinocytes into induced pluripotent stem cells. *Stem Cells and Development*, *21*(6), 965–976. doi: 10.1089/scd.2011.0026.

Nakagawa, M., Koyanagi, M., Tanabe, K., Takahashi, K., Ichisaka, T., Aoi, T., … Yamanaka, S. (2008). Generation of induced pluripotent stem cells without Myc from mouse and human fibroblasts. *Nature Biotechnology*, *26*(1), 101–106. doi: 10.1038/nbt1374.

Nygaard, U. H., Niehues, H., Rikken, G., Rodijk-Olthuis, D., Schalkwijk, J., & van den Bogaard, E. H. (2015). Antibiotics in cell culture: Friend or foe? Suppression of keratinocyte growth and differentiation in monolayer cultures and 3D skin models. *Experimental Dermatology*, *24*(12), 964–965. doi: 10.1111/exd.12834.

Okita, K., Nakagawa, M., Hyenjong, H., Ichisaka, T., &Yamanaka, S. (2008). Generation of mouse induced pluripotent stem cells without viral vectors. *Science*, *322*(5903), 949–953. doi: 10.1126/science.1164270.

Piao, Y., Hung, S. S., Lim, S. Y., Wong, R. C., & Ko, M. S. (2014). Efficient generation of integration-free human induced pluripotent stem cells from keratinocytes by simple transfection of episomal vectors. *Stem Cells Translational Medicine*, *3*(7), 787–791. doi: 10.5966/sctm.2013-0036.

Raab, S., Klingenstein, M., Liebau, S., & Linta, L. (2014). A comparative view on human somatic cell sources for iPSC generation. *Stem Cells International*, *2014*, 768391. doi: 10.1155/2014/768391.

Raab, S., Klingenstein, M., Moller, A., Illing, A., Tosic, J., Breunig, M., … Liebau, S. (2017). Reprogramming to pluripotency does not require transition through a primitive streak−like state. *Scientific Reports*, *7*(1), 16543. doi: 10.1038/s41598-017-15187-x.

Re, S., Dogan, A. A., Ben-Shachar, D., Berger, G., Werling, A. M., Walitza, S., & Grunblatt, E. (2018). Improved generation of induced pluripotent stem cells from hair derived keratinocytes—a tool to study neurodevelopmental disorders as ADHD. *Frontiers in Cellular Neuroscience*, *12*, 321. doi: 10.3389/fncel.2018.00321.

Schlaeger, T. M., Daheron, L., Brickler, T. R., Entwisle, S., Chan, K., Cianci, A., … Daley, G. Q. (2015). A comparison of non-integrating reprogramming methods. *Nature Biotechnology*, *33*(1), 58–63. doi: 10.1038/nbt.3070.

Shen, S., Alt, A., Wertheimer, E., Gartsbein, M., Kuroki, T., Ohba, M., … Tennenbaum, T. (2001). PKCdelta activation: A divergence point in the signaling of insulin and IGF-1-induced proliferation of skin keratinocytes. *Diabetes*, *50*(2), 255–264. doi: 10.2337/diabetes.50.2.255.

Sommer, C. A., Stadtfeld, M., Murphy, G. J., Hochedlinger, K., Kotton, D. N., & Mostoslavsky, G. (2009). Induced pluripotent stem cell generation using a single lentiviral stem cell cassette. *Stem Cells*, *27*(3), 543–549. doi: 10.1634/stemcells.2008-1075.

Steinle, H., Weber, M., Behring, A., Mau-Holzmann, U., Schlensak, C., Wendel, H. P., & Avci-Adali, M. (2019). Generation of iPSCs by nonintegrative RNA-based reprogramming techniques: Benefits of self-replicating RNA versus synthetic mRNA. *Stem Cells International*, *2019*, 7641767. doi: 10.1155/2019/7641767.

Takahashi, K., Tanabe, K., Ohnuki, M., Narita, M., Ichisaka, T., Tomoda, K., & Yamanaka, S. (2007). Induction of pluripotent stem cells from adult human fibroblasts by defined factors. *Cell*, *131*(5), 861–872. doi: 10.1016/j.cell.2007.11.019.

Wagner, T., Gschwandtner, M., Strajeriu, A., Elbe-Burger, A., Grillari, J., Grillari-Voglauer, R., … Mildner, M. (2018). Establishment of keratinocyte cell lines from human hair follicles. *Scientific Reports*, *8*(1), 13434. doi: 10.1038/s41598-018-31829-0.

Warlich, E., Kuehle, J., Cantz, T., Brugman, M. H., Maetzig, T., Galla, M., … Schambach, A. (2011). Lentiviral vector design and imaging approaches to visualize the early stages of cellular reprogramming. *Molecular Therapy*, *19*(4), 782–789. doi: 10.1038/mt.2010.314.

Warren, L., Manos, P. D., Ahfeldt, T., Loh, Y. H., Li, H., Lau, F., … Rossi, D. J. (2010). Highly efficient reprogramming to pluripotency and directed differentiation of human cells with synthetic modified mRNA. *Cell Stem Cell*, *7*(5), 618–630. doi: 10.1016/j.stem.2010.08.012.

Yu, J, , Hu, K., Smuga-Otto, K., Tian, S., Stewart, R., Slukvin, I. I., & Thomson, J. A. (2009) Human induced pluripotent stem cells free of vector and transgene sequences. *Science*, *324*(5928), 797–801. doi: 10.1126/science.1172482.

Reprogramming Urine-Derived Cells using Commercially Available Self-Replicative RNA and a Single Electroporation

Marga J. Bouma,[1,2,4] Christiaan H. Arendzen,[1,2] Christine L. Mummery,[1,2] Harald Mikkers,[1,3] and Christian Freund[1,2]

[1]LUMC hiPSC Hotel, Leiden University Medical Center, Leiden, The Netherlands
[2]Department of Anatomy and Embryology, Leiden University Medical Center, Leiden, The Netherlands
[3]Department of Cell and Chemical Biology, Leiden University Medical Center, Leiden, The Netherlands
[4]Corresponding author: *M.J.Bouma@lumc.nl*

We describe a protocol for efficient generation of human-induced pluripotent stem cells (hiPSCs) from urine-derived cells (UDCs) obtained from adult donors using self-replicative RNA containing the reprogramming factors *OCT3/4*, *SOX2*, *KLF4*, *GLIS1*, and *c-MYC* (ReproRNA-OKSGM). After electroporation, transfection efficiency is quantified by measuring OCT3/4-expressing UDCs using flow cytometry and should be ≥0.1%. hiPSC colonies emerge within 3 weeks after transfection and express multiple pluripotency markers. Moreover, the UDC-derived hiPSCs are able to differentiate into cells of all three germ layers and display normal karyotypes. ReproRNA-OKSGM is available commercially and only requires a single transfection step so that the protocol is readily accessible, as well as straightforward. In addition to a detailed step-by-step description for generating clonal hiPSCs from UDCs using ReproRNA-OKSGM, we provide guidance for basic pluripotency characterization of the hiPSC lines. © 2020 The Authors.

Basic Protocol: Reprogramming of urine-derived cells using ReproRNA-OKSGM
Support Protocol 1: Determination of the pluripotency status of hiPSCs by flow cytometry
Support Protocol 2: Characterization of functional pluripotency of hiPSCs

Keywords: induced pluripotent stem cell • reprogramming • self-replicative RNA • urine

How to cite this article:
Bouma, M. J., Arendzen, C. H., Mummery, C. L., Mikkers, H., & Freund, C. (2020). Reprogramming urine-derived cells using commercially available self-replicative RNA and a single electroporation. *Current Protocols in Stem Cell Biology*, *55,* e124. doi: 10.1002/cpsc.124

INTRODUCTION

Human-induced pluripotent stem cells (hiPSCs) are widely used as in vitro tools for modeling congenital diseases, studying early human development and toxicology screens,

CURRENT PROTOCOLS
A Wiley Brand

Current Protocols in Stem Cell Biology e124, Volume 55
Published in Wiley Online Library (wileyonlinelibrary.com).
doi: 10.1002/cpsc.124

and also hold promise for regenerative medicine (Bellin, Marchetto, Gage, & Mummery, 2012; Singh, Kalsan, Kumar, Saini, & Chandra, 2015). Since the initial reprogramming of human skin fibroblasts from biopsies by Takahashi and Yamanaka (Takahashi et al., 2007) using retroviral vectors to express the reprogramming factors *OCT3/4*, *SOX2*, *KLF4*, and *c-MYC*, many other cell types have been reprogrammed with a variety of vectors. Non-integrating reprogramming vectors are preferred as they circumvent risks of remaining- or reactivated transgene expression or altered endogenous gene expression, which may limit utility. Reprogramming conditions are ideally highly reproducible and avoid intermediate culture splitting that could yield mixed, non-clonal hiPSC colonies. This is important because donors could in principle be mosaic.

Urine-derived cells (UDCs) can be efficiently isolated non-invasively from urine samples and expanded in culture. They are thus an alternative source of somatic cells for reprogramming. UDCs were first reprogrammed using integrating retroviral pMX vectors (Zhou, Benda, Dunzinger, et al., 2012; Zhou, Benda, Duzinger, et al., 2011), and later using non-integrating episomal plasmids (Steichen et al., 2017; Wang et al., 2017; Xue et al., 2013). However, there is a (residual) risk of integration of episomal vectors into the host genome (Okita et al., 2011; Wang et al., 2017). Plasmid integration can be detected by PCR with specific primers, but integration of fragments can only be excluded by whole genome sequencing. In addition, compared with other reprogramming methods, karyotypic abnormalities may occur more frequently using episomal vectors (Schlaeger et al., 2015).

Sendai virus (SeV) is considered entirely non-integrating (Nishimura et al., 2011); SeV has also been used successfully for generating hiPSCs from UDCs (Afzal & Strande, 2015; Hildebrand et al., 2016). Since the virus is replication-deficient, it is normally eliminated by continuous division of the host cells. However, in some cases it has been shown to persist even after multiple passages in culture (Schlaeger et al., 2015); this may adversely affect hiPSC quality and may limit use due to laboratory safety requirements.

Much like SeV, RNA is another "zero footprint" reprogramming vector. Originally messenger (m)RNA was used for reprogramming. Since it is quickly degraded by the intracellular interferon (IFN)α/β-mediated response to foreign RNA, transfection on 11 consecutive days was required to reprogram UDCs, resulting in high workload and extra costs (Gaignerie et al., 2018). As an alternative, Yoshioka et al. developed a self-replicative (sr)RNA, which only requires a single transfection for reprogramming skin fibroblasts. The degradation of srRNA is prevented during reprogramming by addition of B18R, which blocks the INF-y response. Omission of B18R upon emergence of hiPSC-colonies leads to complete srRNA removal (Yoshioka & Dowdy, 2017; Yoshioka et al., 2013). Recently, an srRNA containing *GFP*, *OCT3/4*, *SOX2*, *KLF4*, and *c-MYC* was used for reprogramming UDCs (Steinle et al., 2019). However due to an intermediate culture split, reprogramming efficiencies may have been overestimated and hiPSC colonies were possibly of a mixed origin. Moreover, the protocol required B18R protein supplementation for 26 days, making the experiment costly compared to other methods.

Here we describe a method to reprogram UDCs with commercially available srRNA containing the reprogramming factors *OCT3/4*, *SOX2*, *KLF4*, *c-MYC*, and *GLIS1* (ReproRNA-OKSGM) (Yoshioka & Dowdy, 2017) with defined media on Matrigel. As the ReproRNA-OKSGM vector is large (∼16,500 nt), we tested various transfection methods of which nucleofection proved to be the most suitable in terms of required cell number and transfection efficiency. Flow cytometry analysis performed on day 3 allowed quantification of transfection efficiency, enabling termination of an unsuccessful experiment at an early timepoint. B18R protein is added to the cells for 12 days following transfection. Our experiments using UDCs isolated from three adult donors demonstrated

that 4-82 hiPSC colonies (corresponding to 0.008%-0.17% reprogramming efficiency) can be generated in a single experiment, despite the relatively low percentage of transfected cells. Due to a lack of an intermediate splitting step, hiPSC colonies are likely to be clonal. UDC-derived hiPSCs are free of the reprogramming vector and display a normal karyotype. They express typical pluripotency markers and have in vitro trilineage differentiation capacity. We also provide supporting protocols for the characterization of pluripotency by FACS and pre-labeled antibodies for immunofluorescent staining of derivatives of the three germ layers.

REPROGRAMMING OF URINE-DERIVED CELLS USING ReproRNA-OKSGM

BASIC PROTOCOL

Similar to many other primary cell types it is difficult to transfect UDCs with large vectors using regular lipid-based transfection. Here we describe a step-wise feeder-free protocol to reprogram UDCs with ReproRNA-OKSGM using electroporation as an alternative transfection method, hence combining a non-integrating reprogramming vector with a cell source that can be harvested through non-invasive methods. The first section describes the starting material and how to prepare for the electroporation. In the next set of steps the UDCs are harvested and transfected with ReproRNA-OKSGM and subsequently cultured until hiPSC colony picking. The final section describes how to quantify the transfection efficiency by flow cytometry.

Materials

UGCs (see Zhou, Benda, Dunziner, et al., 2012)
Renal Epithelial Cell Growth (REGM)-medium (Lonza, cat. no. CC-3190)
Transfection (TF) medium (see recipe)
Matrigel, hESC-qualified (Corning, cat. no. 354277)
DMEM-F12 (Gibco, cat. no. 10565018)
ReproRNA-OKSGM (STEMCELL Technologies, cat. no. 05931)
Dulbecco's phosphate-buffered saline (DPBS, Gibco, cat. no. 14190-169)
Trypsin-EDTA, 0.05% (Gibco, cat. no. 25300054)
0.4% Trypan-Blue (Invitrogen, cat. no. T10282)
Neon Transfection System 10 µl kit (Invitrogen, MPK1096) containing:
  Resuspension buffer R
  Buffer E
REGM-medium with B18R (see recipe)
ReproTeSR with B18R (see recipe)
TeSR-E8 (STEMCELL Technologies, cat. no. 05990)
FIX & PERM cell permeabilization kit (Invitrogen, cat. no. GAS003) containing:
  Medium A
Medium BFACS buffer (see recipe)
Anti-OCT3/4 Isoform A-PE antibody (Miltenyi Biotec, cat. no. 130-105-606, RRID: AB_2653084)

Serological pipettes (5-, 10 ml, sterile)
Pipette tips (10-, 200-, 1,000 µl, sterile, RNase-/DNase-free)
Pipettes (0.5 µl to 1,000 µl)
Culture plates (12-well and 6-well, clear, sterile)
37°C, 5% CO_2 humidified incubator
Neon Transfection System (Invitrogen, MPK5000)
Tubes (disposable, 15 ml, sterile)
Centrifuge
Cell counter
Eppendorf tubes (disposable, 1.5 ml, sterile, RNase-/DNase-free)

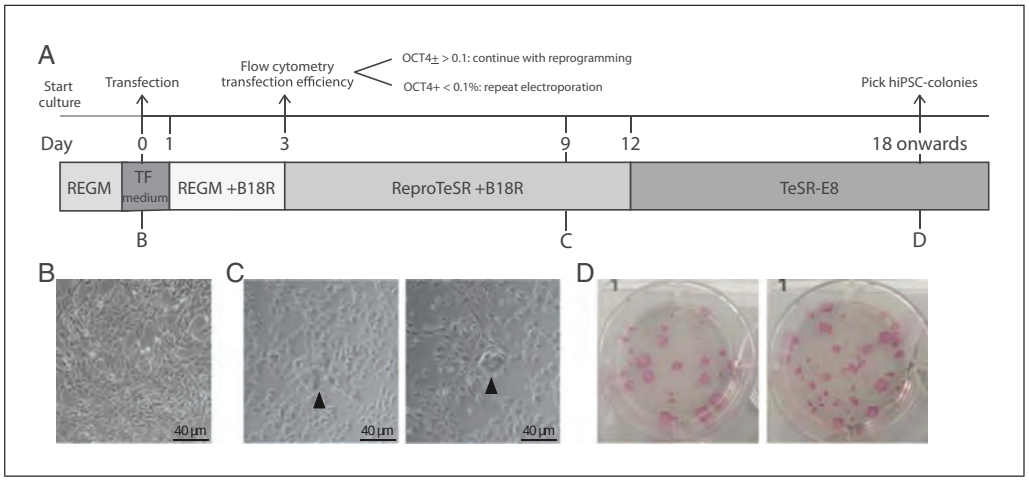

Figure 1 (**A**) Schematic of reprogramming experiment. (**B**) UDCs before transfection. (**C**) Morphology of UDCs at day 9 after transfection. Arrowhead: clusters of UDCs undergoing reprogramming. (**D**) Alkaline phosphatase staining of hiPSC-colonies at day 21 after transfection (6-well format).

Falcon round-bottom test tube with cell strainer (Corning, cat. no. 352235)
Flow cytometer

Treatment of UDCs before transfection

1. Culture early passage UDCs REGM-medium in one well of a 6-well culture plate until 80%-90% confluent. Before reprogramming make sure that the UDCs are mycoplasma negative by using a standard testing kit.

Isolation of UDCs according to Zhou, Benda, Dunzinger, et al. (2012).

2. Refresh UDCs with 1.5 ml transfection (TF) medium 1 h prior to harvesting of the UDCs (step 11) (Fig. 1A/B).

Preparation of Matrigel-coated wells

3. Thaw a Matrigel aliquot on ice and dilute with cold DMEM-F12 according to the manufacturer's instructions.
4. Add 1 ml of the diluted Matrigel into one well of 6-well plate and 0.5 ml into 2 wells of a 12-well plate, respectively.
5. Incubate for at least 30 min at room temperature (RT).
6. Remove the Matrigel solution and add 1.5 ml TF medium to each coated well of the 6-well and 0.75 ml to each coated well of the 12-well-plate.
7. Place in the incubator until further use.

Setting up of the NEON transfection system

8. Set up the NEON pipette station according to manufacturer's instructions.
9. Enter the following transfection parameters manually: 1,200 V, 50 ms, 1 pulse.

Thawing of ReproRNA-OKSGM

10. Thaw the ReproRNA-OKSGM on ice.

Harvesting of UDCs for transfection

11. Wash the UDCs with 2 ml DPBS (RT).
12. Add 0.5 ml of 0.05% Trypsin-EDTA and place in the incubator for 4 min.

Cells should be completely detached after 4 min incubation with Trypsin-EDTA. If still adherent, gently tap the plate to loosen the cells.

13. Add 2 ml REGM medium (RT) to the cell suspension, transfer into a 15-ml conical tube, and centrifuge at for 3 min at 200 × *g*, RT.
14. Discard the supernatant and gently resuspend the pellet in 2 ml TF medium.
15. Take 10 µl of the cell suspension and mix with 10 µl of 0.4% Trypan Blue.
16. Count the number of live (unstained) UDCs using a cell counter. Refer to the manufacturer's guidelines for instructions.
17. Take an aliquot corresponding to 2.4×10^5 live cells and centrifuge for 3 min at 200 × *g*, RT.

Transfection of UDCs

18. Carefully remove the supernatant without disturbing the cell pellet.

    It is important to remove as much volume as possible, to minimize the dilution of Resuspension buffer R in the next step.

19. Resuspend UDCs in 22 µl of resuspension buffer R (Neon Transfection kit).
20. Transfer 11 µl of the cell suspension into a 1.5-ml Eppendorf tube. Keep the remaining cell suspension at RT.
21. Add 1 µl of ReproRNA-OKSGM directly into the cell suspension and mix well by pipetting gently up and down.
22. Aspirate 10 µl of the cell suspension/ReproRNA mix from step 21 with the NEON-pipette, avoid air bubbles.

    Any air bubble in the tip causes arcing, which can result in reduced or failed electroporation of the UDCs.

23. Insert the Neon-pipette vertically in the Neon-tube containing 3 ml Buffer E (Neon Transfection kit) in the Neon Pipette Station (as prepared in step 8).
24. Electroporate the cells using the parameters of step 9. (Fig. 1A)
25. Remove the Neon-pipette from the station and transfer the electroporated cells into a 1.5-ml Eppendorf tube.
26. Plate 5 µl of the transfected UDCs into the Matrigel-coated 6-well plate and 5 µl into one well of the 12-well plate with prewarmed TF medium from step 7. Distribute the cells by gently rocking the plate.
27. Plate 5 µl of untransfected cells from step 19 in the remaining well of the 12-well plate. Distribute the cells by gently rocking the plate.
28. Incubate the cells at 37°C and 5% CO_2 without disturbing them for the next 24 hr.

Reprogramming of transfected UDCs

29. Refresh the cells 24 and 48 hr post-transfection with 1.5 ml REGM-medium with B18R for the 6-well plate and 0.75 ml REGM-medium with B18R for the 12-well plate.

    Attached single cells should be equally distributed throughout the well.

30. Replace REGM-medium with B18R with 1.5 ml ReproTeSR+B18R at 72 hr post-transfection for the 6-well plate. Refresh cells daily until day 11. For the cells in the 12-well plate, proceed with step 32.

Small groups of cells undergoing reprogramming that are surrounded by regular UDCs can be observed from day 7 after transfection (see Fig. 1C).

31. From day 12: refresh cells with 2 ml TeSR-E8 daily until hiPSC colonies are ready for picking.

    At this timepoint wells are often fully confluent with non-reprogrammed UDCs surrounding newly formed hiPSC colonies. This will not compromise the growth of the hiPSC-colonies. However, removal of UDCs around hiPSC colonies by gentle scraping with a pipette tip can accelerate outgrowth of the hiPSC-colony.

    hiPSC colonies are ready for picking and further expansion around day 18-21 post transfection (Fig. 1D).

Flow cytometry analysis to quantify UDC transfection with ReproRNA-OKSGM

32. Wash both wells of the 12-well plate (transfected and untransfected UDCs) with 1 ml DPBS.
33. Add 0.25 ml of 0.05% Trypsin-EDTA to each well and incubate for 4 min at 37°C.

    Cells should be completely detached after 4 min incubation with Trypsin-EDTA. If still adherent, gently tap the plate to loosen the cells.

34. Add 1 ml of REGM-medium to each well and transfer the cell suspensions into a 15-ml tube, prelabeled with either + (transfected-) or – (untransfected).
35. Centrifuge for 3 min at 200 × *g*, RT.
36. Remove the supernatant, resuspend the pellet in 200 µl Medium A (FIX and PERM permeabilization kit) and incubate for 15 min at RT.
37. Add 3 ml FACS buffer and centrifuge the cells for 5 min at 300 × *g*, RT.
38. Remove the supernatant and resuspend the cell pellet in 100 µl Medium B (FIX and PERM permeabilization kit).
39. Add 2 µl of conjugated anti-OCT3/4 antibody (1:50) and incubate for 20 min at RT in the dark.
40. Add 3 ml of FACS buffer and centrifuge for 5 min at 300 × *g*, RT.
41. Remove the supernatant and wash the cells with 3 ml FACS buffer. Centrifuge for 5 min at 300 × *g*, RT.
42. Resuspend the pellet in 200 µl FACS buffer and filter the cell suspension by using a cell strainer in the lid of a Falcon round-bottom test tube.
43. Measure the percentage of OCT3/4$^+$ cells with a flow cytometer. Use the untransfected cells as a negative control.

    If the percentage of OCT3/4$^+$ is below 0.1%, discontinue the reprogramming experiment and repeat the electroporation.

SUPPORT PROTOCOL 1

DETERMINATION OF THE PLURIPOTENCY STATUS OF hiPSCs BY FLOW CYTOMETRY

This method describes a flow cytometry-based characterization of the pluripotency status of undifferentiated hiPSCs, by measuring the expression of pluripotency markers.

Additional Materials *(also see Basic Protocol)*

hiPSC cultures (see the Basic Protocol)
Gentle Cell Dissociation Reagent, GCDR (STEMCELL Technologies, cat. no. 07180)

FIX and PERM cell permeabilization kit (Invitrogen, cat. no. GAS003) containing:
Medium A
Medium B
FACS buffer (see recipe)
Anti-OCT3/4-BV421 antibody (BD Biosciences, cat. no. 565644, RRID: AB_2739320)
Anti-Nanog-PE antibody (BD Biosciences, cat. no. 560483, RRID: AB_1645522)
Anti-SSEA4-FITC antibody (Miltenyi, cat. no. 130-098-371, RRID: AB_2653517)

Flow cytometry of pluripotency markers

Culture hiPSCs according to standard procedures in a 6-well plate. On the day of passaging, use 1 × 6-well for flow cytometry to measure expression of pluripotency markers. You can take along primary cells (e.g., skin fibroblast, HACAT, but do not use UDCs as they express SSEA4 at high levels) as a negative control and Fluorescence Minus One controls for setting up the flow cytometer.

1. Remove culture medium from the hiPSC cultures and add 1 ml GCDR; incubate for 7 min at 37°C.
2. Pipette vigorously up and down several times with a 1000-µl pipette to dislodge the cells and generate a single-cell suspension.
3. Check cell suspension under a brightfield microscope; if cell aggregates persist, repeat step 2.
4. Add 4 ml DMEM/F12 to the cell suspension and transfer into a 15-ml tube.
5. Take 10 µl of the cell-suspension and mix with 10 µl of 0.4% Trypan Blue.
6. Count the number of live cells using a cell counter according to the manufacturer's instructions.
7. Take the volume of the cell suspension corresponding to 1×10^5 cells and centrifuge for 3 min at 200 × *g*, RT.
8. Discard the supernatant, resuspend the cells in 200 µl Medium A (FIX and PERM permeabilization kit), and incubate 15 min at RT.
9. Add 3 ml FACS buffer to the cells and centrifuge for 5 min at 300 × *g*, RT.
10. Remove the supernatant and resuspend the cell pellet in 80 µl Medium B (FIX and PERM permeabilization kit).
11. Add 4 µl conjugated anti-OCT3/4 antibody (1:25), 4 µl conjugated anti-SSEA4 antibody (1:25), and 20 µl conjugated anti-Nanog antibody (1:5) and incubate for 60 min at RT in the dark.
12. Add 3 ml FACS buffer to the cells and centrifuge for 5 min at 300 × *g*, RT.
13. Wash the cells with 3 ml FACS buffer and centrifuge for 5 min at 300 × *g*, RT.
14. Resuspend the cells in 200 µl FACS buffer and filter using the cell strainer of a Falcon round-bottom test tube.
15. Measure the percentage of OCT3/4-/Nanog-/SSEA4-triple positive cells with a flow cytometer.

Set up the flow cytometer using the appropriate controls. At least 75% of the cells should be positive for all three markers.

CHARACTERIZATION OF FUNCTIONAL PLURIPOTENCY OF hiPSCs BY IMMUNOFLUORESCENT STAINING WITH PRE-LABELED ANTIBODIES

The method below describes a way to check the functional pluripotency of hiPSCs by immunofluorescent staining after directed short-term differentiation into derivatives of endo-, ecto-, and mesoderm.

Additional Materials *(also see Basic Protocol)*

100% Ethanol
Stemdiff Trilineage Differentiation Kit (STEMCELL Technologies, cat. no. 05230)
2% Paraformaldehyde (PFA; see recipe)
Permeabilization/Blocking solution (see recipe)
4% Normal Swine Serum (4% NSS; see recipe)
Conjugated antibodies (Cell Signaling Technologies, custom-made, pre-labeled, see Table 1)
0.05% Tween/PBS (see recipe)
DAPI (Invitrogen, cat. no. D3571)
MilliQ water
ProLong Gold Antifade Mountant (Invitrogen, cat. no. P36930)

Glass coverslips (13-mm diameter)
Tweezers
Bunsen burner
Culture plates (24-well, sterile, clear)
Glass microscope slides
(Confocal) Fluorescent microscope

Matrigel coating of coverslips

1. Sterilize a coverslip by dipping it into 100% ethanol using tweezers and subsequent flaming.
2. Place the sterile coverslip in a well of a 24-well plate. Each germ layer differentiation requires one well with a coverslip.

   Use the same plate for meso- and endoderm differentiation (5 days) and a separate plate for ectoderm differentiation (7 days).

3. Thaw a Matrigel aliquot on ice and dilute with cold DMEM-F12 according to the manufacturer's instructions.
4. Add 330 µl of the diluted Matrigel onto each coverslip.

Table 1. Pre-Conjugated Antibody-List Used for Support Protocol 2

Antibody	Cat. no.	Source	Isotype	Conjugated with	Germ layer
anti-FAPB7	D8N3N	Rabbit	IgG	Alexa555	Ectoderm
anti-PAX6	D3A9V	Rabbit	IgG	Alexa647	Ectoderm
anti-Nestin	10C2	Mouse	IgG1	Alexa488	Ectoderm
anti-FOXA2	D56D6	Rabbit	IgG	Alexa555	Endoderm
anti-EOMES	D8D1R	Rabbit	IgG	Alexa488	Endoderm
anti-GATA4	D3A3M	Rabbit	IgG	Alexa647	Endoderm
anti-Vimentin	D21H3	Rabbit	IgG	Alexa647	Mesoderm
anti-CDX2	D11D10	Rabbit	IgG	Alexa555	Mesoderm
anti-Brachyury	D2Z3J	Rabbit	IgG	Alexa488	Mesoderm

Make sure that the coverslip is completely covered with Matrigel. Sometimes coverslips need to be pushed down using a pipette tip.

5. Incubate the plates for at least 30 min at RT before use.

Trilineage differentiation and fixation of coverslips

6. Plate undifferentiated hiPSCs on Matrigel-coated coverslips and perform Trilineage differentiation according to the manufacturer's instructions.
7. At the end of differentiation (day 5 for meso- and endoderm and day 7 for ectoderm), remove medium from the coverslips and gently wash cells with 1 ml DPBS.
8. Remove DPBS and add 1 ml of 2% PFA to the coverslips; incubate for 30 min at RT.
9. Remove 2% PFA and gently wash cells once with 1 ml DPBS.
10. Add 1 ml DPBS to the coverslips and proceed with the immunofluorescence staining.

    If necessary, fixed cells can be stored for several weeks at 4°C before proceeding with the immunofluorescent staining.

Immunofluorescent staining of trilineage differentiation

11. Wash the coverslips once with 200 µl DPBS.
12. Remove DPBS and add 80 µl Permeabilization/Blocking solution to each coverslip and incubate 60 min at RT.
13. Prepare antibody mix for all three germ layers by diluting the antibodies in 4% NSS according to Table 2.
14. Wash the coverslips once with 200 µl DPBS.
15. Add 80 µl of the corresponding antibody-mix to the coverslips (Table 1/2) and incubate for 60 min, at RT, in the dark.
16. Incubate the coverslips three times, each time with 200 µl of 0.05% Tween/PBS for 10 min in the dark.
17. Dilute DAPI stock-solution (1 mg/ml) 1:500 in DPBS.

Table 2. Dilution Factors Antibodies for Support Protocol 2

Antibody mix	Components	Dilution	Volume (µl)
Ectoderm	anti-FAPB7	1:100	1
	anti-PAX6	1:200	0.5
	anti-Nestin	1:200	0.5
	4% NSS		98
Endoderm	anti-FOXA2	1:500	0.2
	anti-EOMES	1:100	1
	anti-GATA4	1:200	0.5
	4% NSS		98.3
Mesoderm	anti-Vimentin	1:400	0.25
	anti-CDX2	1:500	0.2
	anti-Brachyury	1:200	0.5
	4% NSS		99

18. Add 80 µl of the diluted DAPI to the coverslips and incubate for 5 min, at RT, in the dark.
19. Wash the coverslips once with 200 µl MilliQ water.
20. Put a droplet of ProLong Gold (~10 µl) on a pre-labeled glass microscope slide.
21. Remove the MilliQ water from the coverslips and mount coverslip upside down onto the microscope slide.
22. Dry the microscope slide for at least 24 hr in the dark.
23. Image the slides with a (confocal) fluorescent microscope.

REAGENTS AND SOLUTIONS

FACS buffer

Dissolve bovine serum albumin (BSA; Sigma, cat. no. A8022) in DPBS (Gibco, cat. no. 14190-169) at 5 mg/ml. Add EDTA (0.5 M EDTA; ThermoFisher, cat. no. AM9260G) to a final concentration of 0.2 mM. Store FACS buffer up to 4 weeks at 4°C.

Normal swine serum (NSS), 4%

Dilute NSS (Jackson ImmunoResearch Laboratories, cat. no. 014-000-121) at 1:25 in DPBS (Gibco, cat. no. 14190-169)
Prepare fresh

Paraformaldehyde (PFA), 2%

8% PFA (2 L)
Heat 1,500 ml MilliQ water to 80°C
Weigh 160 g Paraformaldehyde (Merck, cat. no. 1.04005.1000) in an Erlenmeyer flask
Place the Erlenmeyer flask on a magnetic stirrer in a chemical hood
Add 1,500 ml MilliQ water of ~74°C to the Paraformaldehyde and stir 5 min until dissolved
Adjust the pH to 7.4 using 5 M NaOH (Merck, cat. no. 1.06498.1000)
Let the solution cool down while stirring
Add 500 ml MilliQ
Sterilize by using a 0.22-µm filter
Store up to 3 months at 4°C
2% PFA
Dilute 8% PFA 1:4 with the phosphate buffer
Prepare fresh

Permeabilization/blocking solution

Prepare a 0.1% Triton X-100/DPBS solution by diluting Triton X-100 (Sigma, cat. no. T8787) at 1:1,000 with DPBS (Gibco, cat. no. 14190-169)
Dilute NSS (Jackson ImmunoResearch Laboratories, cat. no. 014-000-121) at 1:25 with the 0.1% Triton X-100/DPBS solution
Prepare fresh

Phosphate buffer

Prepare a 0.2 M solution of $NaH_2PO_4 \cdot H_2O$ (Merck, cat. no. 1.06346.1000) in MilliQ water
Prepare a 0.2 M solution of $Na_2HPO_4 \cdot 2H_2O$ (Gerbu, cat. no. 1309-1000) in MilliQ water
Add $NaH_2PO_4 \cdot H_2O$ (acid) solution to the $Na_2HPO_4 \cdot 2H_2O$ (base) solution until it reaches a pH of 7.4
Store up to 3 months at 4°C

REGM-medium with B18R

Prepare the REGM-medium according to manufacturer's instructions (REGM Bulletkit, Lonza, cat. no. 3190)

Thaw B18R protein at RT and add at 1:2,500 to the medium

Prepare aliquots of the B18R protein if you do not use the complete volume. Store aliquots at −80°C. Avoid repeated freeze-thaw cyclesm

Warm medium to RT before use.

Complete REGM-medium with B18R can be stored up to 1 week at 4°C.

ReproTeSR with B18R

Prepare ReproTeSR according to manufacturer's instructions (STEMCELL Technologies, cat. no. 05926)

Thaw B18R protein at RT and add at 1:2,500 to the medium

Prepare aliquots of the B18R protein if you do not use the complete volume. Store aliquots at −80°C. Avoid repeated freeze-thaw cycles.

Warm medium to RT before use.

Complete ReproTeSR with B18R can be stored up to 1 week at 4°C.

Transfection (TF) medium

Thaw REGM Singlequots, except GA-1000 (antibiotic) (REGM Singlequots kit, no GA-1000. Lonza, cat. no. CC4127) on ice

Add REGM Singlequots, except GA-1000, to the Renal Epithelial Cell Growth Basal Medium (REBM. Lonza, Cat.no CC3191)

IMPORTANT: *The TF medium must not contain any antibiotics as this can lead to increased cell-death. (Prepare aliquots of the Singlequots when you are not using the complete volume. Store aliquots at −20°C. Avoid repeated freeze-thaw cycles.)*

Thaw B18R protein at RT and add at 1:2,500 to the medium

Prepare aliquots of the B18R protein if you do not use the complete volume. Store aliquots at −80°C. Avoid repeated freeze-thaw cycles.

Warm medium to RT before use.

Complete TF medium can be stored up to 1 week at 4°C.

Tween/PBS, 0.05%

Pipette 49.975 ml of DPBS (Gibco, cat. no. 14190-169) into a 50-ml tube

Cut the end of a 100-µl pipette tip to enlarge the opening

Pipette up 25 µl of Tween-20 (Merck, cat. no. 8.22184.0500) with the pre-cut pipette tip

Tween-20 is very viscous, pipette slowly to ensure aspirating the complete amount.

Add the Tween-20 to the tube containing the DPBS (drop the used pipette tip inside of the tube)

Put the 50-ml tube on a tube rotator until the Tween-20 is properly dissolved

Store for several months at RT

COMMENTARY

Background Information

Zhou et al. were the first to show that cells extracted and expanded from urine samples can be used for reprogramming (Zhou, Benda, Dunzinger, et al., 2012; Zhou, Benda, Duzinger, et al., 2011). These so-called urine-derived cells (UDCs) are a heterogeneous population, which originate mainly from the

renal epithelium. Their identity is based on high expression levels of several epithelial markers (e.g., Occludin and Claudin1) and renal tubular markers (e.g., CD13 and NR3C2) (Dorrenhaus et al., 2000; Rahmoune et al., 2005; Zhou, Benda, Duzinger, et al., 2011). However, expression of urothelial markers and stem cell markers have also been described (Bharadwaj et al., 2011; Zhang et al., 2008).

Zhou et al. were the first to reprogram UDCs with retroviral pMX vectors with an efficiency of 0.1%-4%. The use of retroviruses for reprogramming is unfavorable because stable integration of the retroviral DNA can lead to incomplete transgene silencing or reactivation under certain conditions (Koyanagi-Aoi et al., 2013; Okita, Ichisaka, & Yamanaka, 2007). The latter has been shown to negatively affect the differentiation capacity of hiPSCs and can even cause malignancy (Bouma et al., 2017). Moreover, hiPSCs generated with retroviral vectors have high aneuploidy rates (Schlaeger et al., 2015).

Since the first description of UDCs as a cell source for reprogramming, multiple efforts have been made to reprogram UDCs using different reprogramming methods. Several groups generated hiPSCs from UDCs with episomal plasmids (Steichen et al., 2017; Wang et al., 2017; Xue et al., 2013); however, episomal DNA can occasionally integrate in the host-genome and may increase aneuploidies (Okita et al., 2011; Schlaeger et al., 2015; Wang et al., 2017). As a truly non-integrative approach, Sendai virus has been used for reprogramming of UDCs (Afzal & Strande, 2015; Hildebrand et al., 2016). However, persistence of Sendai virus vectors in hiPSCs of relatively high passage has been observed (Afzal & Strande, 2015; Schlaeger et al., 2015). Commercially available SeV contains temperature-sensitive mutations in a subset of the vectors requiring incubation of hiPSCs at 38°-39°C for 5 days for clearance. However, hiPSCs might be sensitive to culture at elevated temperatures. As an alternative non-integrating vector mRNA has been successfully deployed for the reprogramming of somatic cells including UDCs (Gaignerie et al., 2018; Warren et al., 2010). Due to the low stability of exogenous mRNA the reprogramming procedure requires transfections on multiple consecutive days and is, therefore, laborious, error-prone and expensive.

To overcome these hurdles, Yoshioka et al. (2013) developed a self-replicative (sr)RNA. The original srRNA version is based on a single, synthetic Venezuelan Equine Encephalitis (VEE) RNA replicon encoding the reprogramming factors *OCT3/4*, *KLF4*, *SOX2*, and *c-MYC* or *Glis1*. The continuous expression of the reprogramming factors is ensured by self-replication of the vector and the suppression of RNA degradation by B18R supplementation (Alcami, Symons, & Smith, 2000; Colamonici, Domanski, Sweitzer, Larner, & Buller, 1995). A single transfection with the srRNA is sufficient to successfully reprogram fibroblasts into hiPSCs (Yoshioka et al., 2013). An improved version of the srRNA vector contains all five factors (Yoshioka & Dowdy, 2017).

In 2019, hiPSCs were generated from UDCs using an srRNA with the four Yamanaka factors as well as GFP to monitor transfection efficiency (Steinle et al., 2019). Between 3-25 hiPSC colonies were obtained after a single transfection with lipofectamine. However, the protocol included an intermediate splitting step after transfection, possibly leading to an overestimation of transfection efficiency and the emergence of non-clonal hiPSC colonies.

Our protocol is based on a commercially available and improved srRNA version containing the reprogramming factors *OCT3/4*, *KLF4*, *SOX2*, *GLIS1* and *c-MYC*. Only 1.2×10^5 cells are required for the actual electroporation and the total number of 2.4×10^5 cells for the whole experiment is easily obtained by culturing UDCs in a single well of a 6-well plate. Fewer population doublings reduce the risk of cells becoming senescent, which is known to be counteractive for successful reprogramming in general and has previously been seen for UDCs. (Li et al., 2016). Moreover, in our protocol B18R protein supplementation is only required for 12 days, which significantly reduces the costs compared to other protocols. In addition, we found that puromycin selection as described for fibroblasts was not necessary for UDC reprogramming resulting in a simplified experimental procedure. By measuring the percentage of $OCT3/4^+$ cells 72 hr post-transfection our protocol provides an early checkpoint in order to determine whether an experiment is likely to be successful. Finally, we provide straightforward protocols for the basic characterization of the pluripotency status and differentiation capacity of hiPSCs.

Critical Parameters

UDCs need to be at an early passage and highly proliferative to enable proper reprogramming. Otherwise, the reprogramming

Table 3. Troubleshooting Guide

Step	Problem	Solution
Basic Protocol, step 29	Increased cell-death after transfection	Some degree of cell-death is expected after the transfection of the cells using these electroporation parameters. However, there should be attached cells 24 hr post plating.
Basic Protocol, step 31 (annotation)	No hiPSC colonies appearing (with transfection efficiency >0.1%)	Ensure your UDCs are low passage and proliferative.
Basic Protocol, step 31 (annotation)	hiPSC colonies remain small due to fully confluent non-reprogrammed UDCs	Carefully remove non-reprogrammed UDCs surrounding the hiPSC colony by scraping with a pipette-tip without damaging the colony. Change medium and keep in culture for a couple of days until hiPSC colony is ready for picking.
Basic Protocol, step 43	Transfection efficiency below 0.1%	Repeat the experiment ensuring that: (1) TF medium does not contain antibiotics. (2) Cells appeared as single cells before transfection (3) Transfect the correct number of viable cells. (4) The srRNA has not been degraded. Use RNase-free tubes and tips. Thaw srRNA on ice shortly before use. Avoid repeated freezing and thawing. (5) No error or spark was observed using the Neon transfection system
Support Protocol 1, step 15	Low fluorescent intensity for one or more antibodies	There might be batch-to-batch variation for pre-labeled antibodies. Test different batches and determine the optimal dilution.
Support Protocol 2, step 7 & 8	Cells are detached from coverslips after this step	Avoid adding DPBS and 2% PFA at high speed directly onto the cells. As the cells differentiate and become dense, they tend to detach more easily (as a sheet). Add fluids gently against the well wall.

efficiency decreases dramatically (Li et al., 2016). It is therefore important to start the UDC isolation with sufficiently large volumes of urine (>100 ml) and to process the urine immediately after collection. On average we obtain ~5 UDC colonies per 100 ml of urine; however, there is variability between donors and even separate samples from the same donor can give different isolation efficiencies. When culturing UDCs, they should be passaged at a ratio 1:4 when reaching 80%-90% confluency to ensure proper growth. Normally, it takes 3-5 days before they reach the required confluency again.

UDCs should be transfected as a single-cell suspension to ensure proper transfection using the Neon-system. After centrifugation the culture medium should be removed carefully, without disturbing the cell pellet. We usually remove the supernatant just above the pellet with a pipette tip instead of aspiration by vacuum. Moreover, it is important to avoid any arcing using the Neon system. When a spark has been observed during transfection, transfection efficiency might be reduced. We therefore recommend to always check the transfection efficiency by flow cytometry after 72 hr.

We found that despite low transfection efficiencies a minimum of four hiPSC colonies/clones were obtained per reprogramming experiment. In general, we consider three hiPSC clones per donor as sufficient. At transfection efficiencies of <0.1% we were never able to obtain any hiPSC colonies. In this case we recommend aborting the ongoing experiment and repeating the electroporation in order to save both time and money.

At day 12 during UDC reprogramming we switch culture medium from ReproTeSR + B18R to TeSR-E8 medium, to promote

outgrowth of the formed hiPSC-colonies. Although small hiPSC-colonies might already be observed at an earlier timepoint, it is important not to start with TESR-E8 before day 12 as hiPSC lines established under those conditions seem to have a bias for spontaneous neuroectodermal differentiation.

Troubleshooting

Problems that may arise at different steps and their possible solutions are listed in Table 3.

Understanding Results

Reprogramming time-course for UDCs

Small clusters of cells undergoing reprogramming will be visible from day 7 onwards. Compared to the original UDCs these show morphological changes, such as formation of compact cell clusters, high nucleus-to-cytoplasm ratios and few clearly visible nucleoli. No clear borders are observed yet for all clusters (Fig. 1A−C). When medium is switched to TeSR-E8 at day 12, some clusters will disappear in the following 2-3 days, whereas others transform into compact hiPSC colonies with defined borders. Outgrowth of hiPSC colonies can be accelerated by manual removal of surrounding non-reprogrammed UDCs. Usually at day 18-21 post-transfection, hiPSC colonies are sufficiently large for manual picking (Fig. 1A/D).

Measuring transfection efficiency

UDCs seeded in the 12-well plate after transfection are subjected to flow cytometry to quantify transfection efficiency. This is performed at 72 hr post-transfection, to enable the cells to recover from the electroporation procedure. Due to the transfection stress many cells will die, resulting in a low number of attached cells the day after transfection. Untransfected cells (negative control) will be confluent after 72 hr in most cases. Percentages of OCT3/4-expressing cells was in the range ∼0.2%–1.3% (0.64 ± 0.40%), resulting in 4-86 hiPSC (32 ± 23) colonies for three donors (Fig. 2). Of note, the transfection efficiency is not directly correlated with the reprogramming efficiency but rather seems to be donor-dependent. However, out of 15 performed reprogramming attempts, three failed due to transfection efficiencies below 0.1% (ranging from ∼0.01% to 0.06%).

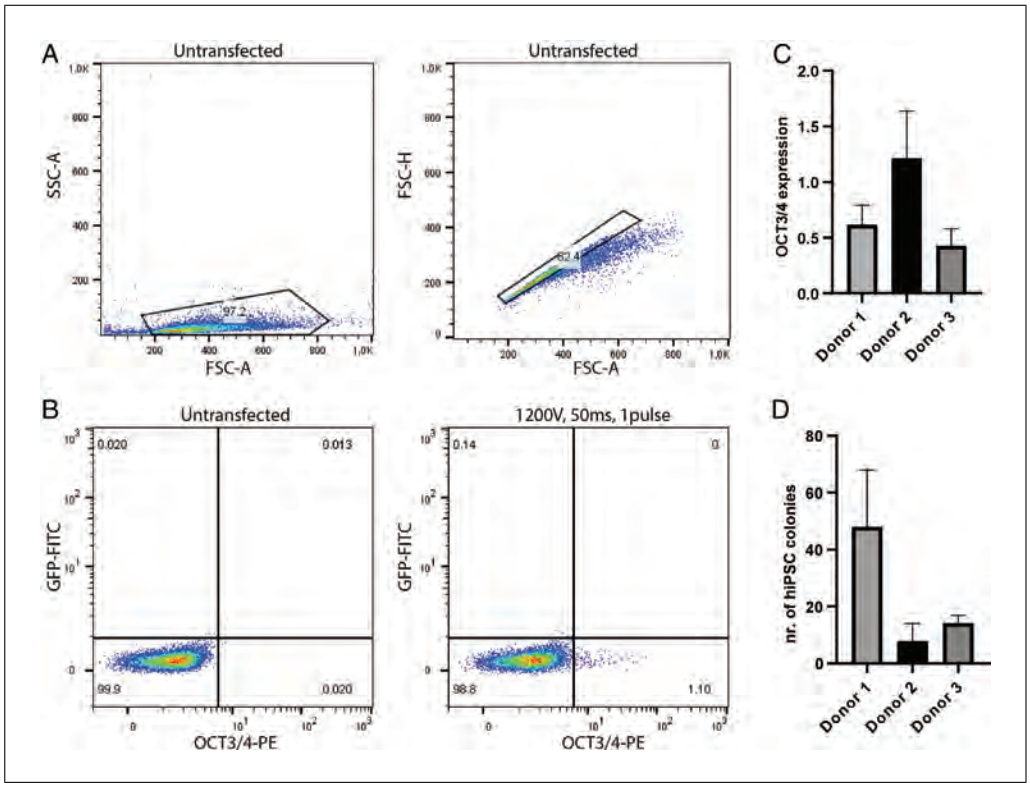

Figure 2 ReproRNA-OKSGM reprogramming of UDCs. (**A**) Flow cytometry gating strategy for live and single cells, respectively to check transfection efficiency. (**B**) Example of transfection efficiency measured by flow cytometry for donor 1. (**C**) OCT3/4 expression measured by flow cytometry for three different donors, 72 hr after transfection (±SD). (**D**) Number of hiPSC colonies at 21 days after transfection for three different donors (±SD) (Donor 1: $n = 7$, donor 2: $n = 3$, donor 3: $n = 2$).

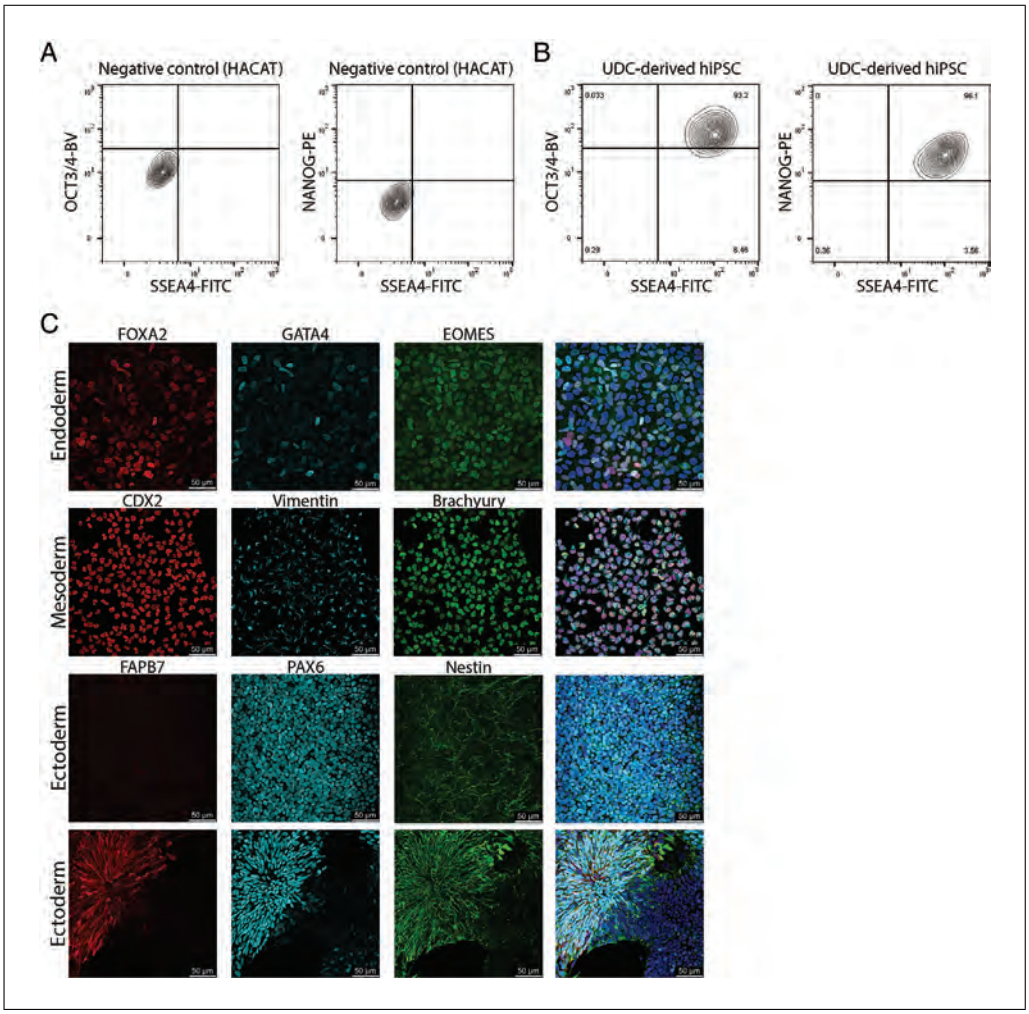

Figure 3 Basic characterization of hiPSC lines. (**A**) Use of an immortalized keratinocyte cell-line (HACAT) as negative control for setting the gates for measuring pluripotency markers. (**B**) Flow cytometry analysis of pluripotency marker expression in UDC-derived hiPSCs. (**C**) Examples of immunofluorescence staining after trilineage differentiation of hiPSC-lines derived from UDCs.

Measuring the pluripotency status of hiPSCs

The pluripotency status of undifferentiated hiPSCs can be determined by flow cytometry, measuring the percentage of cells expressing pluripotency markers OCT3/4, Nanog, and SSEA4. In a maintenance culture with little spontaneous differentiation, the majority of cells are OCT3/4-/Nanog-/SSEA4 triple-positive; in general, 75% is regarded as a threshold for high-quality cells. When cells differentiate they usually first lose the expression of Nanog and OCT3/4, while SSEA4 can remain present for a longer period (Fig. 3A/B).

Characterization of functional pluripotency of hiPSCs

For ecto- and endoderm differentiation, hiPSCs are plated at a density to reach 80%-90% confluency on the next day, while the mesoderm coverslips will be 20%-30% confluent. However, after switching the maintenance medium to differentiation medium, the cells seeded on coverslips for endoderm differentiation may show detaching cells. This only happens on day 1 of the protocol and will not hamper differentiation of the remaining cells. When analyzing the immunofluorescence staining of ectodermal, mesodermal, and endodermal cells we usually obtain the following results: Mesodermal differentiation is homogeneous and most of the cells express Vimentin (cytoplasmic), Brachyury T, and CDX2 (both nuclear). Endoderm differentiation is more heterogeneous with cells expressing a combination of FOXA2, EOMES, and/or GATA4 (all nuclear). The number of positive cells is sometimes lower in comparison with mesodermal differentiation. Ectodermal differentiation is often a mix of 3D structures surrounded by monolayers. Patches of cells expressing PAX6 (nuclear) and Nestin

(cytoplasmic) are commonly found whereas expression of FAPB7 (nuclear and cytoplasmic) is less common. (Fig. 3C)

Time Considerations

Basic Protocol

Steps 1-10: 15 min
Steps 11-17: 20 min
Steps 18-28: 5 min
Step 29-31: ∼21 days
Step 32-43: 1.5 hr

Support Protocol 1

2.5 hr

Support Protocol 2

Steps 1-5: 5 min
Steps 6-10: 7 days
Steps 11-23: 2 days

Literature Cited

Afzal, M. Z., & Strande, J. L. (2015). Generation of induced pluripotent stem cells from muscular dystrophy patients: Efficient integration-free reprogramming of urine derived cells. *Journal of visualized experiments: JoVE*(95), 52032. doi: 10.3791/52032.

Alcami, A., Symons, J. A., & Smith, G. L. (2000). The vaccinia virus soluble alpha/beta interferon (IFN) receptor binds to the cell surface and protects cells from the antiviral effects of IFN. *Journal of Virology*, *74*(23), 11230–11239. doi: 10.1128/jvi.74.23.11230-11239.2000.

Bellin, M., Marchetto, M. C., Gage, F. H., & Mummery, C. L. (2012). Induced pluripotent stem cells: The new patient? *Nature Reviews Molecular Cell Biology*, *13*(11), 713–726. doi: 10.1038/nrm3448.

Bharadwaj, S., Liu, G., Shi, Y., Markert, C., Andersson, K. E., Atala, A., & Zhang, Y. (2011). Characterization of urine-derived stem cells obtained from upper urinary tract for use in cell-based urological tissue engineering. *Tissue Engineering Part A*, *17*(15–16), 2123–2132. doi: 10.1089/ten.TEA.2010.0637.

Bouma, M. J., van Iterson, M., Janssen, B., Mummery, C. L., Salvatori, D. C. F., & Freund, C. (2017). Differentiation-defective human induced pluripotent stem cells reveal strengths and limitations of the teratoma assay and in vitro pluripotency assays. *Stem Cell Reports*, *8*(5), 1340–1353. doi: 10.1016/j.stemcr.2017.03.009.

Colamonici, O. R., Domanski, P., Sweitzer, S. M., Larner, A., & Buller, R. M. (1995). Vaccinia virus B18R gene encodes a type I interferon-binding protein that blocks interferon alpha transmembrane signaling. *Journal of Biological Chemistry*, *270*(27), 15974–15978. doi: 10.1074/jbc.270.27.15974.

Dorrenhaus, A., Muller, J. I., Golka, K., Jedrusik, P., Schulze, H., & Follmann, W. (2000). Cultures of exfoliated epithelial cells from different locations of the human urinary tract and the renal tubular system. *Archives of Toxicology*, *74*(10), 618–626. doi: 10.1007/s002040000173.

Gaignerie, A., Lefort, N., Rousselle, M., Forest-Choquet, V., Flippe, L., Francois-Campion, V., … David, L. (2018). Urine-derived cells provide a readily accessible cell type for feeder-free mRNA reprogramming. *Scientific Reports*, *8*(1), 14363. doi: 10.1038/s41598-018-32645-2.

Hildebrand, L., Rossbach, B., Kuhnen, P., Gossen, M., Kurtz, A., Reinke, P., … Stachelscheid, H. (2016). Generation of integration free induced pluripotent stem cells from fibrodysplasia ossificans progressiva (FOP) patients from urine samples. *Stem Cell Research*, *16*(1), 54–58. doi: 10.1016/j.scr.2015.11.017.

Koyanagi-Aoi, M., Ohnuki, M., Takahashi, K., Okita, K., Noma, H., Sawamura, Y., … Yamanaka, S. (2013). Differentiation-defective phenotypes revealed by large-scale analyses of human pluripotent stem cells. *Proceedings of the National Academy of Sciences*, *110*(51), 20569–20574. doi: 10.1073/pnas.1319061110.

Li, D., Wang, L., Hou, J., Shen, Q., Chen, Q., Wang, X., … Pan, G. (2016). Optimized approaches for generation of integration-free iPSCs from human urine-derived cells with small molecules and autologous feeder. *Stem Cell Reports*, *6*(5), 717–728. doi: 10.1016/j.stemcr.2016.04.001.

Nishimura, K., Sano, M., Ohtaka, M., Furuta, B., Umemura, Y., Nakajima, Y., … Nakanishi, M. (2011). Development of defective and persistent Sendai virus vector: A unique gene delivery/expression system ideal for cell reprogramming. *Journal of Biological Chemistry*, *286*(6), 4760–4771. doi: 10.1074/jbc.M110.183780.

Okita, K., Ichisaka, T., & Yamanaka, S. (2007). Generation of germline-competent induced pluripotent stem cells. *Nature*, *448*(7151), 313–317. doi: 10.1038/nature05934.

Okita, K., Matsumura, Y., Sato, Y., Okada, A., Morizane, A., Okamoto, S., … Yamanaka, S. (2011). A more efficient method to generate integration-free human iPS cells. *Nature Methods*, *8*(5), 409–412. doi: 10.1038/nmeth.1591.

Rahmoune, H., Thompson, P. W., Ward, J. M., Smith, C. D., Hong, G., & Brown, J. (2005). Glucose transporters in human renal proximal tubular cells isolated from the urine of patients with non-insulin-dependent diabetes. *Diabetes*, *54*(12), 3427–3434. doi: 10.2337/diabetes.54.12.3427.

Schlaeger, T. M., Daheron, L., Brickler, T. R., Entwisle, S., Chan, K., Cianci, A., … Daley, G. Q. (2015). A comparison of non-integrating reprogramming methods. *Nature Biotechnology*, *33*(1), 58–63. doi: 10.1038/nbt.3070.

Singh, V. K., Kalsan, M., Kumar, N., Saini, A., & Chandra, R. (2015). Induced pluripotent stem cells: Applications in regenerative medicine, disease modeling, and drug discovery. *Frontiers in Cell and Developmental Biology*, *3*, 2. doi: 10.3389/fcell.2015.00002.

Steichen, C., Si-Tayeb, K., Wulkan, F., Crestani, T., Rosas, G., Dariolli, R., … Krieger, J. E. (2017). Human induced pluripotent stem (hiPS)

cells from urine samples: A non-integrative and feeder-free reprogramming strategy. *Current Protocols in Human Genetics*, *92*, 21.7.1–21.7.22. doi: 10.1002/cphg.26.

Steinle, H., Weber, M., Behring, A., Mau-Holzmann, U., von Ohle, C., Popov, A. F., … Avci-Adali, M. (2019). Reprogramming of urine-derived renal epithelial cells into iPSCs using srRNA and consecutive differentiation into beating cardiomyocytes. *Molecular Therapy - Nucleic Acids*, *17*, 907–921. doi: 10.1016/j.omtn.2019.07.016.

Takahashi, K., Tanabe, K., Ohnuki, M., Narita, M., Ichisaka, T., Tomoda, K., & Yamanaka, S. (2007). Induction of pluripotent stem cells from adult human fibroblasts by defined factors. *Cell*, *131*(5), 861–872. doi: 10.1016/j.cell.2007.11.019.

Wang, L., Chen, Y., Guan, C., Zhao, Z., Li, Q., Yang, J., … Li, J. (2017). Using low-risk factors to generate non-integrated human induced pluripotent stem cells from urine-derived cells. *Stem Cell Research & Therapy*, *8*(1), 245. doi: 10.1186/s13287-017-0698-8.

Warren, L., Manos, P. D., Ahfeldt, T., Loh, Y. H., Li, H., Lau, F., … Rossi, D. J. (2010). Highly efficient reprogramming to pluripotency and directed differentiation of human cells with synthetic modified mRNA. *Cell Stem Cell*, *7*(5), 618–630. doi: 10.1016/j.stem.2010.08.012.

Xue, Y., Cai, X., Wang, L., Liao, B., Zhang, H., Shan, Y., … Pan, G. (2013). Generating a non-integrating human induced pluripotent stem cell bank from urine-derived cells. *Plos One*, *8*(8), e70573. doi: 10.1371/journal.pone.0070573.

Yoshioka, N., & Dowdy, S. F. (2017). Enhanced generation of iPSCs from older adult human cells by a synthetic five-factor self-replicative RNA. *Plos One*, *12*(7), e0182018. doi: 10.1371/journal.pone.0182018.

Yoshioka, N., Gros, E., Li, H. R., Kumar, S., Deacon, D. C., Maron, C., … Dowdy, S. F. (2013). Efficient generation of human iPSCs by a synthetic self-replicative RNA. *Cell Stem Cell*, *13*(2), 246–254. doi: 10.1016/j.stem.2013.06.001.

Zhang, Y., McNeill, E., Tian, H., Soker, S., Andersson, K. E., Yoo, J. J., & Atala, A. (2008). Urine derived cells are a potential source for urological tissue reconstruction. *Journal of Urology*, *180*(5), 2226–2233. doi: 10.1016/j.juro.2008.07.023.

Zhou, T., Benda, C., Dunzinger, S., Huang, Y., Ho, J. C., Yang, J., … Esteban, M. A. (2012). Generation of human induced pluripotent stem cells from urine samples. *Nature Protocols*, *7*(12), 2080–2089. doi: 10.1038/nprot.2012.115.

Zhou, T., Benda, C., Duzinger, S., Huang, Y., Li, X., Li, Y., … Esteban, M. A. (2011). Generation of induced pluripotent stem cells from urine. *Journal of the American Society of Nephrology*, *22*(7), 1221–1228. doi: 10.1681/ASN.2011010106.

Methods for Automated Single Cell Isolation and Sub-Cloning of Human Pluripotent Stem Cells

Valeria Fernandez Vallone,[1,2,6] Narasimha Swamy Telugu,[3,4,6] Iris Fischer,[1,2] Duncan Miller,[3,4,5] Sandra Schommer,[3,4] Sebastian Diecke,[3,4,5,7] and Harald Stachelscheid[1,2,7]

[1]Charité—Universitätsmedizin Berlin, Berlin, Germany
[2]Berlin Institute of Health (BIH), BIH Stem Cell Core Facility, Berlin, Germany
[3]Max Delbrück Center for Molecular Medicine in the Helmholtz Association (MDC), Berlin, Germany
[4]BIH Stem Cell Core Facility, Berlin Institute of Health (BIH), Berlin, Germany
[5]DZHK (German Centre for Cardiovascular Research), partner site Berlin, Berlin, Germany
[6]These authors contributed equally to this work
[7]Corresponding authors: *Sebastian.Diecke@mdc-berlin.de*; *Harald.Stachelscheid@charite.de*

Advances in human pluripotent stem cell (hPSC) techniques have led them to become a widely used and powerful tool for a vast array of applications, including disease modeling, developmental studies, drug discovery and testing, and emerging cell-based therapies. hPSC workflows that require clonal expansion from single cells, such as CRISPR/Cas9-mediated genome editing, face major challenges in terms of efficiency, cost, and precision. Classical sub-cloning approaches depend on limiting dilution and manual colony picking, which are both time-consuming and labor-intensive, and lack a real proof of clonality. Here we describe the application of three different automated cell isolation and dispensing devices that can enhance the single-cell cloning process for hPSCs. In combination with optimized cell culture conditions, these devices offer an attractive alternative compared to manual methods. We explore various aspects of each device system and define protocols for their practical application. Following the workflow described here, single cell−derived hPSC sub-clones from each system maintain pluripotency and genetic stability. Furthermore, the workflows can be applied to uncover karyotypic mosaicism prevalent in bulk hPSC cultures. Our robust automated workflow facilitates high-throughput hPSC clonal selection and expansion, urgently needed in the operational pipelines of hPSC applications. © 2020 The Authors.

Basic Protocol: Efficient automated hPSC single cell seeding and clonal expansion using the iotaSciences IsoCell platform
Alternate Protocol 1: hPSC single cell seeding and clonal expansion using the Cellenion CellenONE single-cell dispenser
Alternate Protocol 2: hPSC single cell seeding and clonal expansion using the Cytena single-cell dispenser
Support Protocol 1: Coating cell culture plates with Geltrex
Support Protocol 2: hPSC maintenance in defined feeder-free conditions
Support Protocol 3: hPSC passaging in clumps
Support Protocol 4: Laminin 521 coating of IsoCell plates and 96-well/384-well plates
Support Protocol 5: Preparation of medium containing anti-apoptotic small molecules
Support Protocol 6: 96- and 384-well target plate preparation prior to single cell seeding

CURRENT PROTOCOLS
A Wiley Brand

Current Protocols in Stem Cell Biology e123, Volume 55
Published in Wiley Online Library (wileyonlinelibrary.com).
doi: 10.1002/cpsc.123

Support Protocol 7: Single cell dissociation of hPSCs
Support Protocol 8: IsoCell-, CellenONE-, and Cytena-derived hPSC clone subculture and expansion

Keywords: automation • hPSC • karyotyping • single cell isolation • sub-cloning

How to cite this article:
Vallone, V. F., Telugu, N. S., Fischer, I., Miller, D., Schommer, S., Diecke, S., & Stachelscheid, H. (2020). Methods for automated single cell isolation and sub-cloning of human pluripotent stem cells. *Current Protocols in Stem Cell Biology*, *55,* e123. doi: 10.1002/cpsc.123

INTRODUCTION

The combination of human induced pluripotent stem cell (hiPSC) reprogramming and CRISPR/Cas9 technology has generated new perspectives in the field of stem cell research that span developmental biology up to translational and therapeutic applications (Rossant & Tam, 2017; Wu & Izpisua Belmonte, 2015; Yamanaka, 2012). CRISPR/Cas9-based gene editing has made it possible to accurately correct or introduce disease-associated mutations in human pluripotent stem cells (hPSCs) to generate isogenic control/disease lines, overcoming the problem of genetic variability between individual hPSC lines. Similarly, transgenic hPSCs containing reporters or expression cassettes knocked into endogenous or safe harbor loci allow cell tracing experiments, functional studies, or gene induction (Doudna & Charpentier, 2014; Hsu, Lander, & Zhang, 2014). Although the combination of hPSC and CRISPR/Cas9 technologies is revolutionizing disease modeling and regenerative medicine, progress is hampered by the lack of standardization, low-throughput processes, and insufficient robustness.

One of the biggest challenges in the genome editing process for hPSCs is the isolation of single cells and derivation of clonal cell populations with the desired genetic modifications. This single-cell cloning bottleneck occurs because hPSCs are sensitive to environmental changes like pH, osmolarity and nutrient supply, mechanical stress/shear forces, and, most importantly, loss of cell-cell and cell-extracellular matrix (ECM) contact. In conventional 2D culture conditions, hPSC typically grow in densely packed colonies on surfaces coated with various ECM components. If these cell-cell and cell-ECM contacts are disturbed, an apoptotic program, known as anoikis, is induced, which causes a significant decrease in single cell survival rate (Chen, Hou, Gulbranson, & Thomson, 2010). A single cell isolation process combined with survival and proliferation enhancement using small molecules and optimized culture conditions is critical for the successful selection and expansion of genome-edited hPSCs. Approaches such as manual picking of single outgrown colonies and/or limiting dilution are not optimal, as they are labor-intensive and inefficient. In addition, these methods do not prove with certainty a successful single cell clonal outgrowth event following the isolation process. Moreover, gene editing protocols usually expose stem cells to harsh conditions that further lead to poor survival (e.g., electroporation); therefore, a gentle single cell isolation and dispensing technique would increase cloning efficiencies. Another challenge to overcome is the length of the process—a typical gene editing workflow takes 2 to 4 months, and a major part of the time is spent on hPSC sub-clone isolation, genotyping, selection, and expansion. Therefore, automated systems that offer quicker and more precise isolation of hPSCs with increased

single cell survival would be highly desirable for research and commercial applications. A variety of devices for single cell dispensing have been developed and are currently commercially available.

The authors of this article have tested three platforms with different working principles that can be applied within a complete hPSC sub-cloning workflow, including isolation, clonal expansion, and further characterization. The Basic Protocol that we describe here is coupled to the iotaScience IsoCell platform, a small-footprint device that enables miniaturization and therefore cost reduction (*https://www.iotasciences.com/*). We provide, in alternate protocols, two additional platforms: the CellenONE X1/F1 (*https://www.cellenion.com/*; see Alternate Protocol 1) and the Cytena c.sight/f.sight (*https://www.cytena.com/*; see Alternate Protocol 2) single cell dispensers. All three platforms have been developed to ensure high cell viability and low rates of contamination, and to increase the confidence of monoclonal efficiency. We describe the relevant cell culture methods and specific device protocols that enable robust and efficient automated sub-cloning of hPSCs for a variety of applications. Finally, we provide example data and highlight karyotypic stability and maintained pluripotency to validate the workflow for each device system.

STRATEGIC PLANNING

The methods described below have been selected and structured in order to ensure an easy workflow focusing on four critical steps (1) hPSC culture quality requirements as starting point, (2) preparation procedures before single cell seeding, (3) automated single cell seeding, and (4) culture and expansion of derived clones (Fig. 1).

Good practices to ensure a high-quality hPSC culture are described in Support Protocols 1, 2, and 3. A description of recommended culture characteristics can be found in Critical Parameters. Procedures such as target plate preparation and derivation of a single cell suspension prior to single cell seeding are described in Support Protocols 4, 5, 6, and 7. Automated single cell seeding is the central part of the workflow and is described for three alternate platforms in Basic Protocol 1 (IsoCell) and Alternate Protocols 1 and 2 (CellenONE and Cytena, respectively). Finally, a protocol for the expansion of the clones following the isolation process is provided in Support Protocol 8 (Fig. 1).

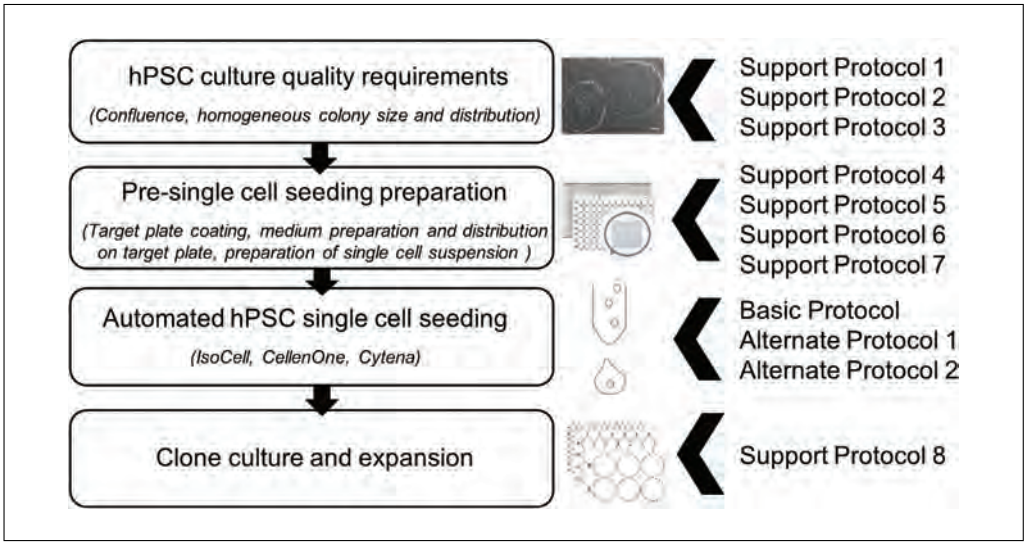

Figure 1 Strategic planning. Overview of the main working blocks and the related protocols to perform hPSC single cell isolation and sub-cloning. The picture next to the first block shows the desired morphology and confluence (70%-80%) that the hPSC cultures should have as starting material. Scale bar: 200 µm.

EFFICIENT AUTOMATED hPSC SINGLE CELL SEEDING AND CLONAL EXPANSION USING THE IotaSciences IsoCell PLATFORM

The IsoCell platform aims to automate single cell seeding and clonal expansion while decreasing hands-on time and scaling the procedure down to a minimal use of consumables and resources. The miniature workflow is based on the formation of a grid between two immiscible fluids. The grid contains chambers that enable cell culture in less than 1 μl of volume. The IsoCell exploits the principle of a fluid-shaping technology (Soitu et al., 2018, 2020; Walsh et al., 2017). Briefly, the IsoCell creates small-scale cell culture chambers on (optionally coated) polystyrene dishes using an aqueous phase (cell medium or substrate coating) and an immiscible liquid overlay (the fluorocarbon oil FC40^{STAR}). This results in an array of 256 cell culture reservoirs that are completely separated from each other by the immiscible FC40^{STAR}. The device applies a technology developed by Walsh and colleagues whereby grids are formed on top of a protein-coated surface of a cell culture dish, in a liquid phase overlaid with FC40^{STAR} (Soitu et al., 2018). The integrated liquid-handling system automates cell isolation, feeding, and harvesting. Single cell seeding follows a Poisson distribution, limiting the number of single-cell chambers to 94 per grid (256 chambers). In-chamber verification of single cells is performed on a standard bright-field microscope using a 40× or 100× magnification. The contents of the chambers are stable, do not mix, and can be manipulated without extra care. The FC40^{STAR} layer on top of the chambers does not mix with the aqueous phase of the culture medium, allows gas exchange, prevents evaporation of such small volumes, and remains in place for the entire cloning workflow.

This protocol describes a workflow in which the IsoCell platform is applied to enable robust, efficient, cost-effective, and easy-to-handle hPSC clone isolation and expansion (Fig. 2A).

NOTE: Special training on how to operate the instrument is recommended. Here we give an overview, but full details are beyond the scope of this protocol. Please contact the manufacturer for further information.

Materials

FC40^{STAR} (Iota Sciences, cat. no. SKU10040)
Dulbecco's phosphate-buffered saline without Ca^{2+} and Mg^{2+} (DPBS; e.g., ThermoFisher Scientific, cat. no. 10010023)
70% ethanol (e.g., Carl Roth, cat. no. T913.3)
hPSC culture (see relevant Current Protocols articles)
StemFlex medium (ThermoFisher Scientific, cat. no. A3349401)
CloneR (Stem Cell Technologies, cat. no. 05888; see Support Protocol 5 for use in medium preparation)
Cell culture−grade water (e.g., Corning, cat. no. 25-055-CM)
TrypLE Select Enzyme (ThermoFisher Scientific, cat. no. 12563011)
Essential 8 medium (ThermoFisher Scientific., cat. no. A1517001) or mTeSR (Stem Cell Technologies, cat. no. 85850)

Laminar flow hood (e.g., Herasafe, ThermoFisher Scientific)
IsoCell device (Iota Sciences)
1.5-ml microcentrifuge tubes (e.g., Eppendorf, cat. no. 30120086)
Clone G kit-A—with tissue-culture treated 6-cm dishes (Iota Sciences, cat. no. SKU 10030)
P1000 repeat pipettor
200- and 1000-μl pipette tips (e.g., Eppendorf, cat. no. 3123000055 and 3123000063)
200- and 1250-μl pipette tips (e.g., Biozyme, cat. no. 770200 and 770600)
5- and 10-ml serological pipettes (e.g., Corning, cat. no. 357543 and 357551)

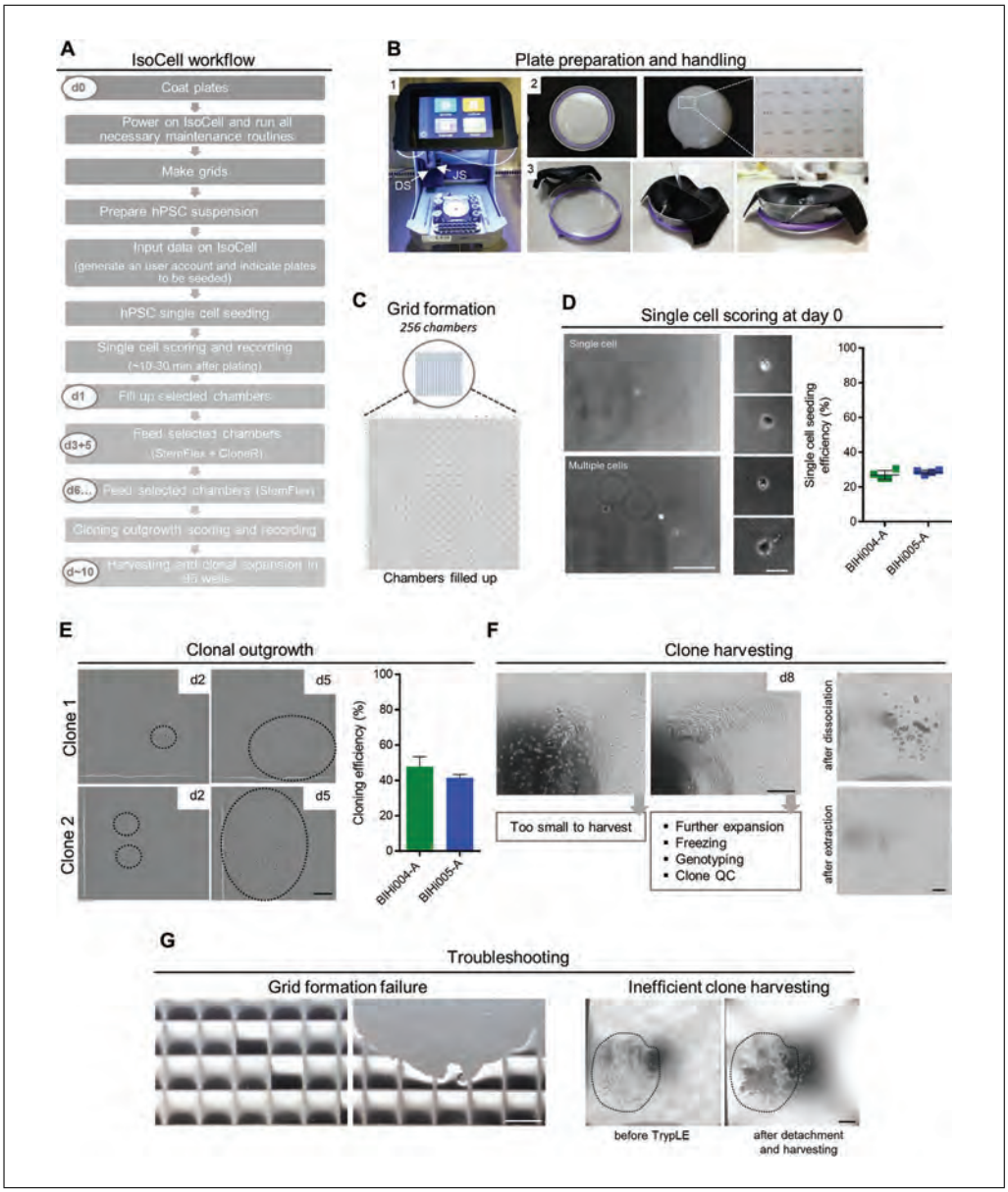

Figure 2 Basic Protocol: IsoCell hPSC single cell isolation and clonal expansion. (**A**) Step-by-step flowchart showing automated hPSC single cell seeding and clone expansion using the IsoCell platform. Time points are defined in days (d) or minutes (min). (**B**) (1) IsoCell device, arrows point to the needles from the dispensing (DS) and the jetting system (JS); (2) adaptor for microscopy counting with chamber coordinates; and (3) pipetting aid for achieving very gentle FC40^{STAR} filling of the plate. (**C**) Scheme of a 256-chamber grid generated in a 60-mm coated culture dish (upper part) and representative picture from a grid after selected chambers were filled up with medium (lower part). (**D**) Representative pictures showing chambers with single or multiple cells to be scored at day 0 (scale bar: 200 µm). On the right, different single cell morphologies that can be seen within 30 min after plating (scale bar: 50 µm). The graph shows single cell seeding efficiencies (mean $\pm$ SD, n $=$ 4) for two different hiPSC lines. (**E**) Representative pictures of clone outgrowth at day 2 and 5 for two hiPSC clones (scale bar: 200 µm). Cloning efficiency (right) is calculated as relative to the number of chambers with single cells at day 0 (mean $\pm$ SD, n $=$ 4). (**F**) Pictures showing examples for colony size in chambers at day 8 (left) and chambers after enzymatic dissociation and extraction (scale bars: 200 µm). (**G**) Troubleshooting: an example of grid formation failure is depicted on the left (scale bar $=$ 2 mm). Inefficient harvesting due to short enzymatic treatment is shown on the right (scale bar: 200 µm). Cell3imager Duos was used for pictures in panel C, a Leica DMi8 microscope with phase contrast was used for pictures in panels D, E, F, and G, and an Olympus SZX16 stereomicroscope was used for grid pictures in panel G.

Inverted microscope with phase-contrast optics, 4×, 10×, and 20× objectives (e.g., DMi8, Leica)
Cell culture incubator (e.g., Binder)
Geltrex-coated 96-well tissue-culture plates (prepared as described in Support Protocol 1)

Additional reagents and equipment for laminin coating of dishes (Support Protocol 4), preparing single cell suspension of hPSCs (Support Protocol 7), preparation of medium containing anti-apoptotic small molecules (Support Protocol 5), and subculture and expansion of hPSC clones (Support Protocol 8)

Grid preparation and single cell seeding (day 0)

Initialize IsoCell device

1. Check FC40^{STAR} level in the reserve bottle on the back of the device.

   FC40^{STAR} level of the reservoir can be manually adjusted from the main display of the instrument ("more" > "FC40^{STAR} levels"). The instrument will then estimate the amount of FC40^{STAR} remaining for further operations and give an alert when the level may be too low. FC40^{STAR} bottle level is an estimation; therefore, it is important to verify it before starting any process.

2. Power on the IsoCell device.
3. Run the start-up routine by following the wizard on the display. 1.5-ml tubes containing sterile water, 70% ethanol, DPBS, and StemFlex medium must be prepared in advance and placed in the corresponding spots in the IsoCell tube rack.
4. If necessary, replace the dispenser needle: from the menu choose "more" > "replace dispenser," then follow the instructions (Fig. 2B).

   The dispenser needle must be changed at least every time a new Clone G kit-A is used.

5. Switch the heater on: from the menu choose "Settings" > "Options" > "heater on."

Prepare grid using FC40^{STAR}

6. Coat the necessary number of 6-cm culture dishes provided in the Clone G kit-A with laminin 521 as described in Support Protocol 4.
7. Carefully remove the coating solution from the 6-cm dish using a P1000 repeat pipettor with a 1000-µl pipette tip.
8. Very carefully add 1 ml of StemFlex medium by placing the pipette at the side wall of the dish and releasing the medium very slowly.
9. Remove the washing medium using the P1000 repeat pipettor with a 1000-µl tip.
10. Repeat step 3, avoiding any bubble formation, and incubate at room temperature for 5-10 min.
11. Remove the StemFlex medium from the dish carefully using the P1000 repeat pipettor with a 1000-µl tip.
12. Place the pipetting aid accessory on top of the culture dish and dispense 2 ml FC40^{STAR} into the center (Fig. 2B).

    This procedure ensures that FC40^{STAR} covers the surface of the dish slowly and without bubble formation. The procedure can be performed without the pipetting aid accessory using a P1000 pipet and slowly pipetting FC40^{STAR} against the side walls of the dish.

13. Proceed immediately to grid preparation on the IsoCell instrument: from the menu choose "isolate" > "Grid," then follow the wizard. A grid with 256 chambers can be seen on the dish (Fig. 2B and C).

    Prepared grids should be used within the same day on which they are generated.

Single cell seeding and scoring

14. Prepare an hPSC single cell suspension by following Support Protocol 7.

15. Re-suspend hPSCs in StemFlex supplemented with CloneR (preparation described in Support Protocol 5, i.e., 1:20 dilution) with a concentration of 10,000 cells/ml.

    The concentration of the cell suspension can be adjusted within a range of 5-10000 cells/ml to achieve optimal numbers of single-cell chambers; see Troubleshooting.

16. Place 0.5-1 ml of cell the suspension in a 1.5-ml tube, resuspend, and place the tube in the IsoCell rack in position that is depicted by the wizard.

    Immediately start the single cell dispensing to avoid cell sedimentation!

17. Perform single cell seeding with the IsoCell device: from the menu choose "Isolate," and follow the instructions.

    The IsoCell device will proceed with deposition of ~200 nl cell suspension per microchamber

18. *Scoring*: Immediately or at least within 10-20 min after seeding, visually identify and record chambers containing single cells using an inverted microscope (10× objective recommended) and the microscope plate adapter provided by Iota Sciences (Fig. 2B and D).

    Adjusting the focal plane up and down allows identification of the chamber or the coordinate of the chamber printed on the plate adapter. The focal plane of the chamber walls is roughly the same as that of the cells.

    It is important to quantify single cell chambers within 30 min of dispensing, when cells are not fully attached and have a round shape and the cell borders appear bright due to their refraction. 30 min to 1 hr after dispensing, mitotic events can occur and become false negative as duplets.

    The GRID is limited to around 94 single-cell chambers out of 256 due to Poisson distribution. With the protocol described here, ~60-80 chambers containing a single cell were achieved. Variations can occur depending on the cell preparation, counting method, and the experience of the operator (Fig. 2D).

19. Place the dish in the incubator at 37°C in a humidified environment, preferably under hypoxic conditions (5% O_2, 5% CO_2) for 24 hr.

    hPSC cultures are preferably maintained in hypoxic conditions to avoid spontaneous differentiation.

20. *Data input in IsoCell (single cell containing-well coordinates)*: First, create the experiment: from the menu choose "More" > "add dish" (name the experiment). Second, register the chambers containing a single cell: from the menu choose "Isolate" > "input data," then select coordinates and save. This allows the IsoCell to automate feeding and harvesting of only the relevant chambers during the subsequent workflow.

21. Shut down the IsoCell device by following the device wizard for shut-down routine.

Clonal culture maintenance in IsoCell chambers (d1 to ~d10)

22. Initialize IsoCell instrument as described in step 1.

23. On day 1 after single cell seeding, perform the fill up routine for the wells registered with a single cell. Follow the wizard: "Culture" > "Fill," then select the dish. Use StemFlex medium supplemented with CloneR.

    This procedure will add 600 nl of medium to each chamber containing a single cell that has been plated in 200 nl of medium. The resulting volume in one chamber is about

800 nl (Fig. 2C). Evaporation of the medium is prevented due to the FC40^{STAR} layer on top.

24. On day 3 and day 5, perform medium change, only in the preselected single-cell containing chambers, with StemFlex supplemented with CloneR following the "Culture" > "Feed" program and the wizard instructions (Fig. 2E)

    Cloning efficiency scoring (number of wells with outgrowth relative to number initially containing a single cell) can be performed at day 5 or later, and is an important quality control for the procedure (Fig. 2E).

25. From day 6 to day ~10, perform daily medium change with StemFlex medium without CloneR as explained in step 24.

    On day 7, cell death can be seen due to the CloneR removal; after that, colonies will re-shape to a more compact morphology with more defined borders, which helps the investigator select well-established cultures for further replating (Fig. 2F).

26. Regularly monitor clone growth and confluence in order to decide the time point for further expansion.

    The cloning efficiency is dependent on the specific hPSC line used. This has to be considered in order to estimate the number of dishes to be plated to isolate a sufficient number of clones.

27. Shut down the IsoCell device by following the device wizard for shut-down routine.

Clone harvesting and transfer to 96-well plate using the IsoCell (after day 10)

Clones with 50%-70% confluency can be re-plated for further expansion and downstream application (genotyping, freezing, etc.; Fig. 2F). The time point of adequate confluence may vary between clones, and is highly dependent on the hPSC line.

28. Prepare in advance 0.2-ml tube strips (provided in the Clone G kit-A) with 120 µl StemFlex medium supplemented with CloneR and five 1.5-ml tubes containing: water, 70% ethanol, DPBS, TrypLE, and StemFlex medium supplemented with CloneR.

29. Prepare a 96-well plate coated with Geltrex as described in Support Protocol 1

30. Remove coating solution from the 96-well plate and add 100 µl StemFlex medium supplemented with CloneR. Place in the incubator at 37°C until use.

31. Select the clones to be re-plated by groups of 8 or 16.

    Up to 16 clones can be detached and harvested per round according to the IsoCell program.

32. Initialize IsoCell device as described in step 1.

33. Cell harvesting should proceed following the wizard: "Harvest" > "Detach," then choose chambers.

    At this point is important to verify cell detachment by microscopy. Poor detachment results in expansion failure. Some hPSC clones may need longer enzymatic incubation (program can be paused) (Fig. 2F).

34. Proceed to "Harvest" > "Extract." IsoCell will collect each detached clone in a 0.2-ml tube already containing 150 µl of StemFlex medium supplemented with CloneR.

    This program can be run for up to 16 samples at the time.

35. Resuspend and manually transfer each cell suspension from step 34 to one well of a 96-well plate using a pipette.

36. Incubate the 96-well plate at 37°C in a humidified environment, preferably in hypoxic conditions (5% O_2, 5% CO_2).

37. Power off IsoCell device according to the shutdown instructions.

38. At day 1 after re-plating, monitor cell attachment.

39. At day 2 after re-plating, perform a 50% medium change with Essential 8 or mTeSR medium.

    If there are only a few cells that are scattered throughout a well, change 50% medium with StemFlex supplemented CloneR daily until they recover.

After adapting the clones to Essential 8 or mTeSR medium (according to the original maintenance/expansion medium), clones may be subjected to further expansion as described in Support Protocol 8. For cell freezing, DNA collection for genotyping etc. standard procedures should be followed that are described elsewhere.

hPSC SINGLE CELL SEEDING AND CLONAL EXPANSION USING THE CELLENION CellenONE SINGLE-CELL DISPENSER

ALTERNATE PROTOCOL 1

The CellenONE instrument utilizes image-based cell detection and acoustic dispensing technology. The equipment performs automated image acquisition combined with fast processing using advanced algorithms in order to identify the cells of interest. Bright-field morphological parameters (diameter, circularity, and elongation) can be combined with up to four fluorescence signals to select specific cells for subsequent isolation. Therefore, application of live/dead dyes, fluorescently labeled antibodies, and fluorescence reporters enables the selection of specific cell subpopulations.

Single cell isolation is performed by drop-on-demand technology. Nanoliter drops are generated by piezo-acoustic technology, which ensures gentle cell isolation (*https://www.cellenion.com/*). Only single cell−containing drops are dispensed in each well of a target plate. Cells can be dispensed in a wide variety of target vessels, including any type of multi-well plate, e.g., 96- or 384-well plates. Empty drops or drops containing multiple cells are collected in a recycling tube for further use.

All acquired images and parameters of the isolated events are recorded by the software, and a final report with statistics can be automatically generated at the end of the process. Therefore, all information about the contents and corresponding parameters of each single well of the target plate is available.

In this alternate protocol, we provide a basic step-by-step procedure including all considerations, parameters, and important variables adapted to hPSC single cell isolation and posterior clonal expansion using CellenONE X1/F1 platform (Fig. 3).

NOTE: Special training on how to operate the instrument is recommended. Here we give an overview, but full details are beyond the scope of this protocol. Please contact the manufacturer for further information.

Materials

sciCLEAN8 (Scienion, cat. no. C-5283)
Bleach solution containing active Cl (e.g., Miltenyi, 130-093-663)
70% ethanol (e.g., Carl Roth, cat. no. T913.3)
Hydrogen peroxide (e.g., Carl Roth, cat. no. 8070.1)
hPSC suspension (see relevant Current Protocols articles)
StemFlex medium (ThermoFisher Scientific, cat. no. A3349401)
Y-27632 (Stem Cell Technologies, cat. no. 72305; see Support Protocol 5 for use in medium preparation)

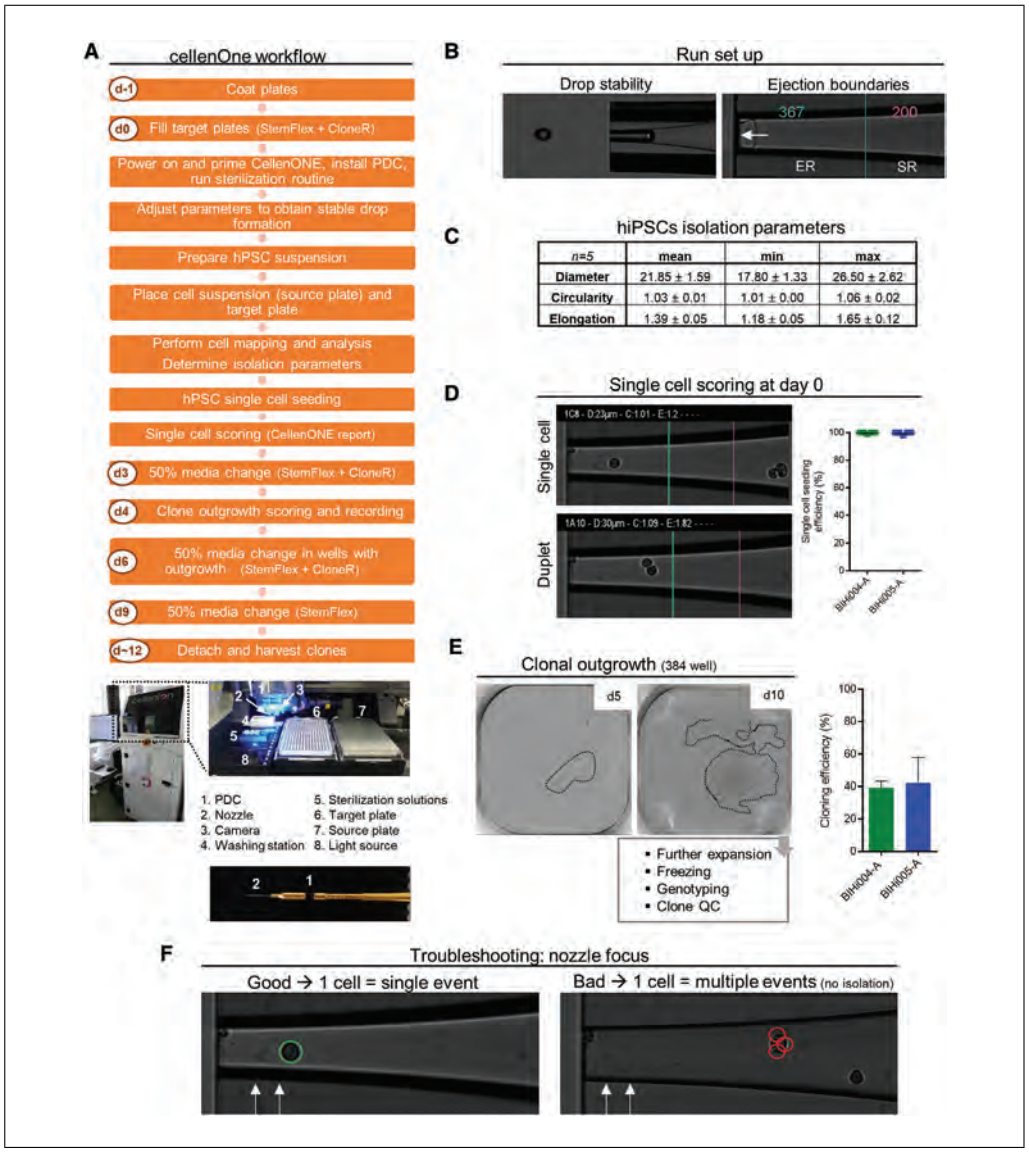

Figure 3 Alternate Protocol 1: CellenONE hPSC single cell isolation and clonal expansion. (**A**) Overview flowchart showing automated hPSC single cell seeding using CellenONE instrument. The instrument and its details are depicted in the lower part. (**B**) left: Representative picture showing a stable drop (no satellite drops or deviations should be visible); right: setting of the ejection boundaries delimiting the ejection and sedimentation regions (ER and SR, respectively), arrow shows the direction of drop ejection. (**C**) Table showing recommended isolation parameters for hPSC dispensing, obtained from the analysis of five independent experiments (**D**) Left: exemplary pictures from CelleONE dispensing report—a single cell event can be evaluated by review of the recorded images. Area between green and pink lines is the so called "safe space"; no element should be present within these boundaries, to ensure single cell isolation. Right: graph showing single cell seeding efficiency for two hiPSC lines using CellenONE (mean ± SD, n = 5). (**E**) Left: representative pictures showing clonal expansion in culture; dotted lines delimit the borders of the colonies (scale bars: 400 µm). Right: graph showing cloning efficiencies for two hiPSC lines (mean ± SD, n = 5). (**F**) Troubleshooting: panel showing the importance of the correct nozzle focus (pointed with white arrows) to guarantee correct isolation and high recovery rate. Cell3imager Duos was used for pictures in panel F. PDC = Piezo Dispense Capillary.

Propidium iodide, 1.0 mg/ml solution in water (ThermoFisher Scientific, cat. no. P3566)

Laminar flow hood (e.g., Herasafe, ThermoFisher Scientific)
CellenONE F1.1 (1 channel: green) or F1.4 (4 channels: blue, green, orange, red)
Piezo Dispense Capillary (PDC; Cellenion, P-20-CM)

384-well sciSOURCE plate (Scienion, CPG-5501-1)
Serological pipettes, 5 and 10 ml (e.g., Corning, cat. no. 357543 and 357551)
Repeat pipettors, 200 and 1000 µl (e.g., Eppendorf, cat. no. 3123000055 and 3123000063)
Pipette tips, 200 and 1250 µl (e.g., Biozyme, cat. no. 770600)
Cell culture incubator (e.g., Binder)

Additional reagents and equipment for preparing target plates (Support Protocols 4 and 6), preparing single cell suspension of hPSCs (Support Protocol 7), preparation of medium containing anti-apoptotic small molecules (Support Protocol 5), and subculture and expansion of hPSC clones (Support Protocol 8)

CellenONE setup (day 0)

This protocol does not include full details for the handling of the device software or hardware. This protocol describes all steps relating specifically to hPSC single cell isolation (Fig. 3A).

1. Power on the instrument and follow the initial routine: filter and de-gas fresh autoclaved water and place it on the system bottle; re-fresh water for the washing procedure; empty waste; check water in the humidification system as well as the chiller.
2. Start the CellenONE software and follow the "prime" instructions.
3. Install the piezo dispenser capillary (PDC) according to the wizard (Fig. 3A).
4. Align the nozzle and correct the offset as recommended by the manufacturer.
5. Adjust pulse and voltage until a stable drop is achieved (Fig. 3B). Verify drop volume.

   Drop instability can be detected by drop deviation or presence of satellite drops.
6. Perform a Sci-Clean task.

   This task ensures that the nozzle is perfectly clean and helps to stabilize the drop. In this step, a diluted detergent and sonication are applied.
7. Perform a sterilization routine.

   This routine includes a serial clean in bleach solution, ethanol, and H_2O_2 to decontaminate the PDC.
8. Check drop stability.

   A stable drop is shown in Figure 3B. A deviation in the drop trajectory or appearance of satellite drops are signs of drop instability. Drop stability should always be validated before and after performing a dispensing task.
9. Set target plate platform at 4°C for the whole process.

   Setting temperature at 4°C ensures higher cell viability.
10. Set chamber humidity greater than 15%.
11. Open the sciSOURCE 384-well plate in a laminar flow hood, seal it with aluminum foil, and place it on the CellenONE source stage (Fig. 3A).
12. If drop is stable, the following steps can be performed.

Single cell isolation (day 0)

13. Prepare the target plates as described in Support Protocols 4 and 6.
14. Prepare hPSC cell suspension as described in Support Protocol 7.

15. Resuspend hPSCs in StemFlex medium supplemented with Y-27632 (preparation described in Support Protocol 5) at a concentration of 200 cells/µl.

    The cell suspension for spotting MUST be prepared with Y-27632 since CloneR is too viscous and generates a film at the end of the nozzle, which makes the drop unstable and therefore not suitable for isolation. In the event that StemFlex medium supplemented with Y-27632 also generates a film, DPBS containing Y-27632 can be used with similar results regarding cell survival.

16. If required, add propidium iodide (final concentration 2 µg/ml) for sorting viable cells by fluorescence discrimination.

17. Transfer 30 µl of cell suspension into one well of the SciSOURCE plate and register the well coordinates of the well in the software.

18. Place the target plate in the corresponding position (Fig. 3A).

    Do NOT forget to remove the lid of the target plate before the isolation procedure starts; not doing so will damage the PDC.

19. Take up 10 µl of hPSC suspension with the PDC and check drop stability.

20. Enter CellenONE (cell isolation) mode.

21. Create a folder for the set of experiments and name the run.

22. Choose continuous dispensing in transmission mode (T) until cells can be seen in the capillary.

23. Change to manual dispensing mode and dispense drops. When no cells are in the observed area, record a background image.

24. Perform a "mapping"; adjust ejection boundaries and save the selection (green and pink line shown in Fig. 3D).

25. Perform "analysis" on 100 events with wide detection parameters (default).

26. Create a gate that includes cells with the desired morphological parameters to ensure single cell isolation, and save the selection.

    Recommended morphological parameters for hPSC isolation are depicted in Figure 3C.

27. If additional fluorescence parameters are to be used for sorting, switch to Transmission>Fluorescence (T > F) mode.

28. Turn on desired channels (blue, green, orange, and/or red) and adjust power for a maximum fluorescence intensity 120.

29. Perform a background subtraction when no cells are in the field of view of the camera.

    If the background signal is high due to some artifact in the capillary, perform a washing task and a manual PDC cleaning with lint-free wipes (e.g., Kimwipes) and 70% ethanol.

30. Perform "analysis" in T > F mode using already selected morphological parameters, and adjust the fluorescence gate for the sorting.

    For propidium iodide staining, a negative gate must be selected for viable cells.

31. By continuously dispensing, verify that single cells with desired parameters are being positively selected (green ring around them), and that aggregates or duplets are shown in red (Fig. 3D).

    If too many events fit the parameters but are aborted (yellow ring around the event), try diluting the sample.

32. Once all is set, select standby mode to avoid clogging of the nozzle by cells that have sedimented.

    Standby mode ejects picoliter drops in a continuous fashion.

33. Select the target plate and the positions to be spotted.

34. Check drop stability.

35. Start the run.

    If the cell suspension is adequate and the desired events frequent enough (high recovery rate), dispensing will take about 3-4 min for a complete 384-well plate.

36. When the run is finished, cover the target plate with the lid and place it in the incubator at 37°C in a humidified environment, preferably under hypoxic conditions (5% O_2, 5% CO_2).

37. Export data folders to be analyzed with the CellenONE report software.

38. Flush the PDC, perform a nozzle wash-removal task, and shut down the CellenONE instrument according to the manufacturer recommendations.

Single cell scoring and quality check

39. Obtain the PDF document name as CellenONE report using the data folders exported in step 37.

    Multiple parameters from the run can be revised and validated using this report. Statistical results can be compared between individual dispensing runs.

40. Review the nozzle images for each event isolated and validate the single cell isolation.

    Percentage of validated single cell events relative to the total spotted events is considered to be the single cell seeding efficiency score (Fig. 3D). This score can be used to calculate cloning efficiency as a quality control parameter for an experiment.

Clone culture maintenance (day 1 to ∼10)

41. On day 3 after seeding, perform a partial medium change with StemFlex medium supplemented with CloneR. In a well of a 96-well plate, remove 40 µl and add 50 µl per well; in the wells of a 384-well plate, remove 20 µl and add 30 µl.

    More medium is added than removed to compensate for medium evaporation, which is especially prevalent in the outer wells of the cell culture plates. A full medium change (100 and 50 µl, respectively) has also been tested and gives similar results.

42. On day 4, monitor clone outgrowth and score wells with a positive outcome (Fig. 3F).

    Cloning efficiency can be calculated as a proportion of wells with outgrowth in relation to the total number of wells containing a single cell directly after dispensing at day 0.

43. On day 6, repeat the partial medium change described step 41 only on wells with cell growth.

    This minimizes the use of reagents and requires less time.

44. On day 9, perform a partial medium change using StemFlex medium without CloneR.

45. From day 10 onwards, perform a full medium change daily with StemFlex medium until the clones are ready to be passaged (70% confluent).

46. Follow Support Protocol 8, describing further clonal expansion for later applications such as freezing, genotyping, and expansion for cell banking.

Standard protocols for such applications can be followed. Detailed procedures are out of the scope of the methods described in this article.

ALTERNATE PROTOCOL 2

hPSC SINGLE CELL SEEDING AND CLONAL EXPANSION USING THE CYTENA SINGLE-CELL DISPENSER

The working principle of the Cytena single-cell dispenser (c.sight/f.sight) or single cell "printer" is an inkjet-like technology using a silicon microfluidic chip within a proprietary disposable cartridge which generates free-flying, picoliter droplets that encapsulate the cells. The microfluidic chip is embedded in the dispensing cartridge. The lower part of the cartridge is called the nozzle, and is the interrogation point for the dispensing event. A microscopy system coupled to a camera detects the droplets and their composition. The cell-containing drop is assessed based on cell size and roundness; single cell−containing droplets are selected and ejected into multi-well plates (96 or 384 wells). The system contains a pneumatic shutter below the nozzle, which remains closed until a positive single cell event occurs, allowing droplets containing more than one cell, or empty droplets, to be aspirated away. The entire sorting procedure is automatically documented as a series of images for each positive droplet recorded by the camera system.

NOTE: Special training on how to operate the instrument is recommended. Here we give an overview, but full details are beyond the scope of this protocol. Please contact the manufacturer for further information.

Materials

Essential 8 medium (ThermoFisher Scientific., cat. no. A1517001)
CloneR (Stem Cell Technologies, cat. no. 05888; see Support Protocol 5 for use in medium preparation)
hPSC culture (see relevant Current Protocols articles)
StemFlex medium (ThermoFisher Scientific, cat. no. A3349401)

Laminar flow hood (e.g., Herasafe, ThermoFisher Scientific)
Cytena c.Sight (no fluorescence option) or f.sight (1 channel = green) connected to computer running Cytena software
Cartridge (Cytena Celllink, cat. no: 42581/40-40 SHC)
Serological pipettes, 5 and 10 ml (e.g., Corning, cat. no. 357543 and 357551)
Repeat pipettors, 200 and 1000 µl (e.g., Eppendorf, cat. no. 3123000055 and 3123000063)
Pipette tips, 100, 200 and 1250 µl (e.g., Biozyme, cat. no. 770200 and 770600)
Cell culture incubator (e.g., Binder)

Additional reagents and equipment for preparing target plates (Support Protocols 4 and 6), preparing single cell suspension of hPSCs (Support Protocol 7), preparation of medium containing anti-apoptotic small molecules (Support Protocol 5), and subculture and expansion of hPSC clones (Support Protocol 8)

Cytena setup (day 0)

1. Start the instrument and the connected computer.
2. Start the Cytena software.
3. Choose the format of the target plate (96-well or 384-well).

Single cell printing (day 0)

4. Prepare the target plates as described in Support Protocols 4 and 6.
5. Prepare an hPSC single cell suspension by following Support Protocol 7.

6. Re-suspend hPSCs in Essential 8 medium supplemented with Y-27632 (preparation described in Support Protocol 5) at a concentration of 1000 cells/µl.

   Essential 8 medium must be used for the cell suspension because it has reduced protein content, which prevents blockage of the cartridge. Slightly longer trypsinization time and the use of a 40-µm cell strainer are recommended to remove cell aggregates from the suspension (see Support Protocol 7).

7. Take a new cartridge and unpack it under sterile conditions.
8. Add 70 µl of the cell suspension into the cartridge using a 200-µl repeat pipettor and pipette tip.
9. Open the lid of the Cytena instrument and mount the cartridge using the provided screw (Fig. 4A).
10. Attach a sterile 100-µl pipette tip to the pipetting arm in such a way that it sits in the cell solution within the cartridge (Fig. 4A).
11. Move arm to camera position.
12. Place the target plate on the substrate carrier.

    Carefully check that the plate is correctly placed, with the plate lid removed.

13. Close the lid and return to the software.
14. Open the droplet quality control (QC) tab to automatically start the process.
15. Ideally, a droplet should appear right away in the QC camera window. It should look as depicted in Figure 4B.

    The droplet should be stable. If the droplet is unstable, it may be necessary to adapt the stroke parameters by changing length and speed values. The settings we recommend are length "10" and speed "120."

16. When the droplet is stable, check the vacuum shutter. Use vacuum setting check box "turn on" to switch on the shutter. The droplet should disappear (Fig. 4B). Once the droplet has been reliably removed, proceed with the cell printing.
17. Set program settings as follows (Fig. 4C):

    Program: Printing
    Number cells/well: 1
    Cell size: 10-30 µm
    Cell roundness: 0.5-1.0.

18. Press the Play button to start the printing process
19. When the printing process has finished, place the plate in the incubator at 37°C in a humidified environment, preferably under hypoxic conditions (5% O_2, 5% CO_2).

Single cell scoring and quality check

20. Export the images generated for the run. A total of five pictures showing the nozzle during the isolation process are recorded for each positive single cell droplet.
21. Review the nozzle images for each event isolated and validate the single cell isolation.

    Percentage of validated single cell events in relation to the total number of spotted events is considered to be the single cell seeding efficiency score (Fig. 4D). This score can be used to calculate cloning efficiency as a quality control parameter for an experiment.

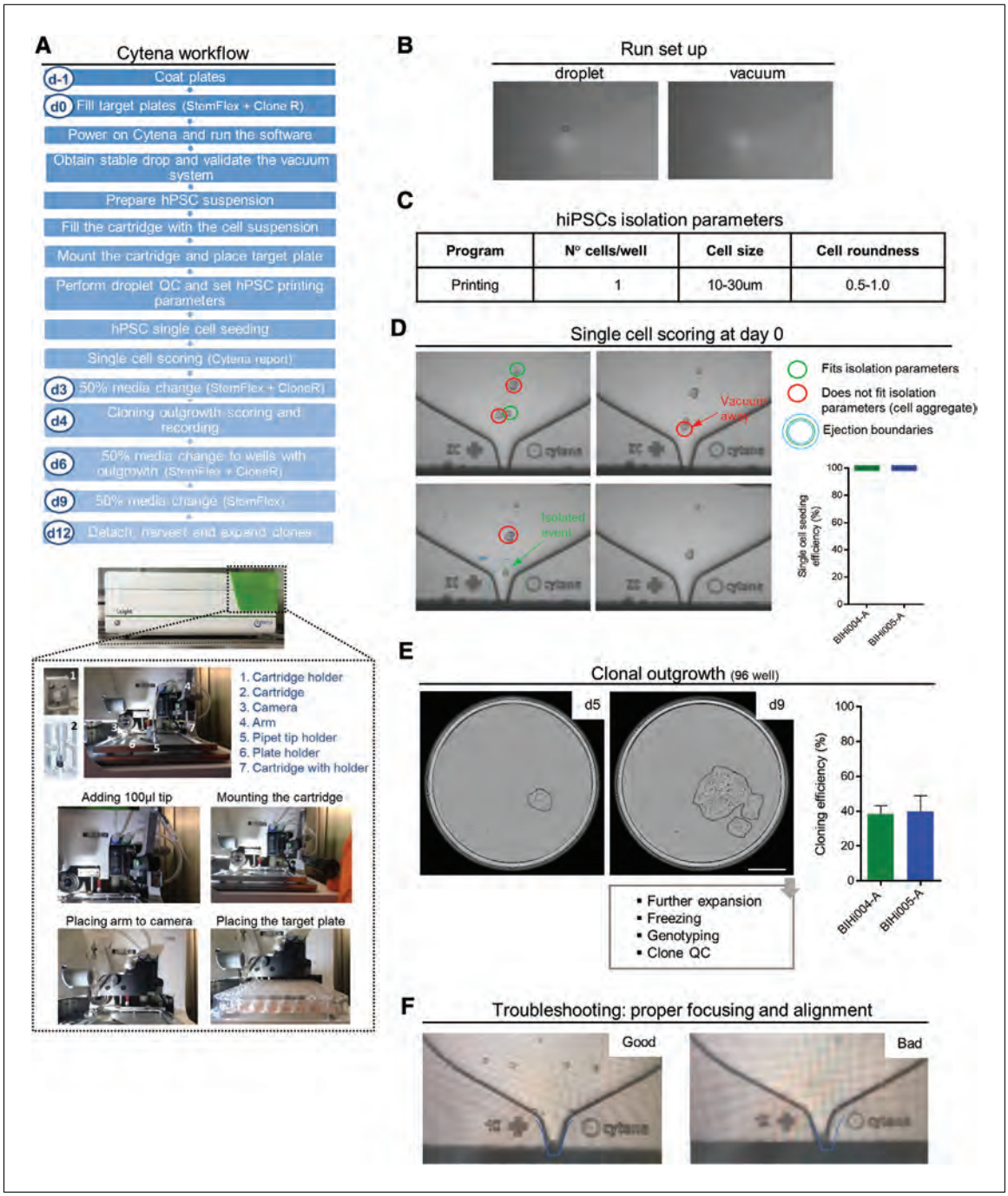

Figure 4 Alternate Protocol 2: Cytena hPSC single cell isolation and clonal expansion. (**A**) Overview flowchart showing automated hPSC single cell seeding using Cytena (c.sight) instrument. Images of the instrument and its main components such as cartridge and pipetting arm are depicted in the lower part. (**B**) Pictures showing the proper droplet formation and the validation of the vacuum system performance. (**C**) Table showing the recommended morphological parameters to ensure single hPSC isolation. (**D**) Left: example of the nozzle images (lower part of the cartridge) taken before and after a single cell printing process; each dispensing event is documented. Right: graph showing single cell seeding efficiency for two hiPSC lines using Cytena (mean ± SD, n = 4) (right). (**E**) Left: Representative pictures showing clonal expansion in culture at different time points (scale bars: 1 mm). Right: graph showing cloning efficiencies for two hPSC lines (mean ± SD, n = 4). (**F**) Troubleshooting: panel showing the correct focus and alignment of cartridge to the camera (good and bad focus are depicted) for successful single cell printing. Incucyte imager was used for pictures in panel E. QC = quality control.

Clone culture maintenance (day 1 to ∼10)

22. On day 3 after seeding, perform a partial medium change with StemFlex medium supplemented with CloneR (preparation described in Support Protocol 5). For 96-well plates: remove 40 µl and add of 50 µl per well; for 384-well plates remove 20 µl and add 30 µl.

    A full medium change (100 and 50 µl, respectively) has also been tested and gives similar results.

23. On day 4, monitor clone outgrowth and record wells with positive outcome.

    Cloning efficiency can be calculated as the proportion of wells with outgrowth in relation to the total number of wells containing a single cell on day 0.

24. On day 6, repeat partial medium change described in step 22 only on wells with cell growth.

    This minimizes the use of reagents and requires less time.

25. On day 9, repeat partial medium change from step 22 using StemFlex medium without CloneR.

26. From day 10 onwards, perform a full medium change daily with StemFlex medium until the clones are ready to be passaged (70% confluent).

27. Follow Support Protocol 8, describing further clonal expansion for later applications such as freezing, genotyping, and expansion for cell banking.

    Standard protocols for such applications can be followed. Detailed procedures are out of the scope of the methods described in this article.

COATING CELL CULTURE PLATES WITH GELTREX

SUPPORT PROTOCOL 1

Soluble forms of basement membrane extract purified from murine Engelbreth-Holm-Swarm tumor cells, such as Geltrex (ThermoFisher Scientific) or Matrigel (Corning), are widely used as a feeder-free alternative to murine embryonic fibroblast feeder cells for hPSC cultures. Here, we briefly describe the coating procedure for standard plastic tissue culture−treated plates using Geltrex.

Materials

Geltrex (ThermoFisher Scientific, cat. no. A1413302)
KnockOut DMEM/F-12 (ThermoFisher Scientific, cat. no. 12660012)

Laminar flow hood (e.g., Herasafe, ThermoFisher Scientific)
50-ml tubes (e.g., Corning Falcon, cat. no. 430290)
Multi-well culture vessels (e.g., 96 well, Corning, cat. no. 353072; see Table 1)
Serological pipettes, 5 and 10 ml (e.g., Corning, cat. no. 357543 and 357551)

Table 1 Coating Solution and Medium Volumes for Different Cell Culture Vessels

Plate	Area (cm^2)/well	Coating solution/well	Culture medium/well
6-well	9.5	1 ml	2 ml
12-well	3.8	0.6 ml	1 ml
24-well	1.9	0.3 ml	0.5 ml
48-well	1	0.2 ml	0.3 ml
96-well	0.32	0.05 ml	0.1 ml
384-well	0.056	0.02 ml	0.06 ml

1.5-ml tubes (e.g., Eppendorf, cat. no. 30120086)
Parafilm M sealing film (Sigma, P6543-1EA)
Cell culture incubator (e.g., Binder)

1. Thaw a frozen Geltrex vial by placing it in ice.

   Geltrex in its concentrated form will start to polymerize and form a gel within a few minutes when warmed up to room temperature; hence, all media and tubes should be pre-cooled to 4°C, and solutions should be kept on ice during handling. It is suggested to thaw stock solutions of Geltrex overnight on ice, aliquot small volumes (0.1-1 ml) into pre-cooled tubes, and re-freeze at −20°C to avoid multiple freeze-thaw cycles. Follow manufacturer's guidelines for handling and dilution where available.

2. Pre-cool a 50-ml Falcon tube containing 49.5 ml DMEM/F12 by placing in ice for 30 min.

3. Add 0.5 ml Geltrex to the 49.5 ml of cold DMEM/F-12 and invert tube gently several times to mix.

   Geltrex dilutions ranging from 1:100 to 1:120 can be used for hPSC culture with similar results.

4. Add appropriate volume of diluted Geltrex solution to desired wells of culture vessels (see Table 1 below).

5. Incubate culture vessels with Geltrex solution for at least 30 min at 37°C before use.

6. For preparation and storage of coated plates for up to 2 weeks, add 1.5× the volume recommended in Table 1 of Geltrex/DMEM/F12 solution, then seal lids on plates using Parafilm and store at 4°C.

   The increased volume is to prevent drying of the plates due to evaporation, which will cause the coating to degrade.

SUPPORT PROTOCOL 2

hPSC MAINTENANCE IN DEFINED FEEDER-FREE CONDITIONS

The quality of the hPSC cultures has a major impact on the downstream application of the cells. Daily medium change and monitoring of cell density and morphology are required to preserve self-renewal, pluripotency, and differentiation capacities.

Materials

hPSC culture (see relevant Current Protocols articles)
Geltrex-coated plates (e.g., 6-well; see Support Protocol 1)
Essential 8 medium (ThermoFisher Scientific., cat. no. A1517001) or mTeSR (Stem Cell Technologies, cat. no. 85850)

Laminar flow hood (e.g., Herasafe, ThermoFisher Scientific)
Inverted microscope with phase-contrast optics, 4×, 10×, 20× objectives (e.g., DMi8, Leica)
Serological pipettes, 5 and 10 ml (e.g., Corning, cat. no. 357543 and 357551)
Pipette tips, 10 µl (e.g., Biozyme, cat. no. 770020)
50-ml tubes (e.g., Corning Falcon, cat. no. 430290)
Glass Pasteur pipette (e.g., VWR, cat. no. 612-1701)
Cell culture vacuum pump (e.g., Integra)
Cell culture incubator (e.g., Binder)
Water bath (e.g., VWR)

Additional reagents and equipment for passaging of hPSC (Support Protocol 3)

1. Most hPSC cultures can be regularly maintained in 6-well Geltrex-coated plates (Support Protocol 1).
2. Use an inverted microscope with phase-contrast optics (4× to 10× objective) to visually monitor the growth and morphology of the hPSC colonies.

   Regions identified as differentiated should be mechanically removed by scraping the bottom of the plate with a plastic pipette tip (10 µl).

3. *For medium change*: Prepare an aliquot of Essential 8 or mTeSR medium in a 50-ml tube with the volume needed for the medium change according to the number of wells (2 ml/well), and warm it to 37°C using a water bath.

   Avoid warming up excess medium, in order to preserve growth-factor activity for a longer period of time.

4. Aspirate medium from the wells using a vacuum system with sterile tip (e.g., glass Pasteur pipette).
5. Add pre-warmed fresh Essential 8 or mTeSR medium according to the hPSC line specification, using 5- or 10-ml pipettes.

   Recommended culture medium volumes for different culture vessels are given in Table 1.

6. When cultures reach 70%-80% confluency, passage according to Support Protocol 3.

hPSC PASSAGING IN CLUMPS

SUPPORT PROTOCOL 3

Standard hPSC cell culture practices include the regular passaging of the cells to maintain self-renewal and pluripotent capacities. Classical enzymatic splitting is harsh for the cells, and the survival rate is lower than with passaging in aggregates or clumps. Here we describe a standard procedure for hPSC splitting using EDTA to "loosen" cell-cell and cell-plate contact without exposing hPSC to single cell dissociation.

Materials

hPSC culture (see relevant Current Protocols articles)
Essential 8 medium (ThermoFisher Scientific., cat. no. A1517001) or mTeSR (Stem Cell Technologies, cat. no. 85850)
0.5 M EDTA, pH 8.0 (ThermoFisher Scientific., cat. no. 15575020)
Dulbecco's phosphate-buffered saline without Ca^{2+} and Mg^{2+} (DPBS; e.g., ThermoFisher Scientific, cat. no. 10010023)

Laminar flow hood (e.g., Herasafe, ThermoFisher Scientific)
Geltrex-coated plates (e.g., 6-well; see Support Protocol 1)
Inverted microscope with phase-contrast optics, 4×, 10×, 20× objectives (e.g., DMi8, Leica)
Cell culture vacuum pump (e.g., Integra)
Glass Pasteur pipette (e.g., VWR, cat. no. 612-1701)
Serological pipettes, 5 and 10 ml (e.g., Corning, cat. no. 357543 and 357551)
50-ml tubes (e.g., Corning Falcon, cat. no. 430290)
Cell culture incubator (e.g., Binder)
Water bath (e.g., VWR)

Additional reagents and equipment for maintaining hPSC in culture (Support Protocol 2)

1. hPSC confluence before splitting should be 70%-80%. Support Protocol 2 provides details on keeping hPSC in culture.

2. Prepare Geltrex-coated tissue culture−treated 6-well plate(s) as described in Support Protocol 1.
3. Aspirate the Geltrex coating solution from the prepared 6-well plate and add 2 ml per well of Essential 8 or mTeSR medium. Keep the plate in the incubator at 37°C until it will be used.
4. Dilute 0.5 M EDTA to a final concentration of 0.5 mM in DPBS

   For example, dilute 500 µl 0.5 M EDTA in 49.5 ml DPBS.
5. Aspirate culture medium from the wells to be split.
6. To wash the wells, add 1 ml of 0.5 mM EDTA to each well and immediately remove it by aspiration.
7. Add 1 ml 0.5 mM EDTA to each well and incubate for 3-4 min at room temperature.

   Monitor the process with an inverted phase-contrast microscope; when cells are rounding up and separate from the neighboring cells, the incubation should be stopped. Cells should not detach!
8. Remove EDTA solution from the wells by aspiration and add 2 ml of Essential 8 or mTeSR medium using a 5-ml serological pipette.
9. Triturate gently using a 1000-µl pipette tip against the culture surface three times to detach the hPSC clumps.
10. Collect the clump suspension and distribute dropwise in the plate prepared in step 3.

    The splitting density will determine how quickly cells will reach confluency for passaging again. Typically, we split 1:6 to 1:20, which would be 333-100 µl volume per well according to the volume in which the clumps were triturated (see step 8), providing about 3-6 days outgrowth.
11. Incubate at 37°C, preferably under hypoxic conditions (5% O_2, 5% CO_2).
12. Change medium every day and monitor the culture as described in Support Protocol 2.

SUPPORT PROTOCOL 4

LAMININ 521 COATING OF IsoCell PLATES AND 96/384-WELL PLATES

hPSC feeder-free cultures need extracellular matrix (ECM) components to successfully attach and generate colonies while keeping pluripotency and self-renewal capacities. Recombinant Laminin 521 is widely used, and in practice increases single cell cloning efficiency compared to commonly used ECMs such as Matrigel or Geltrex. In addition, the purity of Laminin 521 is an advantage for imaging purposes.

Materials

Human recombinant Laminin 521 (Bio Lamina, cat. no. LN521-05)
DPBS with calcium and magnesium (e.g., ThermoFisher Scientific, cat. no. 14040117)

Laminar flow hood (e.g., Herasafe, ThermoFisher Scientific)
Clone G kit-A—with tissue-culture treated 6-cm dishes (Iota Sciences, cat. no. SKU 10030)
96-well tissue-culture treated plates (e.g., Corning, cat. no. 353072)
384-well cell culture plate (e.g., Greiner, 781182)
Serological pipettes, 5 and 10 ml (e.g., Corning, cat. no. 357543 and 357551)

Repeat pipettors, 200 and 1000 µl (e.g., Eppendorf, cat. no. 3123000055 and 3123000063)
Multichannel pipette (e.g., Eppendorf, cat. no. 3125000052)
Pipette tips, 200 and 1250 µl (e.g., Biozyme, cat. no. 770200 and 770600)
15-ml tubes (e.g., Corning Falcon, cat. no. 352096)
50-ml tubes (e.g., Corning Falcon, cat. no. 430290)
Sterile disposable plastic pipetting reservoirs (e.g., ThermoFisher Scientific., cat. no. 95128095)
Parafilm M sealing film (e.g., Sigma, P6543-1EA)
Cell culture incubator (e.g., Binder)

1. Thaw Laminin 521 on ice.
2. Prepare the coating solution by diluting Laminin 521 in DPBS with calcium and magnesium to a final concentration of 5 µg/ml. Total volume depends on number of plates to be coated.

   Prepare 8 ml coating solution per 384-well plate, 5 ml coating solution per 96-well plate, or 2 ml coating solution per 6-cm IsoCell culture-treated dish provided in the Clone G kit-A (Iota Sciences).

3. Add 20 µl coating solution per well of a 384-well plate, 50 µl coating solution per well of a 96-well plate, or 2 ml coating solution per IsoCell culture-treated dish.

   The use of multichannel pipettes or dispensing robots for multi-well plates simplifies the task and reduces the hands-on time.

4. Distribute the coating solution evenly

   For 96- and 384-well plates, centrifuge 1 min at 300 × g to ensure that the bottoms of all wells are covered.

5. Incubate Laminin 521 at least 2 hr at 37°C for multiwell plates before using them, or maximum of 2 hr for 6-cm dishes.

   Best results can be obtained if the plates are prepared fresh. If the plates are not going to be used the same day, they can be sealed with Parafilm and stored immediately after coating at 4°C for up to 1 week, but with a significant reduction in performance.

PREPARATION OF MEDIUM CONTAINING ANTI-APOPTOTIC SMALL MOLECULES

SUPPORT PROTOCOL 5

The use of Rho-kinase (ROCK) inhibitors such as Y-27632 or supplements enhancing cell survival such as CloneR has been shown to play an important role in at least partially blocking apoptotic events in hPSC, among other cell types. We have established the single cell seeding and clonal expansion described in this method paper using these small molecules and supplements to enhance hPSC survival. Here we describe the preparation of culture medium containing anti-apoptotic factors.

Materials

Y-27632 (Stem Cell Technologies, cat. no. 72305)
DMSO (e.g., Sigma-Aldrich, cat. no. D2650)
CloneR (Stem Cell Technologies, cat. no. 05888)
Essential 8 medium (ThermoFisher Scientific, cat. no. A1517001)
mTeSR (Stem Cell Technologies, cat. no. 85850)
StemFlex medium (ThermoFisher Scientific, cat. no. A3349401)

1. Dissolve Y-27632 in DMSO to prepare a 10 mM stock solution.

   Aliquots can be kept at −20°C until use.

Table 2 Anti-Apoptotic Small Molecules and Supplement Dilutions in Medium

Medium	Small molecule stock concentration	Small molecule final concentration	Dilution
StemFlex + CloneR	10×	0.5×	1:20
StemFlex + Y-27632	10 mM	10 µM	1:1000
Essential 8 + Y-27632	10 mM	10 µM	1:1000

2. Thaw a ready-to-use vial of CloneR or aliquot of Y-27632.
3. Calculate the final volume needed of medium containing small molecules.
4. Refer to Table 2 for medium preparation.

SUPPORT PROTOCOL 6

96- AND 384-WELL TARGET PLATE PREPARATION PRIOR TO SINGLE CELL SEEDING

This protocol describes how to prepare the target multi-well culture plates for automated single cell seeding using CellenONE and Cytena instruments. This is a manual procedure; however, the use of liquid-handling robots reduces the hands-on time and standardizes the workflow.

Materials

StemFlex medium containing CloneR, prepared as described in Support Protocol 5
Penicillin/streptomycin (ThermoFisher Scientific, cat. no. 15140122; optional)

Laminar flow hood (e.g., Herasafe, ThermoFisher Scientific)
96- or 384-well tissue-culture treated plates pre-coated with Laminin 521 as described in Support Protocol 4
Multichannel pipette (e.g., Eppendorf, cat. no. 3125000052)
Sterile disposable plastic pipetting reservoirs (e.g., ThermoFisher Scientific., cat. no. 95128095)
Pipette tips, 200 and 1250 µl (e.g., Biozyme, cat. no. 770200 and 770600)
Pipette tips, 300 µl (e.g., Eppendorf, cat. no. 10497221)
Cell culture vacuum pump (e.g., Integra)
Multichannel adaptor for the cell culture pump (e.g., Integra)
Centrifuge (e.g., Eppendorf) with plate adapter

1. Aspirate the coating solution from the plate (see Support Protocol 4, step 5) using the a multichannel pipette and 200-µl pipette tips with adapter connected to the cell culture vacuum pump system.
2. Add StemFlex medium supplemented with CloneR (see Support Protocol 5) using a multichannel pipette.

   Volumes: 60 µl/well (384-well plate); 100 µl/well (96-well plate).

   Optional addition of antibiotics to the medium (penicillin/streptomycin, 1×) for the single cell seeding minimizes the risk of bacterial contamination, especially when using the CellenONE device, and does not affect cell viability.

3. If using 384-well plates, centrifuge plates for 1 min at 300 × *g*, to ensure even surface coverage by the medium and remove any bubbles. If bubbles can be observed after filling of a 96-well plate centrifugation can also be applied.
4. Keep the multi-well plate at 4°C until use within 24 hr.

SINGLE CELL DISSOCIATION OF hPSCs

This protocol describes a procedure, optimized for cell viability, to obtain a homogeneous single cell suspension from hPSC cultures, to be used for automated single cell isolation. Before this point, standard culture conditions for feeder-free hPSC culture using Essential 8 or mTeSR medium should be maintained, as described in Support Protocols 1, 2, and 3, in order to ensure good-quality starting cultures. The procedure is described for hPSCs cultured in 6-well plates. Volumes have to be adapted for other formats taking into account the culture surface, as described in Support Protocol 1 and Table 1.

Materials

hPSC culture (see Support Protocols 1, 2, and 3)
Dulbecco's phosphate-buffered saline without Ca^{2+} and Mg^{2+} (DPBS; e.g., ThermoFisher Scientific, cat. no. 10010023)
TrypLE Select Enzyme (ThermoFisher Scientific, cat. no. 12563011)
Essential 8 medium (ThermoFisher Scientific, cat. no. A1517001) or mTeSR (Stem Cell Technologies, cat. no. 85850)
StemFlex medium (ThermoFisher Scientific, cat. no. A3349401)
CloneR (Stem Cell Technologies, cat. no. 05888; see Support Protocol 5 for use in medium preparation)
Y-27632 (Stem Cell Technologies, cat. no. 72305; see Support Protocol 5 for use in medium preparation)
0.04% Trypan blue (e.g., Sigma-Aldrich, cat. no. T8514-20ML)

Laminar flow hood (e.g., Herasafe, ThermoFisher Scientific)
Inverted microscope with phase-contrast optics, 4×, 10×, 20× objectives (e.g., DMi8, Leica)
Multichannel pipette (e.g., Eppendorf, cat. no. 3125000052)
Sterile disposable plastic pipetting reservoirs (e.g., ThermoFisher Scientific., cat. no. 95128095)
Pipette tips, 200- and 1250-µl (e.g., Biozyme, cat. no. 770200 and 770600)
Pipette tips, 300-µl (e.g., Eppendorf, cat. no. 10497221)
Cell culture vacuum pump (e.g., Integra)
Multichannel adaptor for the cell culture pump (e.g., Integra)
6-well tissue-culture treated plates (e.g., Corning, cat. no. 353046)
Serological pipettes, 5 and 10 ml (e.g., Corning, cat. no. 357543 and 357551)
15-ml tubes (e.g., Corning Falcon, cat. no. 352096)
1.5-ml tubes (e.g., Eppendorf, cat. no. 30120086)
Centrifuge (e.g., Eppendorf)
Automated cell counter with counting chambers (e.g., Countess II, ThermoFisher Scientific) or hemocytometer (Neubauer counting chamber)
Cell culture incubator (e.g., Binder)
Water bath (e.g., VWR)

Additional reagents and equipment for preparation of medium containing anti-apoptotic small molecules (Support Protocol 5) and cell counting (see Current Protocols article: Phelan & May, 2015)

1. Verify 70%-80% hPSC culture confluency using inverted microscope with phase contrast (4× objective).
2. Aspirate and discard medium from the well to be harvested.
3. Wash the well with 1 ml DPBS.
4. Aspirate and discard DPBS. Add 1 ml TrypLE.

Gentle enzymatic dissociation reagents comparable to TrypLE such as Accutase can also be used.

5. Incubate at room temperature until cells are loose (typically 3-5 min). Monitor this step with the microscope. Remove the TrypLE carefully. Make sure the cells are still attached to the bottom of the plate while TrypLE is being removed.

   Unnecessarily long incubations decrease cell viability.

6. Add 1 ml Essential 8 or mTeSR medium to the well to neutralize the enzymatic action, and gently homogenize the cells suspension using a 1000-µl pipette tip.

7. Transfer the cell suspension to a 15-ml tube and centrifuge 5 min at 300 × *g*, room temperature.

8. Aspirate supernatant.

9. Re-suspend the cell pellet with 1 ml of medium.

   Medium for resuspension will be different according to downstream applications: hPSC single cell isolation by IsoCell (StemFlex medium containing CloneR), CellenONE (StemFlex medium or DPBS containing Y-27632), or Cytena (Essential 8 medium containing Y-27632). See Support Protocol 5 for preparation of these media.

10. Prepare an aliquot for cell counting 1:1 in 0.04% trypan blue (e.g., 10 µl cell suspension + 10 µl trypan blue).

11. Homogenize the aliquot and load 10 µl in the cell counting chamber.

    Dedicated chambers are provided specifically for automated counters. A Neubauer chamber (hemocytometer) can also be used, as described in Current Protocols article Phelan & May (2015).

12. Express the result in number of viable cells/ml.

    This value is used for further calculations regarding cell suspension concentrations required for each single cell dispensing method.

SUPPORT PROTOCOL 8

IsoCell-, CellenONE-, AND CYTENA-DERIVED hPSC CLONE SUBCULTURE AND EXPANSION

After hPSC clones derived from single cells have reached 60%-70% confluence, they can be dissociated and further expanded for downstream genotyping, characterization, or freezing. Initial seeding with CellenONE and Cytena instruments will have already been performed in 96- or 384-well plates. For IsoCell, the first expansion step into 96-well plates is described in the Basic Protocol. Here we describe how to passage these clones into larger plate formats. The decision on the plate format to scale up the culture will depend on the several factors: how many clones have to be expanded, workload, possibility of automation, amount of cells needed for downstream purposes, etc.

Materials

StemFlex medium (ThermoFisher Scientific, cat. no. A3349401)
CloneR (Stem Cell Technologies, cat. no. 05888; see Support Protocol 5 for use in medium preparation)
hPSC clones in wells of 96-well plate or 384-well plate (Basic Protocol)
Dulbecco's phosphate-buffered saline without Ca^{2+} and Mg^{2+} (DPBS; e.g., ThermoFisher Scientific, cat. no. 10010023)
TrypLE Select Enzyme (ThermoFisher Scientific, cat. no. 12563011)
Essential 8 medium (ThermoFisher Scientific, cat. no. A1517001) or mTeSR (Stem Cell Technologies, cat. no. 85850)

Laminar flow hood (e.g., Herasafe, ThermoFisher Scientific)
12-well tissue-culture treated plates (e.g., Corning, cat. no. 353043)
Serological pipettes, 5 and 10 ml (e.g., Corning, cat. no. 357543 and 357551)
Repeat pipettor, 200 and 1000 µl (e.g., Eppendorf, cat. no. 3123000055 and 3123000063)
Pipette tips, 200 and 1250 µl (e.g., Biozyme, cat. no. 770200 and 770600)
Cell culture vacuum pump (e.g., Integra)
Inverted microscope with phase-contrast optics, 4×, 10×, 20× objectives (e.g., DMi8, Leica)
Cell culture incubator (e.g., Binder)
48-well tissue-culture treated plates (Corning, cat. no. 353078)
15-ml tubes (e.g., Corning, cat. no. 352096)
Water bath (e.g., VWR)

Additional reagents and equipment for Geltrex coating of cell culture plates (Support Protocol 1) and preparation of medium containing anti-apoptotic small molecules (Support Protocol 5)

To split a 96-well plate of clones

1a. Coat in advance, with Geltrex (Support Protocol 1), the number of wells of 12-well plates according to the number of clones to be passaged (1 × 96-well to 1 × 12 well).

2a. Aspirate and discard the coating solution from the 12-well plate and add 1 ml of StemFlex supplemented with CloneR per well (see Support Protocol 5). Keep the plate in the incubator at 37°C until it will be used.

3a. Aspirate and discard the medium from a well of the 96-well plate with a clone of interest.

4a. Add 200 µl DPBS per well and subsequently discard it to wash the well.

5a. Add 30 µl TrypLE to the well, distribute it evenly, and monitor cell detachment at room temperature using an inverted microscope.

TrypLE incubation time may vary from clone to clone within the range of 3-10 min

6a. Neutralize the TrypLE with 150 µl StemFlex supplemented with CloneR. Pipette up and down three times using a P200 tip on a repeat pipettor set at 150 µl.

7a. Collect the suspension and directly transfer it into one well of the previously prepared 12-well plate (step 2a)

8a. Distribute the cell suspension in the 12-well plate well by a gentle cross movement of the plate.

9a. Incubate at 37°C, preferably under hypoxic conditions (5% O_2, 5% CO_2).

To split a 384-well plate of clones

1b. Coat in advance, with Geltrex (Support Protocol 1), the number of wells in a 48-well plate according to the number of clones to be passaged (1 × 384-well to 1 × 48 well).

2b. Aspirate and discard the coating solution from the 48-well plate and add 0.3 ml per well of StemFlex supplemented with CloneR (see Support Protocol 5). Keep the plate in the incubator at 37°C until it will be used.

3b. Aspirate and discard the medium from a well of the384-well plate with the clone of interest.

4b. Add 80 µl DPBS per well and subsequently discard it to wash the well.

5b. Add 15 µl TrypLE to the well, distribute it evenly, and monitor cell detachment at room temperature using an inverted microscope.

TrypLE incubation time may vary from clone to clone.

6b. Neutralize the TrypLE with 80 µl StemFlex supplemented with CloneR. Pipette up and down three times using a P200 tip on a repeat pipettor set at 80 µl.

7b.. Collect the suspension and transfer it directly to one well of the previously prepared 48-well plate (step 2b)

8b. Homogenize the cell suspension in the 48-well plate by gentle cross movement of the plate.

9b. Incubate at 37°C, preferably under hypoxic conditions (5% O_2, 5% CO_2).

Culture maintenance after clone splitting

10. On day 2 after splitting, adapt clones to the regular cell culture medium (Essential 8 or mTeSR) by changing medium to a 1:1 mixture of StemFlex:Essential 8 or mTeSR.

11. Change medium every day from here on.

12. Further culture expansion follows standard procedures for hPSC culture maintenance and splitting, as described in Support Protocols 1-3.

Other procedures including clone genotyping, characterization, or freezing can be performed using standard protocols that are out of the scope of this article and described in the literature.

COMMENTARY

Background Information

The current standard approaches for hPSC isolation and sub-cloning involve either manual or FACS-based methods. Although there have been improvements in the workflows over the last years, both methods still have limitations, including relatively low survival rates. Various approaches using different recombinant ECM proteins or hydrogels (Higuchi et al., 2016; Rodin, Antonsson, Hovatta, & Tryggvason, 2014), protein inhibitors (Valamehr et al., 2012; Watanabe et al., 2007), mouse embryonic fibroblasts (MEFs; Yang et al., 2013), and human serum-derived protein (Pijuan-Galitó et al., 2016) have shown improved survival of single-cell derived hPSC clones. Recently, FACS sorting in combination with different ECM proteins such as Laminin 521 or with MEF co-culture showed an increased single cell survival (Chen & Pruett-Miller, 2018; Singh, 2019). However, the usability of these methods is often severely compromised due to high cost, the need for MEFs, poor reproducibility, or the requirement for a dedicated operator/facility to maintain and operate the FACS equipment.

Based on preliminary results (data not shown) and the literature, we have included key factors in our workflows such as growth factor−stabilized medium (StemFlex medium) that ensure the activity of growth factors for longer periods of time, as well as a supplement that enhances cell survival (CloneR) and a coating matrix suitable for better hPSC single cell survival, outgrowth, and imaging (Laminin 521) (Chen & Pruett-Miller, 2018). Using these conditions, automated single cell dispensing and follow-up culture were optimized. Other cell isolation and culture conditions than the ones described here can potentially be used as well, but they need to be tested. Classical media used for hPSC culture such as Essential 8 or mTeSR contain unstable components and need to be replaced every day. These medium changes cause stress to the hPSCs and significantly affect the single cell outgrowth potential of the developing clones. The less the cultures are manipulated during the first days after single-cell seeding, the better. In addition, a reduced number of medium changes in high-throughput experiments translates into lower maintenance cost and less hands-on time.

Addition of CloneR to the medium has shown better hPSC single cell survival in our experiments compared to the widely used ROCK inhibitor Y-27632, but, other options available on the market such as RevitaCell (ThermoFisher Scientific) could also be explored. It is important to keep CloneR in the culture medium for at least 5 days. Earlier removal leads to a reduction of cloning efficiency by 5%-7% (data not shown). Regarding the coating of the culture surface, other options such as vitronectin, Geltrex, or Matrigel at various dilutions can be considered; however, vitronectin has shown interference with IsoCell grid formation, and after Geltrex or Matrigel coating, certain debris-like deposits are present that affect imaging procedures and make the single cell scoring process difficult. We have applied three automated systems to generate hPSC sub-cultures with proven mono-clonality, reaching efficiencies of 30%-60%. This percentage refers to the outgrowth observed in wells where a single cell event was registered. However, we also want to point out that the cloning efficiency is cell-line dependent and that it might be important to optimize the conditions for other cell lines. Knowing the cloning efficiency allows estimation of the number of plates and format (96 or 384 wells, or 256 chambers) to be seeded in order to isolate a desired clone. For example, if the frequency of occurrence of a certain homologous directed recombination (HDR) event using CRISPR/Cas9-based gene editing is about 1%-5% and the hPSC line used for this experiment shows 50% cloning efficiency after single cell seeding, about 1-10 clones containing the desired edit can be isolated from 384 initially seeded single cells. This estimation is valid for single cell dispensing with an efficiency equal or greater than 95%, which can be reached using the CellenONE or Cytena instruments (see Fig. 3E and Fig. 4E). Notably, single cell seeding efficiencies reported for CellenONE and Cytena rely on images that show the content of the nozzle at the moment of dispensing, which is a good validation considering the difficulty of finding a single isolated cell in a well post-seeding; however, this is not 100% proof of mono-clonality (Yim & Shaw, 2018). The IsoCell instrument yields lower single cell seeding efficiencies (25%-35%) which results in 60-80 chambers out of 256 containing a single cell (Fig. 2D). This lower single cell seeding efficiency is due to the fact that the instrument relies on a Poisson distribution and the experience of the operator for scoring the wells containing the single cells using an inverted microscope. Therefore, with the IsoCell instrument, a higher number of chambers/dishes must be seeded to isolate a desired clone. This is not necessarily a disadvantage of this platform, as the consumable costs are reduced in comparison to CellenONE or Cytena due to the minuscule medium volumes used in the IsoCell from seeding to clone outgrowth.

Critical Parameters

There are several important parameters that influence the efficient derivation of single cell clones from hPSCs. One of the most important parameters is the quality of the hPSC starting culture from which single cell clones are isolated. Preferably, hPSC in log phase of growth at 70%-80% confluency should be used. To keep the cells in log phase, the culture split ratios must be optimized. In most cases, splitting ratios between 1:4 and 1:8 are optimal, and one should standardize the time between passages at 4 and 5 days. However, the optimal split ratio varies between individual cell lines. The confluency and morphology of the cultures should be observed daily. hPSC colonies should have similar sizes and be distributed evenly in the culture vessel. Variability observed between different hPSC lines makes it necessary to adapt several parameters/procedures to achieve optimal sub-cloning outcomes. These parameters/procedures could include adaptation to specific ECM coating (e.g., Laminin 521) and culture medium (e.g., culture in StemFlex medium supplemented with CloneR for some time prior to the dispensing procedure), or obtaining more homogeneous cultures in terms of hPSC colony size and distribution by performing a single cell split 1 or 2 days before automated single cell seeding. We have not exhaustively explored these alternatives; however, preliminary data indicate that further improvement is possible.

Other critical parameters to pay attention to are possible mycoplasma or other microbial contaminations. In general, the growth kinetics of hPSCs infected with mycoplasma are slower and might eventually reduce the single cell survival rate. Mycoplasma testing at regular intervals is highly recommended. Adding antibiotics to the culture medium during critical steps such as open single cell seeding (CellenONE, Cytena) helps to reduce the risk of microbial contamination and does not affect the culture outcome.

An additional critical step in the protocols is the preparation of the single cell suspension

prior to the dispensing procedure. Here, either too-long or too-short enzymatic incubations affect the outcome of single cell sub-cloning experiments. Insufficient enzymatic dissociation leads to cell aggregates in the suspension, which will interfere with the single cell dispensing process. Prolonged enzymatic incubation as well as harsh pipetting lead to increased cellular stress, resulting in a decreased single cell survival rate.

Furthermore, the time between preparation of the single cell suspension and dispensing should kept as short as possible (maximum 15 min) to preserve hPSC viability and quality. Therefore, the materials needed have to be ready for use before cell harvesting. These include solutions, reagents, and target plates; in addition, equipment must be cleaned, sterilized, and primed as described in the corresponding protocols.

Troubleshooting

Common problems the user may encounter, with possible causes and potential solutions, in all three single cell seeding protocols are described in Table 3.

Understanding Results

In the present protocols, we provide a complete automated workflow to efficiently derive hPSC monoclonal cultures using three alternative platforms—IsoCell, CellenONE, and Cytena—dedicated to the single cell seeding step. Each platform (Table 4) has different characteristics that may be more appropriate depending on the laboratory setup (throughput, operator experience, space, GMP, cost, etc.) or application (gene editing, hPSC mosaicism, etc.). Here we describe application examples using the different technologies—the first two examples aim to derive clones with a normal karyotype from a mosaic hPSC culture consisting of mixed hPSC populations of normal cells and cells with karyotypic abnormalities. In a third example, we demonstrate how the genetic stability and genotype composition of hPSC cultures can be analyzed.

Genetic integrity in hPSC cultures is one of the most important quality controls that must be validated before performing other downstream applications. Methods such as genome-wide SNP analysis using microarrays and G-banding karyotyping are employed to assess genetic integrity in hPSC cultures. Both methods have certain technical limitations that result in the non-detection of certain karyotypic abnormalities. SNP arrays, for example, cannot detect balanced chromosomal relocations or aberrations that are under-represented (below 15% of the entire population) in an overall cell population. G-band karyotyping can be more informative in this regard, since it visually identifies metaphase-stage chromosomal defects and is therefore able to detect balanced translocations. However, G-band karyotyping cannot detect loss of heterozygosity (LOH) or abnormalities below 5 MB, and, due to the low number of cells analyzed, does not have a good threshold of detection. Therefore, the combination of both methods can compensate for the shortcomings of each, and makes it possible to detect a wide variety of chromosomal abnormalities in hPSC cultures.

During our routine analysis of the karyotypic stability of our cell lines, we detected a large common duplication of chromosome 20 (Chr20q11, around 5 MB) in the BIHi050-A line by SNP array analysis (Table 5; Markouli et al., 2019). In an attempt to investigate as well as resolve this large copy number variation, we applied the Basic Protocol utilizing the IsoCell platform following a slightly modified version of Support Protocol 1 (preadaption of the hPSCs to Laminin 521 and StemFlex). We established and subsequently analyzed 18 single cell−derived clonal populations. Out of these clones, 16 showed a karyotype comparable to the parental hPSC (Table 5). The detected copy number differences of the clones are in the range of naturally occurring variants within the human population (Liang & Zhang, 2013). Interestingly, within the region duplicated on Chr20q11 are genes like *BCL2* or *DNMT3* having key roles in pluripotency and cell survival (Markouli et al., 2019). This might give a growth advantage to the cells carrying the aberration, and therefore increase the probability of acquiring compromised clones with the subsequent passages.

In a second application, we used Alternate Protocol 1 and the CellenONE technology to derive a clone with a normal karyotype from an hPSC population (BU3 NG hiPSC line) with a mosaicism of a trisomy of chromosome 12 that had been detected by G banding. Even though 3/21 (14%) of the karyograms analyzed by G banding exhibited this trisomy, the aberration could not be detected using SNP array. Therefore, we estimated that the rate of mosaicism was probably below 10%. We isolated several clones and analyzed the karyotype of five clones using SNP arrays (Table 5). None of the clones showed the chromosome 12 trisomy; however, three of them

Table 3 Troubleshooting for Single Cell Isolation and Sub-Cloning of Human Pluripotent Stem Cells

Problem	Possible causes	Potential solutions
Failure in grid formation and/or grid merging (Fig. 2G) (IsoCell)	• Jetting system is not creating adequate pressure to make the grids • Bubbles in jetting system • Bubbles in a dish • Not enough protein content on the dish surface	• Repeat the startup routine or perform a jetting flush routine • Change the jetting system • Lay solutions on the dish carefully • Use fresh coatings (within 24 hr) • Wash plate 2-3 times with StemFlex medium and perform 5-10 min medium incubation at RT before adding FC40^{STAR}
Low number of chambers with a single cell and difficulty in counting the chambers with a single cell (IsoCell)	• Initial density of cell suspension is not optimal • Cell counting varies from lab to lab or person to person • Cell suspension contains clumps • Excessive cell debris • Long incubation after plating • Extra drops or bubbles are seen in the chamber, which confuses the counting	• Optimize the right cell density for plating using 5000, 7500, and 10000 cells/ml • Optimize TrypLE dissociation time for the each hPSC line (range = 7-10 min at RT) • Use 40-µm cell strainer to filter single cell suspensions • Count within 10-20 min after plating • Change the dispense system
Few cells (or none) are transferred to 96-well plate after enzymatic dissociation from chambers(IsoCell)	• Too short enzymatic incubation time	• Monitor cell detachment using the inverted microscope • Increase enzymatic incubation times needed (automatic program can be paused) • Include an initial wash step with 0.5 mM EDTA in DPBS
High cell abortion rate during the run (CellenONE)	• Cell suspension is too concentrated • Isolation parameters are not adequate • Image focus at the nozzle is not correct (Fig. 3F) • Dirt or fluorescent artifacts in the nozzle are detected as cells	• Dilute cell suspension and perform a new mapping • To improve the adequate cell morphology parameters adequate for the present run, perform a new analysis and generate a gate on the main population • Use nozzle off-set tab to adjust the camera focus and save the new parameters • Take a new background image to avoid the identification of background artifacts as cells
Film formation at the tip of the PDC(CellenONE)	• PDC is dirty • Viscosity of the medium interferes with the drop formation	• Perform wash and SciClean tasks • Gently wipe the PDC with a particle-free tissue soaked with ethanol 70% or SciClean solution • Avoid viscous medium or supplements, e.g., DPBS containing Y-27632 can be used
No cells visible in the nozzle during continuous dispensing (CellenONE)	• An aggregate of cells or debris has blocked the PDC • Bubble formation in the PDC • Uptake sample task was not performed	• Use always standby mode to avoid blockings • Flush out 2-3 µl • Perform AirEx task or flush PDC, perform a wash step, and uptake sample (homogenized cell suspension) from the source plate
Printing does not start (Cytena)	• Cartridge is not well aligned • Focus is not set (Fig. 4F)	• Repeat the alignment process • Adjust the focus

(*Continued*)

Table 3 Troubleshooting for Single Cell Isolation and Sub-Cloning of Human Pluripotent Stem Cells, *continued*

Problem	Possible causes	Potential solutions
Low survival rate of single cells (all devices)	• Missing CloneR supplement in the culture medium • Long/harsh dissociations to obtain single cell suspension • Long time between obtaining single cell suspension and dispensing • Too-sensitive cell lines • Crystal structures in grids or plate due to evaporation	• Make sure you add CloneR supplement (1:20) • Keep CloneR in the medium until day 6 of culture • Optimize right dissociation time • Avoid dissociation times longer than 10 min • Avoid high confluency (>80%) or heterogeneous colony size of initial culture • Dispense the cells immediately • Pre-adapt the culture conditions to StemFlex medium containing CloneR and Laminin 521 coated plates • Make sure incubator conditions (humidity and temperature) are correct

Table 4 Automated Single Cell Dispensers' Characteristics and Utilities for Applications on hPSC Field

Aspect/equipment	IsoCell	CellenONE (F1.1/F1.4)	Cytena (c.sight/f.sight)
Training	Half day	3-5 days	1 day
Deposition volume/cell culture volume	Nanoliter/0.2-0.9 μl	Picoliter/60-100 μl	Picoliter/60-100 μl
Embedding in bigger automated platform	No	Yes	Yes
Sample recovery	No	Yes	No
Proof of clonality	In-chamber verification (manually, microscopy)	Before-chamber verification (automated/imaging)	Before-chamber verification (automated/imaging)
Sterility	Yes	Yes	Yes
	(can be place inside cell culture cabinet)	(open system, uses sterilization routine)	(closed system)
Documentation	Manual	Automated (PDF report)	Automated
Mean number of clones generated	20-40	15-30 (96 well)	30-50 (96 well)
	per dish	70-100 (384 well)	
Isolation using fluorescence	No	Yes (up to 4 channels)	Yes (1 channel)
Isolation using morphological parameters	No	Yes	Yes
Equipment maintenance requirements	Low	Demanding	Low
Handling	Easy	Difficult	Moderate
Hardware acquisition cost	Medium	High	High
Consumable cost (per dispensing run)	Low	Low	High

were carrying an additional deletion in chromosome 18, depicting once more the mosaicism prevalent within hPSC bulk populations, as well as the contrasting features of G banding versus SNP array karyotyping analysis.

Reliable large-scale production of Good Manufacturing Practice (GMP)-compliant hPSC banks is a crucial starting point for cell therapies: therefore, it is important to maintain a stable karyotype and homogenous

Table 5 Single Cell Seeding and Clone Derivation Application Examples

Protocol/ technology	Aim	Parental hPSC	Finding/ reference	Cloning efficiency (%)	n° clones analyzed	n° clones with normal karyotype	Conclusion
Basic Protocol (IsoCell)	Clean up karyotype abnormality	BIHi050-A	Chr20q11, large duplication (detected by SNP array)	68	18	16	Reference hPSC showed mosaicism. Clones with a normal karyotype could be isolated by single cell sub-cloning
Alternate Protocol 1 (CellenONE)	Clean up karyotype abnormality	BU3 NG	Chr12 trisomy (detected by G-banding)	21	5	2	Reference hPSC showed mosaicism. Clones with a normal karyotype could be isolated by single cell sub-cloning
Alternate Protocol 2 (Cytena)	Readout of homogeneity and genetic stability under cGMP conditions	BIHi005-A	Parental hPSC cultured in cGMP conditions show normal karyotype	48	3	2	Single cell subcloning and clone genotyping reveals mosaicism in the parental hPSC

cell population under cGMP culture conditions. It is necessary to develop quality control assays that can efficiently and reproducibly monitor growth kinetics, random differentiation, heterogeneity, and chromosomal integrity during either the adaptation to GMP compliant-hPSC culture conditions or large-scale production, processing, and storage of hPSC banks. More quantitative karyotype analysis of derivative single cell sub-clones would provide an excellent readout of homogeneity and genetic stability of hPSCs derived and cultured under GMP compliant conditions. As a proof of principle, we have studied the control cell line BIHi005-A following adaptation to GMP-grade culture conditions (i.e., using GMP-grade reagents), and analyzed sub-clones derived according to Alternate Protocol 2 using Cytena technology. Compared to the parental bulk line, karyotype analysis indicated that two out of three sub-clones were comparable, with a third exhibiting an additional copy-number variation (Table 5). Although the detected aberration in this particular clone is relatively small, below 3 MB in size, it once more shows the latent frequency of mosaicism within a bulk culture of hPSCs, which should be kept in mind for further downstream applications of hPSC-derived clinical products.

Our experimental data reiterate several important points with regard to an automated single cell isolation workflow. First, they highlight hPSC mosaicism; second, the detection threshold and different characteristics of G banding and SNP array karyotype analysis; and finally the ability to maintain, quantify, or even "clean up" the karyotypes of hPSC sub-clonal lines. Importantly, we find that the automated single cell seeding and subsequent clonal expansion described here results in hPSC clones that preserve pluripotency markers and classical colony morphology, as exemplified in Figure 5.

In summary, the protocols presented here utilizing automated single cell seeding and further clonal expansion enable efficient, precise, reproducible, and quality-controlled derivation of monoclonal hPSCs, and can be

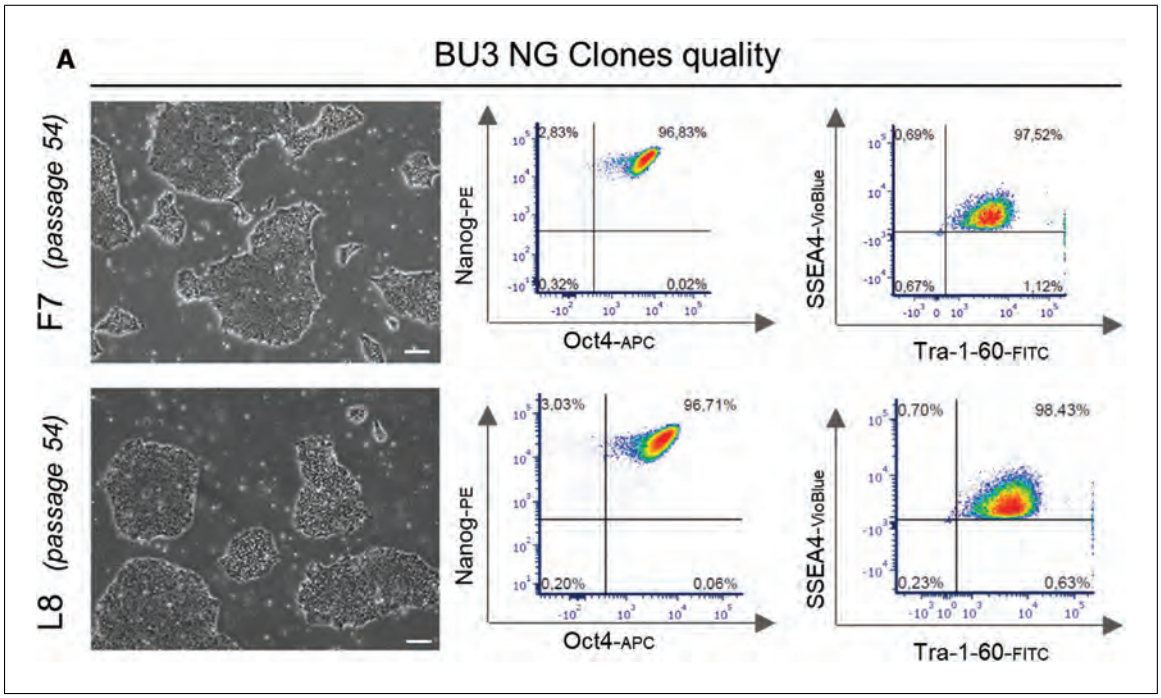

Figure 5 Example data for the validation of hPSC pluripotent morphology and marker expression following automated single cell sub-cloning. (**A**) Pictures showing colonies with typical hPSC morphology of two clones isolated using Alternate Protocol 1 (scale bar: 200 µM). (**B**) FACS analysis showing pluripotent marker expression (Nanog, Oct4, SSEA-4, and Tra-1-60) by almost 100% of the cells in the clones. A Leica DMi8 microscope with phase contrast was used for pictures.

Table 6 Time Considerations

Time required for /equipment	IsoCell	CellenONE (F1.1/F1.4)	Cytena (c.sight/f.sight)
Equipment setup	5-15 min	30-40 min	10-15 min
Single cell seeding	1-2 min per dish	1-2 min per 96-well plate	2-4 min per 96-well plate
		2-3 min per 384-well plate	
Single cell validation	10-15 min	5-10 min	5-10 min
Feeding routine	4-6 min per dish	10-30 min per plate[a]	10-30 min per plate[a]
Until first clone can be expanded	8-10 days	10-12 days	10-12 days
Clone harvesting	15-20 min (8 clones)	5-7 min per clone	5-7 min per clone

[a]Depends on the number of wells with clonal outgrowth selected.

used for stem cell engineering and future stem cell therapy applications.

Time Considerations

Time considerations for key steps and comparing the different platforms are shown in Table 6.

Acknowledgments

Open access funding enabled and organized by Projekt DEAL. We would like to thank all other team members of the BIH Stem Cell Core Facility at the locations Charité and MDC.

Author Contributions

Valeria Fernandez Vallone: Conceptualization; data curation; formal analysis; investigation; methodology; validation; visualization; writing-original draft. **Narasimha Swamy Telugu:** Conceptualization; data curation; formal analysis; investigation; methodology; validation; visualization; writing-original draft. **Iris Fischer:** Conceptualization; data curation; formal analysis; investigation; methodology; software; validation; visualization; writing-review & editing. **Duncan Miller:** Data curation; formal

analysis; investigation; methodology; visualization; writing-review & editing. **Sandra Schommer:** Investigation. **Sebastian Diecke:** Conceptualization; data curation; methodology; project administration; supervision; validation; writing-review & editing. **Harald Stachelscheid:** Conceptualization; Data curation; methodology; project administration; supervision; validation; writing-review & editing.

Literature Cited

Chen, G., Hou, Z., Gulbranson, D. R., & Thomson, J. A. (2010). Actin-myosin contractility is responsible for the reduced viability of dissociated human embryonic stem cells. *Cell Stem Cell*, *7*(2), 240–248. doi: 10.1016/j.stem.2010.06.017.

Chen, Y.-H., & Pruett-Miller, S. M. (2018). Improving single-cell cloning workflow for gene editing in human pluripotent stem cells. *Stem Cell Research*, *31*, 186–192. doi: 10.1016/j.scr.2018.08.003.

Doudna, J. A., & Charpentier, E. (2014). The new frontier of genome engineering with CRISPR-Cas9. *Science*, *346*(6213), 1258096. doi: 10.1126/science.1258096.

Higuchi, A., Kao, S.-H., Ling, Q.-D., Chen, Y.-M., Li, H.-F., Alarfaj, A. A., … Umezawa, A. (2016). Long-term xeno-free culture of human pluripotent stem cells on hydrogels with optimal elasticity. *Scientific Reports*, *5*(1), 18136. doi: 10.1038/srep18136.

Hsu, P. D., Lander, E. S., & Zhang, F. (2014). Development and applications of CRISPR-Cas9 for genome engineering. *Cell*, *157*(6), 1262–1278. doi: 10.1016/j.cell.2014.05.010.

Liang, G., & Zhang, Y. (2013). Genetic and epigenetic variations in iPSCs: Potential causes and implications for application. *Cell Stem Cell*, *13*(2), 149–159. doi: 10.1016/j.stem.2013.07.001.

Markouli, C., Couvreu De Deckersberg, E., Regin, M., Nguyen, H. T., Zambelli, F., Keller, A., … Spits, C. (2019). Gain of 20q11.21 in human pluripotent stem cells impairs TGF-β-dependent neuroectodermal commitment. *Stem Cell Reports*, *13*(1), 163–176. doi: 10.1016/j.stemcr.2019.05.005.

Phelan, K., & May, K. M. (2015). Basic techniques in mammalian cell culture. *Current Protocols in Cell Biology*, *66*, 1.1.1–1.1.22. doi: 10.1002/0471143030.cb0101s66.

Pijuan-Galitó, S., Tamm, C., Schuster, J., Sobol, M., Forsberg, L., Merry, C. L. R., & Annerén, C. (2016). Human serum-derived protein removes the need for coating in defined human pluripotent stem cell culture. *Nature Communications*, *7*(1), 12170. doi: 10.1038/ncomms12170.

Rodin, S., Antonsson, L., Hovatta, O., & Tryggvason, K. (2014). Monolayer culturing and cloning of human pluripotent stem cells on laminin-521−based matrices under xeno-free and chemically defined conditions. *Nature Protocols*, *9*(10), 2354–2368. doi: 10.1038/nprot.2014.159.

Rossant, J., & Tam, P. P. L. (2017). New insights into early human development: Lessons for stem cell derivation and differentiation. *Cell Stem Cell*, *20*(1), 18–28. doi: 10.1016/j.stem.2016.12.004.

Singh, A. M. (2019). An efficient protocol for single-cell cloning human pluripotent stem cells. *Frontiers in Cell and Developmental Biology*, *7*, 11. doi: 10.3389/fcell.2019.00011.

Soitu, C., Feuerborn, A., Tan, A. N., Walker, H., Walsh, P. A., Castrejón-Pita, A. A., … Walsh, E. J. (2018). Microfluidic chambers using fluid walls for cell biology. *Proceedings of the National Academy of Sciences*, *115*(26), E5926–E5933. doi: 10.1073/pnas.1805449115.

Soitu, C., Stovall-Kurtz, N., Deroy, C., Castrejón-Pita, A. A., Cook, P. R., & Walsh, E. J. (2020). Jet-printing microfluidic devices on demand [Preprint]. *Bioengineering*. doi: 10.1101/2020.05.31.126300.

Valamehr, B., Abujarour, R., Robinson, M., Le, T., Robbins, D., Shoemaker, D., & Flynn, P. (2012). A novel platform to enable the high-throughput derivation and characterization of feeder-free human iPSCs. *Scientific Reports*, *2*(1), 213. doi: 10.1038/srep00213.

Walsh, E. J., Feuerborn, A., Wheeler, J. H. R., Tan, A. N., Durham, W. M., Foster, K. R., & Cook, P. R. (2017). Microfluidics with fluid walls. *Nature Communications*, *8*(1), 816. doi: 10.1038/s41467-017-00846-4.

Watanabe, K., Ueno, M., Kamiya, D., Nishiyama, A., Matsumura, M., Wataya, T., … Sasai, Y. (2007). A ROCK inhibitor permits survival of dissociated human embryonic stem cells. *Nature Biotechnology*, *25*(6), 681–686. doi: 10.1038/nbt1310.

Wu, J., & Izpisua Belmonte, J. C. (2015). Dynamic pluripotent stem cell states and their applications. *Cell Stem Cell*, *17*(5), 509–525. doi: 10.1016/j.stem.2015.10.009.

Yamanaka, S. (2012). Induced pluripotent stem cells: Past, present, and future. *Cell Stem Cell*, *10*(6), 678–684. doi: 10.1016/j.stem.2012.05.005.

Yang, L., Guell, M., Byrne, S., Yang, J. L., De Los Angeles, A., Mali, P., … Church, G. (2013). Optimization of scarless human stem cell genome editing. *Nucleic Acids Research*, *41*(19), 9049–9061. doi: 10.1093/nar/gkt555.

Yim, M., & Shaw, D. (2018). Achieving greater efficiency and higher confidence in single-cell cloning by combining cell printing and plate imaging technologies. *Biotechnology Progress*, *34*(6), 1454–1459. doi: 10.1002/btpr.2698.

Internet Resources

https://www.iotasciences.com/

URL of IsoCell manufacturer.

https://www.cellenion.com/

URL of CellenONE manufacturer.

https://www.cytena.com/

URL of Cytena manufacturer.

Cell Banking of hiPSCs: A Practical Guide to Cryopreservation and Quality Control in Basic Research

Aya Shibamiya,[1,2,6] Elisabeth Schulze,[1,2] Dana Krauß,[1,3] Christa Augustin,[4] Marina Reinsch,[1,2] Mirja Loreen Schulze,[1,2] Simone Steuck,[1,2] Giulia Mearini,[1,2] Ingra Mannhardt,[1,2] Thomas Schulze,[1,2] Birgit Klampe,[1,2] Tessa Werner,[1,2] Umber Saleem,[1,2] Anika Knaust,[1,2] Sandra D. Laufer,[1,2] Christiane Neuber,[1,2] Marta Lemme,[1,2] Charlotta Sophie Behrens,[1,2] Malte Loos,[1,2] Florian Weinberger,[1,2] Sigrid Fuchs,[5] Thomas Eschenhagen,[1,2] Arne Hansen,[1,2] and Bärbel Maria Ulmer[1,2,6]

[1]Institute of Experimental Pharmacology and Toxicology, University Medical Center Hamburg–Eppendorf, Hamburg, Germany
[2]DZHK (German Center for Cardiovascular Research), partner site Hamburg/Kiel/Lübeck, Hamburg, Germany
[3]Current address: Institute of Cancer Research, Department of Medicine I, Medical University of Vienna and Comprehensive Cancer Center, Vienna, Austria
[4]Department of Legal Medicine, University Medical Center Hamburg–Eppendorf, Hamburg, Germany
[5]Institute of Human Genetics, University Medical Center Hamburg–Eppendorf, Hamburg, Germany
[6]Corresponding authors: *a.shibamiya@uke.de*; *b.ulmer@uke.de*

The reproducibility of stem cell research relies on the constant availability of quality-controlled cells. As the quality of human induced pluripotent stem cells (hiPSCs) can deteriorate in the course of a few passages, cell banking is key to achieve consistent results and low batch-to-batch variation. Here, we provide a cost-efficient route to generate master and working cell banks for basic research projects. In addition, we describe minimal protocols for quality assurance including tests for sterility, viability, pluripotency, and genetic integrity. © 2020 The Authors.

Basic Protocol 1: Expansion of hiPSCs
Basic Protocol 2: Cell banking of hiPSCs
Support Protocol 1: Pluripotency assessment by flow cytometry
Support Protocol 2: Thawing control: Viability and sterility
Support Protocol 3: Potency, viral clearance, and pluripotency: Spontaneous differentiation and qRT-PCR
Support Protocol 4: Identity: Short tandem repeat analysis

Keywords: cell banking • hiPSC • master cell bank • stem cell quality

CURRENT PROTOCOLS
A Wiley Brand

Current Protocols in Stem Cell Biology e127, Volume 55
Published in Wiley Online Library (wileyonlinelibrary.com).
doi: 10.1002/cpsc.127

How to cite this article:
Shibamiya, A., Schulze, E., Krauß, D., Augustin, C., Reinsch, M., Schulze, M. L., Steuck, S., Mearini, G., Mannhardt, I., Schulze, T., Klampe, B., Werner, T., Saleem, U., Knaust, A., Laufer, S. D., Neuber, C., Lemme, M., Behrens, C. S., Loos, M., Weinberger, F., Fuchs, S., Eschenhagen, T., Hansen, A., & Ulmer, B. M. (2020). Cell banking of hiPSCs: A practical guide to cryopreservation and quality control in basic research. *Current Protocols in Stem Cell Biology*, *55,* e127. doi: 10.1002/cpsc.127

INTRODUCTION

Human induced pluripotent stem cells (hiPSCs) are widely utilized from basic research to clinical applications. Many laboratories create patient-specific or genetically modified hiPSC lines, and need to implement a strategy to cryopreserve not only large quantities of hiPSCs but also high-quality hiPSCs (Stacey, 2012; Stacey, Crook, Hei, & Ludwig, 2013). The basis for this is usually the creation of master and working cell banks (MCBs and WCBs). Basically, a MCB consists of multiple cryopreserved vials of one batch of hiPSCs; some of the vials are used for quality control and others to create WCBs. One WCB cryovial can be thawed per experiment and used without the need for long expansion phases, which are prone to cause genetic aberrations and contamination. This assures a reproducible, validated hiPSC quality that reduces batch-to-batch variability of hiPSC-derived cell types and assays (Volpato et al., 2020). Cell banking with MCBs and WCBs is a central part of quality control during the production of hiPSC-based medical products or hiPSC lines targeted for clinical application (Andrews et al., 2015; Sullivan et al., 2018). Directives and regulations for this are in place (Baghbaderani et al., 2015; Rao et al., 2018; Shafa et al., 2020; see also Internet Resources for EU regulations and directives for Good Laboratory Practice [GLP], Good Cell Culture Practice [GCCP], and Good Manufacturing Practice [GMP]). In addition, consortia such as the International Stem Cell Initiative and Stem Cell COREdinates define best practices and work on a consensus for hiPSC MCB testing, especially for clinical-grade hiPSCs (Andrews et al., 2015; Sullivan et al., 2018). Registries and hiPSC banks such as hPSCreg and EBiSC set gold standards for research-grade hiPSC lines (also see Internet Resources and Key References).

However, these activities are in stark contrast to the common standard of hiPSC quality testing in basic research, where the degree of quality assessment varies widely, with many publications not mentioning any quality control. Thus, a strategy for cell banking and minimal quality control is also necessary to improve reproducibility in the field of basic research.

This protocol is designed to serve as a practical guide to cryopreservation and quality control for basic research. Among other things, it should enable basic scientist to establish a cost-efficient, labor-saving workflow for quality-controlled, reproducible hiPSC-based experiments by detailing a selection of common, well-known assays. The protocol was used to produce MCBs in the course of the IndivuHeart project (ClinicalTrials.gov Identifier: NCT02417311), which attempted to compare hiPSC-derived cardiomyocytes in engineered heart tissues from 60 probands. The protocol details expansion starting from young hiPSC clones between passage numbers (p) 5 and 10 (Basic Protocol 1) and subsequent cell banking of MCBs and WCBs (Basic Protocol 2). Quality controls are described in Support Protocols 1-4.

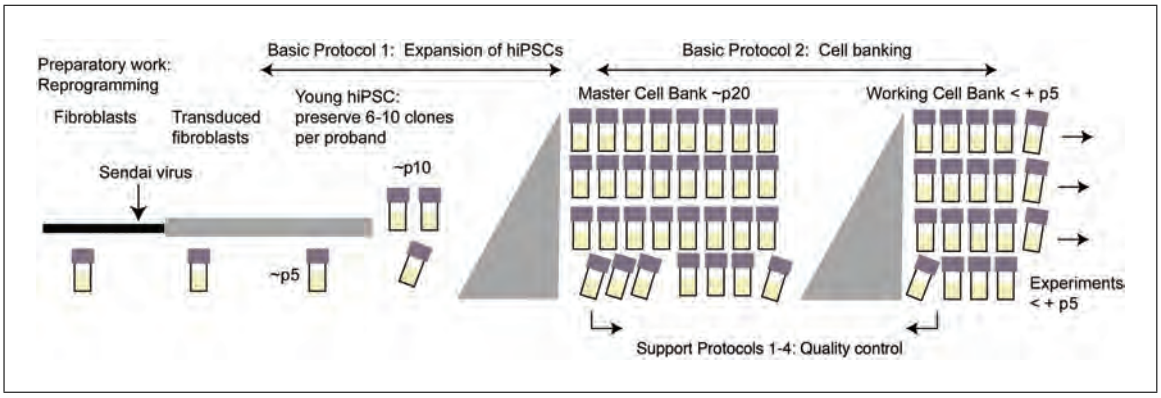

Figure 1 Strategic planning for cryopreservation. Small amounts of backup cryovials of fibroblasts, transduced fibroblasts, and 6-10 Sendai-virus-reprogrammed hiPSC clones per proband at p5-p10 are the basis for this protocol. From these, hiPSCs are expanded (Basic Protocol 1) and Master and Working Cell Banks are prepared (Basic Protocol 2). Some vials are also used for quality control (Support Protocols), and subsequently one vial is thawed for each experiment to ensure reproducible cell quality. WCBs should be prepared within less than 5 passages from MCB (<+ p5), and experiments conducted accordingly from the WCB.

NOTE: Prior approval from the local Institution Safety Board and Ethical Committee is required for research using hiPSCs. All work described in this protocol was reviewed and approved by the Ethical Committee of the University Medical Center Hamburg-Eppendorf (Az. 532/116/9.7.1991 and PV4798/21.10.2014), and all patients gave written informed consent.

NOTE: All procedures are to be performed using sterile materials in a Class II biological hazard flow hood or a laminar-flow hood, and proper aseptic technique should be used accordingly.

STRATEGIC PLANNING

This protocol was developed based on hiPSC lines derived from human dermal fibroblasts reprogrammed with Cytotune™ Sendai virus according to the manufacturer's instructions. We recommend freezing backup cryovials of fibroblasts and transduced fibroblasts, as well as backup vials of 6-10 clones per proband around passage (p) 5-10 (Fig. 1). Here we start with these uncharacterized p5-p10 hiPSC clones and end with the freezing of MCBs and WCBs around p18-p25 or p23-p30 (+ p5), respectively (Fig. 1). Quality controls are detailed in Support Protocols 1-4. The protocol can be adapted to any other reprogramming method, for example episomal transduction of reprogramming factors, by changing quality controls such as transgene clearance controls accordingly. Also, other primary cell types, such as lymphocytes or urinary cells, and other culture methods can be utilized in a similar workflow.

EXPANSION OF hiPSC

BASIC PROTOCOL 1

This protocol describes the thawing and expansion of one cryovial of an uncharacterized hiPSC clone in the range of p5-p10 to derive hiPSCs for an MCB. For details of general hiPSC culture, consult Frank, Zhang, Schöler, & Greber (2012).

Materials

Six-well plates or T75 flasks, coated with Geltrex (see recipe)
FTDA medium with and without Y-27632 (see recipe)
Washing medium (see recipe)
Reprogrammed, uncharacterized hiPSC clones, p5-p10
Y-27632 (rho kinase inhibitor) solution (see recipe)
Dulbecco's Phosphate-Buffered Saline (PBS; e.g., ThermoFisher 14190)

Accutase solution with Y-27632 (see recipe)
Trypan blue dye, optional

Water bath, 37°C
Incubator with CO_2 and N_2 gas supply with an O_2 control system set to 37°C, 90% relative humidity (rH), 5% CO_2, 5% O_2 (hypoxic condition)
Warming cabinet or other dry warming device, 37°C
Freezers, −80°C and −150°C (or liquid nitrogen)
Dry ice
Serological plastic pipets (e.g., Sarstedt 86.1685.001, 86.1254.001, and 86.1253.001)
50- and 15-ml conical centrifugation tubes (e.g., Falcon®)
Centrifuge
Nunclon® Delta Surface six-well plates and T75 flasks (ThermoFisher)
Cell counter (e.g., CASY cell counter) or Neubauer chamber

Thawing of hiPSCs

1. Prewarm water bath and incubator (with Geltrex-coated plate inside). Prewarm washing medium and FTDA (both with Y-27632) in the warming cabinet.

   1 million frozen hiPSCs can be thawed on 9.6 cm^2 in 2 ml FTDA (one well of a six-well plate); adjust plating if necessary.

2. Pick up frozen hiPSC cryovials stored in liquid nitrogen tank or −150°C freezer and transfer to the bench on dry ice. Thaw cryovial in water bath at 37°C for 2-3 min without shaking.

   The water bath is prone to causing contamination, so vials should be sprayed with 70% ethanol or isopropanol after removal from the water bath.

3. Draw up 5 ml washing medium in a pipet. Place the tip of the pipet into the cryovial, and gradually draw up the cell suspension into the washing medium inside the pipet. Slowly let cells and washing medium run down at the inner side of a 50-ml conical centrifugation tube. Centrifuge for 2 min at 200 × *g*, room temperature.

   This will result in a gradual dilution of cells and cryoprotectant in medium, which decreases the osmotic shock for the hiPSCs.

4. Aspirate supernatant, loosen cell pellet by tapping bottom of tube with finger, and resuspend carefully in FTDA medium with Y-27632. Aspirate Geltrex solution from the coated plates and plate cells.

   If hiPSC clones were reprogrammed and frozen under different conditions, thaw them in the original medium and change condition gradually after thawing: e.g., change ratio every second day from 100% to 75%, 50%, and then 25%.

5. Place the cells in an incubator under hypoxic condition at 37°C, 90% rH, 5% CO_2 and 5% O_2.

   Disperse cells equally by moving plate three times back and forth, three times side to side and let cells attach for at least 30 min before moving the plate again.

Feeding of hiPSCs

6. Monitor hiPSCs daily under the microscope.

   Check attachment of the cells to the well or flask, confluency of cell layer, cell morphology, potential beginning of spontaneous differentiation (Fig. 2), and color change of medium.

7. Prepare aliquots of FTDA medium without Y-27632, and prewarm to 37°C.

8. Aspirate most of the medium with one pipet for each cell line. Add 2-4 ml FTDA dropwise to each six-well plate.

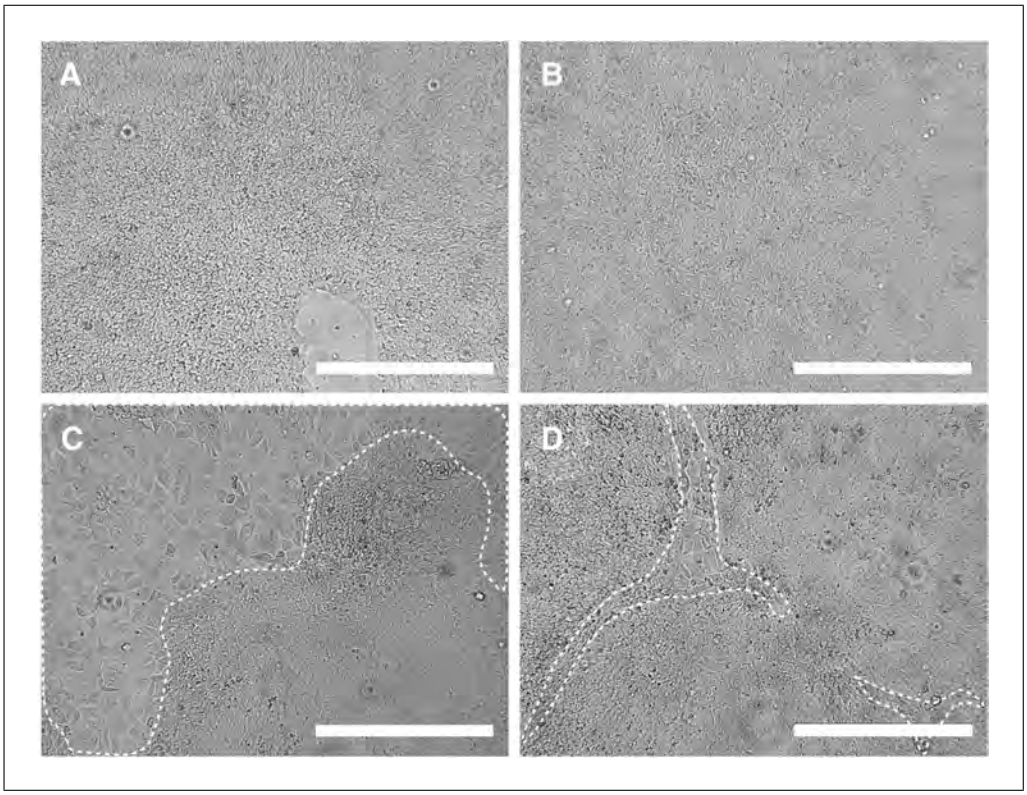

Figure 2 Morphology of hiPSCs during culture. Representative examples of 90% (**A**) and fully (**B**) confluent hiPSC cultures with homogenous good morphology. (**C**, **D**) Examples of hiPSC cultures with islands of cells that have lost stem cell morphology (differentiated hiPSCs), delineated by dashed lines.

Adjust amount of FTDA to medium consumption indicated by the color (pH) of the medium. 90%-100% confluent cells (Fig. 2A) benefit from feeding twice a day and should be passaged the next day.

9. Return the cells into the incubator.

Passaging

10. Prewarm Geltrex-coated plate, PBS, Accutase with Y-27632, and FTDA with Y-27632 to 37°C.
11. Aspirate medium, and wash with 1 ml PBS per 9.6 cm^2 (that is, per six-well plate).
12. Detach cells with 1 ml Accutase with Y-27632 per 9.6 cm^2 for 5-10 min in the incubator.

    Check cells frequently under the microscope for complete detachment.

13. Wash off cells in 2 ml washing medium per 9.6 cm^2 and transfer to a 50-ml conical centrifugation tube.

    All cells from different wells should be pooled and distributed into next passage.

14. Centrifuge 2 min at 200 × *g*, room temperature. Aspirate supernatant, loosen cells by tapping bottom of conical centrifugation tube with finger, and resuspend carefully in 500 µl to 1 ml of FTDA with Y-27632.
15. Count cells with CASY or manually with Neubauer chamber with Trypan Blue dye diluted 1:1 with cell suspension.

    Proliferation (relation of harvested and seeded cells) and viability (percent of living cells) should be documented at every passage. Viability goal for expansion phase is viability

>80%, with harvest density 2.5-3.5 × 10^5 per cm^2. For CASY counting, the aggregation factor (AGG) should be <2.1 according to settings for hiPSCs dissociated with Accutase from the manufacturer's instructions.

16. Dilute cell suspension with FTDA with Y-27632. Aspirate Geltrex solution from the coated plates, and plate cells at a seeding density of 4.5-7 × 10^4 cells per cm^2 surface.

    Plate, e.g., 400,000-650,000 cells in 2 ml FTDA per 9.6 cm^2 (one six-well plate). Depending on seeding density, the next passaging will be necessary after 3-5 days.

17. Incubate at 37°C, 90% rH, 5% CO_2 and 5% O_2, and document data.

    Data documentation includes viability, aggregation factor, cell count, and morphology.

18. Around p12-p15, scale up culture from six-well plates to T75 flasks.

    Feed with 15-30 ml FTDA depending on confluency (see steps 7 and 8), and use 7 ml Accutase to detach cells for transfer into the flask (see step 12).

BASIC PROTOCOL 2

CELL BANKING OF hiPSCS

This section describes the freezing of a master cell bank (MCB) or working cell bank (WCB).

Materials

Two to four T75 flasks of confluent (90%-100%) hiPSCs at p18-p25 (Basic Protocol 1)
Fetal bovine serum, advanced (FBS; Capricorn Scientific GmbH FBS-11A)
Accutase solution with Y-27632 (see recipe)
Washing medium (see recipe)
Freezing medium (see recipe)

Pasteur pipets, sterile, autoclaved
Incubator with CO_2 and N_2 gas supply with an O_2 control system set to 37°C, 90% relative humidity (rH), 5% CO_2, 5% O_2 (hypoxic condition)
50-ml conical centrifugation tube
Cryovials
Cryogenic storage labels or ethanol-resistant markers
Freezing container with isopropanol or freezing machine
Freezer, −80°C and −150°C (or liquid nitrogen tank)

Cryopreservation of MCB

Volumes listed below are suitable for one T75 flask. For six-well plates, adjust according to growth surface. Two T75 will usually give rise to 25-30 cryovials containing 1 million hiPSCs each.

1. Image cell morphology just before harvesting for MCB, and document.
2. Aspirate medium using a sterile, autoclaved Pasteur pipet for each cell line. Wash with 10 ml PBS per T75 flask.
3. Add 7 ml of Accutase with Y-27632 and incubate 7-10 min in incubator.

   Incubate until cells detach completely, with no scraping or tapping.

4. Resuspend cells in 10 ml washing medium. Centrifuge cells in 50-ml conical centrifugation tube for 3 min at 200 × *g*, room temperature.

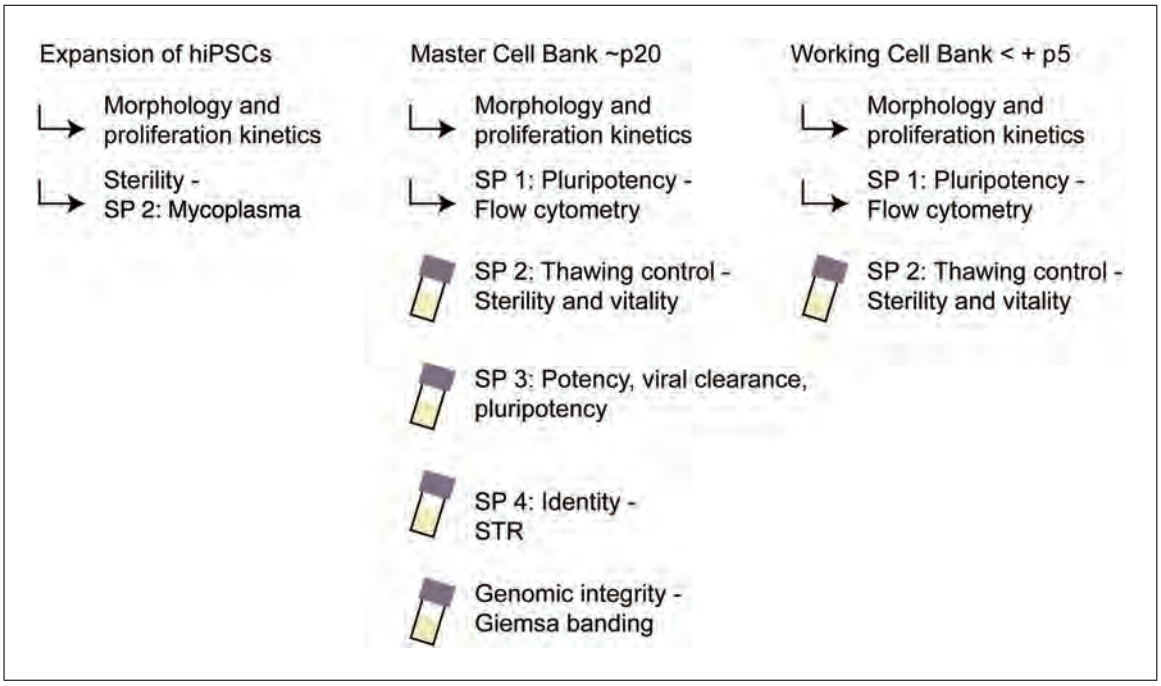

Figure 3 Overview of quality controls. Timing of quality controls is described in Support Protocols (SP) 1-4 or in Breckwoldt et al. (2017): genomic integrity, mycoplasma PCR. Basic quality control and documentation starts during the expansion of hiPSCs. Master cell banks are controlled with all hiPSC quality controls available. For a working cell bank (WCB) prepared from the master cell bank (MCB) within a few passages, quality control can be less extensive. STR, short tandem repeat.

5. Aspirate supernatant, loosen the pellet by tapping bottom of conical centrifugation tube, and carefully resuspend in 2-3 ml FBS.
6. Count cells in CASY or manually with Neubauer chamber.

   Cell count goals: AGG <2.1, viability for freezing >90%, harvest density a bit lower than for passaging, between 1.5 and 2.0 × 10^5 per cm^2, to assure exponential growth phase. Aliquot sample for pluripotency marker test on fresh cells.

   The fresh cell population just before the freezing should be examined, as the expression of surface markers might alter during freeze-thaw (see Anticipated Results).
7. Calculate the amount of freezing medium required to give a final concentration of 1 million cells per 1 ml of freezing medium.
8. Prepare fresh freezing medium (10% DMSO/90% FBS) in an extra tube in advance.

   Calculate FBS amount including the amount used for pre-suspension in the step 5, so that the final concentration of DMSO will be 10%. Add 10% extra for pipetting volume.
9. Add freezing medium to the cells. Invert and pipet very gentle, and aliquot immediately into labeled cryovials.

   Consider using printed labels. The full cell line name with clone number, passage number, MCB/WCB, and freezing date should appear.
10. Transfer MCB vials in the freezing container to a −80°C freezer and let it sit overnight. The next day, transfer to −150°C or liquid nitrogen.

    The freezing container allows gradual freezing at −1°C per minute in the −80°C freezer for the first 24 hr. Avoid moving of the container in the freezer during the freezing procedure. A controlled-rate freezing machine can be used as an alternative.
11. Document all the data in a file, and prepare detailed information in the storage list.

    Redundancy of information is helpful for detecting mistakes, e.g., with numbering.

Cryopreservation of WCB

12. Thaw 1 vial of the MCB, expand further for 3-5 passages, and cryopreserve as WCB by repeating steps 1-11 and quality controls as specified in Figure 3 (see Support Protocols 1-4) .

    Quality controls include proof of pluripotency, potency, sterility, viability, transgene clearance, and genetic stability (Fig. 3). Further forms of characterization should be added depending on project requirements.

SUPPORT PROTOCOL 1

ASSESSMENT OF STEM CELL MARKERS BY FLOW CYTOMETRY

Quantitative live stain of surface markers of stem cells and self-renewal can be done by flow cytometry. For representative results, either sample fresh hiPSCs during cell harvesting for MCB or harvest at least two passages after thawing (see Anticipated Results).

Materials

hiPSCs (Basic Protocol 1 or 2)
FACS buffer (see recipe)
FITC Mouse Anti-human TRA-1-60 (Becton Dickinson cat. no. 560876)
FITC Mouse IgM, Isotype Control (Becton Dickinson cat. no. 553474)
PE Anti-SSEA3 (Becton Dickinson cat. no. 560879)
PE Rat IgM, Isotype Control (Becton Dickinson cat. no. 553943)

Flow cytometry tubes compatible with flow cytometer
Flow cytometer and software: e.g., Canto II Flow Cytometer and Becton Dickinson FACSDiva Software 6.0

Live-cell staining for SSEA3 and TRA-1-60

1. Resuspend 1 million hiPSCs in 1 ml FACS buffer and incubate 15 min on ice.

   Process the staining as fast as possible to minimize cell death. If necessary, store hiPSCs up to 2 days in 100% FBS at 4°C or on ice.

2. Split the cell sample into two flow cytometry tubes.
3. Centrifuge 3 min at 200 × *g*, 4°C, and discard supernatant.
4. Add either PE anti-SSEA3 or FITC mouse anti-human TRA-1-60 antibody, diluted in 100 µl FACS buffer, or the respective isotype control antibodies.

   The appropriate dilutions of antibodies depend on the lot; use working concentrations recommended by the manufacturer.

5. Vortex at low speed to resuspend hiPSCs. Incubate at least 30 min on ice or at 4°C.
6. Add 2 ml FACS buffer, centrifuge 5 min at 200 × *g*, 4°C, and discard supernatant.
7. Repeat step 6 twice with 2 ml PBS.
8. Resuspend in final PBS volume that is adequate for FACS analysis (e.g., 250 µl).
9. Analyze samples by flow cytometry.

   In our hands, most hiPSC lines show >90% SSEA3-positive cells (see Anticipated Results). Cell lines with between 70% and 90% SSEA3 positivity still differentiated well; hiPSC lines with <40% SSEA3 positivity were discarded.

SUPPORT PROTOCOL 2

THAWING CONTROL—VIABILITY AND STERILITY

Controls the viability, enables hiPSC recovery, and tests for bacterial and fungal contamination (Fig. 4). We recommend thawing two vials to check the reliability of the freezing process (Hunt, 2019).

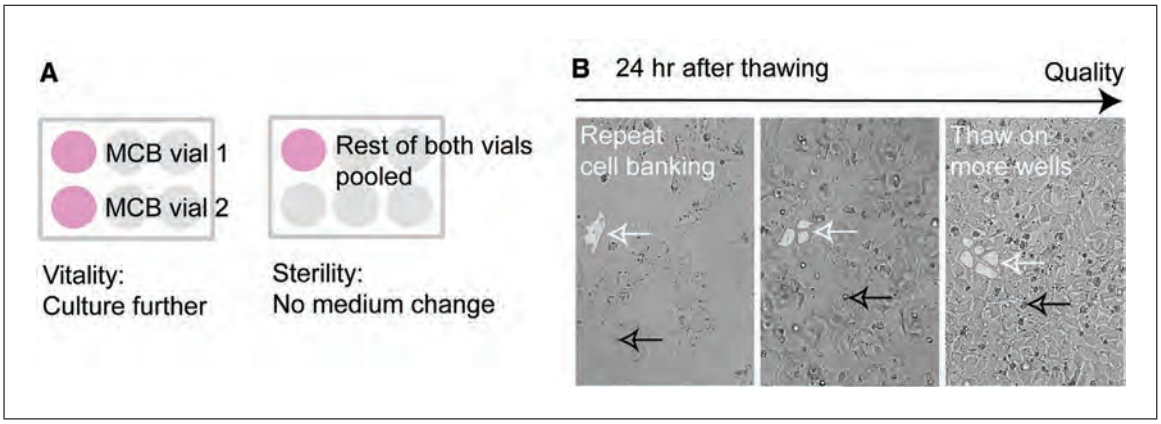

Figure 4 Thawing control to assess viability and sterility. (**A**) Schematic depiction of workflow for thawing controls (Support Protocol 2). (**B**) Photographs of hiPSCs 1 day after plating of 1 million frozen hiPSCs in one well of a six-well plate, before medium change. Black arrows indicate dead cells, white arrows cell morphology; shapes are highlighted. Left: an MCB with low confluency and mediocre cell morphology that should be discarded. Middle and right: good, cobblestone-like stem cell morphology and good confluency, the right panel can be seeded in future in two wells of a six-well plate.

Materials

Two MCB cryovials (see Basic Protocol 2, step 10)
Six-well plates, coated with Geltrex (see recipe)
FTDA with Y-27632 (see recipe)

Microscope with camera for documentation
Material for mycoplasma PCR (see Table 1 and Breckwoldt et al., 2017)

Thaw cells

1. Prepare two separate Geltrex-coated six-well plates: a sterility control plate with one six-well per clone and a viability control plate with two six-well plates per clone.
2. Thaw two MCB cryovials separately as described in Basic Protocol 1, steps 1-5, resuspending cells in 2.3 ml each of FTDA with Y-27632 (Fig. 4A).
3. On the viability control plate, plate into each well 2 ml from each MCB cryovial.
4. On the sterility control plate, pool the remaining 300 µl from both vials and add 1 ml FTDA with Y-27632.

Viability control

5. Document recovery by photographing the cell density of the viability control plate.

   Dependent on their confluency after thawing, it may be desirable to plate the hiPSCs into a larger number of wells in future, or MCB production might need to be repeated (Fig. 4B).

6. Feed hiPSCs daily, and consider subjecting them to further analysis (Support Protocols 3 and 4.

Control for bacterial and fungal contamination including mycoplasma

7. Check regularly for bacterial contamination for 10 days, without changing the medium, by monitoring medium color and potential bacterial motion under the microscope at high magnification, as well as the growth speed and morphology of hiPSCs.

Table 1 List of Primers Used in This Unit

Gene or other sequence	Function	Forward primer sequence (5′-3′)	Reverse primer sequence (5′-3′)
GUSB	Housekeeping gene	AAACGATTGCAGGGTTTCAC	CTCTCGTCGGTGACTGTTCA
Sendai virus	Reprogramming vector	GGA TCA CTA GGT GAT ATC GAG C	ACC AGA CAA GAG TTT AAG AGA TAT GTA TC
Mycoplasma	Bacterial contamination	TGC ACC ATC TGT CAC TCT GTT AAC CTC	ACT CCT ACG GGA GGC AGC AGT A
NANOG	Pluripotency endogenous	GATTTGTGGGCCTGAAGAAA	AAGTGGGTTGTTTGCCTTTG
SOX2	Pluripotency endogenous	AGTCTCCAAGCGACGAAAAA	TTTCACGTTTGCAACTGTCC
BRACHYURY (*TBXT*)	Mesoderm	TGCTTCCCTGAGACCCAGTT	GATCACTTCTTTCCTTTGCATC AAG
TNNT2	Mesoderm	TTTGGTTTGGACTCCTCCAT	CTGGAGAGAGGACGAAGACG
SOX17	Endoderm	CGCACGGAATTTGAACAGTA	GGATCAGGGACCTGTCACAC
AFP	Endoderm	AGAACCTGTCACAAGCTGTG	GACAGCAAGCTGAGGATGTC
FOXA2	Endoderm	GAGCGGTGAAGATGGAAGG	TGTACGTGTTCATGCCGTT
TUBB3	Ectoderm	GGCCAAGGGTCACTACACG	GCAGTCGCAGTTTTCACACTC
PAX6	Ectoderm	TGGGCAGGTATTACGAGACTG	ACTCCCGCTTATACTGGGCTA
SOX1	Ectoderm	ACCAGGCCATGGATGAA	CTTAATTGCTGGGGAATTGG
NCAM1	Ectoderm	ATGGAAACTCTATTAAAGTGA ACCTG	TAGACCTCATACTCAGCATT CCAGT

Usually bacterial contaminants are fast growing and clearly visible after 2-3 days, but slowly growing bacteria (e.g., Stenotrophomonas maltophilia or Burkholderia cepacia) can take 10 days to become apparent. We generally do not recommend using antibiotics in hiPSC cultures.

8. Optional: Send supernatant for sterility check.

   Hospital hygiene departments provide standardized tests and insight into the types of bacterial contamination that can help avoid recurring heavy infections.

9. After 72 hr, sample medium supernatant for detection of mycoplasma by PCR as described by Breckwoldt et al. (2017) or using an alternative commercially available mycoplasma detection test.

   Testing for potential mycoplasma contamination is also highly recommended after thawing young clones and during expansion. Sample medium supernatant of fully confluent hiPSCs to assure that the detection threshold is reached.

   The specificity and sensitivity of mycoplasma tests varies and should be validated (Nikfarjam et al., 2012). The sterility test specified in this protocol assures that cell cultures are in general aseptic. However, this does not assure sterility (Fleming et al., 2006).

SUPPORT PROTOCOL 3

POTENCY, VIRAL CLEARANCE, AND PLURIPOTENCY—SPONTANEOUS DIFFERENTIATION AND qRT-PCR

The protocol combines simple embryoid body (EB) formation with collagenase- (El-Mounayri et al., 2013) and FBS-based spontaneous differentiation medium (Fig. 5). The potency of hiPSCs in regard to differentiation into the three germ layers is examined by qRT-PCR (see Table 1; Bertero et al., 2016; Breckwoldt et al., 2017;

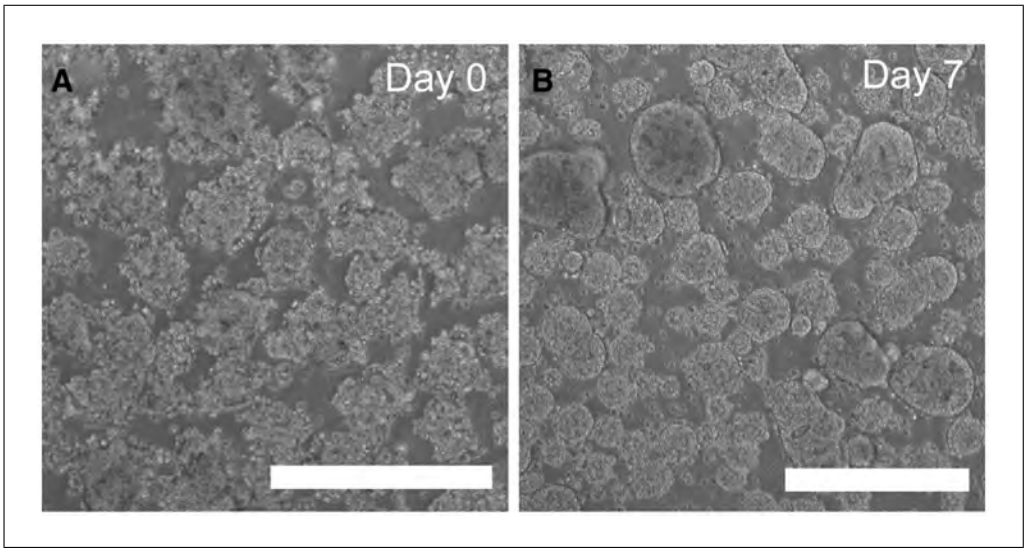

Figure 5 Embryoid-body-based spontaneous differentiation. Representative pictures of cell aggregates at day 0 directly after dissociation with collagenase (**A**) and embryoid bodies (**B**) after 7 days of culture (Support Protocol 3). Scale bars, 500 µm.

Schaaf et al., 2014). The cDNA is also used to check for viral clearance. In addition, qRT-PCR with endogenous pluripotency factors can be used to better assess markers of stem cell status and self-renewal.

Materials

Twice-passaged, almost confluent (90%-100%) hiPSCs thawed from MCB (Basic Protocol 2, step 10)
Collagenase II solution (see recipe)
EB washing medium (see recipe)
Pluronic®-127-coated T25 suspension culture flask or two wells of a six-well plate (see recipe)
EB differentiation medium (see recipe)
RNA isolation kit (e.g., RNeasy Plus Mini kit, Qiagen 74134)
cDNA reverse transcription kit (e.g., High Capacity cDNA RT Kit, Applied Biosystems)
Specific primers (see Table 1)
qPCR mix with carboxyrhodamine (ROX; e.g., Eva Green qPCR Mix, Solis BioDyne)

50-ml conical centrifugation tubes
Liquid nitrogen
Nanodrop TM ND-1000 spectrophotometer (ThermoFisher Scientific)
qPCR machine (e.g., ABI PRISM 7900HT Sequence Detection System, Applied Biosystems)

EB-based spontaneous differentiation

1. Culture hiPSCs to 90%-100% confluency.

   Feeding with FTDA 1-4 hr before starting the dissociation improves EB formation.

2. Aspirate medium, and incubate in 1 ml collagenase solution for 45 min to 2 hr until cell layer lifts off in large junks from the surface.

3. Transfer the cell suspension into a 50-ml conical centrifugation tube.

4. Rinse the wells with 1 ml EB washing medium and add to conical centrifugation tube.
5. Let cell clumps sediment and remove supernatant (first wash step).
6. Add 4 ml EB washing medium and centrifuge 3 min at 200 × *g*, room temperature.
7. Remove supernatant, and resolve the pellet by tapping the conical centrifugation with a finger. Add 4 ml differentiation medium.

   If necessary, gently triturate the cells with a 5-ml pipet to disrupt the cell chunks into smaller clusters (compare Fig. 5A).

8. Transfer 3 ml of cell suspension to a T25 flask previously coated with Pluronic® F127 and washed.
9. Transfer the remaining cell suspension into a 1.5-ml tube as the day 0 sample. Remove supernatant after a short centrifugation, snap-freeze cell pellet in liquid nitrogen, and store at −80°C.
10. Incubate T25 flask at 37°C, 90% rH, 5% CO_2 under normoxic conditions. Cell aggregation will give rise to embryoid bodies overnight (Fig. 5B).
11. Change medium with EB differentiation medium every 2-3 days, for 7 days.
12. On day 7, take sample of EBs and transfer to a conical centrifugation tube. Let this sediment, and remove supernatant so that only about 1 ml of medium with EBs is left. Transfer to a labeled 1.5-ml tube. Centrifuge 1 min at 300 × *g*, room temperature. Remove supernatant, snap freeze cell pellet in liquid nitrogen, and store at −80°C.

RT-qPCR for germ layer markers, viral clearance, and stem cell markers

13. Isolate RNA and transcribe into cDNA.

    Use, for example, the RNeasy Plus Mini Kit and High Capacity cDNA Reverse Transcription according to manufacturer's instructions. Measure RNA concentration and purity with a Nanodrop spectrophotometer.

14. Run RT-qPCR with primers for markers of each germ layer, for endogenous pluripotency genes (as listed in Table 1), and for reprogramming virus primers according to manufacturer's instructions.

    Include negative controls without addition of reverse transcriptase to detect potential genomic artifacts. Also include as positive controls samples from differentiated cells, hiPSC and transduced fibroblasts.

15. Normalize expression to household gene and evaluate expression of differentiated cells as fold of hiPSCs (day 0).

    At least one marker of all three germ layers should be upregulated, and markers of stem cell and self-renewal should be downregulated, on day 7 as compared with day 0. Sendai virus should be detectable only in transduced fibroblasts.

    Clones should be transgene free before functional experiments are conducted. If quality controls need to take place in a laboratory with biosafety level 1 (BSL1), it may be useful to verify viral clearance during expansion, as transgene clearance verification is a prerequisite for the use of S1.

SUPPORT PROTOCOL 4

IDENTITY—SHORT TANDEM REPEAT ANALYSIS

For the identity test (Fig. 6), compare the short tandem repeat (STR) profile of the proband sample (e.g., genomic DNA isolated from buffy coats of blood or buccal swab, or preserved primary cells) to that of the MCB hiPSCs. The discrimination capacity of these

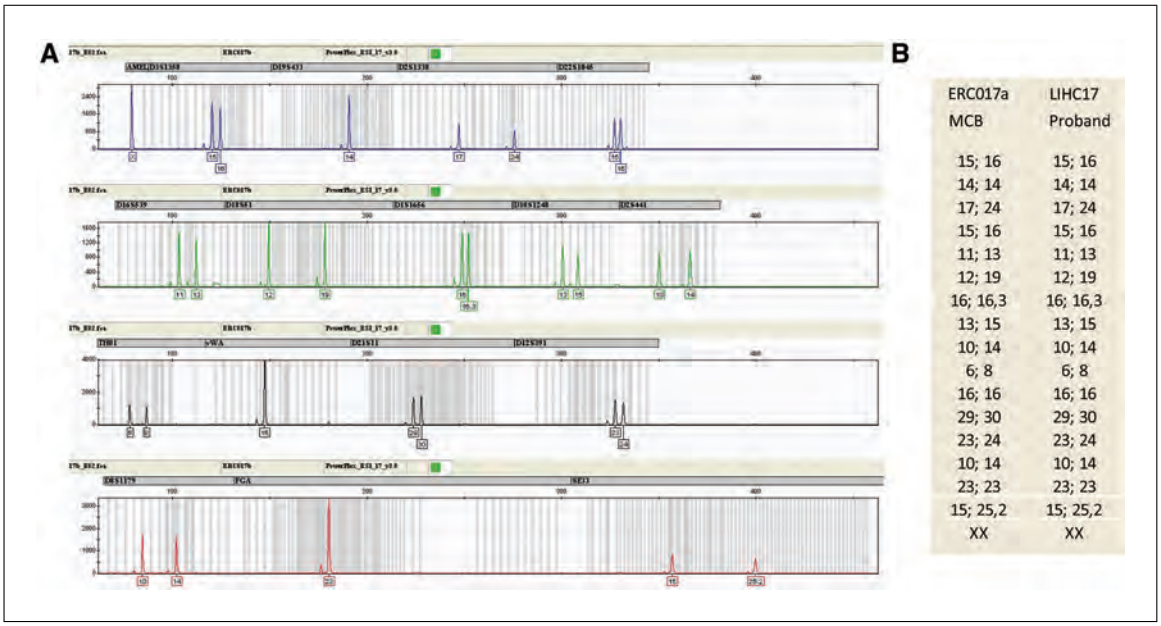

Figure 6 Identity test with short tandem repeat (STR) analysis. (**A**) Electropherogram of a representative female cell line amplified using the PowerPlex ESI17 fast multiplex kit; 16 STR loci from the European Standard Set (ESS) of STRs are depicted, plus amelogenin for sex determination. (**B**) Example of a genotype table derived from the proband sample and cell line depicted in **A**. STR loci differentiate all human beings except identical twins (see Support Protocol 4).

combined STR-loci is high enough to differentiate all human beings except for identical twins.

Materials

Proband sample (e.g., buccal swab)
MCB cryovial (Basic Protocol 2, step 10)
Chelex 100® resin (Bio-Rad 143-2832)
PowerQuant™ System (Promega PQ 5008)
PowerPlex ESI17 Fast™ PCR-amplification multiplex kit (Promega DC 1720) or comparable kit from another company (e.g., ThermoFisher, Qiagen, or Promega)
MicroAmp™ Optical Adhesive Film (Applied Biosystems 4311971)
HiDi Formamide (Applied Biosystems 4311320)
LiChrosolv water for chromatography (Merck 1.15333)

Forensic swabs (Sarstedt 80.634)
Heater, 56°C
96-well PCR plate (e.g., 96 PCR Plate half skirt, Sarstedt 72.1979.202)
ABI 7500 Realtime PCR System
ABI 3130 Genetic Analyser
Genemapper ID 3.2 (software for the identification of the alleles)

Sample preparation

1. Thaw 1 vial of MCB as described in Basic Protocol 1.

   Use a 50-ml Falcon tube in order to reach the bottom more easily.

2. Centrifuge 3 min at 200 × *g*, room temperature, aspirate medium, and take sample with swab from cell pellet at the bottom of Falcon tube.

   As the swabs are sterile, hiPSCs can be plated and utilized for further experiments.

DNA extraction: Chelex method

Chelex®100 is an ion-exchange resin that inactivates DNA destructing nucleases by removing magnesium, exposure to 100°C disrupts the cell membranes, proteins and denatures the DNA yielding single stranded DNA (Butler, 2010; Walsh, Metzger, & Higuchi, 1991).

3. Prepare a 5% suspension of Chelex®100 resin in distilled water.
4. Transfer each swap (one with proband sample, one with MCB sample) into a 1.5-ml reaction tube.
5. Add 500 µl of Chelex®100 suspension to the swab in the tube and shake several times to mix the suspension.
6. Incubate 30 min at 56°C.
7. Remove the tubes from the heater and increase the temperature to 100°C.
8. Incubate the tubes 6 min at 100°C.
9. Vortex the tubes vigorously and centrifuge 1 min at 200 × *g*, room temperature.
10. DNA in the supernatant is now ready for PCR.

    After being stored in the refrigerator for >24 hr, the DNA extract should be vortexed and centrifuged again before using.

Optional: DNA quantification

The most sensitive and specific way to quantify human DNA is real-time quantitative PCR (qPCR). Here, we use the PowerQuant™ System (Promega) and the ABI 7500 Real Time PCR System (ThermoFisher). The PowerQuant™ System simultaneously quantifies the amount of total, of male, and of degraded gDNA. DNA quantification is performed according to the manufacturer´s protocol.

11. Prepare a serial dilution of the PowerQuant™ Male gDNA Standard (provided with PowerQuant kit).

    Our standard consists of the following four concentrations: 50, 2, 0.08, and 0.0032 ng/µl (successively, undiluted; 4 µl 50 ng/µl + 96 µl dilution buffer = 2 ng/µl; 4 µl 2 ng/µl + 96 dilution buffer = 0.08 ng/µl; and 4 µl 0.08 ng/µl + 96 µl dilution buffer = 0.0032 ng/µl)

12. Prepare a reaction mix of PowerQuant™ 2× Master Mix, PowerQuant™ 20× Primer Mix, and water for the number of reactions planned plus 10%. The reaction volume is 20 µl.

    Calculate master mix with DNA samples, eight standard samples, negative (no-template) control, and 0.2 ng DNA 2800 M (provided in the PowerPlex ESI17 multiplex kit).

13. Add 18 µl of the reaction mix to the reaction wells of a 96-well PCR plate.
14. Add 2 µl of the gDNA standards the controls and the unknown DNA samples to the appropriate wells; seal the plate with MicroAmp Optical Adhesive Film. Centrifuge the plate briefly.

    Use two technical replicates for all samples.

15. Start the thermal cycling run according to the manufacturer's instructions.
16. The analysis of the raw data is performed with the HID Real Time PCR software; the data are then imported into the PowerQuant Analysis Tool and stored there.

PCR amplification of STR loci with PowerPlex ESI17 Fast™ multiplex kit (Promega)

The Multiplex Kit PowerPlex ESI 17 fast contains the 16 so-called ESS (European Standard Set of STRs) systems plus amelogenin for sex determination.

17. Prepare a reaction mix:
2 µl 5× master mix including Taq polymerase
1 µl 10× primer mix
0.5 ng template DNA
Water (amplification grade) as needed to 10 µl.

The optimal amount of template DNA for generating well-balanced STR-profiles is 0.5 ng of total template DNA.

17. Run the PCR in the thermocycler for 29 cycles according to the manufacturer´s protocol

18. Store amplified samples at 4°C until ready to perform capillary electrophoresis

Capillary electrophoresis of the PCR products on the ABI 3130 Genetic Analyzer

Five different fluorescent dyes are attached to the primers and to the size standard. The different fragment lengths of the STR alleles and the use of different fluorescent dyes allows simultaneous detection of all loci and alleles in a single run. The capillaries are 36 cm in length and are refilled with a special polymer for the separation of the alleles after each run.

19. Dilute each amplified sample by adding 30 µl of LiChrosolv® water.

20. Prepare a formamide size-standard mix (1000 µl HIDI formamide + 30 µl size standard)

Allelic Ladder ESI17, Size Standard WENILS500ESS, can be used if utilizing the PowerPlex ESI17 multiplex kit.

21. Add 13 µl of this mixture to the number of wells of a 96-well plate that are needed for the amplified samples and allelic ladder. Add 2 µl of each PCR product and 2 µl of the allelic ladder, respectively.

22. Incubate the plate 3 min at 94°C, and then cool for 3 min in a freezer at −18°C.

23. Run the plate in the ABI 3130 Genetic Analyzer according to the manufacturer's protocols.

24. Analyze the raw data with Genemapper ID 3.2 software.

REAGENTS AND SOLUTIONS

NOTE: All media are prepared under sterile conditions and, if not provided sterile by the supplier, vacuum filtered with a 0.2-µm-pore-size filtration set (TPP, 99500).

Accutase containing Y-27632

Add 10 µM Y-27632 solution (see recipe below) to freshly thawed Accutase (Sigma-Aldrich, A6964) by diluting stock solution 1:1000. Store up to 2 weeks at 4°C.

Basic fibroblast growth factor (bFGF) solution

Dissolve bFGF (PeproTech, 100-18B) to a stock concentration of 100 µg/ml in PBS (Gibco, 10010-049) containing 0.1% (w/v) bovine serum albumin (BSA). Working concentration in FTDA is 30 ng/ml. Store aliquots for up to 6 months at −80°C, or thawed aliquots up to 1 week at 4°C. Always add fresh to medium.

Collagenase type 2 solution

Dissolve collagenase type 2 (Worthington LS004176) in DMEM (ThermoFisher 41965-039) to a concentration of 200 U/ml. Incubate at room temperature for 1 hr, divide into aliquots, and store up to 1 year at −20°C. Thaw aliquots at 4°C as needed, and add 6 µl/ml DNase solution fresh before use.

DNase solution

Dissolve 100 mg DNase I, type V (from bovine spleen, Sigma-Aldrich D8764), in 50 ml PBS, and divide into 2-ml aliquots. Store the aliquots up to 1 year at −20°C.

EB differentiation medium

1× L-glutamine (ThermoFisher 25030081)
1 mM HEPES solution (see recipe)
20% fetal bovine serum advanced (FBS, Capricorn Scientific GmbH, FBS-11A)
1% non-essential amino acid (NEAA; ThermoFisher 11140-050)
0.1% 1-thioglycerol (Sigma-Aldrich M6145)
IMDM medium (ThermoFisher 12440-053)
Prepare medium fresh.

EB washing medium

RPMI containing 6 µl/ml DNase II solution and 0.5% (v/v) human serum albumin. Add DNase I fresh to the medium before use.

FACS buffer for blocking and staining (live-cell staining)

PBS supplemented with 5% fetal bovine serum advanced (FBS, Capricorn Scientific GmbH, FBS-11A). Store up to 4 weeks at 4°C.

Freezing medium

Fetal bovine serum advanced (FBS, Capricorn Scientific GmbH, FBS-11A) with 10% DMSO (Sigma-Aldrich, D8418) and 10 µM Y-27632 (1:100 stock solution). Aliquot FBS and thaw fresh for each cryobanking process. DMSO releases heat during mixing with FBS. Alternatively, use Gamma Irradiated FBS (FBS, Capricorn Scientific GmbH, FBS-GI-12A) to avoid contamination with bovine viruses, as FBS cannot be fully sterilized. In addition, use of DMSO-free medium should be considered (Awan et al., 2020).

FTDA containing Y-27632

Supplement FTDA medium with bFGF solution (see recipe), and add Y-27632 solution (see recipe) in 1:1000 dilution to a final concentration of 10 µM.

DMEM/F12 (ThermoFisher 21331-020) containing:	
L-Glutamine (ThermoFisher 25030081)	2 mM
Transferrin-selenium solution (see recipe; 1:10,000)	5 mg/L (transferrin)/ 5 µg/L (Se)
Human Serum Albumin (Biological Industries 05-720-1B)	0.10% (v/v)
Lipid mix (Sigma-Aldrich L5146)	1×
Insulin (Sigma-Aldrich I9278)	5 mg/L
Dorsomorphin (Tocris 3093)	50 nM
Activin A (R&D Systems 314-BP)	2.5 ng/ml
TGFβ1 (PeproTech 100-21C)	0.5 ng/ml
bFGF solution (see recipe; add fresh)	30 ng/ml

Supplement medium with bFGF immediately before use. FTDA without bFGF can be stored up to 2 weeks in the dark at 4°C. We do not recommend using antibiotics in hiPSC culture.

Geltrex solution and coating

Thaw Geltrex (LDEV-Free Reduced Growth Factor Basement Membrane Matrix, ThermoFisher A14132) on ice and dilute 1:100 (v/v) in cold (4°C) DMEM/F12 (ThermoFisher, 21331-020). Use this to coat six-well plate (ThermoFisher, 140675) or T75 flasks (ThermoFisher, 156472) according to manufacturers' instructions (more details is provided by the European Bank for Induced Pluripotent Stem Cells (EBiSC; see Internet Resources). Coated plates or flasks wrapped with Parafilm can be kept up to 2 week at 4°C. Warm before use and aspirate the supernatant.

HEPES, pH 7.4

Dissolve HEPES (Roth, 9105.4) in PBS to a concentration of 1 M. Adjust the pH to 7.4 with potassium hydroxide. Store up to 1 year at 4°C.

Pluronic® F-127 coating for low-attachment culture surface

Add 1 ml of 1% Pluronic® solution (see recipe) per well of a six-well plate or 2.5 ml per T25 flask at least 1 day before use, and incubate in humidified 37°C incubator for up to 2 weeks. Wash twice with PBS before use.

Pluronic® F-127 solution

Dissolve 1% Pluronic® F-127 (Sigma-Aldrich P2443) in 500 ml PBS (ThermoFisher 14190-094, [w/v]; 5 g). Store up to 1 year at 4°C.

Sodium selenite

Dissolve 382 μM sodium selenite (Sigma-Aldrich S5261) in PBS (e.g., 33 mg in 500 ml PBS). Store at 4°C for up to 1 year.

Transferrin–selenium solution

Dissolve 100 mg transferrin (Sigma-Aldrich T8158) in 2 ml sodium selenite (see recipe) and prepare aliquots of 55 μl. Store them up to 1 year at −80°C, and thaw fresh for preparation of FTDA.

Washing medium (for thawing and passaging)

DMEM/F12 (ThermoFisher 21331-020) containing 10 μM Y-27632.

Alternatively, this can be replaced by FTDA containing 10 μM Y-27632.

Y-27632 solution

Dissolve the rho kinase inhibitor Y-27632 (Biorbyt orb60104) in injection-grade water to a stock concentration of 10 mM. Store aliquots up to 1 year at −20°C, and after thawing, up to 1 week at 4°C. Working concentration is 10 μM.

COMMENTARY

Background Information

The techniques described in this protocol aim to (i) fulfill regulatory, ethical, and safety requirements for basic research; (ii) meet common quality criteria for the publication or registration of lines in registries such as hPSCreg.eu, which combine release and informational criteria that characterize the cell lines; and (iii) distinguish hiPSCs of superior versus mediocre quality for successful hiPSC-based experiments (predictive criteria).

The main safety and regulatory aspects are as follows. (i) For basic research, donor consent and viral contamination. Points to consider for donor consent, data protection, and derivation of primary cells have been discussed previously (Lomax, Hull, Lowenthal, Rao, & Isasi, 2013; Morrison et al., 2017; Orzechowski, Schochow, Kühl, & Steger, 2020). Before reprogramming, the proband or the primary cells should be tested for HIV and hepatitis (be negative on viral screening for HIV1, HIV2, HBV, and HCV by qPCR; Andrews et al., 2015). After reprogramming, MCBs free of viral reprogramming vectors (i.e., showing vector clearance in Support

Table 2 Critical Quality Checks Recommended During Expansion, on MCB and WCB level–Release Criteria

Attribute	Criteria	Analytical method	Alternatives
Proliferation	Short doubling time, <1 day	Counting cells during seeding and harvest (Basic Protocol 1)	Proliferation markers
Morphology	Cobblestone-like, small stem cells, no differentiating cells	Microscopic control (Support Protocol 2)	Automated high-content screening
Viability	>80% viable hiPSCs during expansion, >90% for freezing	CASY (Basic Protocol 1)	Trypan Blue staining, viability dye (e.g., eBioscience™ Fixable Viability Dye eFluor™ 450 65-0863-14)
Aseptic culture: mycoplasma	Mycoplasma free	PCR on supernatant of confluent or 72-hr cultured hiPSCs (Support Protocol 2; Breckwoldt et al., 2017)	Broth-agar microbiological culture method, ELISA, DNA stain test
Aseptic culture: bacteria	Contamination free	Microscopic control (Support Protocol 2)	Sterility test by membrane filtration or direct inoculation

Table 3 Additional Quality Checks Recommended on MCB Level to Meet Registration Criteria and Ensure MCB Quality

Attribute	Criteria	Analytical method(s)	Alternatives
Pluripotency	High expression of stem cell markers	Flow cytometry (Support Protocol 1) qRT-PCR (Support Protocol 3)	Pluritest, Scorecard, immunofluorescence, Taqman
Potency	Differentiation into all three germ layers	EB-based spontaneous differentiation and qRT PCR (Support Protocol 3)	Teratoma assay, directed differentiation
Genomic integrity	Normal karyotype	Metaphase cytogenetics, Giemsa banding (Breckwoldt et al., 2017)	FISH, array-CGH, sequencing, spectral karyotyping (SKY) NanoString
Identity	Genomic DNA of hiPSCs at MCB level identical to sample derived directly from donor	STR analysis (Support Protocol 4)	
Viral clearance	No detection of virus genome	Perform RT-PCR according to manufacturer's instructions (Support Protocol 4)	Depending on reprogramming method

Protocol 3) can be considered BSL-1 instead of BSL-2. (ii) Criteria for the registration of cell lines used for basic research purposes include proof of markers of stem cell status and proliferation, differentiation potency, genetic fidelity, and identity (see the Internet Resources and Key References for more detail). (iii) Which criteria are meaningful and assure successful hiPSC-based experiments strongly depends on the type of experiments being conducted in a given laboratory. However, in general, although there are incompletely pluripotent hiPSC lines with intrinsically mediocre quality, it is also possible for hiPSC lines of good quality to lose their differentiation potency during culture. Thus, we recommend evaluating certain parameters (vitality, morphology, signs of contaminations, proliferation, and maybe expression of stem cell markers; Table 2, Fig. 3) frequently during expansion for MCB, for each WCB and for critical experiments.

The assays described are commonly used standard assays that enable a cost- and labor-saving workflow to achieve minimal criteria (Table 3, Fig. 3); however, there are plenty of alternatives (Tables 2 and 3). We strongly encourage changing the quality tests

depending on the requirements of the specific projects.

To assess differentiation potential, we describe EB-based spontaneous differentiation. However, results from EBiSC indicate that hiPSCs that lack spontaneous differentiation still showed differentiation potential in all three germ layers (O'Shea, Steeg, Chapman, Mackintosh, & Stacey, 2020). Directed differentiation, on the contrary, might test very specific pathways, and the optimal assay to use is still under discussion (The International Stem Cell Initiative, 2018). For a predictive assay, most probably directed differentiation into the cell type of interest is the most meaningful readout (Liu et al., 2019).

Human iPSC lines have repeatedly been shown to be prone to accumulate genetic aberrations (Henry, Hawkins, Boyle, & Bridger, 2019; Steinemann, Göhring, & Schlegelberger, 2013; Weissbein, Benvenisty, & Ben-David, 2014), occurring during reprogramming as well as during expansion of hiPSC clones. Moreover, hiPSC have high clonality, and subclones can overgrow the culture in the course of a few passages (Brenière-Letuffe et al., 2018). We assessed karyotype by G-banding; however, genetic aberrations can be analyzed by many other methods. Examples are qPCR to detect common karyotypic abnormalities or mosaicism (Assou et al., 2020), fluorescence in situ hybridization (FISH) or spectral karyotyping (SKY; Moralli et al., 2011), and sequencing approaches (Henry et al., 2019; Kyriakides, Halliwell, & Andrews, 2018).

Global confirmation of marker of stem cell status and self-renewal with methods like Pluritest or Scorecard is clearly more informative than the use of single markers (Fergus, Quintanilla, & Lakshmipathy, 2015; Müller, 2012), but is considerably more expensive.

Cell line identity is an often-neglected part of quality control in hiPSC basic research, although data shows that between 10% and 20% of hiPSC lines are misidentified (De Sousa et al., 2017; O'Shea et al., 2020; Yaffe, Noggle, & Solomon, 2016). Here, we describe STR profiling, which is the standard for authentication of human samples (Barallon et al., 2010).

From basic to translational research: requirements for preclinical or clinical-grade hiPSC banking

The proposed workflow specifies minimal scientific and technical elements of hiPSC quality control to enable reproducibility for basic research, which might be sufficient for preclinical proof-of-concept testing. However, it would clearly fall short of the regulatory requirements needed to generate data to be submitted for regulatory approval or clinical use (see Internet Resources and Key References, below). From a technical and scientific view, the applied assays for quality control of hiPSCs for both clinical and research work are comparable. However, for clinical applications, the scope changes from more informative assays about cell line characteristics to areas including traceability, risk assessment, adventitious agent testing, critical quality attributes, product characterization, and process standardization (Creasey, Stacey, Bharti, Sato, & Lubiniecki, 2019, Crook, Hei, & Stacey, 2010; O'Shea et al., 2020; Stacey, 2009; Stacey et al., 2019). For all reagents and materials that come in contact with hiPSCs, risk-assessment procedures need to be implemented, and processes and equipment must be qualified (e.g., DQ/OQ/IQ/PQ to apply for a GMP product manufacturing license; Rehakova, Souralova, & Koutna, 2020; Shafa et al., 2020; see Internet Resources). Qualification of raw materials and bioanalytics are very different, ranging from the selection of irradiated FBS to the gas quality for incubators. The occurrence of karyotypic and other genetic abnormalities in clinical-use hiPSCs affects genetic safety, as it might result in higher teratogenicity (Merkle et al., 2017; Rebuzzini, Zuccotti, Alberto, & Garagna, 2016; Stacey et al., 2019), and there is no clear consensus regarding methods for tumorigenicity assessment (Abbot et al., 2018; Andrews et al., 2015; Liu et al., 2019; Sato et al., 2019; Stacey et al., 2013). The use of the rho kinase inhibitor described here might increase the malignant potential by inducing subchromosomal abnormalities (Bai et al., 2015).

One other important aspect is documentation: Naming hiPSCs according to the standard nomenclature specified by (Kurtz et al., 2018) and recording the most important hiPSC parameters (see Basic Protocol 1) is recommended for any hiPSCs research project. However, for any more formal quality-management systems, e.g., for Good Laboratory Practice (GLP) or the more specific Good Cell Culture Practice (GCCP), accurate and extensive records are needed (Coecke et al., 2005).

Critical Parameters

The success of the cell-banking approach depends on the quality of the preserved stem

Table 4 Troubleshooting Table

Problem(s)	Possible cause(s)	Solution(s)
Cells are not evenly distributed in culture well or flask	Poor distribution of cells during plating	Move six-well plate or flask back and forth from side to side three times to generate a wave. Check under the microscope after 30 min incubation whether cells are dispersed optimally across the well or flask surface.
Cells detach during feeding	Suboptimal coating Harsh feeding Contamination	Control Geltrex coating. Feed dropwise. Early sign of contamination.
Cell layer is less confluent than expected after 3-4 days of culture	Low seeding density due to miscounting Slow cells growth	Pool wells of the same cell line, e.g., two into one. Slow cell proliferation can be a sign of technical problems, loss of pluripotency, or contamination.For MCB production, only exponentially growing cell cultures should be used.
Medium is turbid, yellow, or pink Bacterial movement or brown molecular motion is observed	Warning signs that might indicate bacterial contamination	Eliminate infected cultures and sterilize all equipment and consumables. Quarantine all the cultures running in parallel.
Spontaneous differentiation occurs during expansion, or no recovery of bad morphology occurs	Poor quality of the original cell clone Technical problem(s) during stem cell culture	Do not proceed to MCB—use other clones. If not available, consider iPSC pool purification e.g., using magnetic-activated cell sorting (MACS) of TRA-1-60 or SSEA4.
No EB formation occurs	hiPSCs too confluent before starting collagenase treatment	Start at 90% confluency (see Figures 2A and 4B).
MCB vials have thawed	Blackout or freezer broken	Distribute MCB vials to several locations as mirror backups, ideally in another building or institution.
PCR results during STR analysis are unclear	Amount of template DNA not optimal	DNA quantification is optional, but strongly recommended, as the subsequent PCR of STR markers will give much better results.

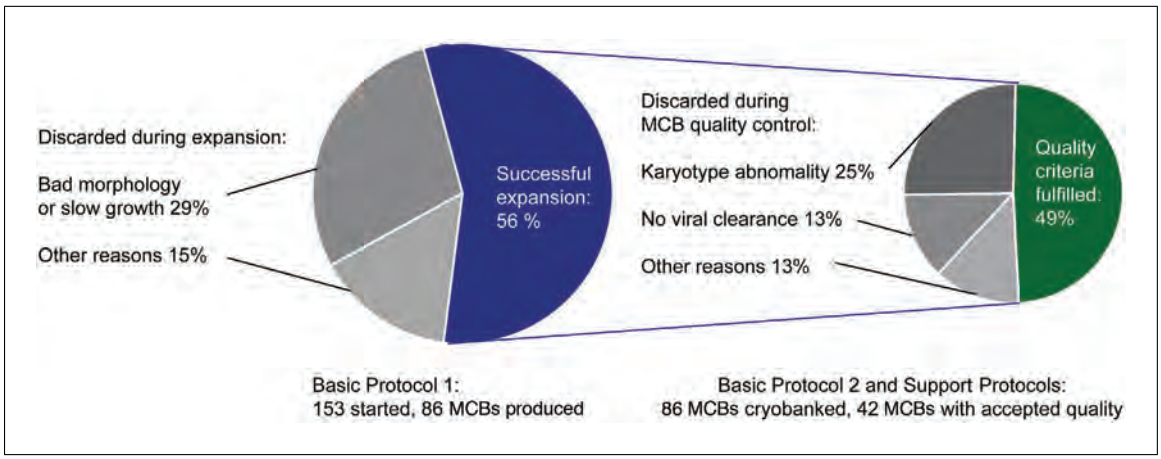

Figure 7 Expected percentages of hiPSC lines meeting all quality criteria. Shown is the number of cell lines that were discarded due to failure to reach quality criteria when utilizing this protocol as standard operating procedure to produce MCBs in the course of the IndivuHeart project (ClinicalTrials.gov identifier: NCT02417311).

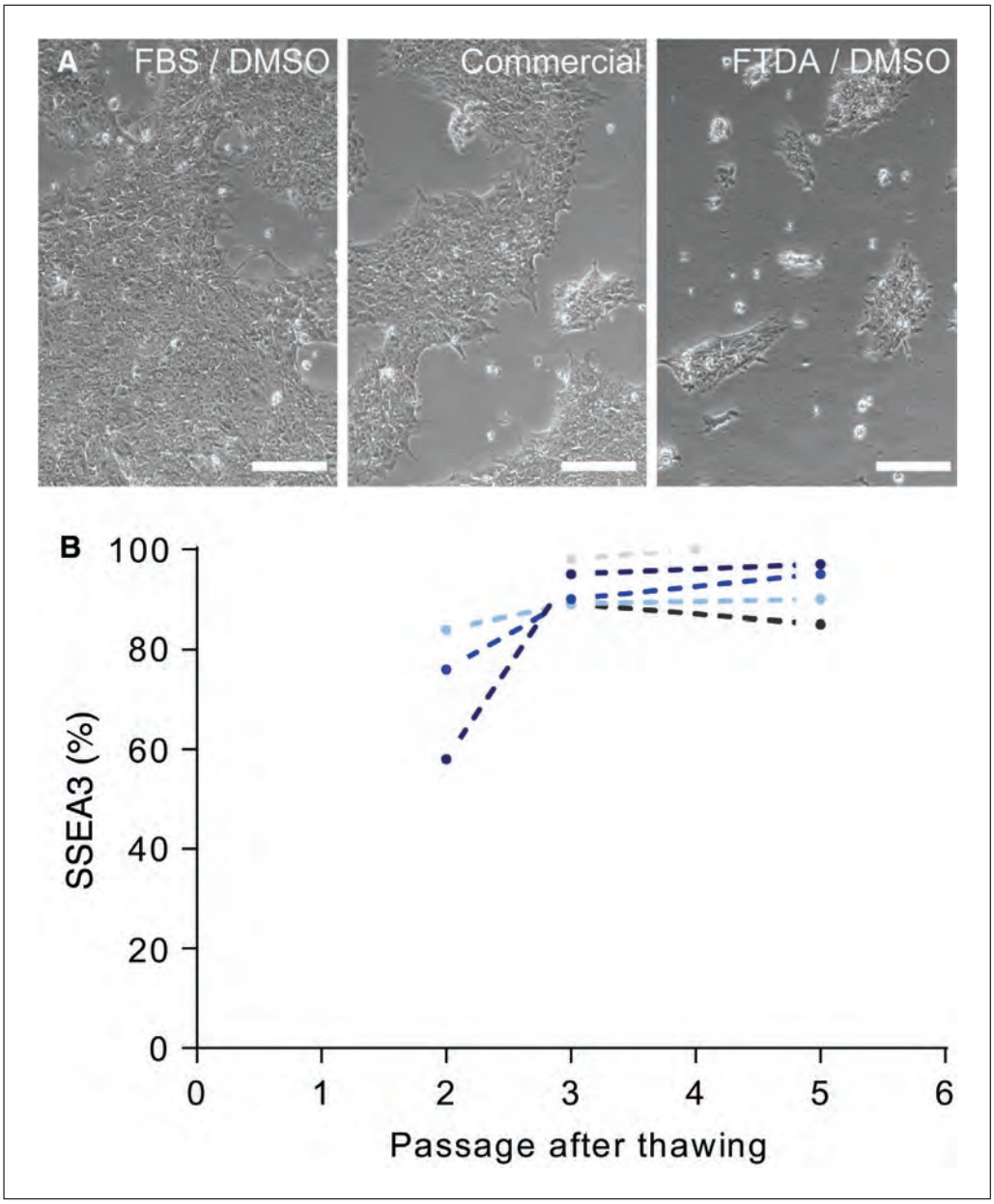

Figure 8 Recovery of pluripotency after thawing of MCB. (**A**) Batch- and time-matched comparison of freezing media, with healthy female control cell line, pictured 24 hr after thawing following medium change. Left, freezing medium (see recipe; FBS/DMSO based). Middle, representative serum-free commercial freezing medium. Right, 90% FTDA containing 10 µM Y-27632 and 10% DMSO. Bars, 600 µm. (**B**) Percentages of cells positive for the pluripotency marker SSEA3, evaluated by flow cytometry (Support Protocol 2) over the first passages after thawing the MCB. Depicted are the time courses for five clones from three healthy female donors.

cells. Most time-consuming are the quality checks at the MCB level (Table 3); thus, it is critical to preselect hiPSC lines based on the parameters specified in Table 2. We recommend freezing only fast-growing hiPSCs, as an accepted indicator for pluripotency (Kuo et al., 2020), and only cells with excellent morphology. Stringently discard lines that show evidence of spontaneous differentiation during expansion for MCB (Fig. 2). In addition, the passage number for the MCB should be kept as low as possible: On the one hand, genetic aberrations accumulate over culture time, whereas on the other hand a stable reprogramming state and full clearance of reprogramming vectors has to be ensured. Hence, passage number depends on both the reprogramming and culture methods. As the cells are passaged with high confluency two to three times per week in this protocol, cryobanking at around p20 corresponds to a comparably low number of population doublings. We found that lower passage

numbers were inferior in regard to pluripotency and (cardiac) differentiation potency and included a higher frequency of clones that retained Sendai virus (data not shown).

Troubleshooting

Table 4 lists problems that may arise with these procedures, as well as their possible causes and solutions.

Understanding Results

Only a fraction of MCB meets all quality criteria

Stringent quality controls result in many hiPSC lines that need to be discarded. We produced MCBs that met all quality criteria for 42 probands with the workflow described in this protocol. In this process, we discarded 67 clones during the expansion phase. Most of the discarded clones (65%) showed morphological signs of differentiation, and the rest slow growth, technical problems, or bacterial contamination. The first MCB passed all quality controls in only one-quarter of probands. Two MCBs had to be prepared for half of the probands and 3-5 MCBs for another quarter. The causes were mostly chromosomal aberrations (50%) or lack of Sendai virus clearance (25% of discarded clones, Fig. 7). We thus recommend thawing 3-6 young hiPSC clones per proband in parallel to account for the selection process.

Recovery of thawed hiPSCs in 2-3 passages

Cell banking relies on the fast recovery of cells after thawing. We chose 90% FBS/10% DMSO as cryopreservation medium; however, there are a variety of xeno-free commercial freezing media available. In our hands, however, FBS-based medium was superior to commercial freezing medium (as determined by batch and time matched freezing and thawing, Fig. 7A). With Basic Protocol 2 described here, hiPSCs regularly regain pluripotency and vitality within 2-3 passages after thawing (Fig. 7B), allowing experiments (e.g., directed differentiation) to be started after three passages.

Time Considerations

For an efficient workflow, parallel cell culture of six to ten hiPSC lines, typically three to six clones from two probands, is recommended. From thawing of young clones at p10 to MCB at p20, about 5 weeks with daily hands-on work need to be scheduled. In-house quality control (Support Protocols 1-4) will take about 4-6 additional weeks.

Acknowledgments

We thank June Uebeler for expert technical help with mycoplasma detection. The FACS analysis was done with support from the HEXT FACS Core unit of the UKE. Jennifer Kaiser helped with karyotype analysis. We thank Prof. Kaomei Guan for sharing the protocol for spontaneous differentiation medium and expert advice for hiPSC characterization. Dr. Boris Greber and Dr. Nicole Dubois generously provided protocols for hiPSC culture and EB formation as well as hands-on training.

This study was supported by the European Research Council (ERC-AG IndivuHeart), the Deutsche Forschungsgemeinschaft (DFG Es 88/12-1, DFG HA 3423/5-1), and the German Centre for Cardiovascular Research (DZHK). Open access funding enabled and organized by Projekt DEAL.

Author Contributions

Aya Shibamiya: Conceptualization; data curation; formal analysis; investigation; methodology; project administration; validation; visualization; writing-original draft; writing-review & editing. **Elisabeth Schulze:** Investigation; methodology; project administration; writing-review & editing. **Dana Krauß:** Investigation; methodology. **Christa Augustin:** Conceptualization; data curation; investigation; methodology; project administration; supervision; visualization; writing-original draft; writing-review & editing. **Marina Reinsch:** Investigation; methodology; validation. **Mirja Loreen Schulze:** Investigation; methodology; visualization. **Simone Steuck:** Investigation; methodology. **Giulia Mearini:** Investigation. **Ingra Mannhardt:** Investigation; methodology. **Thomas Schulze:** Investigation. **Birgit Klampe:** Investigation. **Tessa Werner:** Investigation. **Umber Saleem:** Investigation. **Anika Knaust:** Investigation. **Sandra D. Laufer:** Investigation. **Christiane Neuber:** Investigation. **Marta Lemme:** Investigation. **Charlotta Sophie Behrens:** Investigation. **Malte Loos:** Investigation. **Florian Weinberger:** Project administration; supervision; writing-review & editing. **Sigrid Fuchs:** Investigation; methodology; visualization. **Thomas Eschenhagen:** Conceptualization; funding acquisition; project administration; resources; supervision; writing-review & editing. **Arne Hansen:** Project administration; resources; supervision; writing-review & editing. **Bärbel Maria Ulmer:** Conceptualization; data curation; formal analysis; funding acquisition; investigation;

methodology; project administration; supervision; validation; visualization; writing-original draft; writing-review & editing.

Literature Cited

Abbot, S., Agbanyo, F., Ahlfors, J. E., Baghbaderani, B. A., Bartido, S., Bharti, K., … Zoon, K. (2018). Report of the international conference on manufacturing and testing of pluripotent stem cells. *Biologicals*, *56*, 67–83. doi: 10.1016/j.biologicals.2018.08.004.

Andrews, P. W., Baker, D., Benvinisty, N., Miranda, B., Bruce, K., Brüstle, O., … Zhou, Q. (2015). Points to consider in the development of seed stocks of pluripotent stem cells for clinical applications: International Stem Cell Banking Initiative (ISCBI). *Regenerative Medicine*, *10*(2 Suppl), 1–44. doi: 10.2217/rme.14.93.

Andrews, P. W., Ben-David, U., Benvenisty, N., Coffey, P., Eggan, K., Knowles, B. B., … Stacey, G. N. (2017). Assessing the safety of human pluripotent stem cells and their derivatives for clinical applications. *Stem Cell Reports*, *9*(1), 1–4. doi: 10.1016/j.stemcr.2017.05.029.

Assou, S., Girault, N., Plinet, M., Bouckenheimer, J., Sansac, C., Combe, M., … De Vos, J. (2020). Recurrent genetic abnormalities in human pluripotent stem cells: Definition and routine detection in culture supernatant by targeted droplet digital PCR. *Stem Cell Reports*, *14*(1), 1–8. doi: 10.1016/j.stemcr.2019.12.004.

Awan, M., Buriak, I., Fleck, R., Fuller, B., Goltsev, A., Kerby, J., … Stacey, G. N. (2020). Dimethyl sulfoxide: A central player since the dawn of cryobiology, is efficacy balanced by toxicity? *Regenerative Medicine*, *15*(3), 1463–1491. doi: 10.2217/rme-2019-0145.

Baghbaderani, B. A., Tian, X., Neo, B. H., Burkall, A., Dimezzo, T., Sierra, G., … Rao, M. S. (2015). CGMP-manufactured human induced pluripotent stem cells are available for preclinical and clinical applications. *Stem Cell Reports*, *5*(4), 647–659. doi: 10.1016/j.stemcr.2015.08.015.

Bai, Q., Ramirez, J. M., Becker, F., Pantesco, V., Lavabre-Bertrand, T., Hovatta, O., … De Vos, J. (2015). Temporal analysis of genome alterations induced by single-cell passaging in human embryonic stem cells. *Stem Cells and Development*, *24*(5), 653–662. doi: 10.1089/scd.2014.0292.

Barallon, R., Bauer, S. R., Butler, J., Capes-Davis, A., Dirks, W. G., Elmore, E., … Kerrigan, L. (2010). Recommendation of short tandem repeat profiling for authenticating human cell lines, stem cells, and tissues. *In Vitro Cellular and Developmental Biology - Animal*, *46*(9), 727–732. doi: 10.1007/s11626-010-9333-z.

Bertero, A., Pawlowski, M., Ortmann, D., Snijders, K., Yiangou, L., De Brito, M. C., … Vallier, L. (2016). Optimized inducible shRNA and CRISPR/Cas9 platforms for in vitro studies of human development using hPSCs. *Development (Cambridge)*, *143*(23), 4405–4418. doi: 10.1242/dev.138081.

Breckwoldt, K., Letuffe-Brenière, D., Mannhardt, I., Schulze, T., Ulmer, B., Werner, T., … Hansen, A. (2017). Differentiation of cardiomyocytes and generation of human engineered heart tissue. *Nature Protocols*, *12*(6), 1177–1197. doi: 10.1038/nprot.2017.033.

Brenière-Letuffe, D., Domke-Shibamiya, A., Hansen, A., Eschenhagen, T., Fehse, B., Riecken, K., & Stenzig, J. (2018). Clonal dynamics studied in cultured induced pluripotent stem cells reveal major growth imbalances within a few weeks. *Stem Cell Research & Therapy*, *9*(1), 165. doi: 10.1186/s13287-018-0893-2.

Butler, J. M. (2010). *Fundamentals of forensic DNA typing*. San Francisco: Academic Press. doi: 10.1016/C2009-0-01945-X.

Coecke, S., Balls, M., Bowe, G., Davis, J., Gstraunthaler, G., Hartung, T., … Stokes, W. (2005). Guidance on good cell culture practice: A Report of the Second ECVAM Task Force on good cell culture practice. *ATLA Alternatives to Laboratory Animals*, *33*(3), 261–287. doi: 10.1177/026119290503300313.

Creasey, A. A., Stacey, G., Bharti, K., Sato, Y., & Lubiniecki, A. (2019). A strategic road map to filing a Biologics License Application for a pluripotent stem cell derived therapeutic product. *Biologicals*, *59*, 68–71. doi: 10.1016/j.biologicals.2019.03.007.

Crook, J. M., Hei, D., & Stacey, G. (2010). The international stem cell banking initiative (ISCBI): Raising standards to bank on. *In Vitro Cellular and Developmental Biology - Animal*, *46*(3–4), 169–172. doi: 10.1007/s11626-010-9301-7.

De Sousa, P. A., Steeg, R., Wachter, E., Bruce, K., King, J., Hoeve, M., … Allsopp, T. E. (2017). Rapid establishment of the European Bank for induced Pluripotent Stem Cells (EBiSC) - the Hot Start experience. *Stem Cell Research*, *20*, 105–114. doi: 10.1016/j.scr.2017.03.002.

El-Mounayri, O., Mihic, A., Shikatani, E. A., Gagliardi, M., Steinbach, S. K., Dubois, N., … Husain, M. (2013). Serum-free differentiation of functional human coronary-like vascular smooth muscle cells from embryonic stem cells. *Cardiovascular Research*, *98*(1), 125–135. doi: 10.1093/cvr/cvs357.

Fergus, J., Quintanilla, R., & Lakshmipathy, U. (2015). Characterizing pluripotent stem cells using the TaqMan® hPSC scorecard™ panel. *Methods in Molecular Biology*, *1307*, 25–37. doi: 10.1007/7651_2014_109.

Fleming, D. O., & Hunt, D. L. (2006). *Biological safety: Principles and practices* (4th ed.). Washington, DC: ASM Press.

Frank, S., Zhang, M., Schöler, H. R., & Greber, B. (2012). Small molecule-assisted, line-independent maintenance of human pluripotent stem cells in defined conditions. *PLoS ONE*, *7*(7), e41958. doi: 10.1371/journal.pone.0041958.

Henry, M. P., Hawkins, J. R., Boyle, J., & Bridger, J. M. (2019). The genomic health of human pluripotent stem cells: Genomic instability and

the consequences on nuclear organization. *Frontiers in Genetics*, *10*(JAN), 623. doi: 10.3389/fgene.2018.00623.

Hunt, C. J. (2019). Technical considerations in the freezing, low-temperature storage and thawing of stem cells for cellular therapies. *Transfusion Medicine and Hemotherapy*, *46*, 134–149. doi: 10.1159/000497289.

Kim, J. H., Alderton, A., Crook, J. M., Benvenisty, N., Brandsten, C., Firpo, M., … Stacey, G. N. (2019). A report from a workshop of the international stem cell banking initiative, held in collaboration of global alliance for iPSC therapies and the harvard stem cell institute, Boston, 2017. *Stem Cells*, *37*(9), 1130–1135. doi: 10.1002/stem.3003.

Kuo, H. H., Gao, X., DeKeyser, J. M., Fetterman, K. A., Pinheiro, E. A., Weddle, C. J., … Burridge, P. W. (2020). Negligible-cost and weekend-free chemically defined human iPSC culture. *Stem Cell Reports*, *14*(2), 256–270. doi: 10.1016/j.stemcr.2019.12.007.

Kurtz, A., Seltmann, S., Bairoch, A., Bittner, M. S., Bruce, K., Capes-Davis, A., … Xu, R. H. (2018). A standard nomenclature for referencing and authentication of pluripotent stem cells. *Stem Cell Reports*, *10*(1), 1–6. doi: 10.1016/j.stemcr.2017.12.002.

Kyriakides, O., Halliwell, J. A., & Andrews, P. W. (2018). Acquired genetic and epigenetic variation in human pluripotent stem cells. *Advances in Biochemical Engineering/Biotechnology*, *163*, 187–206. doi: 10.1007/10_2017_22.

Liu, L. P., & Zheng, Y. W. (2019). Predicting differentiation potential of human pluripotent stem cells: Possibilities and challenges. *World Journal of Stem Cells*, *11*, 375–382. doi: 10.4252/wjsc.v11.i7.375.

Lomax, G. P., Hull, S. C., Lowenthal, J., Rao, M., & Isasi, R. (2013). The DISCUSS project: Induced pluripotent stem cell lines from previously collected research biospecimens and informed consent: Points to consider. *Stem Cells Translational Medicine*, *2*(10), 727–730. doi: 10.5966/sctm.2013-0099.

Merkle, F. T., Ghosh, S., Kamitaki, N., Mitchell, J., Avior, Y., Mello, C., … Eggan, K. (2017). Human pluripotent stem cells recurrently acquire and expand dominant negative P53 mutations. *Nature*, *545*(7653), 229–233. doi: 10.1038/nature22312.

Moralli, D., Yusuf, M., Mandegar, M. A., Khoja, S., Monaco, Z. L., & Volpi, E. V. (2011). An improved technique for chromosomal analysis of human ES and iPS cells. *Stem Cell Reviews and Reports*, *7*(2), 471–477. doi: 10.1007/s12015-010-9224-4.

Morrison, M., Bell, J., George, C., Harmon, S., Munsie, M., & Kaye, J. (2017). The European General Data Protection Regulation: Challenges and considerations for iPSC researchers and biobanks. *Regenerative Medicine*, *12*(6), 693–703. doi: 10.2217/rme-2017-0068.

Müller, F.-J. (2012). Assessment of human pluripotent stem cells with PluriTest. In *StemBook* (Vol. 10, Issues 2008–2012). Cambridge (MA): Harvard Stem Cell Institute. doi: 10.3824/stembook.1.84.1.

Nikfarjam, L., & Farzaneh, P. (2012). Prevention and detection of mycoplasma contamination in cell culture. *Cell Journal*, *13*, 203–212. doi: 10.22074/cellj.2012.1190.

O'Shea, O., Steeg, R., Chapman, C., Mackintosh, P., & Stacey, G. N. (2020). Development and implementation of large-scale quality control for the European bank for induced Pluripotent Stem Cells. *Stem Cell Research*, *45*, 101773. doi: 10.1016/j.scr.2020.101773.

Orzechowski, M., Schochow, M., Kühl, M., & Steger, F. (2020). Donor information in research and drug evaluation with induced pluripotent stem cells (iPSCs). *Stem Cell Research and Therapy*, *11*(1), 126. doi: 10.1186/s13287-020-01644-4.

Rao, M. S., Pei, Y., Garcia, T. Y., Chew, S., Kasai, T., Hisai, T., … Zeng, X. (2018). Illustrating the potency of current Good Manufacturing Practice–compliant induced pluripotent stem cell lines as a source of multiple cell lineages using standardized protocols. *Cytotherapy*, *20*(6), 861–872. doi: 10.1016/j.jcyt.2018.03.037.

Rebuzzini, P., Zuccotti, M., Alberto, C., & Garagna, S. (2016). Achilles' heel of pluripotent stem cells : Genetic, genomic and epigenetic variations during prolonged culture. *Cellular and Molecular Life Sciences*, *73*(13), 2453–2466. doi: 10.1007/s00018-016-2171-8.

Rehakova, D., Souralova, T., & Koutna, I. (2020). Clinical-grade human pluripotent stem cells for cell therapy: Characterization strategy. *International Journal of Molecular Sciences*, *21*, 2435. doi: 10.3390/ijms21072435.

Sato, Y., Bando, H., Di Piazza, M., Gowing, G., Herberts, C., Jackman, S., … van der Laan, J. W. (2019). Tumorigenicity assessment of cell therapy products: The need for global consensus and points to consider. *Cytotherapy*, *21*, 1095–1111. doi: 10.1016/j.jcyt.2019.10.001.

Schaaf, S., Eder, A., Vollert, I., Stöhr, A., Hansen, A., & Eschenhagen, T. (2014). Generation of strip-format fibrin-based engineered heart tissue (EHT). *Methods in Molecular Biology*, *1181*, 121–129. doi: 10.1007/978-1-4939-1047-2_11.

Seltmann, S., Lekschas, F., Müller, R., Stachelscheid, H., Bittner, M. S., Zhang, W., … Kurtz, A. (2016). hPSCreg-the human pluripotent stem cell registry. *Nucleic Acids Research*, *44*(D1), D757–D763. doi: 10.1093/nar/gkv963.

Shafa, M., Walsh, T., Panchalingam, K. M., Richardson, T., Menendez, L., Tian, X., … Baghbaderani, B. A. (2020). Long-term stability and differentiation potential of cryopreserved cGMP-compliant human induced pluripotent stem cells. *International Journal of Molecular Sciences*, *21*(1), 108. doi: 10.3390/ijms21010108.

Stacey, G. N. (2009). Consensus guidance for banking and supply of human embryonic stem

cell lines for research purposes: The international stem cell banking initiative. *Stem Cell Reviews and Reports*, *5*(4), 301–314. doi: 10.1007/s12015-009-9085-x.

Stacey, G. N. (2012). Banking stem cells for research and clinical applications. *Progress in Brain Research*, *200*, 41–58. doi: 10.1016/B978-0-444-59575-1.00003-X.

Stacey, G. N., Andrews, P. W., Barbaric, I., Boiers, C., Chandra, A., Cossu, G., … Wagey, R. (2019). Stem cell culture conditions and stability: A joint workshop of the PluriMes Consortium and Pluripotent Stem Cell Platform. *Regenerative Medicine*, *14*(3), 243–255. doi: 10.2217/rme-2019-0001.

Stacey, G. N., Crook, J. M., Hei, D., & Ludwig, T. (2013). Banking human induced pluripotent stem cells: Lessons learned from embryonic stem cells? In *Cell Stem Cell*, *13*, 385–388. doi: 10.1016/j.stem.2013.09.007.

Steinemann, D., Göhring, G., & Schlegelberger, B. (2013). Genetic instability of modified stem cells—a first step towards malignant transformation? *American Journal of Stem Cells*, *2*, 39–51.

Sullivan, S., Stacey, G. N., Akazawa, C., Aoyama, N., Baptista, R., Bedford, P., … Song, J. (2018). Quality control guidelines for clinical-grade human induced pluripotent stem cell lines. *Regenerative Medicine*, *13*(7), 859–866. doi: 10.2217/rme-2018-0095.

The International Stem Cell Initiative (2018). Assessment of established techniques to determine developmental and malignant potential of human pluripotent stem cells. *Nature Communications*, *9*, 1925. doi: 10.1038/s41467-018-04011-3.

Volpato, V., & Webber, C. (2020). Addressing variability in iPSC-derived models of human disease: Guidelines to promote reproducibility. *DMM Disease Models and Mechanisms*, *13*(1), dmm042317. doi: 10.1242/dmm.042317.

Walsh, P. S., Metzger, D. A., & Higuchi, R. (1991). Chelex® 100 as a medium for simple extraction of DNA for PCR-based typing from forensic material. *BioTechniques*, *10*(4), 506–513. doi: 10.2144/000114018.

Weissbein, U., Benvenisty, N., & Ben-David, U. (2014). Quality control: Genome maintenance in pluripotent stem cells. *The Journal of Cell Biology*, *204*(2), 153–163. doi: 10.1083/jcb.201310135.

World Health Organization. Recommendations for the evaluation of animal cell cultures as substrates for the manufacture of biological medicinal products and for the characterization of cell banks. Proposed replacement of TRS 878, Annex 1, (2010). Retrieved from https://www.who.int/biologicals/Cell_Substrates_clean_version_18_April.pdf.

Yaffe, M. P., Noggle, S. A., & Solomon, S. L. (2016). Raising the standards of stem cell line quality. *Nature Cell Biology*, *18*, 236–237. doi: 10.1038/ncb3313.

Key References

Breckwoldt et al. (2017). See above.

Description of cardiac differentiation and generation of engineered heart tissues containing some quality controls mentioned in this protocol.

Frank et al. (2012). See above.

Description of FTDA-based cell culture FTDA medium for robust long-term maintenance of diverse hPSC lines.

Andrews et al. (2015). See above.

Description of the requirements for early seed stocks of stem cell lines intended for clinical applications according to the International Stem Cell Banking Initiative (ISCBI); consensus on MCB testing is provided in the supplement.

Sullivan et al. (2018). See above.

Quality control guidelines for clinical-grade hiPSCs.

Coecke et al. (2005). See above.

Guidance on Good Cell Culture Practice.

Kurtz et al. (2018). See above.

Standard nomenclature guideline for hiPSC lines.

O'Shea et al. (2020). See above.

Recent report of lessons learned from the European Bank for Induced Pluripotent Stem Cells.

Stacey (2009). See above.

Consensus guidance for cell banking based on knowledge of embryonic stem cell.

Stacey et al. (2013). See above.

Review of lessons learned from embryonic stem cells.

Internet Resources

European registries and cell banks

hPSCreg.eu

Registry and certification of pluripotent stem cell lines (Seltmann et al., 2016). Collaboration with many partners worldwide allows a broad overview about accessible hiPSC lines.

https://ebisc.org/

European Bank for Induced Pluripotent Stem Cells, a not-for-profit iPSC bank. Source for protocols, expert support, QC testing, and hiPSC lines (De Sousa et al., 2017; O'Shea et al., 2020).

International and European societies and consortia

https://www.iscbi.org

International Stem Cell Banking Initiative providing cell banking knowledge and consensus guidance on embryonic and also hiPSC banking (Crook et al., 2010; Stacey, 2009). Regular meeting reports provide helpful updates: (e.g.: Andrews et al., 2017; Kim et al., 2019)

https://coredinates.org/

Stem Cell COREdinates is a group of core facilities working with hiPSCs sharing their expertise.

https://isscr.org

International Society for Stem Cell Research, released helpful guidelines in 2016.

https://gscn.org

German society for stem cell research.

International and European regulations

https://www.iccbba.org/home

Provides information on ISBT 128, the standard regarding terminology, identification, coding, and labeling of medical products of human origin, mandatory for cell lines intended for clinical use.

https://www.iso.org/

International Standards: Includes Organization ISO9001:2000, a general quality-management standard for provision of services and products; ISO17025, for laboratory testing and monitoring including the use of cell lines for "batch release" testing of medical products; ISO13485, for diagnostic testing procedures including the use of cells or cell-derived reference materials; and ISO34 Guide for the preparation of reference materials (Stacey, 2009).

https://www.who.int/

The "Recommendations for the evaluation of animal cell cultures as substrates for the manufacture of biological medicinal products and for the characterization of cell banks proposed replacement of TRS 878, Annex 1, 2010", providing recommendations for the characterization of cell banks.

https://eur-lex.europa.eu/

Commission Directive 2006/86/EC implementing Directive 2004/23/EC of the European Parliament and of the Council: Requirements for the coding, processing, preservation, storage, and distribution of human tissues and cells; Commission Directive 2006/17/EC implementing Directive 2004/23/EC: requirements for the donation, procurement, and testing of human tissues and cells.

Simple Workflow and Comparison of Media for hPSC-Cardiomyocyte Cryopreservation and Recovery

Duncan C. Miller,[1,2,4] Carolin Genehr,[1] Narasimha S. Telugu,[1] Silke Kurths,[1] and Sebastian Diecke[1,2,3,4]

[1]Core Facility Stem Cells, Max-Delbrück-Centrum, Berlin, Germany
[2]DZHK (German Centre for Cardiovascular Research), partner site Berlin, Berlin, Germany
[3]Berlin Institute of Health (BIH), Berlin, Germany
[4]Corresponding authors: *duncan.miller@mdc-berlin.de*; *sebastian.diecke@mdc-berlin.de*

Great progress has been made with protocols for the differentiation and functional application of hPSC-cardiomyocytes (hPSC-CMs) in recent years; however, the cryopreservation and recovery of hPSC-CMs still presents challenges and few reports describe in detail the protocols and general workflow. In order to facilitate cryopreservation and recovery of hPSC-CMs for a wide range of applications, we provide detailed information and step-by-step protocols. The protocols are simple and use common reagents. They are comprised of a fast dissociation, cryopreservation using standard equipment, and gentle recovery following thawing. We discuss various features of the protocols, as well as their utilization in the context of common hPSC-CM differentiation and application workflows. Finally, we compare two proprietary and two common in-house formulations of cryopreservation media used for hPSC-CMs, and despite differences in their price and composition find broadly similar recovery rates and cellular function after thawing. © 2019 The Authors.

Basic Protocol 1: Dissociation and cryopreservation of hPSC-CMs
Basic Protocol 2: Thawing and recovery of cryogenically frozen hPSC-CMs

Keywords: cardiomyocytes • cryopreservation • freezing media • functional recovery • human pluripotent stem cells

How to cite this article:
Miller, D. C., Genehr, C., Telugu, N. S., Kurths, S., & Diecke, S. (2020). Simple workflow and comparison of media for hPSC-cardiomyocyte cryopreservation and recovery. *Current Protocols in Stem Cell Biology*, *55,* e125. doi: 10.1002/cpsc.125

INTRODUCTION

The usability of human pluripotent stem cell-derived cardiomyocytes (hPSC-CMs) for applications within regenerative medicine, toxicology screening, and disease modelling, depends heavily on efficient reproducible bioprocesses. One of these bioprocesses is hPSC-CM cryopreservation, as it enables the generation, transportation, and application of large differentiation batches, which simplifies supply chains and should reduce variability and cost (Dunn & Palecek, 2018; Preininger, Singh, & Xu, 2016). Even on a small scale, reliable freezing and thawing of hPSC-CM batches greatly facilitates project

CURRENT PROTOCOLS
A Wiley Brand

Current Protocols in Stem Cell Biology e125, Volume 55
Published in Wiley Online Library (wileyonlinelibrary.com).
doi: 10.1002/cpsc.125

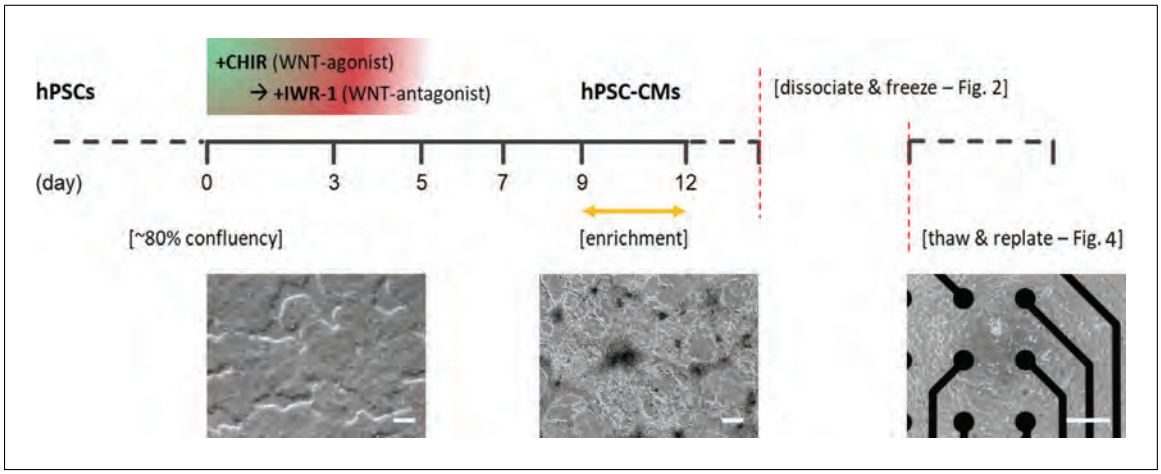

Figure 1 Overview of general hPSC-CM differentiation and handling workflow. Schematic and representative microscopy images of an hPSC-CM differentiation protocol in an adherent monolayer. Following an optional CM enrichment around days 9-12, and after at least 2 days recovery in normal CM Maintenance medium, hPSC-CMs can be dissociated and cryopreserved. They can subsequently be thawed and re-plated at a desired density for downstream application, e.g., analysis by multi electrode array (MEA). Bars = 250 µm.

management and experimental reproducibility. However, hPSC-CMs appear to be less robust towards freeze-thawing than many other cell types, with reported viable recovery rates varying greatly from 50% to 84% (Burridge, Holmström, & Wu, 2015; Chen et al., 2015; van den Brink et al., 2020; Xu et al., 2011). Over nearly a decade, various options in terms of protocols and reagents for cryopreservation have appeared, and although a few papers provide some detail or investigate the functional effects of cryopreservation on hPSC-CMs, there is not yet a consensus with regards to workflow or best practice. For more in-depth discussion please see Background Information and Understanding Results.

In this article, we outline a simple workflow for the step-by-step dissociation, cryopreservation, and functional recovery of hPSC-CMs that have been differentiated in adherent monolayer culture (Fig. 1). This can be performed without specialized equipment and should be applicable to many hPSC-CM differentiation protocols and downstream applications (see Strategic Planning). We provide analytical data, as well as a comparison of four common hPSC-CM freezing medium (Table 1; see Basic Protocol 2 "Sample data"). The protocols are as follows:

- Dissociation and cryopreservation of hPSC-CMs (Fig. 2)–includes sample data of effect of differentiation day on dissociation and freezing (Fig. 3)
- Thawing and recovery of cryogenically frozen hPSC-CMs (Fig. 4)–includes sample data of functional recovery and comparison of freezing media (Fig. 5)

STRATEGIC PLANNING

The simple workflow for cryopreservation and recovery described here is ideally integrated within the wider context of monolayer differentiation, quality control (QC), and functional application of hPSC-CMs. The most commonly used differentiation protocols including the one used in experiments here are based on small molecule inhibition of WNT signaling, which may also include a CM enrichment step (Fig. 1) (Lian et al., 2012; Tohyama et al., 2013). This cryopreservation workflow should work comparably well with hPSC-CMs generated using other similar differentiation protocols or kits (see Background Information). For generating batches of hPSC-CMs for cryopreservation, we would recommend differentiation of 1-4 multi-well plates, usually 6- or 12-well, and find that this can generate up to 2.5×10^8 cells. We and others have found several key parameters affecting hPSC-CM differentiation efficiency and yield. Batch variability in

Table 1 Overview of Selected Media for Cryopreservation of hPSC-CMs[a]

Freezing medium	Cost (100 ml)[b]	Component features	Recommended protocol[c]	hPSC-CM references[d]
CryoStor® CS10	360€	Fully defined, xeno-free, protein-free, cGMP-manufactured	None available	Chen et al. (2015); Gerbin, Yang, Murry, & Coulombe (2015); Liu et al. (2018); Xu et al. (2011)
FBS-DMSO 10%	121€	NA	None available	Breckwoldt et al. (2017); Burridge et al. (2015)
KSR-DMSO 10%	69€	Defined except for lipid rich-BSA	None available	van den Brink et al. (2020)
STEMdiff™ cardiomyocyte freezing medium	270€	Fully defined, xeno-free	Freezing density of 0.5×10^6 CMs/ml. To be used in conjunction with STEMdiff CM dissociation and maintenance kits. Pipette thawed CMs directly into resuspension medium. Viability >70% (assume trypan blue exclusion).	None available

[a] All media listed contain 10% DMSO as cryoprotective agent (CPA); see Reagents and Solutions.
[b] List price in Germany as of April 2020.
[c] Where manufacturer instructions for hPSC-CMs are available and differ from this article.
[d] Selection of primary research articles using indicated media, not including all subsequent derivative articles–see Background Information and Understanding Results for further discussion.

certain reagents, particularly B-27 and CHIR, may have significant impacts on differentiation. For several of our hPSC lines, 6 μM CHIR for the first days of differentiation works well, but across many lines and published protocols the range is 6-12 μM, and an optimal concentration often has to be determined individually for hPSC lines and specific protocols. Cell density at the start of differentiation is also very important, with ∼80% being regarded as ideal (Allen_Institute, 2018; Burridge et al., 2014; D'Antonio-Chronowska et al., 2019; Kempf et al., 2016).

Before freezing hPSC-CMs, it is important to roughly estimate the expected cell number before dissociation and have an adequate amount of medium and number of labelled cryovials and cryostorage boxes prepared before starting. As a guideline, we generate an average of $4.01 \pm 1.44 \times 10^7$ cells per 6-well plate ($n = 5$, ±SD). Similarly before thawing and re-plating hPSC-CMs, it is important to calculate how many cells are required and in what format for their downstream application and prepare sufficient media and coated plates beforehand. See Basic Protocol 2 and Table 2 for more information on coating and plating densities.

In order to determine the cell number before freezing and after thawing, cell counting including live/dead exclusion must be performed. There are various approaches and equipment available for this, which will tend to generate slightly different numbers relative to each other. It is advisable to use just one method across experiments so that numbers remain consistent. In this article we have used an automated cell counter and trypan blue exclusion; however, manual counting using a hemacytometer will work equally well, notwithstanding variability between individual users.

Table 2 Coating/media Volumes and hPSC-CM Seeding Densities for Different Cell Culture Plates[a]

Plate	cm^2/well	Coating/well	Cells/well ($\times 10^5$)	Medium/well
6-well	9.5	1.5 ml	15-30	3 ml
12-well	3.8	0.6 ml	5-10	1 ml
24-well	1.9	0.3 ml	2.5-5.0	0.5 ml
48-well	1	0.2 ml	1.0-2.0	0.3 ml
96-well	0.32	0.06 ml	0.3-0.5	0.1 ml
384-well	0.056	0.03 ml	0.04-0.08	0.05 ml
8-well chamber slide	0.78	0.2 ml	0.8-1.2	0.25 ml
48-well MEA[b]	—	0.008 ml droplet	0.3-0.5	0.3 ml

[a]Prepare Geltrex-coated plates on the day or up to 2 weeks in advance according to manufacturer's instructions (Thermo Fisher Scientific, 2013). Suggested densities should generate a fairly complete monolayer of cells 5 days following recovery from thawing (Fig. 5B). A range is indicated to allow for optimization, the lower figure being most appropriate following optimally recovered cryogenically frozen or freshly dissociated hPSC-CMs.
[b]Coating of wells and subsequent plating of hPSC-CMs in Axion Biosystems Cytoview or E-Stim+ plates must be done the same day, and may only cover the electrodes in the center of the well, hence both coating and cell plating must be done as successive 8 µl droplets, with maintenance medium topped up after 1.5-2 hr. Geltrex at half the normal dilution was found to work well. For more information refer to *https://www.axionbiosystems.com/resources*.

BASIC PROTOCOL 1

DISSOCIATION AND CRYOPRESERVATION OF hPSC-CMs

This protocol describes the careful dissociation and cryopreservation of hPSC-CMs (Fig. 2). There are several critical aspects to preserving the viability of hPSC-CMs during this process. The first is effective dissociation without degradation of the cells. This presents a challenge as often differentiating hPSC-CM monolayer cultures have a high cell density (Fig. 3A), and tend to increase the amount of extra cellular matrix proteins they secrete and cell-cell junctions they generate, which all need to be digested. The most often cited approach uses fast but powerful enzymatic dissociation, which is what is described here. An alternative is more slow but gentle dissociation, requiring different reagents and protocol (see Background Information). The next important aspect is gentle handling of the cells. Slow regular trituration generating a minimal amount of effervescence and sheer stress is strongly advised. Finally, slow but steady cooling of −1°C/min and protection against intracellular ice formation via a cryoprotective agent (CPA) is important for all conventional cell cryopreservation. Here this is handled via proprietary Mr. Frosty™ cryopreservation boxes; however, other products and even controlled rate freezing machines such as ViaFreeze™ should work well. The impact of different cryopreservation media is discussed in Basic Protocol 2 and Understanding Results.

Materials

hPSC-CMs in 6- or 12-well plates (see Fig. 1 and Strategic Planning)
CM Freezing medium (see recipe)
CM Suspension medium (see recipe)
DPBS without Ca^{2+}/Mg^{2+} (PBS^-) (e.g., Thermo Fisher, cat. no. 14190144)
TrypLE Select, 10× (Thermo Fisher, cat. no. A1217701)
Trypan blue solution (e.g., Sigma Aldrich, cat. no. T8154)

Cryogenic storage boxes (e.g., Mr Frosty™, Thermo Fisher, cat. no. 5100-0001)
37°C, 5% CO_2 incubator
15- and 50-ml Falcon™ polypropylene tubes (e.g., Corning, cat. nos. 352096 and 352070)

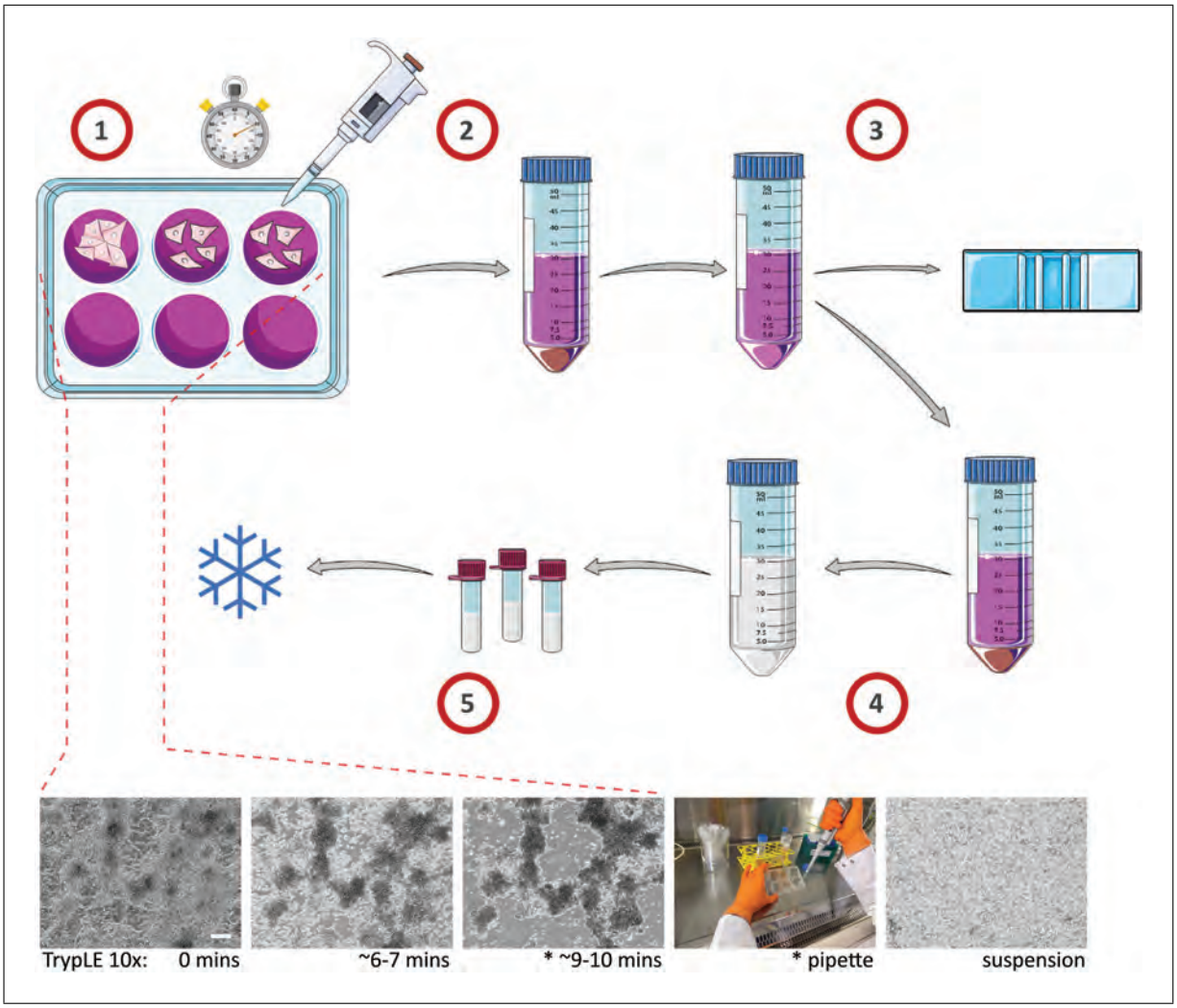

Figure 2 Schematic of hPSC-CM dissociation and freezing (Basic Protocol 1). 1.Dissociate hPSC-CMs by incubating with 10× TrypLE and gently pipetting; 2. Transfer hPSC-CMs to CM Suspension medium and centrifuge; 3.Resuspend hPSC-CMs, count and centrifuge again; 4Resuspend hPSC-CMs in CM Freezing medium; 5Transfer 0.5-1 ml cell suspension/cryovial, add to cooled cryostorage boxes and place overnight at −80°C before transferring to liquid N_2. Lower panel: Phase-contrast microscopy showing time course for dissociation of hPSC-CMs using TrypLE 10×, bar = 250 µm.

Microscope (e.g. Leica DMi1)
1000-µl manual pipette plus 1000-µl filter tips (e.g., Eppendorf, 613-0866; Biozym, cat. no. VT0270)
Centrifuge (e.g., Eppendorf 5810R, Thermo Fisher, cat. no. 10012724)
Pipette gun and 5- to 10-ml stripettes (e.g., INTEGRA Biosciences, cat. no. 156400; Sarstedt, 86.1253.001; Sarstedt86.1254.001)
Countess™ II automated cell counter (Thermo Fisher, cat. no. AMQAX1000)
Countess™ cell counting slides (Thermo Fisher, cat. no. C10228)
Cryovials (e.g., CryzoTraq 2 ml, Ziath, cat. no. 590010)

NOTE: Perform all centrifugation steps at room temperature.

NOTE: The following protocol steps are based on the dissociation and cryopreservation of 2 × 6-well plates of hPSC-CMs at around day 14 of differentiation (Fig. 3A), which would generate approximately 6–10 × 10^7 cells. Dissociation of the two individual plates is slightly staggered to reduce disparity in 10× TrypLE incubation times.

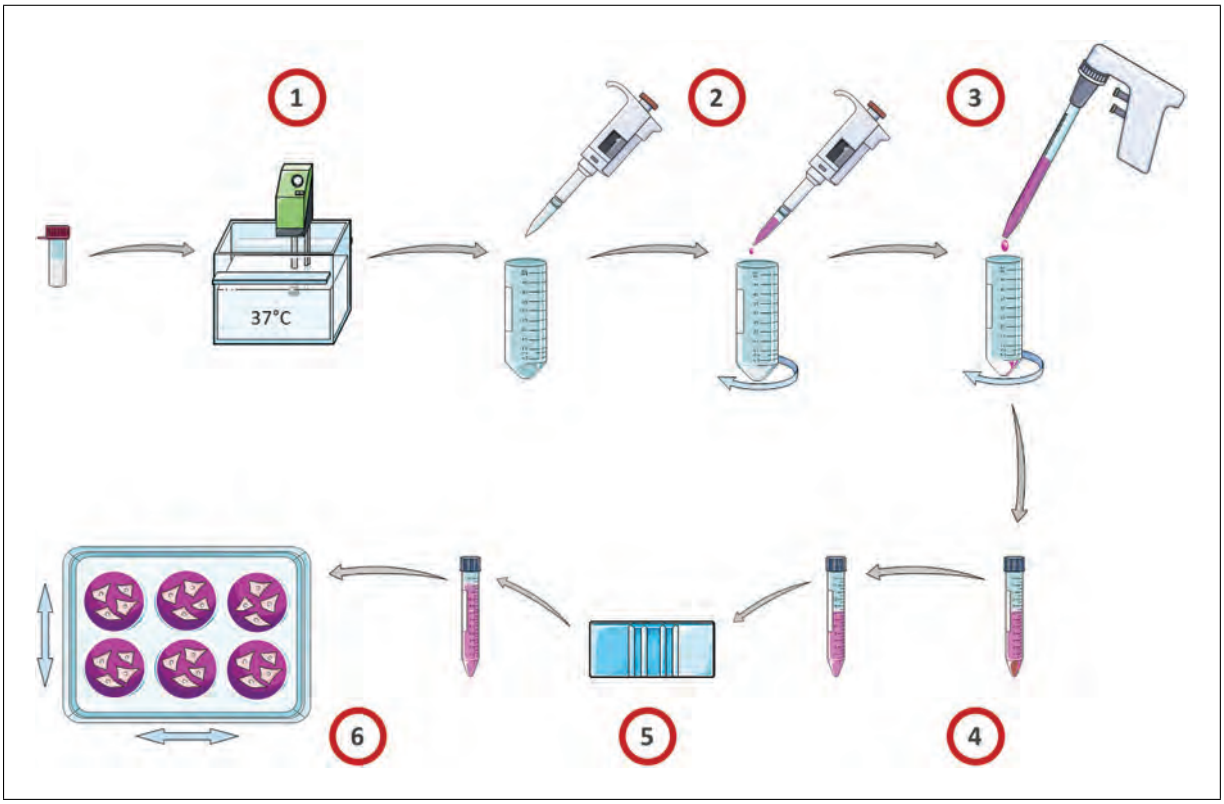

Figure 3 Schematic of hPSC-CM thawing and re-plating (Basic Protocol 2). 1. Quick thaw of hPSC-CMs in water bath; 2.Transfer thawed hPSC-CMs into 50-ml Falcon tube and slow dropwise addition of 1 ml CM Suspension medium, swirling in between; 3. Slow dropwise addition of 5 ml CM Suspension medium, swirling in between, and then transfer into 15-ml Falcon tube; 4. Centrifugation and resuspension in CM Suspension medium; 5. Cell count and adjustment of volume to desired cell density; 6. Addition to pre-coated culture plates and incubation.

1. Ensure a sufficient amount of the following reagents and equipment are pre-cooled by placing them for 30 to 60 min at 4°C before starting (if not already stored there): cryostorage boxes, CM Freezing medium.
2. Ensure a sufficient amount of the following reagents are brought to room temperature for 30-60 min before starting: CM Suspension medium, 10× TrypLE, PBS^-.
3. Aspirate culture medium from hPSC-CMs, wash wells once with 1.5 ml PBS^- each, and aspirate.
4. Add 1 ml of 10× TrypLE to each well of the first culture plate of hPSC-CMs and incubate at 37°C, 5% CO_2 (Fig. 2_1).

   NOTE: If hPSC-CM cell density is significantly lower than that shown in Figure 3A, 10× TrypLE can be slightly diluted to 5-8× using PBS^-. See Troubleshooting.
5. After 2 min, add 1 ml of 10× TrypLE to each well of the second culture plate and incubate at 37°C, 5% CO_2.

   NOTE: If a cell shaker is available in the incubator, place plates on this at a speed of 50-70 rpm, and reduce total incubation time by 1-2 min. See Troubleshooting.
6. Prepare a 50-ml Falcon tube for collection of cells, with 1.5 ml CM Suspension medium added per well.

   NOTE: For 2 × 6-well plates, add 18 ml.
7. After 6-7 min incubation, remove each plate from incubator to check under the microscope for cell rounding and loosening (Fig. 2, lower panel).

8. Replace cells in incubator and check again after 1-4 min, until almost the whole culture has rounded into individual cells and clusters, but with only a few free-floating cells or small cell clusters detached from the culture plate surface (Fig. 2, lower panel).

   CRITICAL STEP: *Judging the period of time for dissociation is a critical parameter. Different hPSC lines and differentiation protocols cause variability in the cell density and adherence; hence, total dissociation time will generally vary within the range of 8-12 min. See Troubleshooting.*

9. Remove cells from incubator and using a 1000-µl pipette, gently triturate cells in each well, tilting the plate towards you and pipetting around the far side of the well in a semi-circular motion 3-4 times, then tilting the plate away from you and pipetting around the near side of the well in a semi-circular motion 3-4 times (Fig. 2, lower panel).

   CRITICAL STEP: *Steady but gentle pipetting at this stage is crucial to dissociate the cells fully but avoid effervescence and shear stress leading to cell degradation and clumping later on. See Troubleshooting.*

10. Carefully transfer the TrypLE-cell suspension into the 50-ml collection Falcon containing CM Suspension medium.

    NOTE: *Albumin and other factors in CM Suspension medium partially quench the protease activity of 10× TrypLE.*

11. Add an additional 1 ml fresh CM suspension medium to each well and using a 1000-µl pipette gently wash and elute final remaining cells, adding them to the 50-ml collection Falcon.

Counting and Freezing

12. Centrifuge the cells for 3 min at 200 × *g*, (Fig. 2_2).

    NOTE: *We have found that lower centrifugation speeds usually pellet cells as effectively as higher speeds, and importantly help to reduce clumping of hPSC-CMs. If significant amounts of cells are still in suspension following centrifugation, perform a second centrifugation for 2-3 min at 300 × g.*

13. Aspirate the supernatant and very gently flick the bottom of the Falcon tube to help disperse the large cell pellet.

14. Carefully add 1 ml fresh CM Suspension medium directly to the cells at the bottom of the tube using a 1000-µl pipette, and gently pipette up and down several times.

15. Add an additional 9 ml CM Suspension medium to the cells using a stripette (Fig. 2_3).

    NOTE: *This step is important as a wash step to remove excess protease, as well as cellular debris, which allows a more accurate viable cell count. If significant cell clumping has occurred, it can also be more easily identified at this stage. See Troubleshooting.*

16. Invert to mix, remove a 10-20-µl sample of cells and perform a viable cell count using Trypan Blue (Fig. 3B).

    NOTE: *For Countess II, use default settings, and perform at least one and ideally two cell counts on each side of a counting chamber.*

    NOTE: *It is advisable to extract any cells required at this stage for re-plating fresh without cryopreservation, or sampling, e.g., for QC by flow cytometry (Fig. 3D).*

17. Centrifuge again for 3 min at 200 × *g*.

18. Aspirate the supernatant and resuspend hPSC-CMs in cooled CM Freezing medium to a density of 2-10 $\times$ 10^6 cells/ml, pipetting gently to mix (Fig. 2_4).

    NOTE: *For discussion on cell freezing density see Background Information.*

19. Pipette 0.5-1 ml hPSC-CM cell suspension into cryovials and place in cooled cryostorage boxes (Fig. 2_5).

20. Place cryostorage boxes at −80°C for at least 4 hr (generally overnight) before transferring cryovials to the vapor phase of liquid N_2 for long-term storage.

Sample data

Following cardiac differentiation of hPSCs (Fig. 1), we investigated the effect of dissociation and cryopreservation on hPSC-CMs. We found that the time point (differentiation day) for initial (first) dissociation may make a difference to the viability of the hPSC-CMs. In our hands, the viability of hPSC-CMs tends to decrease with a later time point for initial dissociation, day 14 tending to be better than day 21 (Fig. 3B), with a mean viability of 84% ±2.9 (SEM). Where possible we would therefore suggest an initial dissociation at an earlier time point i.e., around day 14 of differentiation (see Background Information and Understanding Results). However, dissociation and freezing of hPSC-CMs at later time points additionally to an initial dissociation at an earlier time point does not significantly affect the recovery of cells (Fig. 3C). As a general workflow, we would also recommend taking a sample of ∼1 $\times$ 10^6 cells for QC by flow cytometry following dissociation (Fig. 3D) (e.g., see Berg Luecke, Waas, & Gundry, 2019). Together these data and simple protocol should facilitate the preparation and handling of hPSC-CMs for dissociation and cryopreservation at specified time points during differentiation.

BASIC PROTOCOL 2

THAWING AND RECOVERY OF CRYOGENICALLY FROZEN hPSC-CMs

Similar to many other cell types, maintaining good recovery and viability of hPSC-CMs during thawing is dependent on a controlled but fast thaw and a gentle resuspension in culture medium (Fig. 4). For hPSC-CMs, slow dropwise resuspension using a relevant culture medium is particularly important for avoiding osmotic shock and maintaining viability (see Background Information).

Cryopreserved cells should be kept frozen until all downstream steps for thawing and recovery have been prepared first. Most importantly this includes coated cell culture plates for the downstream application of the cells. Differentiated hPSC-CMs can be re-plated at specified densities onto different types of cell culture plate (Table 2) coated with various forms of extra cellular matrix (ECM). Re-plating can be done either immediately following dissociation or after thawing from cryopreservation. In our hands, Geltrex is largely equivalent to Matrigel and works well for applications where a complete monolayer is desired, including on glass and plastic bottom plates, and those containing electrodes. Fibronectin is also widely used, especially where a lower density of cells on glass bottom plates is required, e.g., for patch clamping. Other ECMs such as Laminin-221/211 are known to work.

Materials

Geltrex (Thermo Fisher, cat. no. A1413302)
DMEM/F-12 (Thermo Fisher, cat. no. 11330032)
CM Suspension medium (see recipe)
Dry ice *or* liquid nitrogen
Cryovials of cryopreserved hPSC-CMs (see Basic Protocol 1)
RevitaCell™ Supplement 100× (Thermo Fisher, cat. no. A2644501)
CM Maintenance medium (see recipe)
Trypan blue solution (e.g., Sigma Aldrich, cat. no. T8154)

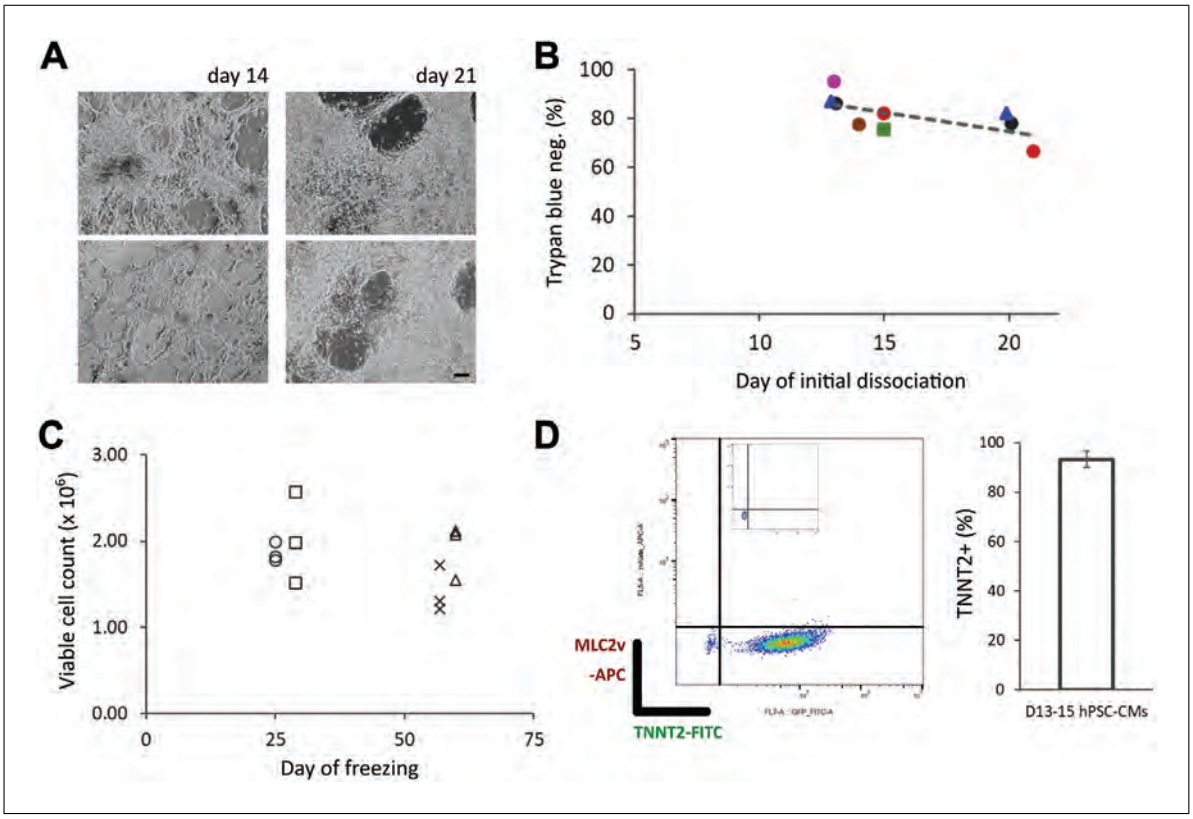

Figure 4 Effects of dissociation and cryopreservation time points on hPSC-CMs. (**A**) Phase-contrast microscopy of hPSC-CM monolayers at day 14 or 21 of differentiation prior to initial dissociation. Bar = 100 µm. (**B**) Viability staining with trypan blue following initial dissociation of hPSC-CMs at different time points during differentiation. Points represent individual differentiation experiments from three different hPSC lines (represented by circles, triangles or squares), except for red, blue, and black, which are corresponding experiments dissociated at different time points. Regression analysis showed $R^2 = 0.45$, with a coefficient $y = -0.016\times + 107$ ($p = 0.048$), indicating that around half the change in viability is due to day of dissociation. (**C**) Cell recovery following freezing and thawing of hPSC-CMs at different time points during differentiation. hPSC-CMs had been dissociated and re-plated at an earlier time point (~days 12-16) and subsequently dissociated a second time before freezing at 3×10^6 cells/vial using CryoStor CS10. Mean recovery = $1.8 \times 10^6 \pm 0.13$ cells/vial ±SEM (60%), $p = 0.22$ (one-way ANOVA). (**D**) Representative flow cytometry plot and mean CM marker expression in dissociated fixed hPSC-CMs at day 13-15 of differentiation. Inset shows isotype control staining. hPSC-CMs from this differentiation batch were cryopreserved using different cryopreservation media, see Figure 5C. Mean TNNT2 expression at days 13-15 across multiple differentiation batches and lines was 94.3% ± 2.7 ($n = 5$, ±SEM).

Multi-well culture plates (e.g., 24-well, Greiner Bio-One, cat. no. 662160)
Parafilm® M sealing film (Sigma, cat. no. P6543-1EA)
Isothermal ice bucket (e.g., Fisherbrand™ Polyurethane Ice Buckets, Fisher Scientific, cat. no. 11324085)
Water bath (e.g., VWR, cat. no. 462-0554)
1000-µl manual pipette plus 1000-µl filter tips (e.g., Eppendorf, cat. no. 613-0866; Biozym, cat. no. VT0270)
15- and 50-ml Falcon™ polypropylene tubes (e.g., Corning, cat. nos. 352096 and 352070)
Pipette gun and 5-10-ml stripettes (e.g., INTEGRA Biosciences, cat. no. 156400; Sarstedt, 86.1253.001; Sarstedt86.1254.001)
Centrifuge (e.g., Eppendorf 5810R, Thermo Fisher, cat. no. 10012724)
37°C, 5% CO_2 incubator
Countess™ II automated cell counter (Thermo Fisher, cat. no. AMQAX1000)
Countess™ cell counting slides (Thermo Fisher, cat. no. C10228)

Table 3 Volumes of CM Suspension Medium Required for the Resuspension of hPSC-CMs Immediately After Thawing[a]

No. cryovials	Volume frozen cells	Volume initial resuspension	Top up volume
1	0.5-1 ml	1 ml	5 ml
2	1-2 ml	2 ml	8 ml

[a]The volume of initial resuspension is to be added dropwise using a 1000 pipette-µl, with the top up volume subsequently added dropwise using a 5-10-ml stripette.

NOTE: *Perform all centrifugation steps at room temperature.*

NOTE: *Follow safety guidance when handling cryogenically frozen material and liquid N_2 storage containers.*

NOTE: *The following protocol steps are intended for defrosting 1× or simultaneously 2× cryovials of hPSC-CMs pooled into one Falcon tube (see Table 3).*

Thawing and Resuspension

1. Dilute Geltrex using DMEM/F12 and prepare Geltrex-coated plates according to manufacturer's instructions (Thermo Fisher Scientific, 2013), ensuring adequate numbers of desired wells/plates are incubated at 37°C 60 min before thawing cells (see Table 2).

   NOTE: *Plates can be prepared up to 2 weeks beforehand and stored at 4°C after sealing with Parafilm.*

   NOTE: *Ensure no area of the culture surface is allowed to dry out following Geltrex coating or during storage.*

2. Allow an adequate volume of CM Suspension medium to reach room temperature for 30-60 min before thawing cells (Tables 2 and 3).

3. Using dry ice or liquid nitrogen, collect cryovial(s) of cryopreserved hPSC-CMs from liquid N_2 and bring to cell culture.

4. Perform a quick thaw in a 37°C water bath. Occasionally gently swirl tubes in the bath, avoiding immersion above the level of the cap. Continue until about 90% defrosted (Fig. 4_1).

5. Sterilize the tube exterior before taking into laminar flow hood e.g., by wiping with 70% ethanol solution.

6. Using a 1000-µl pipette with 1000-µl pipette tip, remove cells from cryovial(s) and gently pipette into the bottom of a 50-ml conical Falcon tube.

   NOTE: *Check the lids of cryovials as some models can retain large droplets of medium.*

7. Using a fresh 1-ml pipette, add 1 ml CM Suspension medium to the cryovial to recover any last microliters of leftover cells.

   NOTE: *If defrosting 2× vials, pipette the same 1 ml of CM Suspension medium from one vial into the other.*

8. Using the same pipette tip, take up the 1 ml of CM Suspension medium now in the cryovial.

9. Dropwise and slowly, add the recovered 1 ml of CM Suspension medium into the 50-ml Falcon tube, aiming for about 1-2 drops every 3-5 s, gently swirling between (Fig. 4_2).

   CRITICAL: *Slow resuspension of hPSC-CMs is crucial to avoid osmotic shock.*

NOTE: *If thawing 2× cryovials, repeat this dropwise addition of 1 ml medium to the Falcon again (Table 3).*

10. Using a stripette and pipette gun, add an additional 5 ml CM Suspension medium to the cells dropwise and slowly, again aiming for several drops every 3-5 s, swirling between (Fig. 4_3).

    NOTE: *If thawing 2× cryovials, an additional 8 ml rather than 5 ml should be added (Table 3).*

11. Transfer the cell suspension into a 15-ml Falcon tube.

Counting and Replating

12. Centrifuge for 3 min at 300 × *g*, and aspirate the supernatant (Fig. 4_4).

13. Gently resuspend the cell pellet in half the amount of CM Suspension medium + RevitaCell (1% v/v) corresponding to the cell density/number of wells desired (see Table 2).

    NOTE: *This allows precise adjustment of cell density later, since the recovery of cells from frozen is 50%-70% (Fig. 3C; Fig. 5A)*

    NOTE: *If using a different kind of medium for general hPSC-CM maintenance, it may be a suitable alternative for CM Suspension medium from this point provided RevitaCell or another kind of anti-apoptosis inhibitor is added prior to plating, see Background Information.*

14. Perform a cell count including trypan blue live/dead staining using Countess II and counting slides, followed by an adjustment of the volume using CM Suspension medium + RevitaCell (1% v/v) to the desired cell density (Fig. 4_5).

15. Remove Geltrex coating solution from intended culture plates and add the cell suspension to Geltrex-coated wells (Fig. 4_6).

    NOTE: *For most hPSC-CM applications, plates should be gently rocked side to side then back and forth at this point to distribute the cells evenly across the well; however, for MEA plates this is not advised (Table 2).*

16. Incubate the cells at 37°C, 5% CO_2.

17. The next day, change medium to CM Maintenance medium (Table 2).

18. Continue culturing hPSC-CMs in CM Maintenance medium for at least 5 days before use in downstream applications (Fig. 5B-E), changing medium every 2 to 3 days.

Sample data

By following Basic Protocols 1 and 2 described here, a hPSC-CM recovery rate of between 50% and 70% can generally be expected (Fig. 3C; Fig. 5A). We investigated potential differences between certain cryopreservation media (Table 1). In our hands, different media appear to have only marginal effects on hPSC-CM viability and recovery. An exhaustive study would be required; however, in a limited study we find that viability and recovery upon thawing are comparable between four common freezing media (Fig. 5A), with a coupled spontaneously contracting monolayer exhibiting typical hPSC-CM morphology forming after 5 days (Fig. 5B), and similar levels of CM marker expression (Fig. 5C). We further investigated the three more chemically defined freezing media (Table 1) and found recovered hPSC-CMs to have a similar intracellular morphology and expression of cytoskeletal components and cardiac markers (Fig. 5D), as well as a comparable electrophysiological profile (Fig. 5E). These data show that the workflow outlined here in combination with potentially any of the four media tested can provide effective

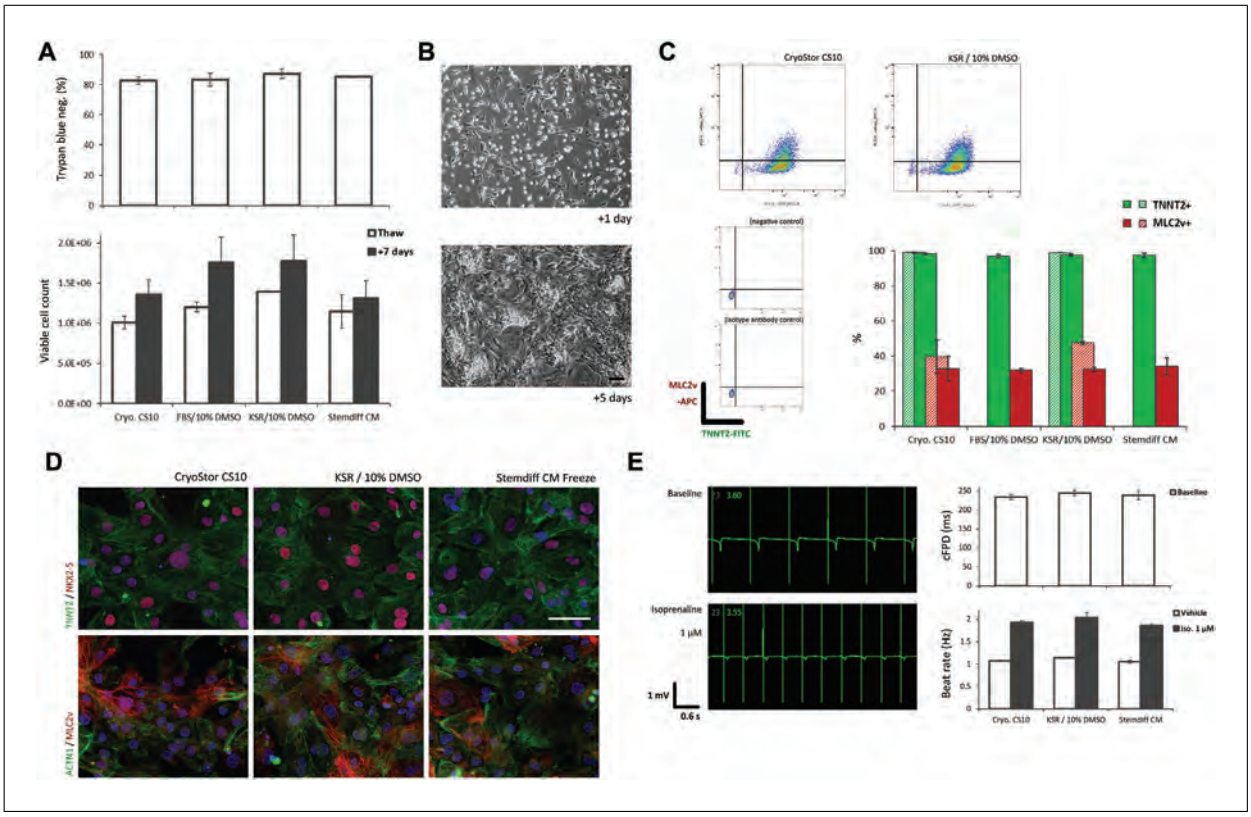

Figure 5 Comparison of hPSC-CM viability, recovery, marker expression, and electrophysiological function following thawing from different cryopreservation media. (**A**) Viability and recovery of thawed hPSC-CMs frozen at differentiation day 13 in 1 ml of cryopreservation medium at 2×10^6 cells/vial. N = 1× differentiation experiment with 3× vials per condition, error bars ±SD. (**B**) Phase-contrast microscopy of hPSC-CMs one or 5 days following thawing. Bar = 100 µm. (**C**) Representative flow cytometry plots and mean CM marker expression in dissociated fixed hPSC-CMs 7 days following thawing from different cryopreservation media. Negative control used was undifferentiated hPSCs. Differentiation experiments using two different lines BIHi005-A (striped) and BIHi050-A (block) are shown, N = 3× vials per line/condition, error bars ±SD. (**D**) Immunofluorescence microscopy of hPSC-CMs fixed and immunostained 5 days following thawing from different cryopreservation media. Blue nuclear counterstain was performed using DAPI. Bar = 100 µm. (**E**) Analysis of hPSC-CM field potential (FP) using Axion Biosystems MEA and CytoView 48-well plate 5 days following thawing from different cryopreservation media. After recording baseline spontaneous contraction, 1 µM isoprenaline or equivalent vehicle was added and contraction analyzed. Correction of FP duration was done using Fridericia's formula (cFPD). N = 1× cryovial across 4× wells per cryopreservation medium, subsequently divided into 2× wells each for vehicle or drug, error bars ±SD.

cryopreservation and functional recovery of hPSC-CMs. Please see Background Information and Understanding Results for further discussion.

REAGENTS AND SOLUTIONS

CM Freezing media

- CryoStor™ CS10 (Stem Cell Technologies, cat. no. 07930)
- FBS/10% DMSO: –Fetal bovine serum (FBS) heat-inactivated (Thermo Fisher, cat. no. 16140071); Dimethyl sulfoxide (DMSO; Sigma-Aldrich, cat. no. D2650). It is recommended to defrost stock FBS and divide into 9- or 36-ml aliquots and freeze for up to 3 months at −20°C. Defrost a 9- or 36-ml FBS aliquot until it reaches room temperature, and then add 1 or 4 ml DMSO (10% v/v) and invert to mix. Store complete medium for up to 2 weeks at 4°C.
- KSR/10% DMSO: –It is recommended to defrost stock KSR and divide into 9- or 36-ml aliquots and freeze for up to 3 months at −20°C. Defrost a 9- or 36-ml KSR aliquot until it reaches room temperature, and then add 1 or 4 ml DMSO (10% v/v) and invert to mix. Store complete medium for up to 2 weeks at 4°C.

- STEMdiff™ Cardiomyocyte Freezing Medium (Stem Cell Technologies, cat. no. 05030).

CM Maintenance medium

Add 10 ml B-27 supplement (Thermo Fisher, cat. no. 17504044) to 490 ml RPMI basal medium (Thermo Fisher, at. no. 11875-093) (2% v/v) and invert to mix. Alternatively, for less frequent use, defrost and divide 10 ml of B-27 supplement into 1-ml aliquots and freeze for up to 3 months at −20°C, and then defrost a 1-ml aliquot and add to 49 ml RPMI basal medium. Store complete medium up to 2 weeks at 4°C.

CM Suspension medium

Add 4 ml KnockOut™ serum replacement (KSR; Thermo Fisher, cat. no. 10828028) to 36 ml CM Maintenance medium (10% v/v; see recipe) and invert to mix. Store complete medium up to 2 weeks at 4°C.

COMMENTARY

Background Information

Two fundamental aspects of hPSC-CM bioprocessing for downstream applications are efficient reproducible differentiation and viable cryopreservation. In general, and particularly for diverse smaller scale research applications of hPSC-CMs, the simplicity of the workflows for these processes greatly facilitates their utilization. While simple hPSC-CM differentiation protocols have become much more precise and efficient (Denning et al., 2016), there is a slight dearth of improvement and understanding with regards to cryopreservation. The review by Preininger and colleagues is a helpful navigator (Preininger et al., 2016). Among the publications that do openly report or specifically investigate cryopreservation of hPSC-CMs, as noted in the Introduction, there are widely varying rates of recovery (Burridge et al., 2015; Chen et al., 2015; van den Brink et al., 2020; Xu et al., 2011), and anecdotally recovery rates tend to be lower. Early reports also cryopreserved hPSC-CMs that had been differentiated at a lower purity and consistency (Xu et al., 2011); hence, their methods and recovery rates may not be wholly applicable now. A high recovery rate of 84% ±5.2 is reported by Chen and colleagues; however, hPSC-CMs were differentiated as 3D clusters in stir tank bioreactors and dissociated using a two-step protocol (see below; Chen et al., 2015). Few studies address the potential effects of cryopreservation on hPSC-CMs with detailed analysis, and to our knowledge there are no in-depth comparisons of cryopreservation media. One report by Brink and colleagues investigates the effect of cryopreservation on the electrophysiology and transcripts of two hPSC lines (van den Brink et al., 2020). Interestingly, they find that following cryopreservation there is mostly no effect on key electrophysiological parameters, although one hPSC line did exhibit slight increases in ventricular, ion channel, and cytoskeletal marker expression compared with non-cryopreserved hPSC-CMs (van den Brink et al., 2020).

The reagents and techniques comprising the workflow described here derive from in-house development, as well as a variety of contemporary protocols and guidelines. The inclusion of KSR in CM Suspension and Freeze media is likely to be beneficial to hPSC-CMs by bolstering B-27 in terms of survival factors (e.g., insulin and transferrin), and increasing the amount of protein via bovine serum albumin (BSA), which among other things will help to quench protease activity following dissociation with 10× TrypLE. Slow dropwise resuspension as a way of avoiding osmotic shock to hPSC-CMs immediately following thawing is noted as critical in several protocols and papers (e.g., Breckwoldt et al., 2017; NCardia, 2018; van den Brink et al., 2020). RevitaCell is a pro-survival supplement commonly used in hPSC culture to avoid anoikis during single-cell passaging, containing a Rho-associated kinase (ROCK) inhibitor and anti-oxidant factors. The application of RevitaCell or some other pro-survival supplement for the first day following re-plating of hPSC-CMs by us and others (Breckwoldt et al., 2017; van den Brink et al., 2020) is partly based on observations by Laflamme et al., whereby inclusion of a pro-survival cocktail increased engraftment size of hESC-CMs in rat hearts (Laflamme et al., 2007). Although we have not rigorously compared hPSC-CM recovery after re-plating with or without RevitaCell, we would nonetheless

recommend inclusion of some kind of pro-survival supplement in the medium on the day of thawing.

Viability and recovery of hPSC-CMs using this workflow should be comparable when using other commercial kits, published differentiation protocols, and CM maintenance medium (e.g., from NCardia, Cellular Dynamics, or Miltenyi) (Allen_Institute, 2018; Birket et al., 2015; Burridge et al., 2014). However, it is advised to follow manufacturer guidelines where available and adjust media and conditions to optimize processes. A small amount of variability can also be expected. This can derive from differences between hPSC lines, differentiation protocols, the cellular composition (CMs vs. non-CMs) of individual differentiation batches, as well as other technical details such as reagent batches and individual user technique. There are certain adjuncts to the protocols that we have also observed as potentially beneficial for cell viability and recovery although they have not been rigorously tested. In particular–addition of DNase I during dissociation with 10× TrypLE to reduce clumping and increase viability; a higher cell freezing density of $>10 \times 10^6$ cells/ml and/or a freezing volume <0.5 ml/vial to provide a more consistent freezing rate, although there is slightly conflicting data regarding this (see Preininger et al., 2016). Furthermore, the use of controlled rate freezing machines such as ViaFreeze may also offer significant benefits; however, this again would require further optimization, as well as an increased financial outlay.

An alternative to the fast dissociation protocol described here exists in the form of a longer two-stage protocol. hPSC-CM monolayers or 3D clusters are partially dissociated slowly by incubating in collagenase type I (Sigma) in PBS^+/20% FBS or Liberase (Roche) plus DNase I for 20-60 min, followed by a quick final digestion with trypsin-EDTA or TrypLE for 3-10 min (Berg Luecke et al., 2019; Chen et al., 2015; Mills et al., 2017). This protocol may confer one advantage in reducing the total time exposed to strong protease activity, which may be beneficial in particular for 3D clusters due to the increased density and gradient of exposure to the dissociation solution. However, a strong protease step is still required, and the workflow is more complex. Unfortunately to our knowledge there are no available direct comparisons between the two approaches.

Critical Parameters

There are several critical parameters influencing dissociation, cryopreservation, and thawing of hPSC-CMs that can each be individually addressed to maximize recovery of cells. The dissociation time with 10× TrypLE can be adjusted based on the cell density and availability of a cell shaker, and will vary based on the hPSC line, and differentiation protocol and time point. Gentle initial pipetting to dissociate the cells in TrypLE, as well as handling in subsequent steps is also important to avoid shear stress. Cell clumping as a result of excessive cell death and subsequent release of DNA and other cellular debris can be reduced by using a cell shaker during dissociation, reducing pipetting, and including DNase I. Different hPSC lines and differentiation protocols will exhibit varying amounts of cell clumping. If it does occur, use of a 70-100-μm cell strainer can partially rescue the situation. A steady rate of freezing is crucial to cryopreservation of all cells, hence all parts of the protocol especially equipment and freezing medium must be well prepared and pre-cooled, and the process conducted in a time-efficient manner. A fast thaw combined with a slow regulated resuspension avoiding osmotic shock is also crucial to maintaining viability when recovering hPSC-CMs.

Troubleshooting

See Table 4 for troubleshooting possible problems encountered during the protocols.

Understanding Results

In this article, we have described a simple workflow for the dissociation, cryopreservation, and recovery of hPSC-CMs. We have also investigated aspects of these protocols, including the effects of differentiation day and cryopreservation media. We hope this will provide a benefit for users in standardizing and simplifying hPSC-CM workflows, in order to improve reproducibility in downstream applications.

A key parameter used in this report and those discussed above is hPSC-CM viability. We use trypan blue exclusion as an indicator of viability throughout the workflow, i.e., how many cells are degraded and/or apoptotic and no longer exclude trypan blue. Viability can also be assessed by immunostaining and flow cytometry. The values derived from these two methods can slightly differ, given the different mechanism, sensitivity, and timing of the two

Table 4 Troubleshooting

Problem	Possible causes	Potential solutions
Severe cell clumping following dissociation of hPSC-CMs	• Cell line or differentiation protocol • Excessive pipetting	• Addition of DNase I (Stem Cell Technologies) to TrypLE/dissociation solution • Use cell shaker and/or increase TrypLE incubation time by 1-4 min to improve dissociation and reduce pipetting • Following centrifugation and resuspension, pass clumped cell suspension through 70-100-µm cell strainer into a fresh Falcon tube, and gently wash strainer through with 5-10 ml CM Maintenance medium
Dense monolayers or clusters of hPSC-CMs not dissociating	• Cell line or differentiation protocol	• Wash twice with 2 ml PBS^- per well before dissociation • Use cell shaker to improve dissociation • If clumps detach whole, transfer into 50-ml Falcon together with 3-6 ml TrypLE and place in 37°C water bath for 8-12 min until dissociated, gently swirling every 2 min
Low viability upon cell count following dissociation	• Excessive pipetting • Excessive incubation time in TrypLE	• Increase TrypLE incubation time by 1-4 min and reduce pipetting • Reduce TrypLE incubation time by 1-4 min and/or dilute TrypLE to 5-8× with PBS^-
Poor functional recovery after thawing	• Problem with reagent(s) • Problem with cryopreservation box or storage arrangement	• Check reagent batches and expiry dates • If cryostorage boxes use isopropanol, check and replace with fresh. Check freezer temperatures, ensure cold chain handling from −80°C to liquid N_2 is maintained, store cryovials in vapor phase of liquid N_2

procedures; however, in practice it is quicker and cheaper to generate an indicative number by trypan blue.

We observe a tendency to lose viability with later days for initial dissociation of hPSC-CMs (Fig. 3B). This may be due to the increase in cell density and cell-cell junctions that likely occurs with a longer period in differentiation culture (Fig. 3A), requiring longer incubation in TrypLE and/or more pipetting to dissociate. A preference for dissociating hPSC-CMs earlier to apply to more complex 3D cultures is emerging, as this may be beneficial for their maturation and functional fidelity in these contexts due to a maturation window which cells pass through soon after lineage commitment (Breckwoldt et al., 2017; Mills et al., 2017; Ronaldson-Bouchard et al., 2018). Together these observations and trends would suggest that dissociation and cryopreservation of hPSC-CMs at around day 14 of differentiation would be a good general workflow for many hPSC-CM applications. It should be noted; however, that for some applications this would then require a longer time in culture subsequent to thawing and re-plating, since older hPSC-CMs even in simple monolayer cultures exhibit a slightly more mature transcriptional and functional profile (Kumar et al., 2019), which may be important for certain assays. Interestingly, we have observed a phenomenon whereby raised expression in MLC2v (MYL2) can be seen at ∼day 21 following dissociation and re-plating of hPSC-CMs at ∼day 14, with or without cryopreservation (compare Fig. 3D and Fig. 5C), with negligible expression of MLC2v at day 21 in parallel hPSC-CMs left un-split (data not shown). This would suggest that initiation of a more mature ventricular CM identity requires dissociation and re-plating. This may be due to space restriction in differentiation cultures before dissociation and re-plating, or perhaps because dissociation and re-plating permits increased cell-cell junction and syncytia formation between hPSC-CMs.

In terms of differences between the four media we have tested for cryopreservation of

hPSC-CMs, the data presented here, as well as our general observations indicate that they are largely comparable despite markedly different formulations. This may be partly due to the fact they all contain the same CPA and are applied with an optimized workflow. Our investigation does not eliminate the possibility that repeated, or more in-depth analyses may reveal some differences, e.g., at the metabolic or transcriptional level. However, any such differences may also be temporary given the brief period the cells are present in cryopreservation media. That said, we excluded FBS/10% DMSO from downstream functional analysis for several reasons. Although it has a long standing as a basis for cryopreservation medium, and is still used in some protocols and by many groups, it suffers from several drawbacks compared to the other three media investigated here–it is not the cheapest, it is the most likely to suffer from batch variability and price fluctuations, some effects on hPSC-CM function when included in maintenance medium have been observed (Dambrot et al., 2014), and it is more difficult to convert to current good manufacturing practice (cGMP).

We have studied the applicability of four common cryopreservation media in this report but would like to note several other observations and options. Despite being by far the most widely used CPA, it is acknowledged that DMSO can have some detrimental effects on cells in culture (Verheijen et al., 2019). We compared 5% rather than 10% DMSO in KSR- or FBS-based freezing media; however, found this resulted in poorer recovery of hPSC-CMs and/or a slight negative impact on TNNT2 expression (data not shown). Similarly, we found BamBanker less good for recovery of hPSC-CMs (data not shown), as noted in Burridge et al. (2015). Other media such as Synth-a-freeze, StemMACS CryoBrew, and NutriFreeze may be viable options for hPSC-CM cryopreservation but require testing.

Conclusion

Application of this simple workflow should allow cryopreservation of hPSC-CM batches with a recovery of up to 70% with no specialized or expensive equipment. The four different cryopreservation media tested here appear to give similar results in terms of critical parameters for hPSC-CM recovery and function. Cost and compatibility of media components then need to be considered for the downstream application of cells.

Time Considerations

Basic Protocol 1: ∼30 min preparation, 45-60 min handling.

Basic Protocol 2: ∼60 min preparation (including pre-coating of plates), ∼45 min handling.

Acknowledgments

This work was supported by funding from the DZHK (German Centre for Cardiovascular Research), partner site Berlin, Standortprojekt 81Z0100101. We would also like to acknowledge the use of several pieces of artwork as part of Figure 2 and 4 from Servier Medical Art (*https://smart.servier.com/*), obtained and used under a Creative Commons Attribution 3.0 Unported License (*https://creativecommons.org/licenses/by/3.0/*). Open access funding enabled and organized by Projekt DEAL.

Author Contributions

Duncan C. Miller: Conceptualization; data curation; formal analysis; investigation; methodology; project administration; resources; supervision; validation; visualization; writing-original draft; writing-review & editing. **Carolin Genehr:** Investigation; methodology; project administration; resources; validation; writing-review & editing. **Narasimha S. Telugu:** Investigation; methodology; writing-review & editing. **Silke Kurths:** Investigation; methodology; resources. **Sebastian Diecke:** Conceptualization; funding acquisition; resources; supervision; writing-review & editing.

Literature Cited

Allen_Institute. (2018). *Cardiomyocyte Differentiation Methods v1.2*. Retrieved from https://www.allencell.org/methods-for-cells-in-the-lab.html.

Berg Luecke, L., Waas, M., & Gundry, R. L. (2019). Reliable protocols for flow cytometry analysis of intracellular proteins in pluripotent stem cell derivatives: A fit-for-purpose approach. *Current Protocols in Stem Cell Biology*, *50*(1), 1–26. doi: 10.1002/cpsc.94.

Birket, M. J. J., Ribeiro, M. C. C., Kosmidis, G., Ward, D., Leitoguinho, A. R. R., van de Pol, V., … Mummery, C. L. L. (2015). Contractile defect caused by mutation in MYBPC3 revealed under conditions optimized for human PSC-cardiomyocyte function. *Cell Reports*, *13*(4), 733–745. doi: 10.1016/j.celrep.2015.09.025.

Breckwoldt, K., Letuffe-Brenière, D., Mannhardt, I., Schulze, T., Ulmer, B., Werner, T., … Hansen, A. (2017). Differentiation of cardiomyocytes and generation of human engineered heart tissue. *Nature Protocols*, *12*(6), 1177–1197. doi: 10.1038/nprot.2017.033.

Burridge, P. W., Holmström, A., & Wu, J. C. (2015). Chemically defined culture and cardiomyocyte differentiation of human pluripotent stem cells. *Current Protocols in Human Genetics*, *87*, 21.3.1–21.3.15. doi: 10.1002/0471142905.hg2103s87.

Burridge, P. W., Matsa, E., Shukla, P., Lin, Z. C., Churko, J. M., Ebert, A. D., … Wu, J. C. (2014). Chemically defned generation of human cardiomyocytes. *Nature Methods*, *11*, 855–860. doi: 10.1038/nMeth.2999.

Chen, V. C., Ye, J., Shukla, P., Hua, G., Chen, D., Lin, Z., … Couture, L. A. (2015). Development of a scalable suspension culture for cardiac differentiation from human pluripotent stem cells. *Stem Cell Research*, *15*(2), 365–375. doi: 10.1016/j.scr.2015.08.002.

D'Antonio-Chronowska, A., Donovan, M. K. R., Young Greenwald, W. W., Nguyen, J. P., Fujita, K., Hashem, S., … Frazer, K. A. (2019). Association of human iPSC gene signatures and X chromosome dosage with two distinct cardiac differentiation trajectories. *Stem Cell Reports*, *13*(5), 924–938. doi: 10.1016/j.stemcr.2019.09.011.

Dambrot, C., Braam, S. R., Tertoolen, L. G. J., Birket, M., Atsma, D. E., & Mummery, C. L. (2014). Serum supplemented culture medium masks hypertrophic phenotypes in human pluripotent stem cell derived cardiomyocytes. *Journal of Cellular and Molecular Medicine*, *18*(8), 1509–1518. doi: 10.1111/jcmm.12356.

Denning, C., Borgdorff, V., Crutchley, J., Firth, K. S. A., George, V., Kalra, S., … Young, L. E. (2016). Cardiomyocytes from human pluripotent stem cells: From laboratory curiosity to industrial biomedical platform. *Biochimica et Biophysica Acta - Molecular Cell Research*, *1863*(7), 1728–1748. doi: 10.1016/j.bbamcr.2015.10.014.

Dunn, K. K., & Palecek, S. P. (2018). Engineering scalable manufacturing of high-quality stem cell-derived cardiomyocytes for cardiac tissue repair. *Frontiers in Medicine*, *5*(APR)doi: 10.3389/fmed.2018.00110.

Gerbin, K. A., Yang, X., Murry, C. E., & Coulombe, K. L. K. (2015). Enhanced electrical integration of engineered human myocardium via intramyocardial versus epicardial delivery in infarcted rat hearts. *PLoS ONE*, *10*(7), e0131446. doi: 10.1371/journal.pone.0131446.

Kempf, H., Olmer, R., Haase, A., Franke, A., Bolesani, E., Schwanke, K., … Zweigerdt, R. (2016). Bulk cell density and Wnt/TGFbeta signalling regulate mesendodermal patterning of human pluripotent stem cells. *Nature Communications*, *7*, 13602. doi: 10.1038/ncomms13602.

Kumar, N., Dougherty, J. A., Manring, H. R., Elmadbouh, I., Mergaye, M., Czirok, A., … Khan, M. (2019). Assessment of temporal functional changes and miRNA profiling of human iPSC-derived cardiomyocytes. *Scientific Reports*, *9*(1), 1–16. doi: 10.1038/s41598-019-49653-5.

Laflamme, M. A., Chen, K. Y., Naumova, A. V., Muskheli, V., Fugate, J. A., Dupras, S. K., … Murry, C. E. (2007). Cardiomyocytes derived from human embryonic stem cells in prosurvival factors enhance function of infarcted rat hearts. *Nature Biotechnology*, *25*(9), 1015–1024. doi: 10.1038/nbt1327.

Lian, X., Hsiao, C., Wilson, G., Zhu, K., Hazeltine, L. B., Azarin, S. M., … Palecek, S. P. (2012). Robust cardiomyocyte differentiation from human pluripotent stem cells via temporal modulation of canonical Wnt signaling. *Proceedings of the National Academy of Sciences*, *109*(27), E1848–E1857. doi: 10.1073/pnas.1200250109.

Liu, Y. W., Chen, B., Yang, X., Fugate, J. A., Kalucki, F. A., Futakuchi-Tsuchida, A., … Murry, C. E. (2018). Human embryonic stem cell-derived cardiomyocytes restore function in infarcted hearts of non-human primates. *Nature Biotechnology*, *36*(7), 597–605. doi: 10.1038/nbt.4162.

Mills, R. J., Titmarsh, D. M., Koenig, X., Parker, B. L., Ryall, J. G., Quaife-Ryan, G. A., … Hudson, J. E. (2017). Functional screening in human cardiac organoids reveals a metabolic mechanism for cardiomyocyte cell cycle arrest. *Proceedings of the National Academy of Sciences of the United States of America*, *114*(40), E8372–E8381. doi: 10.1073/pnas.1707316114.

NCardia. (2018). Pluricyte ® Cardiomyocytes. In *user manual*. Retrieved from https://ncardia.com/files/documents/manuals/PluricyteCardiomyocyte_Manual_v2.pdf.

Preininger, M. K., Singh, M., & Xu, C. (2016). Cryopreservation of human pluripotent stem cell-derived cardiomyocytes: Strategies, challenges, and future directions. In *Advances in Experimental Medicine and Biology*. doi: 10.1007/978-3-319-45457-3_10 .

Ronaldson-Bouchard, K., Ma, S. P., Yeager, K., Chen, T., Song, L. J., Sirabella, D., … Vunjak-Novakovic, G. (2018). Advanced maturation of human cardiac tissue grown from pluripotent stem cells. *Nature*, *556*(7700), 239–243. doi: 10.1038/s41586-018-0016-3.

Thermo Fisher Scientific. (2013). *Geltrex® hESC-qualified Ready-To-Use Reduced Growth Factor Basement Membrane Matrix*. Retrieved from https://tools.lifetechnologies.com/content/sfs/manuals/geltrex_ready_to_use_man.pdf.

Tohyama, S., Hattori, F., Sano, M., Hishiki, T., Nagahata, Y., Matsuura, T., … Fukuda, K. (2013). Distinct metabolic flow enables large-scale purification of mouse and human pluripotent stem cell-derived cardiomyocytes. *Cell Stem Cell*, *12*(1), 127–137. doi: 10.1016/j.stem.2012.09.013.

van den Brink, L., Brandão, K. O., Yiangou, L., Mol, M. P. H., Grandela, C., Mummery, C. L., … Davis, R. P. (2020). Cryopreservation of human pluripotent stem cell-derived cardiomyocytes is not detrimental to their molecular and functional properties. *Stem Cell Research*, *43*(June 2019), 101698. doi: 10.1016/j.scr.2019.101698.

Verheijen, M., Lienhard, M., Schrooders, Y., Clayton, O., Nudischer, R., Boerno, S., … Caiment, F. (2019). DMSO induces drastic changes in human cellular processes and epigenetic landscape in vitro. *Scientific Reports*, *9*(1), 4641. doi: 10.1038/s41598-019-40660-0.

Xu, C., Police, S., Hassanipour, M., Li, Y., Chen, Y., Priest, C., … Gold, J. D. (2011). Efficient generation and cryopreservation of cardiomyocytes derived from human embryonic stem cells. *Regenerative Medicine*, *6*(1), 53–66. doi: 10.2217/rme.10.91.

Internet Resources

https://www.axionbiosystems.com/resources

Repository of information and protocols for Axion Biosystems. Includes "Application Documents" and "Culture Protocols" for thawing, plating, and analyzing iCell® (Fuji Cellular Dynamics International) or Pluricyte®/Cor.4U (NCardia, formerly Pluriomics) hPSC-CMs on E-Stim+ and CytoView MEA plates.

https://hpscreg.eu/

International registry of hPSC lines including those used here (BIHi005-A, BIHi005-A-3, and BIHi050-A).

https://www.allencell.org/methods-for-cells-in-the-lab.html

Allen Cell Explorer from the Allen Institute. Has several comprehensive SOP-style protocols including one for hPSC-CM differentiation, as well as a catalog of tagged hPSC lines and many other useful resources.

Differentiation Protocol for 3D Retinal Organoids, Immunostaining and Signal Quantitation

Hannah Döpper,[1,4] Julia Menges,[1,4] Morgane Bozet,[1] Alexandra Brenzel,[2] Dietmar Lohmann,[1] Laura Steenpass,[1,3,5,6] and Deniz Kanber[1,5,6]

[1]Institute of Human Genetics, University Hospital Essen, University of Duisburg-Essen, Essen, Germany
[2]Institute for Experimental Immunology and Imaging, Imaging Center Essen (LMU), University Hospital Essen, University of Duisburg-Essen, Essen, Germany
[3]Present address: Department of Human and Animal Cell Lines, Leibniz Institute DSMZ—German Collection of Microorganisms and Cell Cultures GmbH, Braunschweig, Germany
[4]These authors contributed equally to the work.
[5]These authors share last authorship.
[6]Corresponding authors: *laura.steenpass@uk-essen.de*; *laura.steenpass@dsmz.de*; *deniz.kanber@uni-due.de*

Structures resembling whole organs, called organoids, are generated using pluripotent stem cells and 3D culturing methods. This relies on the ability of cells to self-reorganize after dissociation. In combination with certain supplemented factors, differentiation can be directed toward the formation of several organ-like structures. Here, a protocol for the generation of retinal organoids containing all seven retinal cell types is described. This protocol does not depend on Matrigel, and by keeping the organoids single and independent at all times, fusion is prevented and monitoring of differentiation is improved. Comprehensive phenotypic characterization of the in vitro–generated retinal organoids is achieved by the protocol for immunostaining outlined here. By comparing different stages of retinal organoids, the decrease and increase of certain cell populations can be determined. In order to be able to detect even small differences, it is necessary to quantify the immunofluorescent signals, for which we have provided a detailed protocol describing signal quantitation using the image-processing program Fiji. © 2020 The Authors.

Basic Protocol 1: Differentiation protocol for 3D retinal organoids
Basic Protocol 2: Immunostaining protocol for cryosections of retinal organoids
Support Protocol: Embedding and sectioning protocol for 3D retinal organoids
Basic Protocol 3: Quantitation protocol using Fiji

Keywords: embedding • immunostaining • organoids • quantitation • retina

How to cite this article:
Döpper, H., Menges, J., Bozet, M., Brenzel, A., Lohmann, D., Steenpass, L., & Kanber, D. (2020). Differentiation protocol for 3D retinal organoids, immunostaining and signal quantitation. *Current Protocols in Stem Cell Biology*, *55,* e120. doi: 10.1002/cpsc.120

CURRENT PROTOCOLS
A Wiley Brand

Current Protocols in Stem Cell Biology e120, Volume 55
Published in Wiley Online Library (wileyonlinelibrary.com).
doi: 10.1002/cpsc.120

INTRODUCTION

Human stem cell–based retina models have become popular, as they have opened the road to studying human retinogenesis in development and disease. These models generate retinal organoids that not only contain all seven retinal cell types, but also show distinct layering similar to the in vivo retina, and thus, at present, are the best in vitro model for retinogenesis. Moreover, 3D culturing in combination with CRISPR/Cas technology enable modeling of genetic diseases affecting cells of the retina, and therefore allow drug testing. Several protocols for 3D differentiation toward neural retina have been published (Llonch, Carido, & Ader, 2018). In principle, the protocols are based on the ability of the pluripotent stem cells to self-reorganize after dissociation, which, in combination with certain supplemented factors, can be specifically driven toward neural retina differentiation. Basic Protocol 1 below is based on a combination of Kuwahara et al. (2015) and Browne et al. (2017) with some modifications, and results in the generation of retinal organoids containing all seven retinal cell types arising in their natural order during differentiation. For phenotypic characterization, an immunostaining protocol (Basic Protocol 2), and for a detailed analysis of cell number, a quantitation protocol using Fiji (Basic Protocol 3) is provided.

BASIC PROTOCOL 1

DIFFERENTIATION PROTOCOL FOR 3D RETINAL ORGANOIDS

In this protocol, the stable and reproducible generation of 3D retinal organoids is described. The human embryonic stem cell line H9 is differentiated to 3D retinal organoids using a combination of two already published protocols (Browne et al., 2017; Kuwahara et al., 2015) with some modifications. This protocol describes the procedure for one 70%-80% confluent well of a 6-well plate. Briefly, 12,000 single cells are seeded into each well of a 96-well U-bottom plate (low-adhesion). The formed organoids are transferred to a 48-well flat-bottom plate coated with agarose at day 21 (d21), keeping one organoid per well during long-term culturing (>22 weeks), which prevents fusion of organoids and improves medium supply and monitoring of organoids. Using this protocol, retinal organoids with all seven retinal cell types are obtained. One has to be aware that bipolar and Müller glia cells are late-born cell types, and therefore will appear after d126 of culturing. However, at this time there will be no ganglion cells left, as they disappear over time, probably because of malnutrition (diffusion of the medium into the inner organoid decreases with time). Figures 1 and 2 illustrate the different stages of the differentiation process.

NOTE: All cell culture work is performed under sterile conditions in a laminar flow hood.

NOTE: All solutions and equipment that come into contact with living cells must be sterile.

NOTE: Cells and organoids should be incubated in a humidified tissue culture incubator at 37°C with 5% CO_2 under normoxic conditions.

NOTE: This protocol is described for cells from one well of a 6-well plate, resulting in one 96-well U-bottom plate (low-adhesion) and later in two 48-well flat-bottom plates.

NOTE: Start on a Wednesday for weekend-free culturing.

NOTE: Before performing a medium change, the corresponding medium should be at room temperature.

Materials

Embryonic stem cell line H9 (WiCell, WA09; please note that restrictions on importation and use of hESCs might apply in some countries, e.g., Germany)

For reagents and consumables used in this protocol, see Tables 1 and 2, respectively

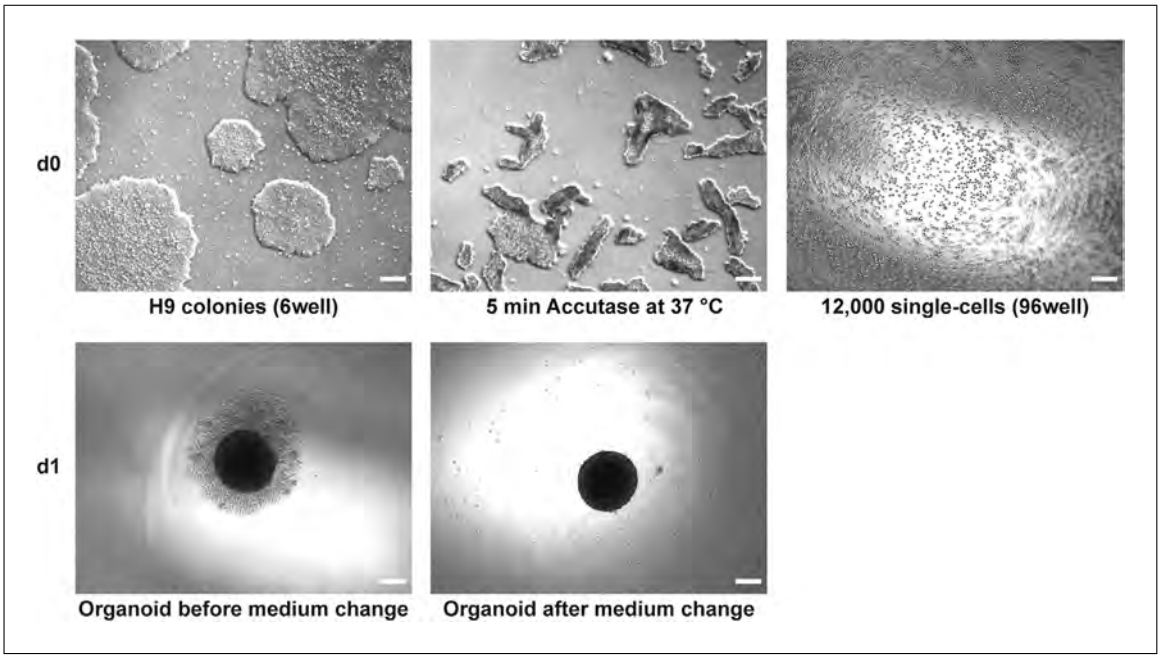

Figure 1 3D retina differentiation: d0 and d1. d0: H9 colonies before starting the protocol and after 5-min incubation with Accutase at 37°C. All colonies are lifted from the bottom and start dissociating. The picture of the 12,000 cells was taken immediately after seeding into a 96-well U-bottom plate. Scale bar: 200 µm. d1: One organoid has formed in each well of the 96-well U-bottom plate at d1. Before medium change, a ring of single cells around the organoid is detectable. These cells were not included in the organoid. The size of the ring can vary from setup to setup and cell line to cell line. After medium change, these "unused" single cells are gone, as they were aspirated. Scale bar: 200 µm.

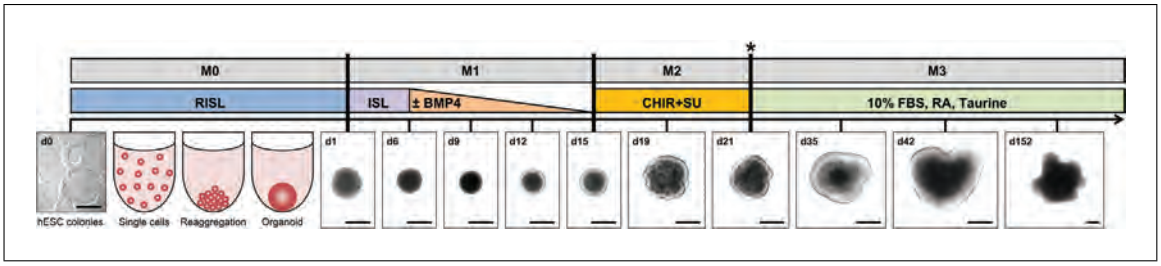

Figure 2 Differentiation timeline for retinal organoids. The graphical overview of the differentiation protocol indicates the addition of different factors at specific time points and shows the development of the neural retina. The formed organoid at d1 develops a bright outer layer at d12 that resembles the neural retina. This layer becomes thicker over time. *d21: Transfer organoids to 48-well flat-bottom. M0, medium for organoid formation; M1, medium for retina formation; M2, medium for RPE formation; M3, medium for long-term culturing. R, Y-27632 ROCK inhibitor; I, IWR1-endo; S, SB-431542; L, LDN-193189; CHIR, CHIR99021; SU, SU5402; RA, retinoic acid. Scale bar: 500 µm.

Additional reagents and equipment for basic cell culture techniques including counting cells with a hemocytometer and mycoplasma testing (see Current Protocols article: Phelan & May, 2017)

d0

1. Prepare 4 ml DMEM/F12-GlutaMAX™ Supplement with 20 µM Y-27632 ROCK inhibitor.
2. Prepare 3 ml AggreWell medium with 20 µM Y-27632 ROCK inhibitor.
3. Prepare 10 ml of medium M0 as described in Reagents and Solutions (Table 8).
4. Wash the cells (one well of a 6-well plate) with 2 ml D-PBS (room temperature), aspirate, and add 1 ml Accutase to the well.
5. Incubate for 5-10 min at 37°C (in a humidified 5% CO_2 incubator).

Table 1 Reagents Used in Basic Protocol 1

Item	Cat. no.	Supplier	Stock conc.	Final conc.
DMEM/F12-GlutaMAX™ Supplement	31331-093	ThermoFisher Scientific	–	–
Y-27632 ROCK inhibitor	S1049	Selleckchem	10 mM	20 µM
Medium M0	see recipe in Reagents and Solutions (Table 8)			
AggreWell medium	5893	StemCell Technologies	–	–
D-PBS (1×)	14190-169	ThermoFisher Scientific	–	–
StemPro Accutase	A11105-01	ThermoFisher Scientific	–	–
IWR1-endo	S7086	Selleckchem	10 mM	3 µM
SB-431542	S1067	Selleckchem	20 mM	10 µM
LDN-193189	S2618	Selleckchem	1 mM	100 nM
Medium M1	see recipe in Reagents and Solutions (Table 8)			
Recombinant Human BMP4	314-BP/CF	R&D Systems	50 µg/ml	55 ng/ml
Medium M2	see recipe in Reagents and Solutions (Table 8)			
CHIR99021	S1263	Selleckchem	5 mM	3 µM
SU5402	SML0443-5MG	Sigma-Aldrich	10 mM	5 µM
peqGOLD Universal Agarose	732-2789	VWR	1%	1%
Water	1.153.332.500	Merck Millipore	–	–
Medium M3	see recipe in Reagents and Solutions (Table 8)			
Retinoic acid	R-2625-50 mg	Sigma-Aldrich	100 µM	0.5 µM

Table 2 Consumables used in Basic Protocol 1

Item	Cat. no.	Company
Nunclon-Sphera 96-well U-bottom plate, sterile, with lid	174925	ThermoFisher Scientific
48-well flat-bottom suspension culture plate, sterile, with lid	677102	Greiner
Reagent reservoir, sterile	4-0016	neoLab
DISTRIMAN repetitive pipette	F164001	Gilson
DISTRITIP Maxi syringe tips, 12.5 ml	F164150	Gilson

6. Place 2 ml of DMEM/F12-GlutaMAX™ Supplement with 20 µM Y-27632 ROCK inhibitor (prepared in step 1) in a 15-ml tube during the incubation in step 5.
7. Confirm under the microscope that all cells are detached (Fig. 1). After 10 min, all cells should be detached—do not incubate for longer.
8. Transfer cell suspension (1 ml) into the prepared tube (step 6) and rinse the well with 1 ml of the rest of DMEM/F12-GlutaMAX™ Supplement containing 20 µM

Y-27632 ROCK inhibitor (the 15-ml tube contains now 4 ml). Avoid too much pipetting, as cells are very sensitive—transfer cells all at once and rinse one to two times.

9. Centrifuge 5 min at 300 × *g*, room temperature.
10. Aspirate supernatant and resuspend the cell pellet in 1 ml AggreWell medium containing 20 µM Y-27632 ROCK inhibitor (prepared in step 2). Do not pipette too much, as cells are very sensitive (this depends on the cell line used).
11. Count viable cells using a hemocytometer (see Current Protocols article: Phelan & May, 2017).
12. Prepare 8 ml cell suspension with 1.6×10^5 cells/ml using medium M0 (prepared in step 3).
13. Count viable cells again using a hemocytometer (optional).

    The result should be ~1.6×10^5 cells/ml.
14. Pipette 75 µl (12,000 cells) of cell suspension into each well of a 96-well U-bottom plate (Fig. 1) and place the plate in the incubator.

    Do not forget to harvest cells at d0 for mycoplasma testing; usually, the rest of cells not needed for seeding should be sufficient.

d1

15. Prepare 60 ml of medium M1 as described in Reagents and Solutions (Table 8). Add IWR1-endo, SB-431542, and LDN-193189 to 10 ml of M1 at final concentrations of 3 µM, 10 µM, and 100 nM, respectively, and perform a complete medium change on the cells from step 14. To do that, aspirate the medium carefully without destroying the built organoid and carefully add 100 µl of the prepared medium to each well using a repetitive pipette (Fig. 1).

    For a medium change, always tilt the plate toward you so that the visible organoid sinks to the edge, and aspirate the medium as much as possible (complete medium change) or take off the given amount of medium (half-medium change).
16. Place the plate in the incubator until d6.

d6

17. Add BMP4 to 20 ml of M1 for a final concentration of 55 ng/ml and perform a complete medium change on the cells. Aspirate the medium carefully without destroying the organoid, and carefully add 200 µl of the prepared medium to each well using a repetitive pipette.
18. Place the plate in the incubator until d9.

d9 and d12

19. Perform a half-medium change on d9 as well as on d12 (on each day a total of 10 ml of medium M1 is needed). Carefully take off 100 µl medium without disturbing the organoid using a 200-µl pipette and carefully add 100 µl of medium M1 using a multichannel pipette and a reagent reservoir (add 10 ml of medium to the reagent reservoir).
20. Place the plate in the incubator until d12 and d15, respectively.

d15

21. Prepare 60 ml of medium M2 as described in Reagents and Solutions (Table 8).
22. Add CHIR99021 and SU5402 to 20 ml of M2 at final concentrations of 3 µM and 5 µM, respectively, and perform a complete medium change on the cells. Aspirate

almost all medium carefully without disturbing the organoid, and carefully add 200 µl of the prepared medium to each well using a repetitive pipette.

23. Place the plate in the incubator until d16.

d16

24. Add CHIR99021 and SU5402 to 10 ml of M2 at final concentrations of 3 µM and 5 µM, respectively, and perform a half-medium change on the cells. Take off 100 µl of the medium carefully, without disturbing the organoid, using a 200-µl pipette, and carefully add 100 µl of the prepared medium to each well using a multichannel pipette and a reagent reservoir (add 10 ml of medium to the reagent reservoir).

25. Place the plate in the incubator until d19.

d19

26. Add CHIR99021 and SU5402 to 20 ml of M2 for final concentrations of 3 µM and 5 µM, respectively, and perform a complete medium change on the cells. Carefully aspirate as much as possible of the medium without destroying the organoid, and gently add 200 µl of the prepared medium to each well using a repetitive pipette.

27. Place the plate in the incubator until d21.

d21

28. Prepare 380 ml medium M3 as described in Reagents and Solutions (Table 8).

    This is the amount that will be needed for 2 weeks. Store at 4°C

29. Coat two 48-well flat-bottom plates with 1% agarose dissolved in ultra-pure water. Weigh 1 g agarose and dissolve in 100 ml ultra-pure water, then boil in the microwave until agarose is completely dissolved. Let it cool down a bit and pipette 300 µl into each well. Add retinoic acid (RA) to 50 ml of medium M3 for a final concentration of 0.5 µM, and add 400 µl of the prepared medium to each well using a repetitive pipette when agarose has hardened (the rest of the prepared medium is needed in step 30).

    As retinoic acid is light sensitive, the light should be turned off during the medium change.

30. Perform a complete medium change. Aspirate the medium carefully without destroying the organoid, and carefully add 100 µl of medium M3 containing freshly added 0.5 µM retinoic acid to each well of the 96-well U-bottom plate using a repetitive pipette (use 10 ml of the medium prepared in step 29).

31. Transfer each organoid to a well of the 48-well flat-bottom plates (step 29)—each organoid is kept separately. If you started with a full 96-well U-bottom plate at d0, you will need two 48-well flat-bottom plates at this step. For the transfer use a 200 µl pipette with tips that were cut (sterile; size of opening should be ∼3 mm as the organoids at this point have a size of ∼1-1.5 mm) so that the organoid will not be destroyed.

    The transfer is necessary because the organoids grow and need more medium.

    The tips should be cut under sterile conditions (use sterile scissors, cut under laminar flow hood).

    Keeping one organoid per well avoids fusion and building of chains of several organoids, which is seen when organoids are cultured together in a 10-cm dish. Moreover, monitoring of organoids is improved, as the development of each organoid can be followed separately.

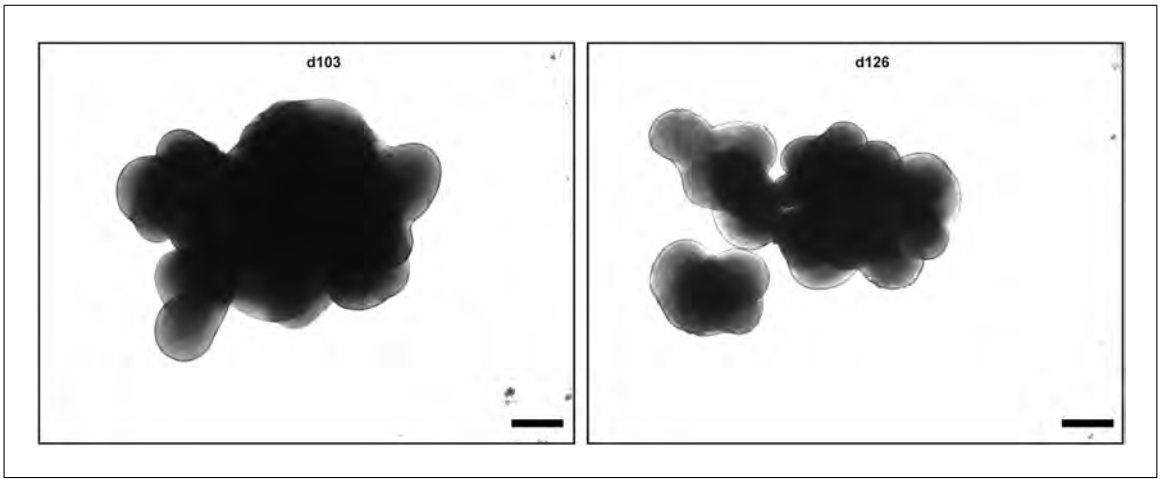

Figure 3 Organoids can fall apart into several smaller organoids during differentiation. Some organoids might disintegrate during differentiation. In this case, several smaller organoids can be observed in a single well. All of these smaller organoids have a bright outer layer. Scale bar: 500 µm.

32. Place the plate in the incubator until d23.

d23

33. Add retinoic acid to 60 ml of medium M3 for a final concentration of 0.5 µM and perform a complete medium change every Monday, Wednesday, and Friday for long-term culturing until d152 or beyond. Aspirate the medium carefully without destroying the organoid and carefully add 600 µl of the prepared medium to each well using a repetitive pipette. The last addition of retinoic acid is on d119.

    At later time points, some of the organoids might break into several small organoids that have a nice bright retinal layer (Fig. 3). Immunostaining of these small organoids reveal normal results.

34. Harvest organoids for RNA and DNA analysis and embedding/immunofluorescent staining at desired time points during differentiation. Embed and section as in Support Protocol, then proceed to Basic Protocol 2.

    Light-microscopic images of the organoids are also advantageous for monitoring retinal differentiation.

IMMUNOSTAINING PROTOCOL FOR CRYOSECTIONS OF RETINAL ORGANOIDS

BASIC PROTOCOL 2

Detailed analysis of, e.g., cell composition, spatial cell organization, and cell proliferation in the in vitro–generated retinal organoids is performed by immunostaining of cryosections (which generally result in better detection of antigens compared to paraffin sections) of the organoids (Fischer, Jacobson, Rose, & Zeller, 2008; Hira et al., 2019). Presence, absence, localization, and distribution of certain cell types can be determined by using specific antibodies for marker proteins (Fig. 4). This protocol is based on Browne et al. (2017).

Materials

Organoids, embedded and sectioned, on slides (Support Protocol)
Primary antibodies (Table 3)
Secondary antibodies (Table 4)
For reagents and consumables used in this protocol, see Tables 5 and 6, respectively

1. Take the slides out of the −80°C freezer and place them on a 37°C heating plate for 15 min.

Table 3 Primary Antibodies Used in Basic Protocol 2

Marker	Cell type	Antibody				Dilution	Host
RX (G-12)	Retinal progenitors	Santa Cruz Biotechnologies	sc-271889	mc	RRID:AB_10708730	1:200	mouse
VSX2	Retinal progenitors	Exalpha Biologicals	X1179P	pc	Not provided	1:300	sheep
CRX (4G11)	PR progenitors, immature PRs	Abnova	H00001406-M02	mc	RRID:AB_606098	1:1000	mouse
BRN3 (C-13)	Ganglion cells	Santa Cruz Biotechnologies	sc-6026[a]	pc	RRID:AB_673441	1:100	goat
PROX1	Horizontal cells	Merck Millipore	AB5475	pc	RRID:AB_177485	1:2000	rabbit
AP2α	Amacrine cells	DSHB	3B5-s	mc	Not provided	2 µg/ml	mouse
RXRγ	Cones (early marker)	SpringBioscience	E4332	pc	RRID:AB_11218714	1:500	rabbit
ARR3	Cones	LifeSpan Biosciences	LS-C382134-100	pc	Not provided	1:250	rabbit
NRL	Rods (early marker)	R&D Systems	AF2945	pc	RRID:AB_2155098	1:100	goat
PRKCA (H-7)	Bipolar cells	Santa Cruz Biotechnologies	sc-8393	mc	RRID:AB_628142	1:100	mouse
VIM (E-5)	Müller glial cells	Santa Cruz Biotechnologies	sc-373717	mc	RRID:AB_10917747	1:100	mouse

[a]Discontinued, but sc-390780 works also fine (monoclonal; clone A4; 1:100; mouse).
mc, monoclonal; pc, polyclonal; PR, photoreceptor.

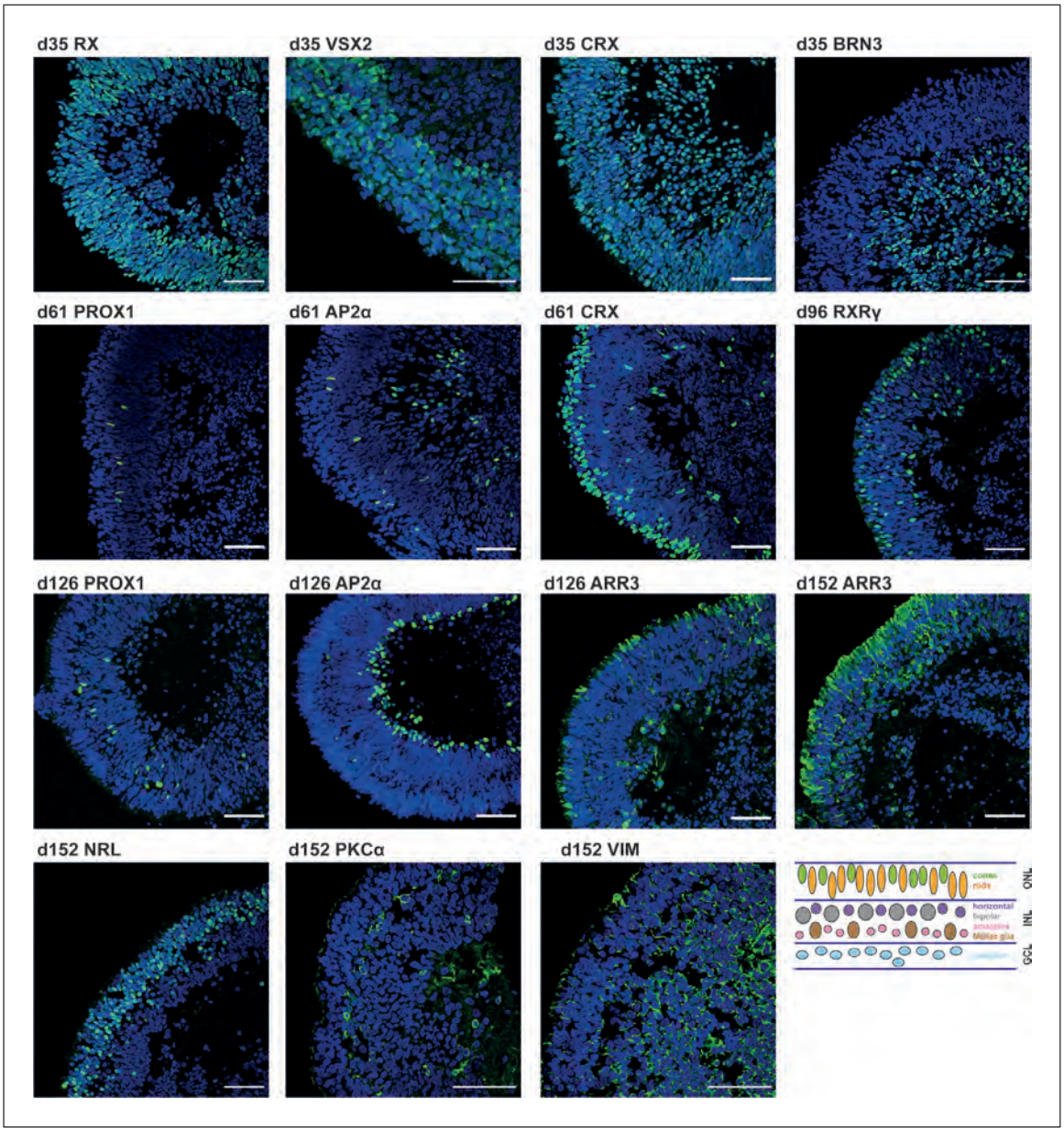

Figure 4 Immunostaining for early retinal markers and all retinal cell types. At d35, the outer layer stains positive for the early eye field marker RX. Moreover, in the outer part, retinal progenitor cells (VSX2), and in the inner part, ganglion cells are present (BRN3). CRX, a marker for retinal progenitors and immature photoreceptors, is present at d35, and a shift to the outer layer can be detected at d61. Horizontal cells (PROX1) and amacrine cells (AP2α) are present in the inner nuclear layer (d61, d126). Cone photoreceptors (RXRγ, ARR3; d96, d126, d152) and rod photoreceptors (NRL; d152) are present in the outer nuclear layer. Bipolar cells (PKCα) and Müller glia cells (VIM) are present in the inner nuclear layer (d152). A schematic overview of the retina with the seven different cell types organized in specific layers is given. Secondary antibodies were labeled in green (AlexaFluor 488), and nuclei were stained with DAPI (blue). Scale bar: 50 µm.

2. Prepare humid chamber in the meantime (metal or plastic box with lid, lined with tissues that are wetted with water).
3. Outline the sections with a pap pen and label the slides (three staining areas on a slide, Fig. 5A).
4. Post fix with 4% PFA for 5 min at room temperature (80 µl per section). Add the 4% PFA solution directly onto the organoids on the slide (Fig. 5A small black rectangle) and aspirate after 5 min.

Table 4 Secondary Antibodies Used in Basic Protocol 2

Secondary antibody	Cat. no.		Company	Dilution
Rabbit anti-Goat IgG (H+L), Alexa Fluor® 488 conjugate	A-11078	RRID:AB_2534122	ThermoFisher Scientific	1:1000
Donkey anti-Sheep IgG (H+L), Alexa Fluor® 555 conjugate	A-21436	RRID:AB_2535857	ThermoFisher Scientific	1:1000
Anti-mouse IgG (H+L), F(ab′)2 Fragment (Alexa Fluor® 488 Conjugate)	4408S	RRID:AB_10694704	Cell Signaling	1:1000
Anti-Rabbit IgG (H+L), F(ab′)2 Fragment (Alexa Fluor® 488 Conjugate)	4412S	RRID:AB_1904025	Cell Signaling	1:1000

Table 5 Reagents Used in Basic Protocol 2

Item	Cat. no.	Company
IMMEdge hydrophobic barrier PAP pen	H-4000	VECTOR Laboratories
4% paraformaldehyde (PFA)	see recipe in Reagents and Solutions (Table 8)	
TBS-T	see recipe in Reagents and Solutions (Table 8)	
Blocking buffer 1	see recipe in Reagents and Solutions (Table 8)	
Blocking buffer 2	see recipe in Reagents and Solutions (Table 8)	
DAPI (1 mg/ml in water)	62248	ThermoFisher Scientific
TrueBlack Lipofuscin Autofluorescence Quencher, 20× in dimethylformamide (DMF)	B-23007	Biotium
Ethanol	1.00983.2500	Merck Millipore
D-PBS (1×)	14190-169	ThermoFisher Scientific
VECTASHIELD Mounting Medium	VEC-H-1000	VECTOR Laboratories
CoverGrip™ Coverslip Sealant	23005	Biotium

Table 6 Consumables Used in Basic Protocol 2

Article	Cat. no.	Company
Metal or plastic box with lid	–	–
DISTRIMAN repetitive pipette	F164001	Gilson
DISTRITIP Maxi syringe tips, 12.5 ml	F164150	Gilson

This step improves adherence of cryosections to the slide.

CAUTION: *4% PFA is a hazardous substance and requires special waste disposal.*

5. Wash three times with TBS-T, each time for 5 min with 100 µl per staining area; use repetitive pipette; aspirate solution between washes.

In the steps below, the antibody, buffer, or washing solution is added directly to the specimen on the slide for the indicated time period, and then aspirated.

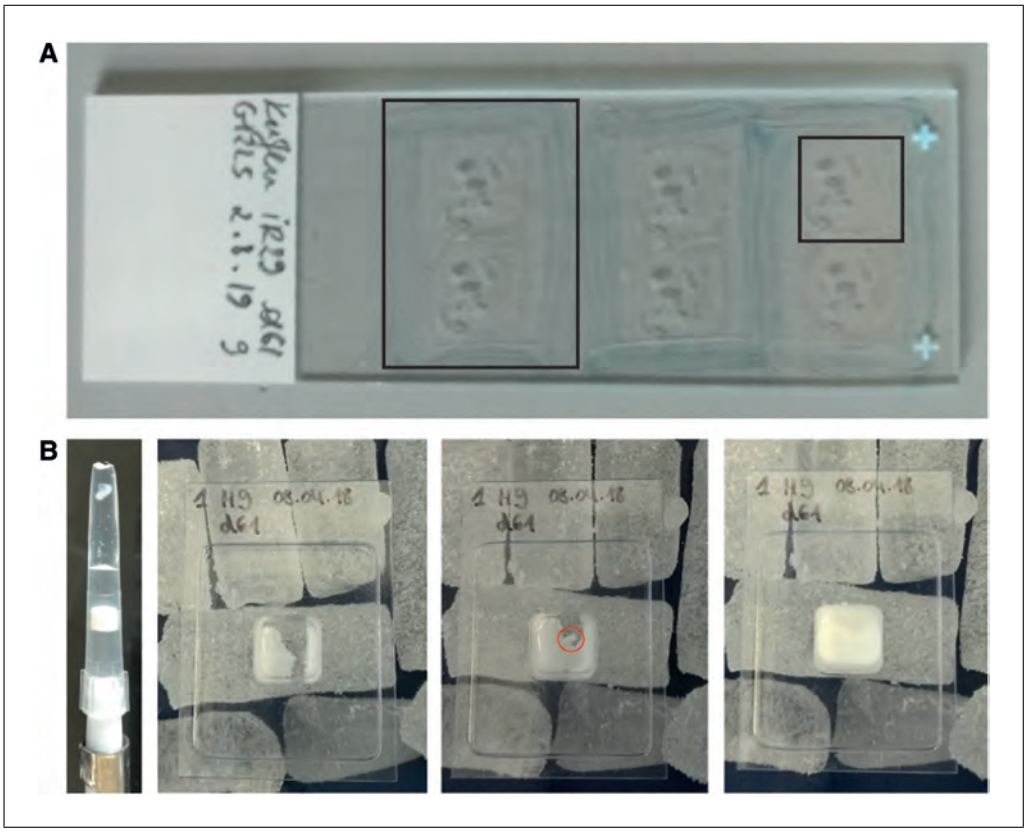

Figure 5 Outlined sections and embedding of organoids. (**A**) SUPERFROST microscope slide with three outlined immunostaining areas (big rectangle). In each area, two cryosections are present (small rectangle shows one cryosection). If outlined with a pap pen, each area can be used for a different staining. (**B**) Embedding of an organoid at d61 is shown. On the left, the organoid in a pipette tip is shown (ready for transfer into the tissue mold). The tissue mold filled with ~100 µl O.C.T. compound on dry ice is shown—as soon as the O.C.T. compound starts to freeze (turns from clear to white), the organoid is transferred into the tissue mold (red circle). The completely frozen block appears white.

6. Block for 1 hr with blocking buffer 1 at room temperature in the humid chamber (100 µl per staining area; use repetitive pipette).
7. Incubate overnight with primary antibody diluted in blocking buffer 1 at 4°C in the humid chamber (80 µl per staining area).
8. Wash three times with TBS-T, each time for 5 min with 100 µl per staining area; use repetitive pipette; aspirate solution between washes.
9. Incubate 1 hr with secondary antibody diluted in blocking buffer 2 at room temperature in the humid chamber (keep dark, 80 µl per staining area).
10. Wash twice with TBS-T, each time for 5 min with 100 µl per staining area protected from light; use repetitive pipette; aspirate solution between washes.
11. Wash once with TBS-T containing DAPI (1:1000 or final conc. 1 ng/µl) for 5 min protected from light (100 µl per staining area, use repetitive pipette, aspirate).
12. Treat with TrueBlack (dilute stock to 1× in ethanol; use 100 µl per staining area) for 30 s to reduce autofluorescence; aspirate and immediately wash with D-PBS (100 µl per staining area for 5 min, protected from light, do NOT use repetitive pipette).
13. Repeat wash step with D-PBS twice, protected from light (100 µl per staining area, use repetitive pipette, aspirate).

Table 7 Reagents and Consumables Used in the Support Protocol

Article	Cat. no.	Company
D-PBS (1×)	14190-169	ThermoFisher Scientific
4% PFA	see recipe in Reagents and Solutions (Table 8)	
Sucrose	84097-1KG	Sigma-Aldrich
Tissue-Tek O.C.T. compound	4584	Sakura
Tissue-Tek cryomold (10 mm × 10 mm × 5 mm)	4564	Sakura
Superfrost Plus microscope slides	J1800AMNZ	ThermoFisher Scientific

14. Coverslip the slide using VectaShield (∼5 µl per staining area) and seal with coverslip sealant.
15. Keep the slides at −20°C and in the dark until and after microscopic analysis.

SUPPORT PROTOCOL

EMBEDDING AND SECTIONING PROTOCOL FOR 3D RETINAL ORGANOIDS

Good embedding is essential for good sectioning. If embedding is poorly executed, you will have trouble at the cryotome while sectioning the cryoblocks, as several or a whole series of sections can be torn, resulting in loss of information. This Support Protocol describes the individual steps to improve embedding and thus immunostaining.

Materials

Organoids in wells of 48-well plate (Basic Protocol 1)
Cryotome
For reagents and consumables used in this protocol, see Table 7

1. Transfer organoid together with medium (100-200 µl) from the 48-well flat-bottom-plate to a 1.5-ml tube using cut 200-µl pipette tips to avoid destruction of the organoid (see Basic Protocol 1, step 31).
2. Let the organoid sink, and remove supernatant (medium) carefully. Wash once for 3 min with 1 ml D-PBS at room temperature. Let the organoid sink and remove D-PBS carefully.
3. Fix for 15 min at room temperature in 400 µl 4% PFA.

   CAUTION: *4% PFA is a hazardous substance and requires special waste disposal.*
4. Wash three times, each time for 10 min with D-PBS.
5. Incubate in 1 ml of 30% sucrose in D-PBS at 4°C for ∼1 hr.

   Organoids will swim up immediately after adding 30% sucrose. Incubation is finished when the organoids have sunk (∼1 hr).

   If after 1 hr the organoids have not sunk, incubate overnight and proceed the next day.
6. Aspirate supernatant, add ∼500 µl O.C.T. compound, and incubate for 30 min at room temperature.
7. Transfer the organoid into a fresh tube with 1 ml fresh O.C.T. compound. Avoid transfer of too much "old" O.C.T. compound. Use cut 200-µl pipette tips to avoid destroying the organoid (see Basic Protocol 1, step 31).

8. Label a tissue mold (10 mm × 10 mm), pipette ∼100 µl O.C.T. compound into it at room temperature, and place it on dry ice. As soon as the O.C.T. compound starts to freeze, transfer the organoid into the mold using a cut 200-µl pipette tip to avoid destroying the organoid (see Basic Protocol 1, step 31). Avoid air bubbles. Immediately fill up the rest of the tissue mold with fresh O.C.T. compound and let it freeze on dry ice (∼15-30 min; Fig. 5B).

   If air bubbles occur in the tissue mold, remove them immediately with a pipette tip.

9. Wrap up the tissue mold in aluminum foil that has been labeled, and keep the cryoblock at −80°C overnight.

10. Section the cryoblock using a cryotome (prepare 10-µm sections). As soon as you have reached the organoid, you will see white/yellowish tissue in the cryoblock and on the test slide. From this point on, place six sections on a labeled Superfrost slide, as shown in Figure 5A. Two sections will be one staining area (Fig. 5A). Store slides at −80°C until used for immunostaining.

QUANTITATION PROTOCOL USING FIJI

BASIC PROTOCOL 3

In order to use immunostaining to analyze possible differences regarding specific cell types, it is necessary to quantify either cell number or the area of specifically labeled fluorescence signals. This protocol describes how to quantify cell numbers using macros in Fiji (Schindelin et al., 2012). For quantitation, TIFF images are acquired on a confocal microscope. In this case, a Leica SP8 confocal laser scanning microscope is used, and according to experience, a pixel size of 150 nm is set as default. However, this may vary depending on the microscope used. To increase precision, at least four pictures are taken per organoid, with three organoids per differentiation and three biological replicates of differentiations (36 images in total). As the described macro is based on a DAPI mask, it is mandatory to take an image of the DAPI channel for each picture to make sure that only nucleated cells are included into the results.

On the DAPI channel image, a watershed algorithm will be performed which is only sufficient to separate sparsely touching cell-cell events in a single cell layer derived from, e.g., cell culture slides. However, in thicker tissue slices, more than one layer of cells will be present, and the density of nuclei will be too high for precise quantitation of single cells. The DAPI area will be eroded by a fixed factor to mimic the true size of a cell. Subsequently, a mask for the fluorescent signal of the immunostaining will be created by a fixed threshold value that is to be tested by the user for each condition. It is also important to adapt the macro for different cellular localizations of the fluorescence staining. In the next step, the fluorescence marker label will be compared with the previously created nuclei mask. Only signals within the DAPI mask will be used for final outputs. After thresholds have been determined for a staining, all images can be processed as a batch. The results table of the macro script will show absolute cell numbers and area values (integrated density). Depending on the type of slides/samples used—monolayer cell culture slides or tissue sections—the respective number can be used for calculations. Calculation of the ratio between the fluorescence area values and the DAPI area values results in cell quantitation on a percentage basis.

Materials

Macro for cell quantitation (Supporting Information Macro S1)

1. Install the Fiji software including the Biovoxxel toolbox (Brocher, 2014, 2015).

2. Because the macro is provided as a `.docx` file, it needs to be converted to a `.ijm` file, which can be processed by Fiji. Open Fiji, then open the macro editing window

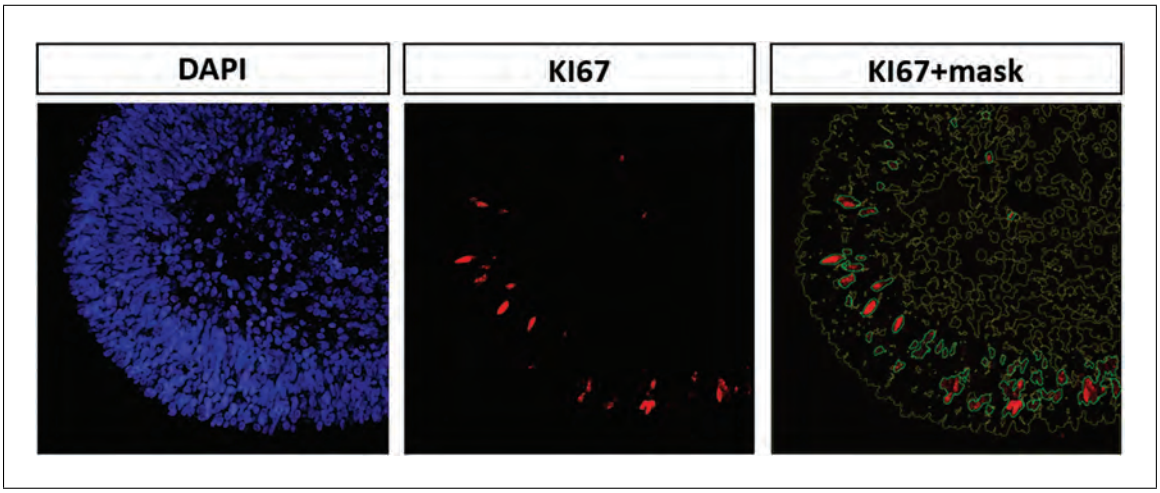

Figure 6 Example of an analysis using the macro for cell counting. Left: picture of the DAPI signal (blue); middle: proliferating cells were stained with an anti-KI67 antibody (red); right: image of the red KI67 signal overlaid with the mask which was created using the DAPI signal (yellow lines). Green lines indicate the areas that are counted as actual KI67 positive signal. Thresholds used here: particle size threshold, 500 pixels to infinity; red signal threshold, brightest 5%.

by clicking on the tab "Plugins" in the task bar. Next, choose the tab "New" from the drop-down menu, and finally the tab "Macro." Copy the text from the `.docx` file into the macro editing window. Click on the tab "Language,"select "IJ1 Macro," and save the macro.

3. For automated cell counting, it is necessary to find the best threshold for each staining. Drag and drop the converted macro into the Fiji taskbar to open it in editing mode. Adjust the percentage for the threshold of your staining (line 91 of the macro). Start, for example, with a threshold of 95. The macro will hereby take only the brightest 5% of the signal into account. Run the macro and select a destination folder in which to save the results.

4. Make sure that the threshold suits the staining as exactly as possible by taking a close look at the resulting pictures. In the resulting pictures, the microscope image is overlaid with the mask that was created from the DAPI signal (cells/areas outlined in yellow; Fig. 6). Green lines indicate the signals that were counted as the brightest 5% of the signal in step 3. If the threshold is too low, many signals will not be counted (and therefore many fluorescent areas will not be encircled by green lines). If the threshold is too high, too much background will be counted as signal (negative areas will be encircled by green lines). Testing several different thresholds for each staining will help to find the perfect fit. It is also important to consider testing thresholds for all different time points of each staining of the experiment.

5. To adjust the pixel range for the particle size (defining the size of stained areas to be taken into account), proceed as described for the fluorescence signal threshold in step 3 (line 163 of the macro; here: 500 to infinity; Fig. 7). This step helps to discriminate between background, staining artifacts, and the actual fluorescence signal. Try different particle-size thresholds to find the one that fits for your analyses. If needed, adjust particle-size threshold for all channels separately.

6. Before running the macro, create a folder for the results.

7. Run the macro with the adjusted thresholds for all pictures to be analyzed and select the destination folder.

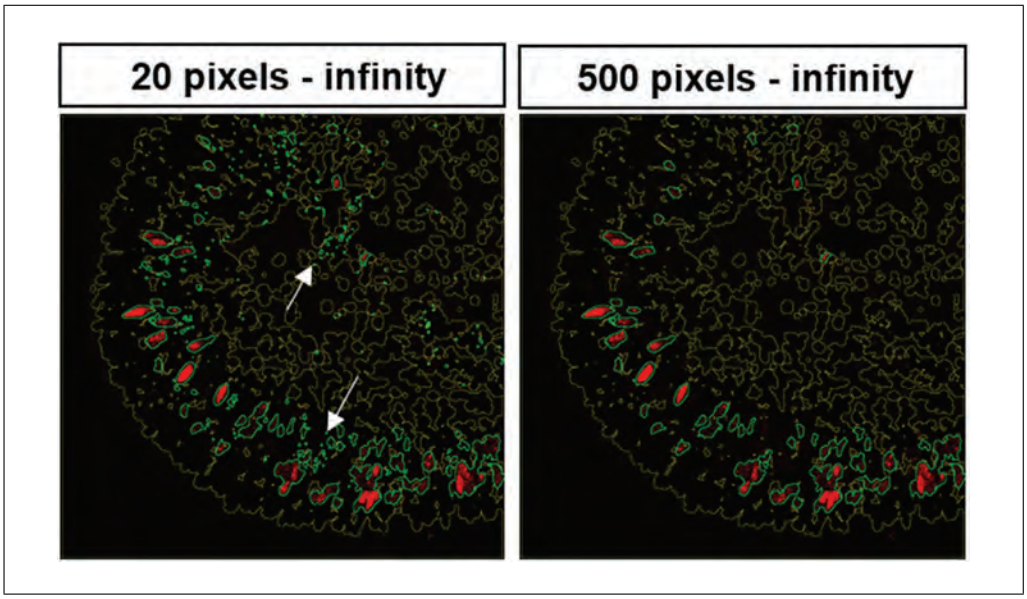

Figure 7 Example of different particle size thresholds. Image of the red KI67 signal. Green lines indicate the areas which are counted as actual KI67 positive signal. Left: particle size threshold, 20 pixels to infinity; right: particle size threshold, 500 pixels to infinity. Note that in the left image, there are too many small particles counted as signal (white arrows).

8. A summary of the analyses will be saved as a text file in the results folder. Copy the data to Excel or any statistics program of choice.
9. One approach to calculating the percentage of immunofluorescence-positive cells among all nucleated cells is to use the area values of the DAPI signal and the area values of the fluorescent signal for calculation. In order to do this, the mean value of the DAPI signal of all 36 pictures is calculated. This value represents the average number of nucleated cells or the average area of nucleated cells.
10. Calculate the mean value of the fluroescent signal for each set of the four images per organoid. This will result in nine values (three organoids, three differentiations).
11. To calculate the percentage of cells positive for the fluorescent signal, each of the nine mean values for the fluorescent signal (calculated in step 10) is divided by the mean DAPI value (calculated in step 9) and the result is multiplied by 100. This set of nine percentage values can be used for statistics.
12. For quantitation of cells grown on cell culture slides, it would also be possible to directly use the number of counted fluorescence signals, which are listed in the results table (as absolute number of stained cells). In this case, cells need to be very evenly distributed in a single layer and should not be too close together. It is also necessary to make sure that there is only one fluorescent signal per nucleated cell (to be checked when adjusting the thresholds).

REAGENTS AND SOLUTIONS

Table 8 lists recipes for media and solutions used in this article.

COMMENTARY

Background Information

The retina is a complex tissue consisting of seven different cells types that are arranged in certain layers. Retinal development starts from cells of the neuroectoderm. An optic vesicle evaginates form the rostral diencephalon and subsequently invaginates, building a double-walled optic cup (Fig. 8; Eiraku, Adachi, & Sasai, 2012). The outer wall of this optic cup forms the retinal pigment epithelium

Table 8 Media and Solutions Used in Basic Protocols 1 and 2 and the Support Protocol

Ingredient		Final conc.	Comment
Blocking buffer 1[a]			
Donkey serum	Merck Millipore, S30-100ML	5%	v/v
Bovine serum albumin (BSA)	Sigma-Aldrich, A9418-10G	3%	w/v
Tris-buffered saline (TBS)	Prepare from Pierce 20× TBS buffer (ThermoFisher Scientific, 28358)	1×	–
Triton X-100	Sigma-Aldrich, T9284-100ML	0.2%	v/v
Blocking buffer 2[a]			
Bovine serum albumin (BSA)	Sigma-Aldrich, A9418-10G	2%	w/v
Tris-buffered saline (TBS)	Prepare from Pierce 20× TBS buffer (ThermoFisher Scientific, 28358)	1×	–
Triton X-100	Sigma-Aldrich, T9284-100ML	0.2%	v/v
M0 medium (day 0)[b]			
AggreWell medium	StemCell Technologies, 5893	–	–
Y-27632 ROCK inhibitor	Selleckchem, S1049	20 µM	–
IWR1-endo	Selleckchem, S7086	3 µM	–
SB-431542	Selleckchem, S1067	10 µM	–
LDN-193189	Selleckchem, S2618	100 nM	–
M1 medium (day 1 to day 15)[c]			
Hams F12, GlutaMAX™ Supplement	Gibco, 31765-027	45%	v/v
IMDM, GlutaMAX™ Supplement	Gibco, 31980-022	45%	v/v
KnockOut Serum Replacement (KSR)	ThermoFisher Scientific, 10828010	10%	v/v
Chemically defined lipid concentrate	Gibco, 11905-031	1×	–
Monothioglycerol	Sigma-Aldrich, M6145-25ML	450 µM	–
Penicillin-streptomycin	ThermoFisher Scientific, 15140122	100 U/ml penicillin; 100 µg/ml streptomycin	–
IWR1-endo	Selleckchem, S7086	3 µM	Add briefly before use only on d1
SB-431542	Selleckchem, S1067	10 µM	Add briefly before use only on d1
LDN-193189	Selleckchem, S2618	100 nM	Add briefly before use only on d1
BMP4[d]	R&D Systems, 314-BP/CF	55 ng/ml	Add briefly before use only on d6
M2 medium (day 15 to day 21)[c]			
DMEM/F12-GlutaMAX™ Supplement	ThermoFisher Scientific, 31331-093	–	–

(*Continued*)

Table 8 Media and Solutions Used in Basic Protocols 1 and 2 and the Support Protocol, *continued*

Ingredient		Final conc.	Comment
N2 Supplement, 100×	ThermoFisher Scientific, 17502-148	1×	–
Penicillin-streptomycin	ThermoFisher Scientific, 15140122	100 U/ml penicillin; 100 µg/ml streptomycin	–
CHIR99021	Selleckchem, S1263	3 µM	Add briefly before use
SU5402	Selleckchem, SML0443-5MG	5 µM	Add briefly before use
M3 medium (long-term medium)[c]			
DMEM/F12-GlutaMAX™ Supplement	ThermoFisher Scientific, 31331-093	–	–
Fetal bovine serum (FBS)	Gibco, 10270106	10%	v/v
N2 Supplement, 100×	ThermoFisher Scientific, 17502-048	1×	–
Penicillin-streptomycin	ThermoFisher Scientific, 15140122	100 U/ml penicillin; 100 µg/ml streptomycin	–
Taurine	Sigma-Aldrich, T8691-25G	0.1 mM	–
Amphotericin B	Thermo Scientific, 15290018	0.25 µg/ml	–
Retinoic acid[e]	Sigma-Aldrich, R2625-50 mg	0.5 µM[e]	Add briefly before use; last addition on d119
Paraformaldehyde (PFA), 4%[a]			
16% Formaldehyde	ThermoFisher Scientific, 28906	4%	v/v; dilute in D-PBS (ThermoFisher Scientific, 14190-169)
Sucrose, 30%[f]			
Sucrose		30%	w/v; dilute in D-PBS (ThermoFisher Scientific, 14190-169)
TBS-T[g]			
Pierce 20× TBS Buffer	ThermoFisher Scientific, 28358	1×	–
Triton X-100	Sigma-Aldrich, T9284-100ML	0.05%	v/v

[a]Store 1-ml aliquots at −20°C and use within 6 months.
[b]Prepare fresh and use up at d0.
[c]Store at 4°C and use within 2 weeks—before feeding the organoids keep at room temperature for 20-30 min.
[d]Store aliquots of stock solution (50 µg/ml) at −20°C and use within 3 months.
[e]Store aliquots of stock solution (100 µM) at −80°C and use within 3 months.
[f]Store at 4°C and use within 4 weeks.
[g]Store at room temperature and use within 4 weeks.

(RPE), whereas the inner wall forms the neural retina. In the early eye field, markers like RX, SIX3, SIX6, LHX2, and PAX6 are detected; later, these progenitor cells differentiate into the different neuronal cells (ganglion, horizontal, amacrine, photoreceptor, and bipolar cells) and glia cells (Müller glia cells) of the retina (Heavner & Pevny, 2012; Meyer et al., 2009). These different retinal cell types arise in a distinct order: the early-born cell types are ganglion, horizontal, and amacrine cells, as well as cone photoreceptors, whereas late-born cell types are rod photoreceptors, bipolar cells, and Müller glia cells. After their emergence, they migrate to their specific positions in the retina—photoreceptors form the outer nuclear layer; horizontal, bipolar, amacrine, and Müller glia cells form the inner nuclear

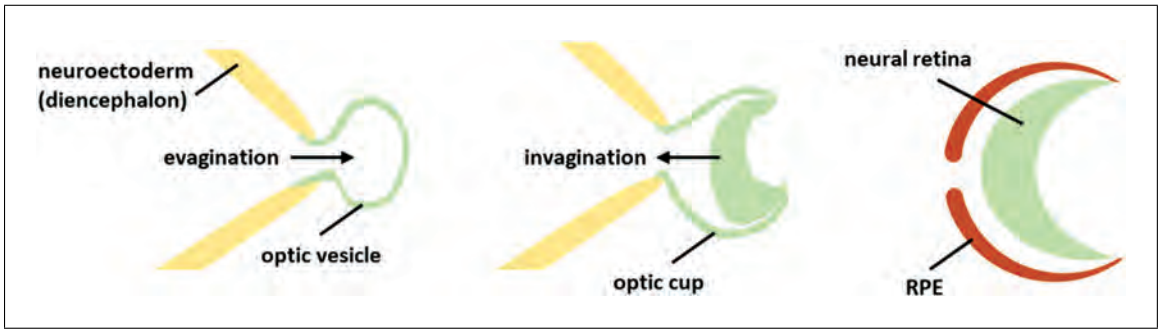

Figure 8 Simplified presentation of early eye development. An optic vesicle evaginates out of the diencephalon and subsequently invaginates, forming a double-walled optic cup. The outer wall of this optic cup forms RPE and the inner wall forms the neural retina.

layer; and the ganglion cells build the ganglion cell layer (Fig. 4; Centanin & Wittbrodt, 2014; Kapatai et al., 2013]).

Organoid technology now makes it possible to study this process by modeling retinogenesis. Different protocols have been established, all based on the self-organizing nature of pluripotent stem cells. Nakano et al. (2012) published the first 3D differentiation protocol for retinal organoids from human embryonic stem cells. In this protocol, Matrigel was used, which is a complex protein mixture consisting of up to 1851 different proteins. The main component is laminin, which promotes formation of a rigid neuroepithelial structure (Eiraku & Sasai, 2012; Hughes, Postovit, & Lajoie, 2010). In 2012, Eiraku and Sasai showed that Matrigel induced the eye field in the generation of retinal organoids (Eiraku & Sasai, 2011, 2012). However, Matrigel shows lot-to-lot differences in protein composition, and therefore influences reproducibility. This problem was overcome with the protocol of Kuwahara et al. (2015), where the use of Matrigel is omitted. Instead, bone morphogenetic protein–4 (BMP4) is used to induce eye field formation. Moreover, in contrast to the Nakano protocol, no manual manipulation like excision of the neural retina from floating aggregates is necessary. Similar to what happens in vivo, retinal organoids develop all seven retinal cell types in a distinct order. However, when the latest-born cell types, the bipolar and Müller glia cells, arise, the earliest-born ganglion cells have already vanished (Capowski et al., 2019; Browne et al., 2017; Zhong et al., 2014). This is possibly due to malnutrition of the inner part of the organoid as the neural retina becomes thicker during differentiation and vascularization is missing, or due to apoptosis because no functional neuronal connections are formed. The layering in retinal organoids is close to the in vivo retina morphology. However, ectopic photoreceptors can be detected in the inner nuclear layer of the retina, which could be due to the lack of contributions from other missing structures (Capowski et al., 2019; Hallam et al., 2018; Phillips et al., 2018). Nevertheless, these stem cell–based retinal models are the best in vitro models for human retinogenesis at this time. 3D culturing in combination with patient-derived iPSCs or CRISPR/Cas technology enables models of genetic diseases, which are promising in terms of drug testing (Crespo et al., 2017; Deng et al., 2018; Jin, Okamoto, Xiang, & Takahashi, 2012; Parfitt et al., 2016; Tucker et al., 2013). Furthermore, organoids have the potential for transplantation therapies because, e.g., retinal organoids can serve as a source of certain retinal cell types to treat retinal degeneration (Gagliardi et al., 2018; Gonzalez-Cordero et al., 2017; Mandai et al., 2017; McLelland et al., 2018). Even personalized therapy might be possible, as the required retinal cell type can be generated from patient-specific iPSCs where gene correction was performed using CRISPR/Cas technology, eliminating rejection responses.

Critical Parameters and Troubleshooting

3D retina differentiation should only be set up with starting cells of good quality. Colonies should not show any signs of differentiation and should not be more than 70%-80% confluent. As a matter of course, the mycoplasma test at d0 should be negative. Quality of starting cell population is critical.

Supplements should be aliquotted into ready-to-use aliquots to avoid repeated thawing and freezing, and strict attention should be paid to shelf life. The medium should only be warmed at room temperature and never at 37°C. In addition, due to its undefined nature, which could hinder consistent differentiation, FBS should be tested before use. Differentiation up to d61 and

Table 9 Troubleshooting

Observation	Possible cause	Remarks
No organoid formed on d1	Not enough cells	Make sure counting is correct and seed 12,000 cells per well
	Medium composition wrong	Aliquot supplements in ready-to-use aliquots, do not refreeze Make sure Y-27632 ROCK inhibitor was added
	Cells of poor quality	No signs of differentiation should be visible, confluency not more than 70%-80%
No bright retinal layer visible at d12	Media composition wrong; final concentration of small molecules wrong	Aliquot supplements in ready-to-use aliquots, do not refreeze. Make sure the end concentration of all supplements used is correct.
Organoids form atypical characteristics, e.g., cysts	Media composition wrong; final concentration of small molecules wrong	Aliquot supplements in ready-to-use aliquots, do not refreeze Make sure the end concentration of all supplements used is correct Make sure that all supplements are added at the correct time point Make sure FBS batch was tested before
Organoids lost by aspiration	Pump speed too high	Adjust the pump speed
Too much autofluorescence	Wash not performed properly	Be sure to perform all washing steps TrueBlack is an autofluorescence quencher that is used in tissue sections for immunofluorescence staining

immunostainings at d35 and d61 should be performed to determine whether the batch can be used for differentiation or not. To avoid repeated testing, purchase of a larger quantity of FBS from the tested batch should be considered.

Whether your differentiation is going in the right direction can be judged by light microscopy. If you see a bright outer layer that becomes thicker with time, the differentiation is correct (Fig. 2). On d19 and d21, you should see some loops forming. Thereafter, the layer starts thickening. If organoids or rather the outer bright layer do not grow, or other unusual characteristics appear, one should consider stopping that run of differentiation (see Supporting Information Figure S1). Of course, immunostaining for specific markers at that point should be considered to support the decision of ending the differentiation. Usually, if immunostaining at d35 stains positive for RX, VSX2, CRX, BRN3, and at d61 stains positive for CRX, PROX1, and AP2α, the differentiation is good and can be continued (Fig. 4).

Another point to consider is that different cell lines can behave differently, resulting in poor results (Bar-Nur, Russ, Efrat, & Benvenisty, 2011; Hiler et al., 2015; Mellough et al., 2019). In these cases, the differentiation protocol may be adjusted to the specific cell line (e.g., try different seeding densities). We have used the hESC line H9 for this protocol and have obtained stable and reproducible results.

Table 9 lists possible problems that can occur with the differentiation, as well as their possible causes and solutions.

Understanding Results

Using this protocol, you should obtain retinal organoids with all seven retinal cell types that arise in their natural order and are organized in the known retinal layers, i.e., the ganglion cell layer, inner nuclear layer, and outer nuclear layer. At d1, an organoid is formed that develops a bright outer layer which is clearly visible at d12 (Figs. 1 and 2). This bright layer is the neural retina, and becomes thicker during differentiation (Fig. 2). The first-born retinal cell type is ganglion cells (d35, Fig. 4). These cells, however, disappear during differentiation as the retinal layer thickens and the supply of medium becomes poorer. At d61, horizontal cells, amacrine cells, and cone

photoreceptors should be present. The rod photoreceptors arise a bit later and are present at d96. The bipolar cells and Müller glia cells are the late-born retinal cell types and will not be present before d126. It could be that you observe organoids falling apart into several small organoids (Fig. 3). All of these smaller organoids should still have a bright outer layer and stain positive for retinal markers.

Time Considerations

The 3D differentiation protocol needs at least 22 weeks and will result in a fully stratified neural retina—although at this time point ganglion cells will be missing for the aforementioned reason. If ganglion cells are the point of interest, following the protocol for 5 weeks is sufficient. Embedding the organoids will take 1 day, followed by 1 day for sectioning and 2 days for immunostaining.

Acknowledgments

We would like to thank Jennifer Aparicio and David Cobrinik (both affiliated with The Vision Center, Department of Surgery, Children's Hospital Los Angeles, Los Angeles, California, United States) for helpful discussions.

The monoclonal antibody AP2α, developed by T.J. Williams (University of Colorado, Denver) was obtained from the Developmental Studies Hybridoma Bank, created by the NICHD of the NIH, and maintained at The University of Iowa, Department of Biology, Iowa City, Iowa.

Open-access funding was enabled and organized by Projekt DEAL. This work was funded by the *Deutsche Forschungsgemeinschaft* (STE 1987/6-1) and partly by the *Ernst und Berta Grimmke-Stiftung* (9/18). Use of hESCs for this work has been reviewed and approved by the Central Ethical Review Board for Stem Cell Research at the Robert Koch Institut, Berlin, Germany (Az.3.04.02/0101) and the Ethical Review Board of the University Duisburg-Essen (16-7215-BO).

Literature Cited

Bar-Nur, O., Russ, H. A., Efrat, S., & Benvenisty, N. (2011). Epigenetic memory and preferential lineage-specific differentiation in induced pluripotent stem cells derived from human pancreatic islet beta cells. *Cell Stem Cell*, *9*(1), 17–23. doi: 10.1016/j.stem.2011.06.007.

Brocher, J. (2014). Qualitative and quantitative evaluation of two new histogram limiting binarization algorithms. *International Journal of Image Processing (IJIP)*, *8*(2), 30–48.

Brocher, J. (2015). The BioVoxxel Image Processing and Analysis Toolbox. EuBIAS Conference, 2015, Jan 5, Institut Curie, Paris, France.

Browne, A. W., Arnesano, C., Harutyunyan, N., Khuu, T., Martinez, J. C., Pollack, H. A., … Cobrinik, D. (2017). Structural and functional characterization of human stem-cell-derived retinal organoids by live imaging. *Investigative Ophthalmology & Visual Science*, *58*(9), 3311–3318. doi: 10.1167/iovs.16-20796.

Capowski, E. E., Samimi, K., Mayerl, S. J., Phillips, M. J., Pinilla, I., Howden, S. E., … Gamm, D. M. (2019). Reproducibility and staging of 3D human retinal organoids across multiple pluripotent stem cell lines. *Development (Cambridge, England)*, *146*(1), dev171686. doi: 10.1242/dev.171686.

Centanin, L., & Wittbrodt, J. (2014). Retinal neurogenesis. *Development*, *141*(2), 241–244. doi: 10.1242/dev.083642.

Crespo, M., Vilar, E., Tsai, S. Y., Chang, K., Amin, S., Srinivasan, T., … Chen, S. (2017). Colonic organoids derived from human induced pluripotent stem cells for modeling colorectal cancer and drug testing. *Nature Medicine*, *23*(7), 878–884. doi: 10.1038/nm.4355.

Deng, W. L., Gao, M. L., Lei, X. L., Lv, J. N., Zhao, H., He, K. W., … Jin, Z. B. (2018). Gene correction reverses ciliopathy and photoreceptor loss in iPSC-derived retinal organoids from retinitis pigmentosa patients. *Stem Cell Reports*, *10*(6), 2005. doi: 10.1016/j.stemcr.2018.05.012.

Eiraku, M., & Sasai, Y. (2011). Mouse embryonic stem cell culture for generation of three-dimensional retinal and cortical tissues. *Nature Protocols*, *7*(1), 69–79. doi: 10.1038/nprot.2011.429.

Eiraku, M., & Sasai, Y. (2012). Self-formation of layered neural structures in three-dimensional culture of ES cells. *Current Opinion in Neurobiology*, *22*(5), 768–777. doi: 10.1016/j.conb.2012.02.005.

Eiraku, M., Adachi, T., & Sasai, Y. (2012). Relaxation-expansion model for self-driven retinal morphogenesis: A hypothesis from the perspective of biosystems dynamics at the multicellular level. *Bioessays*, *34*(1), 17–25. doi: 10.1002/bies.201100070.

Fischer, A. H., Jacobson, K. A., Rose, J., & Zeller, R. (2008). Cryosectioning tissues. *CSH Protocols*, *2008*, pdb prot4991. doi: 10.1101/pdb.prot4991.

Gagliardi, G., Ben M'Barek, K., Chaffiol, A., Slembrouck-Brec, A., Conart, J. B., Nanteau, C., … Goureau, O. (2018). Characterization and transplantation of CD73-positive photoreceptors isolated from human iPSC-derived retinal organoids. *Stem Cell Reports*, *11*(3), 665–680. doi: 10.1016/j.stemcr.2018.07.005.

Gonzalez-Cordero, A., Kruczek, K., Naeem, A., Fernando, M., Kloc, M., Ribeiro, J., … Ali, R. R. (2017). Recapitulation of human retinal development from human pluripotent stem cells generates transplantable populations of cone

photoreceptors. *Stem Cell Reports*, *9*(3), 820–837. doi: 10.1016/j.stemcr.2017.07.022.

Hallam, D., Hilgen, G., Dorgau, B., Zhu, L., Yu, M., Bojic, S., … Lako, M. (2018). Human-induced pluripotent stem cells generate light responsive retinal organoids with variable and nutrient-dependent efficiency. *Stem Cells*, *36*(10), 1535–1551. doi: 10.1002/stem.2883.

Heavner, W., & Pevny, L. (2012). Eye development and retinogenesis. *Cold Spring Harbor Perspectives in Biology*, *4*(12), a008391. doi: 10.1101/cshperspect.a008391.

Hiler, D., Chen, X., Hazen, J., Kupriyanov, S., Carroll, P. A., Qu, C., … Dyer, M. A. (2015). Quantification of retinogenesis in 3D cultures reveals epigenetic memory and higher efficiency in iPSCs derived from rod photoreceptors. *Cell Stem Cell*, *17*(1), 101–115. doi: 10.1016/j.stem.2015.05.015.

Hira, V. V. V., de Jong, A. L., Ferro, K., Khurshed, M., Molenaar, R. J., & Van Noorden, C. J. F. (2019). Comparison of different methodologies and cryostat versus paraffin sections for chromogenic immunohistochemistry. *Acta Histochemica*, *121*(2), 125–134. doi: 10.1016/j.acthis.2018.10.011.

Hughes, C. S., Postovit, L. M., & Lajoie, G. A. (2010). Matrigel: A complex protein mixture required for optimal growth of cell culture. *Proteomics*, *10*(9), 1886–1890. doi: 10.1002/pmic.200900758.

Jin, Z. B., Okamoto, S., Xiang, P., & Takahashi, M. (2012). Integration-free induced pluripotent stem cells derived from retinitis pigmentosa patient for disease modeling. *Stem Cells Translational Medicine*, *1*(6), 503–509. doi: 10.5966/sctm.2012-0005.

Kapatai, G., Brundler, M. A., Jenkinson, H., Kearns, P., Parulekar, M., Peet, A. C., & McConville, C. M. (2013). Gene expression profiling identifies different sub-types of retinoblastoma. *British Journal of Cancer*, *109*(2), 512–525. doi: 10.1038/bjc.2013.283.

Kuwahara, A., Ozone, C., Nakano, T., Saito, K., Eiraku, M., & Sasai, Y. (2015). Generation of a ciliary margin-like stem cell niche from self-organizing human retinal tissue. *Nature Communications*, *6*, 6286. doi: 10.1038/ncomms7286.

Llonch, S., Carido, M., & Ader, M. (2018). Organoid technology for retinal repair. *Developmental Biology*, *433*(2), 132–143. doi: 10.1016/j.ydbio.2017.09.028.

Mandai, M., Fujii, M., Hashiguchi, T., Sunagawa, G. A., Ito, S. I., Sun, J., … Takahashi, M. (2017). iPSC-derived retina transplants improve vision in rd1 end-stage retinal-degeneration mice. *Stem Cell Reports*, *8*(4), 1112–1113. doi: 10.1016/j.stemcr.2017.03.024.

McLelland, B. T., Lin, B., Mathur, A., Aramant, R. B., Thomas, B. B., Nistor, G., … Seiler, M. J. (2018). Transplanted hESC-derived retina organoid sheets differentiate, integrate, and improve visual function in retinal degenerate rats. *Investigative Ophthalmology & Visual Science*, *59*(6), 2586–2603. doi: 10.1167/iovs.17-23646.

Mellough, C. B., Collin, J., Queen, R., Hilgen, G., Dorgau, B., Zerti, D., … Lako, M. (2019). Systematic comparison of retinal organoid differentiation from human pluripotent stem cells reveals stage specific, cell line, and methodological differences. *Stem Cells Translational Medicine*, *8*(7), 694–706. doi: 10.1002/sctm.18-0267.

Meyer, J. S., Shearer, R. L., Capowski, E. E., Wright, L. S., Wallace, K. A., McMillan, E. L., … Gamm, D. M. (2009). Modeling early retinal development with human embryonic and induced pluripotent stem cells. *Proceedings of the National Academy of Sciences of the United States of America*, *106*(39), 16698–16703. doi: 10.1073/pnas.0905245106.

Nakano, T., Ando, S., Takata, N., Kawada, M., Muguruma, K., Sekiguchi, K., … Sasai, Y. (2012). Self-formation of optic cups and storable stratified neural retina from human ESCs. *Cell Stem Cell*, *10*(6), 771–785. doi: 10.1016/j.stem.2012.05.009.

Parfitt, D. A., Lane, A., Ramsden, C. M., Carr, A. J., Munro, P. M., Jovanovic, K., … Cheetham, M. E. (2016). Identification and correction of mechanisms underlying inherited blindness in human iPSC-derived optic cups. *Cell Stem Cell*, *18*(6), 769–781. doi: 10.1016/j.stem.2016.03.021.

Phelan, K., & May, K. M. (2017). Mammalian cell tissue culture techniques. *Current Protocols in Molecular Biology*, *117*, A.3F.1–A.3F.23. doi: 10.1002/cpmb.31.

Phillips, M. J., Capowski, E. E., Petersen, A., Jansen, A. D., Barlow, K., Edwards, K. L., & Gamm, D. M. (2018). Generation of a rod-specific NRL reporter line in human pluripotent stem cells. *Scientific Reports*, *8*(1), 2370. doi: 10.1038/s41598-018-20813-3.

Schindelin, J., Arganda-Carreras, I., Frise, E., Kaynig, V., Longair, M., Pietzsch, T., … Cardona, A. (2012). Fiji: An open-source platform for biological-image analysis. *Nature Methods*, *9*(7), 676–682. doi: 10.1038/nmeth.2019.

Tucker, B. A., Mullins, R. F., Streb, L. M., Anfinson, K., Eyestone, M. E., Kaalberg, E., … Stone, E. M. (2013). Patient-specific iPSC-derived photoreceptor precursor cells as a means to investigate retinitis pigmentosa. *Elife*, *2*, e00824. doi: 10.7554/eLife.00824.

Zhong, X., Gutierrez, C., Xue, T., Hampton, C., Vergara, M. N., Cao, L. H., … Canto-Soler, M. V. (2014). Generation of three-dimensional retinal tissue with functional photoreceptors from human iPSCs. *Nature Communications*, *5*, 4047. doi: 10.1038/ncomms5047.

Internet Resources

https://imagej.net/Fiji/Downloads

Fiji website.

https://www.biovoxxel.de/development/

Biovoxxel website.

Human iPSC-Derived Blood-Brain Barrier Models: Valuable Tools for Preclinical Drug Discovery and Development?

Antje Appelt-Menzel,[1,2] Sabrina Oerter,[1,2] Sanjana Mathew,[2] Undine Haferkamp,[3] Carla Hartmann,[4] Matthias Jung,[4] Winfried Neuhaus,[5] and Ole Pless[3,6]

[1]Fraunhofer Institute for Silicate Research ISC, Translational Center Regenerative Therapies (TLC-RT), Röntgenring 11, Würzburg, Germany
[2]University Hospital Würzburg, Chair Tissue Engineering and Regenerative Medicine (TERM), Röntgenring 11, Würzburg, Germany
[3]Fraunhofer IME ScreeningPort, Schnackenburgallee 114, Hamburg, Germany
[4]University Hospital Halle, University Clinic and Outpatient Clinic for Psychiatry, Psychotherapy, and Psychosomatic Medicine, Julius-Kuehn-Strasse 7, Halle (Saale), Germany
[5]AIT Austrian Institute of Technology GmbH, Center Health and Bioresources, Competence Unit Molecular Diagnostics, Giefinggasse 4, Vienna, Austria
[6]Corresponding author: *ole.pless@ime.fraunhofer.de*

Translating basic biological knowledge into applications remains a key issue for effectively tackling neurodegenerative, neuroinflammatory, or neuroendocrine disorders. Efficient delivery of therapeutics across the neuroprotective blood-brain barrier (BBB) still poses a demanding challenge for drug development targeting central nervous system diseases. Validated *in vitro* models of the BBB could facilitate effective testing of drug candidates targeting the brain early in the drug discovery process during lead generation. We here review the potential of mono- or (isogenic) co-culture BBB models based on brain capillary endothelial cells (BCECs) derived from human-induced pluripotent stem cells (hiPSCs), and compare them to several available BBB *in vitro* models from primary human or non-human cells and to rodent *in vivo* models, as well as to classical and widely used barrier models [Caco-2, parallel artificial membrane permeability assay (PAMPA)]. In particular, we are discussing the features and predictivity of these models and how hiPSC-derived BBB models could impact future discovery and development of novel CNS-targeting therapeutics. © 2020 The Authors.

Keywords: blood-brain barrier (BBB) *in vitro* model • CNS disease • drug permeability screening • human-induced pluripotent stem cells (hiPSC) • preclinical drug discovery

How to cite this article:
Appelt-Menzel, A., Oerter, S., Mathew, S., Haferkamp, U., Hartmann, C., Jung, M., Neuhaus, W., & Pless, O. (2020). Human iPSC-derived blood-brain barrier models: Valuable tools for preclinical drug discovery and development?. *Current Protocols in Stem Cell Biology*, *55,* e122. doi: 10.1002/cpsc.122

CURRENT PROTOCOLS
A Wiley Brand

Current Protocols in Stem Cell Biology e122, Volume 55
Published in Wiley Online Library (wileyonlinelibrary.com).
doi: 10.1002/cpsc.122

INTRODUCTION

Effectively targeting diseases of the central nervous system (CNS) remains an unmet clinical need. Efficient delivery of therapeutics across the blood-brain barrier (BBB) poses a demanding challenge for CNS drug development and translation of basic biological findings towards application. 98% of small-molecule and nearly 100% of large-molecule drugs are not able to cross the BBB (Pardridge, 2005). Furthermore, clinical studies reported by the largest companies involved in drug discovery and development indicate a continued low translation between first-in-man studies and approval of novel therapeutics, particularly in CNS-linked diseases, where the overall success rate is low, even though the clinical candidates have previously been tested in cellular *in vitro* or *in vivo* models (Dowden & Munro, 2019; Kola & Landis, 2004; Waring et al., 2015). This indicates the urgent need for alternative methods and implementation of appropriate testing strategies. One of the key determinants for the below-average success in targeting CNS disease is the non-standardized and often contradictory use of *in vitro* and *in vivo* test systems for characterizing the effects of potential therapeutic agents (small molecule compounds and biologicals, in particular antibodies). The reasons behind this phenomenon are complex and specific to the respective drug development program but include on- and off-target related toxicities, insufficient efficacy, inadequate validation of the disease-target linkage (poor target validation), and insufficient availability of the agent at the intended site of action in the brain. Accurate determination of efficacy of a test substance is a key readout parameter in early drug discovery projects. In addition, the establishment and validation of disease-relevant *in vitro* and *in vivo* models is essential to program success. If the intended compound cannot enter the brain, then efficacy cannot be achieved, regardless of the degree of target validation and failure is guaranteed. Therefore, data on the permeability of substances across the BBB are ultimately indispensable for estimating the availability and effectiveness of CNS drugs. However, some aspects have to be considered for a reliable prediction of the BBB permeability, e.g., species differences between humans and non-human primates/rodent models, as well as the substitution of brain capillary endothelial cells (BCECs) with peripheral tissue-specific endothelial cell (EC) sources. Cell sources with divergent functional characteristics, for example epithelial cell lines (e.g., Caco-2 or MDCK) or ECs of non-cerebral origin (e.g., HUVEC), provide another reason why these transport models are inadequate for the task at hand. Compounding this problem are the lack of regulatory guidelines to assist in the validation of new models for BBB permeation. Functionally relevant and validated human BBB models accurately predicting the transport of substances into the brain together with other methods such as serum binding, brain slice uptake, or brain homogenate binding assays will greatly reduce the requirement for *in vivo* testing of compound distribution and action in the brain and is highly relevant for all CNS-related toxicity, pharmacokinetic, pharmacodynamics and efficacy studies. A physiological and disease-relevant BBB model would act as a pre-screening platform to evaluate the capability of chemical or biological agents to penetrate or actively overcome the BBB. Only substances with the potential to cross the BBB would be taken into account to determine direct and indirect neurotoxic effects. Preclinical safety and efficacy studies for newly developed drug candidates could be a main field of application of human BBB models. Especially in the early phase of lead optimization, it is expected to induce an improved selection of the drug candidates but also an improved predictivity in later developmental stages. In 2012, the first BBB models derived from human-induced pluripotent stem cells (hiPSCs) were invented and are now reaching a level of validation that might make them suitable for utilization in preclinical drug development programs in the pharmaceutical industry. In addition, these models could provide insights into mechanisms of CNS diseases, which are often associated with general or specific pathophysiological alterations at the BBB.

In this review we discuss how hiPSC-derived BBB models compare to widely applied barrier test systems, such as Caco-2 and parallel artificial membrane permeability assay (PAMPA), as well as to BBB models from primary human or non-human BCECs and rodent *in vivo* models. In particular, we are focusing on the predictivity of the model types, the current technological status to generate hiPSC-derived BBB models and future trends in pharmaceutical development.

STRUCTURE AND FUNCTION OF THE BBB IN HEALTH AND DISEASE

The average adult human brain consists of ∼100 billion neurons and weighs around

1.5 kg with a volume of around 1.2 L. Although it constitutes only 2% of the total body weight, around 20% of the basal metabolic energy is consumed. Proper functioning of the vasculature supplying the brain with nutrients is required to maintain this high energy demand. The capillaries of the brain parenchyma have a length of around 600 km with a diameter of 7 μm (Keller, 2013; Wong et al., 2013). The circumference of these brain capillaries are lined with specialized ECs, representing the main component of the BBB and interacting with pericytes, astrocytes, neurons, microglial cells, and extracellular matrix components (ECM). The complex and dynamic association and communication of the elements led to the definition of the term neurovascular unit (NVU). The BCECs show specialized characteristics due to lack of fenestrations, higher mitochondria numbers, minimal pinocytotic activities, low rate of transcytosis, low expression of leucocyte adhesion molecules, higher pericyte coverage, special astrocyte end feet coverage, and the expression of dense tight junctions (TJs), as well as an increased expression of solute carriers and efflux transporters when compared to peripheral vasculature (Hawkins & Davis, 2005; Keller, 2013). This complex interaction of the cell types and functionalities make up the BBB. The main functions of the BBB can be divided into three subgroups, the physical-, metabolic-, and transport-barrier (Neuhaus & Noe, 2010). The BBB regulates and modulates biochemical and activated cellular traffic at the NVU thereby maintaining the homeostasis of the brain microenvironment (Abbott & Friedman, 2012).

Tight Junctions at the BBB

Entry of hydrophilic molecules and immune cells to the CNS is restricted by the presence of junctional protein complexes. These complexes are responsible for sealing the paracellular space and the degree of BBB tightness is determined via interaction of junctional proteins on neighboring BCECs. TJs limit the paracellular transport of substances to the brain and are also crucial for the polarization of the BCECs. The main transmembrane proteins involved in the formation of TJs are claudins, occludins, and junction adhesion molecules (JAMs). Adherence junctions (AJs) represent an additional type cellular junctions of BCECs and are a prerequisite for proper TJ formation. Especially claudin-5 is highly expressed in rodent BMECs. KO mice lacking claudin-5 are characterized by a size-selective leakage of the BBB. Occludin is highly enriched in CNS BCECs compared to other tissues. JAMs are known to regulate leucocyte extravasations, particularly JAM4 has been identified in the BBB of mice. The tight junction complexes are linked to the cytoskeleton via a series of adaptors and cytoplasmic accessory proteins such as zonula occludens (ZO)-1 and -2, cingulin, jacop, membrane-associated guanylate kinases, afadin, and 7H6 antigen. Additionally, the TJs interact with AJs. Main proteins of AJs are vascular endothelial cadherin (VE-cadh) and platelet EC adhesion molecule (PECAM-1), which are further linked to the cytoskeleton via catenins (Bauer, Krizbai, Bauer, & Traweger, 2014; Daneman & Prat, 2015; Liu, Wang, Zhang, Wei, & Li, 2012; Sweeney, Zhao, Montagne, Nelson, & Zlokovic, 2019; Weiss, Miller, Cazaubon, & Couraud, 2009). These TJs are responsible for barrier integrity which can for example be measured by the transendothelial electrical resistance (TEER). In frogs, average TEER values of around 1900 $\Omega*cm^2$ (Crone & Olesen, 1982) and in rats of around 1500 $\Omega*cm^2$ (Butt, Jones, & Abbott, 1990) were determined. Until now, no human *in vivo* reference TEER data is available.

Transporters at the BBB

The high energy demand of neurons is met by the selective entry of various monosaccharides, amino acids, and ions. Glucose is actively transported via glucose transporters-1 (GLUT-1) and GLUT-3. Small hydrophobic molecules, gases, and uncharged polar molecules can pass the membrane by simple diffusion. Short chain monocarboxylic acids, such as L-lactate, acetate, pyruvates, thyroid hormones, aromatic amino acids, and ketone bodies are transported via monocarboxylic acid transporters (MCTs) (Vijay & Morris, 2014). Proteins, such as insulin-like growth factors, vasopressin and transferrin, are transported into the brain via receptor-mediated transcytosis mechanisms (RMT). RMT mechanisms are specially investigated in the delivery of drugs to the brain, among the most importantly studied ones are the transferrin receptors (Tfr), low density lipoprotein receptors (LDLR) and insulin receptors (INSR) (Pulgar, 2018). Multispecific transporters of the ATP-binding cassette transporter families (ABCs) and solute carrier families (SLC) play crucial roles in regulating the entry of blood-delivered molecules, such as drugs into the brain. They recognize active endogenous compounds such as prostaglandins, leukotrienes,

and steroid hormones and prevent the brain from potential over-accumulation of these compounds. ABC transporters are responsible for the efflux of lipophilic and amphiphilic toxic compounds including several anti-inflammatory, anti-infectious, anti-depressant, and psychotropic agents (Strazielle & Ghersi-Egea, 2015). These transporters include P-glycoprotein (P-gp/ABCB1), breast cancer resistance protein (BCRP/ABCG2), and several multidrug-resistance associated proteins (MRPs/ABCCs). P-gp actively effluxes various xenobiotic compounds. P-gp, BCRP and MRPs show overlaps in substrate specificities thereby preventing the therapeutic entry of pharmaceuticals into the brain (Wevers & de Vries, 2016). BCRPs exclude therapeutics such as cytostatics and MRPs are known to efflux neutral organic drugs. Almost all transporters not belonging to the ABC transporter family belong to the SLC group, which consists of three main sub families. These carriers can be either unidirectional or bidirectional. The SLC22 subfamily includes charged organic transporters called organic anionic transporters (OATs) and organic cationic transporters (OCTs). The SLC21/SLCO forms a family of organic anion transport polypeptides (OATPs). SLCO members accept a broad range of substrates like environmental pollutants, nucleosidic antiviral drugs and non-steroidal anti-inflammatory agents. Members of the SLC15 family are required to transport endogenous di- and tri-peptides, peptidomimetic drugs (β-lactam) and antibiotics (Strazielle & Ghersi-Egea, 2015; Sweeney et al., 2019).

Disease- and Age-Associated Changes at the BBB

Altered BBB functions are shown in numerous brain disorders such as stroke, epilepsy, brain trauma, multiple sclerosis, Huntington´s disease, amyotrophic lateral sclerosis, schizophrenia (SCZ), Parkinson´s disease (PD), and Alzheimer´s disease (AD) (Greene et al., 2018; Neuwelt et al., 2011). Munji and co-workers recently analyzed BBB endothelial cells in mice suffering from neurological diseases including stroke, multiple sclerosis, traumatic brain injury, and seizures (Munji et al., 2019). BBB endothelial cells were analyzed using transcriptomics, and obtained gene expression profiles exhibited comparable gene expression changes in the context of different diseases. These data suggest that different diseases share common disease mechanisms affecting BBB functionality. One major result is that these changes induce loss of BBB characteristics and support a peripheral identity. Mice with seizures showed changes likely due to the increased metabolic activity of neurons highlighting that BCECs dynamically alter their properties in response to neural activity. Viruses such as poliovirus, adenovirus, Epstein-Barr virus, and West Nile virus can directly infect the BCECs while targeting JAMs or GLUTs. These infections can downregulate TJ proteins promoting chemokine production while host immune responses can attenuate BBB damage (Sweeney et al., 2019). In addition, the Zika virus infects and replicates in BCECs strain-independent, but changes in BBB permeability occurred strain-dependent (Leda et al., 2019). With the recent outbreak of the Coronavirus disease 2019 (COVID-19), researchers debate the need for neurological tissue models to understand the biology of SARS-CoV-2 infections. The brain has been reported to express angiotensin converting 2 enzyme (ACE-2) receptors, responsible for virus uptake, and brain autopsies of patients suffering from severe acute respiratory syndrome (SARS) presented with virus-infected brain tissue (Puelles et al., 2020). Furthermore, recent studies have proposed these manifestations in hospitalized patients affirming the neurotropic potential of the virus (Mao et al., 2020). Nevertheless, current data do not allow to conclude that SARS-CoV-2 can permeate across the BBB. It is known that the thickness of the basement membrane of the BBB increases during postnatal development and continually increases in aged animals. Other changes include gliofibrillar proliferations, loss of BCECs, decreased mitochondria/mitochondrial dysfunction, and region-specific alterations in cross-sections of capillary walls and lumens (Erdo, Denes, & de Lange, 2017; Goodall et al., 2018). Notably, interspecies differences in these phenotypes exist: Recent studies in mice revealed ultrastructural changes of the BBB of mice with increasing age, showing an enhanced thickness and lipid accumulations compared to the human BBB (Ceafalan et al., 2019). Some studies using advanced magnetic resonance imaging were able to quantify regional BBB permeability in living human brains, showing an age-dependent BBB breakdown in the hippocampus (Montagne et al., 2015). In this article we will focus on disease-associated alterations at the BBB in AD. AD is the most common cause of dementia with a

steep increase of 5.8 million Americans diagnosed with AD with around 122,019 deaths in 2018 compared to previous years ("2020 Alzheimer's disease facts and figures," 2020). AD is characterized by impaired cognitive functions. The two main pathologies in AD affected brains are the formation of amyloid β (Aβ) plaques and tau tangles. A "two hit hypothesis" was suggested to explain the etiology of AD: Initially, damage occurs at the blood vessels resulting in BBB dysfunctions which in turn leads to Aβ accumulation in the brain and neurodegeneration. Studies from AD *post mortem* brains applying immunohistochemistry and immunoblotting show reduced TJ protein expression and capillary leakages of blood derived proteins, in particular albumins, immunoglobulins, thrombins, iron-containing proteins, and fibrinogens in brain areas with increased plaque depositions. Imaging studies show leaky BBBs in AD patients suggesting this phenotype to be an early biomarker for AD (Neuwelt et al., 2011; Sweeney, Sagare, & Zlokovic, 2018). In addition to non-specific leakages, nonfunctional BBB transport can drive AD pathology. Molecular changes such as low levels of GLUT-1 expression in BCECs were shown to result in diminished glucose transport (Erickson & Banks, 2019). The efflux transporters P-gp and the receptor LRP-1 are major regulators of Aβ CNS levels. Patients with AD show decreased protein levels of LRP-1 and P-gp. This led to the hypothesis that inefficient efflux at the BBB can lead to progression of AD via reduced clearance of Aβ from brain parenchyma. LRP-1 surface receptors on BCECs are responsible for Aβ clearance. They were shown to be diminished in AD brain microvessels leading to reduced clearance of Aβ promoting intracerebral accumulations. AD mouse models with an EC-specific knockout of LRP-1 show increased levels of soluble brain Aβ and severe learning and memory deficits while P-gp deficiency decreases Aβ clearance rates (Banks, 2016; Desai, Monahan, Carvey, & Hendey, 2007). In addition, BBB breakdown also leads to the increased uptake of inflammatory mediators like cytokines, chemokines, peripheral leukocytes, and CD4+T cells into the brain parenchyma thereby accelerating disease progression. Red blood cell extravasation, as well as infiltration by peripheral macrophages and neutrophils reported in AD *post mortem* studies further suggest innate immune system activation in the brain contributing to the pathophysiological changes (Engelhardt, Vajkoczy, & Weller, 2017; Nishihara et al., 2020; Sweeney et al., 2019). ABCA7, which shares a significant sequence homology to ABCA1, mainly promotes cholesterol and phospholipid transport across membranes, but involvement in phagocytic activity and Aβ clearance pathway was also shown in mouse models (Jehle et al., 2006; Kaminski et al., 2000; Kim et al., 2013; Sakae et al., 2016). ABCA7 levels were found to be increased in AD brains due to a compensatory regulation as suggested by the authors (Karch et al., 2012; Vasquez, Fardo, & Estus, 2013). Further, ABCA7 was identified by GWAS as a susceptibility locus contributing to the late-onset form of AD and loss-of-function variants of ABCA7 were reported for AD patients (Almeida, dos Santos, Trancozo, & de Paula, 2018; Hollingworth et al., 2011; Lambert et al., 2013; Steinberg et al., 2015; Vasquez et al., 2013). Recently, it was shown that an ABCA7 polymorphism (rs3764650) within apolipoprotein E carriers of a homozygous risk haplotype (APOE-ε4) results in memory impairment and functional network connectivity in AD patients (Chang et al., 2019). Many mechanisms underlying the onset, progression, and severity of CNS diseases are not completely understood, in particular with regard to BBB functionality (Profaci, Munji, Pulido, & Daneman, 2020). Furthermore, it is not yet understood if the disease-specific BBB degradation is cause or effect of neurological diseases.

APPLICATION OF BBB MODELS IN PRECLINICAL DRUG DISCOVERY

Value of BBB Models for Drug Discovery and Development

The increasing age of the world's population is significantly associated with a growing number of CNS-related diseases, including AD, PD, brain cancer, or stroke, resulting in an urgent need to develop cost-effective packages of medical and social care. A major problem in the CNS drug discovery process is the BBB penetration of effective therapeutic agents in sufficient amounts (Ghose, Herbertz, Hudkins, Dorsey, & Mallamo, 2012). This is one of the reasons for low success rates in CNS drug discovery, resulting in halted drug development programs in pharmaceutical companies for these indications. The increasing number of patients, however, is reflecting the dramatic need of effective drugs: Only for dementia it is predicted that the number of patients in the United Nations population will double every

20 years from 36 million people in 2010 to 115 million in 2050 (Prince et al., 2013). In order to increase the market release of CNS drugs, two major issues need to be overcome in preclinical development: First, the understanding of physicochemical and structural drug characteristics, which correlate with good penetrability needs to be improved; second, better translational models have to be provided to evaluate BBB penetration capability and efficacy of CNS therapeutics. BBB *in vitro* models are useful tools to study BBB permeability and to predict pharmacological availability of drugs, such as small molecules, antibodies, proteins, and peptides. The pharmaceutical industry seeks for standardized and predictive human BBB *in vitro* models in order to differentiate between CNS active and non-active compounds early on in the drug development process.

Currently Applied BBB Models in Early Stage Drug Discovery

Due to the high demand for test systems in basic and preclinical research of drug development and transport studies, a range of different BBB models have been implemented. Besides the *in silico*, acellular *in vitro* and *in vivo* models, numerous cell-based BBB models have been developed. However, standardized models based on immortalized human cell lines show only moderate TJ expression and possess low barrier integrity, which is detected through TEER values below 150 Ω*cm^2 (Deli, Ábrahám, Kataoka, & Niwa, 2005). In comparison, the TEER values in animal experiments reached average values of more than 1500 Ω*cm^2 at the BBB (Butt et al., 1990; Crone & Olesen, 1982). These values are valuable benchmarks from *in vivo* experiments for the *in vitro* model validation, but it should be highlighted that also significantly lower and higher values have been measured in these reports. The availability of human primary BBB cells and healthy human brain tissue is very limited and ethically troublesome. Isolated primary cells change their characteristics rapidly during *in vitro* cultivation. Furthermore, the limited possibility to subculture or cryo-preserve primary cells make them unsuitable for a standardized industrial application. Most widely used primary BBB models in the pharmaceutical industry are based on bovine and porcine brain microvascular endothelial cells (BMECs), but the isolation and cultivation processes are very labor intensive and lead to variable results (Reichel, 2006). In this regard, it should be mentioned that the isolation of pure BCECs is quite difficult. Most procedures yield BMECs and not BCECs, since many protocols end up with a mixture of BCECs with other cells from the microvasculature such as brain arteriole or venule endothelial cells. Furthermore, due to the increasing knowledge of BBB-specific species differences, reproducible human *in vitro* models become more and more important. Most prominent differences are known in the expression of the transporters P-gp *versus* MDR as well as claudin subtypes in rodents and humans (Aday, Cecchelli, Hallier-Vanuxeem, Dehouck, & Ferreira, 2016). By aid of quantitative targeted absolute proteomics (QTAP) of human brain transporters and receptors, it was shown that P-gp expression in humans is 2.33-fold less compared to mdr1a expression in mice. More than 2-fold differences in protein expression were also detected for multidrug resistance-associated protein 4 (ABCC4/MRP4), monocarboxylate transporter 1 (MCT1/SLC16A1), l-type amino acid transporter (LAT1/SLC7A5), and organic anion transporter 3 (OAT3/SLC22A8) in comparative studies of human and rat BBBs. The amounts of ABCG2/BCRP, SLC2A1/GLUT-1, and INSR were similar in both species. These data together with others highlighted that the expression of ABCG2/BCRP was higher than the one of ABCB1/P-gp in humans (Shawahna et al., 2011). Moreover, the specific transporter MRP could not be detected in humans but is reported to be expressed in the rodent BBB. In addition, the expression level of LAT1/SLC7A5 was decreased 5-fold compared to mice (Hoshi et al., 2013; Uchida et al., 2011). Thus, intraspecies differences have an important impact on reproducibility and translation of drug transport efficacy studies (Aday et al., 2016; Bhalerao et al., 2020). Beside the expression of transporters, differences in the presence and quantity of tight junction proteins as well as receptors are reported between humans and rodents. The expression of claudin-3, -5, and -12 was reported to be most relevant in mouse models (Krause et al., 2008; Pfeiffer et al., 2011) until recently the role of claudin-3 and -12 for the barrier function of the BBB in mice was questioned (Castro Dias, Coisne, Baden et al., 2019; Castro Dias, Coisne, Lazarevic et al., 2019). On the contrary, the expression of claudin-1 was only evident at the human BBB (Berndt et al., 2019; Liebner et al., 2000). Claudin-5 expression dominates the BBB *in vitro*, but this

does not reflect the *in vivo* situation. The expression profile of mouse and human TJ proteins *in vivo* is much more complex, but their complexity is largely lost under *in vitro* conditions (Berndt et al., 2019). In general, the properties of BCECs *in vivo* are better comparable to primary human BBB models than to immortalized cell lines (Bagchi et al., 2019). Due to the simple and cost-efficient usage, cell-free PAMPA assays and non-cerebral cell lines, such as Caco-2 or kidney epithelial cells (MDCK), are widely utilized in BBB assays. The MDCK cell line for example is characterized by a tighter barrier and has therefore been used to rank order passive permeation characteristics. Despite its routine use, permeability data obtained by the intestinal cell line Caco-2 cannot be used to evaluate CNS penetration, due to lacking tissue-specificity and, therefore, significance (Reichel, 2006). PAMPA assays are based on transwell systems containing a lipid artificial membrane in order to predict BBB permeation. PAMPA represents a predictive surrogate test for transcellular passive diffusion. Using this assays, compounds can be classified into high, low or uncertain BBB permeation categories. In general, PAMPA assays are considered a high throughput, low cost, and reproducible method. Nevertheless, active transport processes cannot be examined using PAMPA assays, resulting in an overestimation of *in vivo* penetration of tested substances (Bicker, Alves, Fortuna, & Falcao, 2014). In summary, no currently applied *in vitro* test system is able to mimic the *in vivo* complexity of the BBB and its properties (Bicker et al., 2014). As long as the ideal model, representing all critical aspects of BBB penetration characteristics at the same time, is not available, industry-driven drug development programs rely on the combination of several models to separately investigate the passive permeability and specific transport processes of compounds (Reichel, 2006). An alternative to avoid the aforementioned problems and to provide standardized human BBB models by the use of reproducible conditions, could be the application of hiPSC-derived test systems.

CURRENT TECHNOLOGICAL STATUS IN HIPSC-DERIVED BBB MODELING

Comparison of Differentiation Methods and Cellular Characterization

Within the last eight years a variety of different hiPSC-derived BBB models have been established, following alternative differentiation strategies and test system complexities. As summarized in Table 1, numerous methods of successful *in vitro* hiPSC differentiation, under reproducible conditions, were already developed. The BCECs were examined for the presence and the functionality of endothelial-specific markers, as well as specific transporters using transcriptional and proteomic methods. The most extensively used protocol for the derivation of BCECs is the co-differentiation protocol developed by Lippmann and colleagues (Lippmann et al., 2012). The protocol comprises of the following main steps: Firstly, the hiPSCs are differentiated to neural cells and ECs, followed by selective maturation of ECs and finally the elimination of neural subtypes via sub-culture onto collagen IV and fibronectin ECM. Furthermore, retinoic acid (RA) was identified as a suitable component in the enhancement of BBB phenotypes (Lippmann, Al-Ahmad, Azarin, Palecek, & Shusta, 2014; Stebbins et al., 2016; Wilson, Canfield, Hjortness, Palecek, & Shusta, 2015). The protocol has been reproduced by us and various other groups (Appelt-Menzel et al., 2017; Appelt-Menzel, Cubukova, & Metzger, 2018; Katt, Xu, Gerecht, & Searson, 2016; Yamashita, Aoki, Hashita, Iwao, & Matsunaga, 2020). Updates have been made to the original method in accelerating the differentiation process, use of serum-free media or efforts to eliminate additional purification steps (Hollmann et al., 2017; Neal et al., 2019; Ribecco-Lutkiewicz et al., 2018). Inhibition of TGFβ pathway induced the expression of cellular markers and cell-specific characteristics, as well as reduced damages induced by freezing/thawing processes (Yamashita et al., 2020). The use of embryoid bodies (EBs) and co-culture with rat glioma cells or conditioned medium has been explored (Minami et al., 2015). A shift from the co-differentiation protocol to direct BCECs generation was achieved by using chemically defined factors (Grifno et al., 2019; Praca et al., 2019; Qian et al., 2017). Recent advancements have been focused on the overexpression of transcription factors in upregulating BBB phenotypes (Roudnicky et al., 2020). Here, Roudnicky et al. identified 17 transcription factors, including among others TAL1, SOX7, SOX18, ETS1, and LEF1, to improve the direct differentiation of vascular endothelial cells and analyzed them using gain-of-function assays (Patsch et al., 2015; Roudnicky et al., 2020).

Table 1 Overview of the Differentiation Methods to Generate hiPSC-derived BCECs and Comparison of the Cellular Characteristics

Strategy	Co-differentiation						Directed differentiation		Transcription factor overexpression	EBs + Co-culture
Original reference	Lippmann et al. (2012)	Lippmann et al.,(2014)	Hollmann et al.,(2017)	Ribecco-Lutkiewicz et al. (2018)	Neal et al. (2019)	Yamashita et al. (2020)	Qian et al. (2017)	Praca et al. (2019)	Roudnicky et al. (2020)	Minami et al. (2015)
Days required	~13	~13	~8	~21	~8	~13	~10	~15-20	~6	~14
Purification step	+	+	+	-	+	+	-	+	-	+
TEER (Ω*cm^2) monoculture	~200	~3000	~1000-4500	~300-800	~2000-8000	~1500-4000	~3000	~50-60	~20-25	~22-28
TEER (Ω*cm^2) co-culture (cells/ conditioned medium)	~1500	~5000	~6500	~1000-1500	~9000-10,500	N/A	~4000	~50-60	N/A	~55
Tube formation *in vitro*	+	N/A	N/A	N/A	N/A	+	+	N/A	N/A	+
Marker expression (immuno-fluorescence)	Claudin−5, GLUT−1, occludin, PECAM−1, P−gp, VE−cadh, von Willebrand Factor (vWF), ZO−1	BCRP, claudin−5, GLUT−1, MRP−1, occludin, PECAM−1, P−gp, VE−cadh	Claudin−5, GLUT−1, occludin, PECAM−1, VE−cadh	Claudin-5, GLUT−1, occludin, P−gp, PECAM−1,vWF, ZO−1	Claudin−5, GLUT−1, occludin, PECAM−1, VE−cadh	BCRP, claudin−5, GLUT−1, occludin, P−gp, VE−cadh, ZO−1	BCRP, claudin−5, GLUT−1, occludin, MRP−1, PECAM−1, P-gp, VE−cadh, vWF, ZO−1	Claudin−5, GLUT−1, occludin, PECAM−1, P−gp, Tie−2, VE−cadh, vWF, ZO−1	Claudin−5, occludin, VE−cadh, ZO−1	PECAM−1, vWF

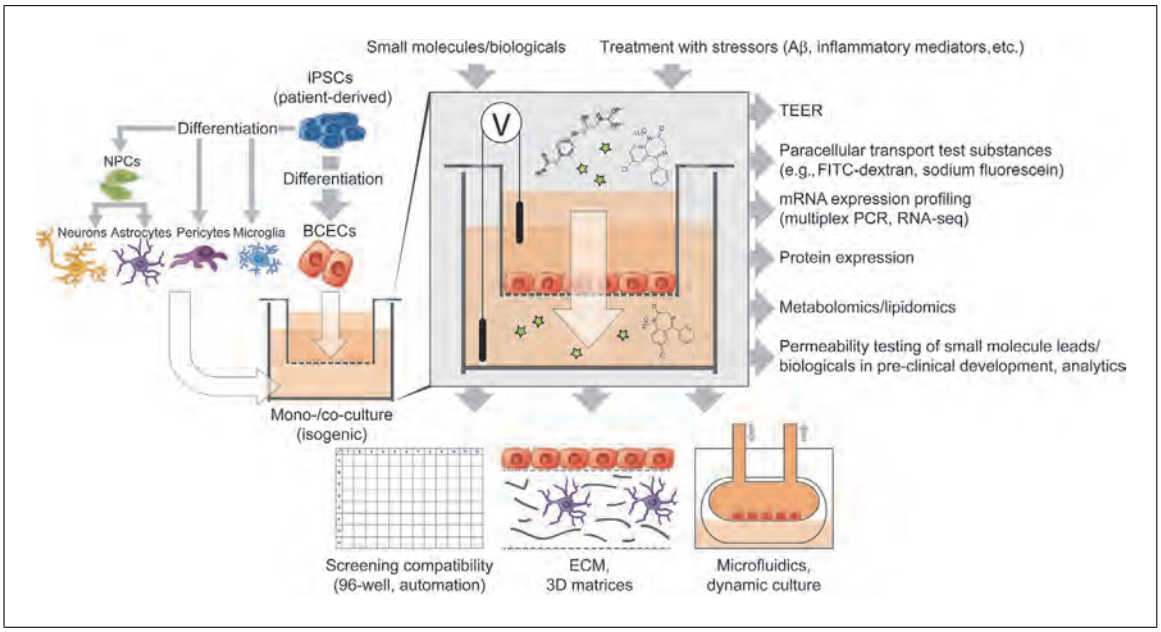

Figure 1 Features of hiPSC-derived BBB models. BCECs are differentiated from healthy or diseased hiPSCs and seeded in the apical compartment of a transwell plate. Patient-specific hiPSC-derived neurons, astrocytes, pericytes, and/or microglia in the basolateral compartment can be used to recapitulate the cellular composition of the NVU and to establish isogenic models. In such a setup, various read-outs are possible either interrogating the BCEC barrier properties, such as TEER measurements or analysis of paracellular transport of test substances is possible. Furthermore, the permeability of small molecule leads and biologicals in preclinical development can be tested. Moreover, additional parameters such as RNA or protein expression levels, as well as metabolomics and lipidomics profiles can be studied. In addition, both compartments can be used to treat or challenge the barrier with soluble factors and to imitate disease-specific environmental stressors (e.g., Aβ or inflammatory mediators). Of note, this setup also allows for the application of HTS formats (up to 96-well transwell plates) and at least partially automatization, dynamic/microfluidic culture resulting in BCEC stimulation by shear stress or the usage of advanced extracellular matrix constituents and three-dimensional structures.

Types of hiPSC-Derived *In Vitro* BBB Models

Static transwell models in mono- and co-culture

Transwell-based models mainly consist of BCECs cultured on a semipermeable cell culture membrane, providing a separated apical and basolateral culture compartment. These models are easy to use; the main advantage is the suitability for unsophisticated co-culture, TEER measurement, and permeability studies. This model is static and the plastic insert membrane acts as an extrinsic barrier, which can be considered as a drawback (Gastfriend, Palecek, & Shusta, 2018). Depending on the protocol used for differentiation, BBB models using these mono-cultures led to varying TEER values (brief summary provided in Table 1) (Delsing et al., 2018; Hollmann et al., 2017; Katt, Linville, Mayo, Xu, & Searson, 2018; Lippmann et al., 2014; Lippmann et al., 2012; Lippmann, Al-Ahmad, Palecek, & Shusta, 2013; Neal et al., 2019; Qian et al., 2017; Ribecco-Lutkiewicz et al., 2018; Stebbins et al., 2016). Recent comparisons of these models have been made to porcine-based systems, resulting in similar drug permeability data for a set of 23 CNS targeting compounds with a correlation coefficient of $R^2 = 0.8$. In addition, activity differences of transporters were highlighted for efflux transporters, as well as GLUT-1 and LAT-1 (Di Marco et al., 2020). Co-culture with pericytes or hiPSC-derived ACs and neurons increased TEER values in transwell models by 30%, while monocultures had values around 3000 Ω*cm^2 (Qian et al., 2017). HiPSC-derived BCECs and PCs co-cultures enhanced BBB phenotypes with reduced levels of transcytosis (Stebbins et al., 2019). Previously, we have analyzed a set of ten different BBB culture models using hiPSC-derived BCECs, multipotent (fetal) neural stem cells, ACs, and PCs. The most complex culture models were able to investigate the distinct upregulation of typical BBB genes, as well as significant increase of TEER compared to the mono-cultures (Appelt-Menzel et al., 2017; Appelt-Menzel et al., 2018). Studies like ours confirmed that the combination of cell types of the NVU enhances barrier properties

compared to mono-cultures of hiPSC-derived BCECs. Ribecco and colleagues developed the first syngeneic stem cell model to study receptor-mediated transcytosis and its application in evaluation of antibody-based BBB carriers. The mono-cultures yielded TEER between 300 and 800 $\Omega*cm^2$, while with AC conditioned medium the TEER is elevated to $\sim$1000 $\Omega*cm^2$ (Ribecco-Lutkiewicz et al., 2018). Transwell models based on hiPSC-derived BCECs can generally also be used to mimic aspects of neurological diseases, as already shown for example for cerebral ischemia (Kokubu, Yamaguchi, & Kawabata, 2017; Page, Raut, & Al-Ahmad, 2019), Huntington's disease (Lim et al., 2017), MCT8 deficiency (Vatine et al., 2017) or cerebral amyloid angiopathy (CAA) and AD (Blanchard et al., 2020). An overview of hiPSC-derived transwell models is provided in Figure 1.

Planning and performing co-culture experiments face challenges like choosing the ideal media composition for every cell type of the NVU to ensure e.g., viability of co-cultured cells and the maintenance of cell type-specific markers. Considering the effect of cell maturity to signaling pathways, another aspect is finding the optimal timing of bringing together several cell types or various differentiation protocols to one timepoint.

Microfluidic models

Compared to transwell models the microfluidic test systems offer benefits like imitation of fluid flow and shear stress conditions found in physiological situation; however, the scalability and requirement of special expertise is a drawback when using these models for drug discovery applications (Gastfriend et al., 2018). Perfused hydrogels show that hiPSC-derived BCECs form confluent 3D monolayers with barrier integrity up to 3 weeks in culture. Perfusion of the cell-lined channels in low stress conditions stabilizes the barrier integrity over non-perfused controls, hence, indicating that perfusion with shear stress enables long-term barrier functions due to mechanical cues and continuous medium circulations. As a downside, angiogenesis was reported in the perfused channels, presumably due to lack of other NVU cell types and their secreted factor or cell-cell contacts (Faley et al., 2019). DeStefano and colleagues have shown that shear stress does not significantly affect the proliferation, rate of apoptosis, elongation, alignment, and gene expressions in hiPSC-derived BCECs (DeStefano, Jamieson, Linville, & Searson, 2018). Recently, hiPSC-derived BCECs co-cultured with ACs in perfused microfluidic channels were reported to maintain *in vivo*-like TEER values for 12 days, whereby the authors concluded that shear forces were not essential for the establishment of strong intercellular junctions but required to stabilize barrier integrity over time (Wang, Abaci, & Shuler, 2017). HiSC-derived BCECs co-cultured with rat primary ACs in a pumpless microfluidic platform for 10 days showed maintained TEER of $\sim$2000 $\Omega*cm^2$. This system was used as a drug candidate screening platform (Wang et al., 2017). A first-of-a-kind human hypoxic BBB chip model permitting analysis of BBB penetrating peptides and TfRc shuttling mechanisms has been described by Park and colleagues (Park et al., 2019). Channels with cylindrical geometry mimicking the three-dimensional architecture of the BBB have been introduced in proof-of-concept studies (Grifno et al., 2019; Katt et al., 2018; Linville et al., 2019).

Isogenic models

Canfield and colleagues reported for the first time that an NVU transwell model with hiPS-derived neurons, ACs, and BCECs in physiological cell ratios facilitated the investigation of the BBB. The endothelial stimulation by neurons, as well as ACs to the co-culture models induced barrier tightening, tight junction continuity and elevated TEER values, while P-gp efflux transport activity remained unchanged. The main limitation in this study was the absence of isogenic PCs (Canfield et al., 2016; Xiang, Andjelkovic, Wang, & Keep, 2017). In order to overcome the limitation of the previous study, the authors further included the effects of isogenic PCs in a new study, which led to the reduction of the rate of non-specific transcytosis. In this model, the authors noticed no differences in efflux activity compared to mono-cultures, although the co-cultures demonstrated barrier tightening and significant increases in expression of junctional proteins, especially occludin (Canfield et al., 2019). Patel and colleagues investigated the variability on phenotype and cell yield after differentiation in isogenic BBB models using asymptomatic patient samples. Differences in differentiation efficiencies of hiPSC-derived BCECs were noticed for PECAM-1, GLUT-1, and P-gp expression and drug efflux pump activities. The observation of such differences suggest interindividual polymorphisms or sexual dimorphisms; therefore, these observations must be taken into consideration for isogenic disease model

development (Patel, Page, & Al-Ahmad, 2017). Recently, novel isogenic NVU chip models are developed supporting co-culture of hiPSC-derived BCECs and ACs. These chip models support media flow, which can be beneficial in recapitulating physiological conditions (Motallebnejad, Thomas, Swisher, & Azarin, 2019).

Preclinical Permeability Prediction and Potential Application of hiPSC-derived BBB Models

Robust and standardized hiPSC-derived BBB *in vitro* models could be valuable tools for preclinical drug-discovery because they fulfill two fundamental important criteria: They demonstrate physiological BBB relevant *in vivo*-like characteristics and simultaneously are compatible with the high-throughput demands of the pharmaceutical industry. Upscaling technologies using stirred tank bioreactors, spinner or suspension flasks are already routinely used for standardized hiPSC maintenance, as well as differentiation (Ackermann et al., 2018; Halloin et al., 2019; Kropp et al., 2016; Schwedhelm et al., 2019; Silva et al., 2015). On this basis, a high-throughput drug-compatible BBB assay should be feasible. For every developed CNS targeting compound, but also for substances acting in the periphery in order to exclude CNS-mediated side effects, it is mandatory to determine the brain targeting efficacy, as well as the toxicity. BBB *in vitro* models can be applied to perform transport studies, visualize transport routes, analyze drug transporter functionalities, perform drug interaction, or targeting studies, ensure pharmacological safety, examine disease-relevant BBB functions and conduct drug discovery studies (Prieto et al., 2004). The process of developing novel therapeutic agents follows a strategy that is based on the same principle across the entire pharmaceutical industry. Usually, the process of drug discovery is divided into different phases sequentially including target identification, hit identification, lead identification, and lead optimization. There are, however, differences between companies, in particular concerning the detailed organization of the various phases of the drug discovery and development processes. For compounds destined to act within the CNS, the penetrability of the BBB is an important additional property, which is typically investigated during lead generation (Reichel, 2006). A typical high-throughput screen (HTS) results in up to 1% hits of the initial screening library, which after hit validation (comprising of confirmation of single dose hits from the primary screen in replicates, assessment of compound identity and purity) and hit qualification (comprising of *in vitro* potency and selectivity towards related targets, early structure-activity relationships, physiochemistry, pharmacokinetics, and toxicology) narrow down to a handful of lead series (ideally providing a chemically diverse lead-like compound series with sufficient potential for chemical optimization). The characterization of lead compounds and lead series involves *in silico* tools, *in vitro* models and *in vivo* studies to examine pharmacological, pharmacokinetic and early toxicological properties. In programs aiming for the development of CNS therapeutics, the pharmacokinetic studies involve tests for CNS penetration, ranging from *in silico* classification systems, *in vivo* permeability assays, and for selected compounds the determination of brain-to-plasma or CSF-to-plasma ratios *in vivo*. Leads will serve as starting points for iterative steps of chemical optimization with the goal to increase *in vitro* potency and selectivity and to improve *in vivo* pharmacokinetic and pharmacodynamics properties by rational medicinal chemistry efforts. Ultimately, compounds need to be efficacious in relevant animal disease models in order to be progressed. The most promising compounds of these lead series which show *in vivo* efficacy are thoroughly characterized in order to identify the most critical properties and hence, the determining characteristics for the direction of chemical optimization in the subsequent drug development phase. The transition from discovery to development represents a major decision point, as all further activities on the candidate drug will demand a substantial commitment in terms of manpower, resources and budget. Drug development begins with a preclinical phase, which investigates in great detail the metabolism and pharmacokinetics, as well as the toxicology and safety profile of the compound in several (rodent and non-rodent) animal species in order to prepare the testing of the compound into human studies. Current strategies aim at combining elements of drug discovery and development phases earlier in the process to optimize safety and efficacy parameters. Clinical studies establish the safety and pharmacokinetics of the compound in humans (phase I study), from which the dosing scheme is derived for the subsequent phase II and phase III studies to demonstrate clinical efficacy in multi-center trials. To prevent

misinterpretations and incorrect predictions resulting from species differences with regard to the expression of transporters, receptors and TJ proteins which influence BBB permeability, predictive human *in vitro* BBB models should also to be taken into account in drug discovery studies to complement the results (Aday et al., 2016). Obviously, the importance of the BBB and their integrity should be considered to estimate the penetration capacity of newly developed drugs and their metabolites, but on the other hand should also not be ignored in neurotoxicity screenings. The combination of predictive and robust BBB models with downstream located neurological systems can be a future testing strategy of choice. To increase standardization and simplicity, as well as to reduce workload and cell culture costs, cryopreserved hiPSC-derived BCECs can potentially be utilized for customer-specific applications (Wilson, Faubion, Hjortness, Palecek, & Shusta, 2016). The cryopreservation and banking of hiPSC-derived BCECs or respective progenitors will be a future trend for a standardized application of hiPSC-derived BBB models in drug discovery. Several pan-European, US, and Japanese strategies led to the establishment of sophisticated cell banks to address this need over the last decade and could serve as a source for high-quality reference lines used for hiPSC-derived BCEC progenitor generation (De Sousa et al., 2017; McKernan & Watt, 2013; O'Shea, Steeg, Chapman, Mackintosh, & Stacey, 2020).

In Vitro-In Vivo Correlation of Permeability Data Obtained from hiPSC-derived BBB Models

Especially *in vitro* models derived from human cell lines and stem cells have been demonstrated as useful tools for preclinical drug discovery (Aday et al., 2016). During the last years, different hiPSC-derived BBB *in vitro* models were evaluated for their applicability to predict drug permeability of novel treatment modalities, providing promising future concepts for CNS drug development. After differentiation of hiPSCs into BCECs and model characterization, the group of Lippmann et al. correlated in 2012 for the first time permeability values with *in vivo* rodent brain uptake measured by *in situ* brain perfusion, confirming high correlative values for the transport prediction of small molecules with a correlation coefficient of $R^2 = 0.98$ (Lippmann et al., 2012). Le Roux and colleagues differentiated hiPSCs in accordance to protocols described by Lippmann et al. and included an additional puromycin-based selection process for EC purification. The morphology of the differentiated cells was comparable to primary human BMECs and expression of ZO-1, as well as claudin-5 was confirmed on protein level. Except for PECAM-1 and ABCB1, the mRNA expression level of transporters and receptors including ABCC1, ABCG2, TfRc, and INSR was similar to primary cell cultures. Furthermore, they compared BBB permeability of eight clinical positron emission tomography (PET) radioligands in comparison to the human BBB *in vivo*, showing a highly significant correlation ($R^2 = 0.83$, $P = 0.008$) (Roux et al., 2019). With another panel of 18 compounds, the group aimed to further evaluate the ability of the hiPSC-derived BBB *in vitro* test systems to distinguish between CNS and non-CNS drugs. Indeed, the permeability values between both groups significantly differed, showing high values of CNS active drugs (mean Papp $= 30.1 \pm 4 \times 10^{-6}$ cm/s) and only low transport rates of non-CNS drugs (mean Papp $= 2.1 \pm 0.6 \times 10^{-6}$ cm/s), but a relationship between permeability and physicochemical properties of the compounds could not be established. In this context, Papp describes the apparent permeability coefficient and is often used to describe transport velocities of drugs. In intestinal models this value correlates with the absorption. Moreover, species-related transport differences could be confirmed comparing the transport data to an *in vitro* BBB model based on primary rat cells. Prediction of *in vivo* human BBB permeability was also investigated by Ohshima and colleagues using hiPSC-derived mono- and co-culture models (Ohshima et al., 2019). Transporter expression profiles of the hiPSC-derived BCECs was similar to that of human primary BMECs, barrier integrity with TEER values $>1000\ \Omega*cm^2$ and expression of relevant TJ markers, such as claudin-5, ZO-1, and occludin was confirmed. In detail, the expression of transporters and other tissue relevant markers was not affected by co-cultures with pericytes, astrocytes, or neurons. Especially the expression level of P-gp/ABCB1 was similar between the different BBB set-ups, but significantly lower than in the analyzed Caco-2 models. Drug permeability assays yielded a better correlation between hiPSC-derived BBB models and data obtained from *in vivo* assays than rat BBB models or Caco-2 assays. Antibody-triggered

RMT was studied by Ribecco-Lutkiewicz and colleagues (Ribecco-Lutkiewicz et al., 2018). The applied hiPSC-derived BBB model expressed RMT-associated receptors, as LDLR, TfR, INSR, or TMEM30A (receptor for BBB-crossing antibody FC5) and allowed the discrimination of species-selective antibody-mediated transcytosis mechanisms. Correlation of Papp values derived from specific antibody transport and the apparent CNS exposure in rat [simultaneous pharmacokinetic measurements of antibodies in cerebrospinal fluid (CSF) and in the serum] was significantly high with $R^2 = 0.96$.

REGULATORY REQUIREMENTS FOR PRECLINICAL DRUG TESTING AT THE BBB

Regulatory Status Quo

A related key problem within the domain of drug permeability testing at the BBB is that until now no regulatory guidelines for the validation of *in vitro* models are available. An exception are Caco-2 models mimicking the gut epithelium (Volpe, 2011; Volpe et al., 2007). Already in 1993, the European Union Reference Laboratory for alternatives to animal testing (EURL ECVAM) defined the prevalidation and validation of non-animal methods for predicting the penetration of chemicals through the BBB as a current priority (*https://cordis.europa.eu/article/id/10815-alternative-methods-in-biosciences*, accessed on 21.04.2020). Furthermore, within the report of the ECVAM Workshop 49, the need for *in vitro* models to determine BBB transport was again underlined. As there are large quantitative and qualitative differences in BBB systems, EURL ECVAM defined the presence of a restrictive paracellular permeability, the presence of a physiologically plausible cell architecture/morphology, the expression of *in vivo* relevant transporter mechanisms, as well as the simplicity of cell culture as minimal requirements for useful BBB models (Prieto et al., 2004). To sum up the recommendations for the evaluation of the performance of promising *in vitro* models, it was suggested to use an appropriate and defined set of selected compounds to better characterize and standardize the models. To define acceptance criteria of *in vitro* models, the expression of BBB relevant (active) transporters has to be compared to the *in vivo* situation. To ensure the comparability and model standardization, all applied methods have to be defined in standard operation procedures. Moreover, a more precise definition of the abovementioned minimal requirements for model characterization is required, stressing in particular the importance on studying cellular polarity and the restriction of paracellular transport. Model performance has been evaluated by analyzing influx and efflux rates, as well as barrier integrity. All obtained permeability and CNS toxicity data should be provided for setting up an EURL ECVAM database. Endpoints for model validation prior to substance testing have to be defined for valid BBB *in vitro* models. This includes for example the specification of permeability values describing the paracellular tightness of the barrier as well as the transport velocities of BBB relevant reference drugs. Furthermore, the definition of relevant substances, as well as optimal testing concentrations for the (pre-)validation of BBB models are missing, thereby providing an adequate model quality control. Moreover, this topic remains challenging due to the insufficient availability of human *in vivo* data. Nevertheless a wide acceptance of a validated human BBB *in vitro* model is prognosed, urging the supply of a guidance provided by regulatory authorities.

Requirements in Preclinical Drug Discovery

To develop more effective neuropharmacological drugs with the capability to cross the BBB, standardized, robust and highly predictive humanized BBB models should be applied to determine the penetration capacity, as well as to understand the related expression and functionality of transporters at the BBB. The results obtained by use of adequate human BBB test systems should valorize the toxicological results generated in animals, in order to improve the outputs of toxicity tests and to enhance the evaluation of risk and safety in comparison with clinical data in humans (Cecchelli et al., 2007). A challenge to be fulfilled for permeability screenings is the application of *in vitro* models that recapitulate essential aspects of the *in vivo* physiology of the BBB and are compatible with the high-throughput requirements of the pharmaceutical industry (Bicker et al., 2014). In order to evaluate efficiently the large numbers of compounds generated by the pharmaceutical and chemical industry, assays have to be compatible to 96- or 384-well formats, allowing at least a partial automatization of the experimental workflow and resulting data analysis. Furthermore, a simplified handling of the test systems should be feasible, including an easy

assay procedure with well-defined ready-to-use components/reagents ("mix-and-ready") and robust readout parameters using state-of-the-art detection technologies. An appropriate turnaround time ensures the milestone-based compound progression. Beside time efficiency, the assay costs have to be justifiable. A successful usage of hiPSC-derived BBB models in preclinical testing requires the availability of robust *in vitro* test systems, characterized by the presence of a physiologically relevant morphology and cellular polarity, a reproducible permeability of reference compounds, an adequate screening capacity, and the expression of complex tight junction proteins and transporters, as well as their functionality (Cecchelli et al., 2007). To avoid misinterpretations of preclinical toxicity and bioavailability data and to efficiently translate this towards the clinic, the following criteria should be considered: According to the EURL ECVAM principle on test validation, robust protocols to reproducibly generate hiPSC-derived BCECs and resultant BBB models should be provided, describing the purpose of the test method, especially specifying the test system, the readout of the method, defined endpoints, the derivation and expression of results, acceptance criteria, the interpretation of the results and the implementation of adequate controls. Secondly, within-laboratory variability of the assay over time as well as the transferability to another laboratory have to be examined. In addition, the between-laboratory reproducibility should be addressed using a group of at least three qualified laboratories/test facilities at different sites performing a blinded study (Hartung et al., 2004). Advices in good cell culture practice for human primary and stem cell-derived models should be complied to increase the reproducibility of the assay and to ensure high-quality control standards (Pamies et al., 2018). By comparing the obtained results with a reference method, as for example the expression profile of cell-specific markers and transporters to human brain tissue biopsies or freshly isolated BMECs, the predictiveness of the test system can be evaluated. Furthermore, the transport results have to be compared to established *in vivo* and *in vitro* assays (e.g., PAMPA, Caco-2, *in vivo* studies of analyze brain penetration) to determine the robustness of the developed *in vitro* assay. For validation of transport studies a panel of well-defined reference substances, including BBB relevant drugs, small molecules, and biopharmaceuticals of different substance classes, covering the whole spectrum of permeability rates from slow to fast permeating substances, also including substrates of active transporters, should be used. If the predictive power of the hiPSC-derived BBB models should be compared to different species, it is advisable to investigate similar transport targets and processes, but also to include *in vivo* as well as *in vitro* models of the other species in order to exclude *in vitro* model set-up dependent effects. In order to increase the successful development of neurotherapeutics, particular attention has to be focused on the identification of disease-relevant transport targets and mechanisms, taking into account the relevant cellular populations based on hiPSC-derived disease models and variations in gene expression depending on age, sex, or disease stage. To advance the exchange of improved knowledge and to make data available, for example by installation of a online database, for academia as well as for industry, exchange of permeability data from *in vitro* and *in vivo* studies, protocols of standardized test procedures and drug reference sets might lead to an improved data quality for proper comparison of the results obtained by different researchers. This could enable faster validation and approval processes, as well as an increased predictive power of transport studies performed by means of *in vitro* models including an increased correlation to *in vivo* data.

FUTURE TRENDS IN DRUG DEVELOPMENT APPLYING HIPSC-DERIVED BBB MODELS

Monolayer models of the human BBB using transwells as a basis are most frequently used to study signaling pathways, transporter kinetics, binding affinities, or to characterize leads. To fully simulate the BBB integrity and complexity, including cell-cell communications and cell-matrix interactions more complex models are required (Bagchi et al., 2019). The interaction between different brain cell types, directly or indirectly via secreted soluble factors, as well as dynamic shear stress increase for example the expression of EC transporters, as well as TJs and promote cellular polarity. Implementing these factors might be decisive in the future development of e.g. personalized and disease-relevant BBB models.

Precision Medicine

Precision medicine (PM), also known as personalized medicine, is a novel approach of medical treatment taking into account the

individual characteristics of each patient. The approach relies on tailored therapeutic strategies based on identifying and understanding a person's unique molecular and genetic profile and vulnerability to certain diseases. Compared to the traditional approach ("one size fits all"), PM takes into account a patient's genetic and epigenetic risk factors or other biomarkers in addition to clinical information and can increase the chance to predict the most effective and safe medical treatment. Individual BBB properties recently became more and more relevant in this context (Vatine et al., 2019).

Patients suffering from AD and PD show altered BBB functionality at the beginning of the disease and a BBB breakdown in later stages, which is accompanied with neuronal dysfunction, loss of neuronal connectivity, and neurodegeneration (Bowman et al., 2007; Gray & Woulfe, 2015). PM taking into account patient-specific BBB properties could improve therapeutic success for patients suffering from neurodegenerative disorders like AD or PD because alterations of the BBB accompany disease progression (Sweeney et al., 2018). However, modifying BBB functions for treating AD still remains challenging for different treatment strategies including antibody-based approaches, increasing brain clearance of Aβ or antagonize aggregation (Panza, Lozupone, Logroscino, & Imbimbo, 2019). PM focuses on the analysis of genetic mutations of patients to identify suitable drug targets for therapy or risk assessment including the prediction of negative side-effects and the exclusion of non-responders. In AD, this may include considering the genotypes of APOE and ACE (both expressed in BCECs) as recently reported for the treatment with ACE inhibitors (de Oliveira, Chen, Smith, & Bertolucci, 2018). Moreover, modulation of calcineurin-nuclear factor of activated T cell (NFAT) signaling could be another therapeutic option in APOE4-mediated CAA and AD (Blanchard et al., 2020).

HiPSC-based therapies for treating age-related macular degeneration have been successfully conducted (Zarbin, Sugino, & Townes-Anderson, 2019) and cell replacement therapies for human brain cells are currently being tested in clinical trials. A fascinating approach in PM is the transplantation of autografts into the CNS aiming for a curative approach of neurological disease (Barker, Parmar, Studer, & Takahashi, 2017), in particular in PD. The increasing number of clinical trials involving therapies based on hiPSC-derived cells shows the general applicability of autologous clinical-grade stem cells for cell replacement therapies. Additionally, gene therapy is discussed as a promising technology to restore functionality in diseased tissue. Recently, primary rodent BCECs were successfully transduced targeting the lysosomal cholesterol storage disease Niemann Pick type C2 (Hede et al., 2019). To target AD- and PD-related BBB symptoms, there is a need to first understand the consequence of disease-associated genetic variants. Then, patient-specific hiPSCs could be genetically modified to produce healthy BBB tissue for autologous transplantation, although current technologies and associated costs are still prohibitive.

Disease Models Mimicking BBB Alterations

The major promises of disease models are to improve our understanding of pathomechanisms and associated biomarkers. This could be achieved by hiPSCs since one key limitation in drug development for disorders of the CNS is the inaccessibility of (intact) brain tissue. Accordingly, there is a lack of adequate models with high predictive value.

The application of disease models with patient- and disease-specific hiPSC-derived cell types opens up the possibility (i) to develop more effective personalized therapies, (ii) to characterize novel drugs, (iii) to characterize disease-associated mutations and resulting malformations that occur in embryogenesis, childhood, adulthood or old age, (iv) to develop disease- and/or tissue-specific disease models *in vitro*, and (v) to mimic disease-associated mutations or to introduce artificial mutations (e.g. gene knockout) by gene editing (e.g. CRISPR/cas technology).

Diseases of the CNS are often multifactorial including a variety of environmental and genetic risk factors. Genetic risk factors are DNA variations including copy number variations (CNVs), single-nucleotide polymorphisms (SNPs), and functional homozygous mutations. DNA variations influence onset, progression, and treatment of neurodevelopmental and neurodegenerative diseases as well. In this context, DNA variations in genes regulating BBB functionality may not only have an impact on disease onset and progression, but may also play a role for disease treatment. Accordingly, the APOE status is detected as a biomarker in many preclinical studies. Disease models provide a powerful tool to interpret findings from

genetic studies including the validation of AD risk variants such as loss-of-function mutation found in ABCA7 representing a transporter expressed on BCECs (Sims et al., 2017). To investigate BBB dysfunction depending on individual genetic differences, individual cellular models need to be established according to patient-specific genetic profiles. HiPSC-derived models are ideal candidates for disease recapitulation enabling the analysis of molecular and cellular pathways in order to nominate suitable molecular targets addressing a dysfunctional BBB. Patient-derived hiPSCs can be used to investigate the underlying genetically driven pathomechanisms and pathways in BBB dysfunction, since they most likely maintain patient-specific genetic mutations also after transduction and differentiation. Genetic studies have already been conducted for over 20 years and the first familial AD-correlated mutation on chromosome 21 was already suggested in 1987 (St George-Hyslop et al., 1987). Later on, highly multiplexed genotyping sped up the identification of genetic causes of neurological disorders in patients (Sims et al., 2017). Following results from these genome-wide association studies, numerous projects aimed for the identification of disease-specific mutations and the resulting dysregulation or functional impairment of proteins in neurodegenerative disorders. The number of genetic risk factors associated with BBB dysfunction in neurodegenerative disorders is constantly growing due to the growing number of cohort studies and the enlargement of existing cohorts (Savage et al., 2018). The technological advancement in multi-omics technologies will further accelerate and enlarge such studies. Meta-analysis and epidemiological studies will support these developments. These data will help to fill gaps in our knowledge regarding of the contribution of altered BBB functionality in AD, PD, and other diseases. However, identifying the causal relationship between specific mutations and pathophysiological changes of the BBB and especially BCECs has only been addressed scarcely.

Cellular two-dimensional and organotypic three-dimensional hiPSC-derived *in vitro* models hold a great promise for the functional characterization of DNA variations necessary to further advance the field of translational medicine aiming at the transfer of insight from neuroscience research to clinical application. Patient-specific hiPSC-derived cells can also mimic aspects of BBB associated glial cell types including microglia which are key modulators of CNS disease (Ormel et al., 2018). Complex BBB models are suggested to be more predictive for disease modeling and toxicity screenings (Qian et al., 2018). Advanced co-culture CNS models composed of patient-specific hiPSC-derived cell types allow for the analysis of cell-cell communication and provide deeper insights into complex brain physiology (Raja et al., 2016; Smits et al., 2019). Thus, the impact of disease-associated mutations on BBB integrity in AD and PD patients can be studied in different cell types of the NVU. It is important to mention that mutations associated with AD occur in genes that are expressed by a variety of different cell types including BCECs, PCs, ACs, and neurons (Anttila et al., 2013; Blanchard et al., 2020; Challen et al., 2011). Therefore, in complex diseases such as AD and PD, however, multifactorial etiologies have to be considered, thus just cultivating AD hiPSC-derived BCECs might be not sufficient to mimic the disease phenotype and factors such as additional cell types of the NVU, inflammatory cytokines, growth medium adaptations or further disease-relevant stimuli have to be considered for *in vitro* model optimization.

Personalized *in vitro* cell models of the BBB, generated from patient-derived hiPSCs, could be used to validate drug candidates or to repurpose launched drugs for different indications. In preclinical testing, these models might have the potential to improve the success rate in clinical trials of CNS disorders affecting the BBB including AD and PD. Over 5000 clinical trials analyzing a variety of interventions for the treatment of neurodevelopmental diseases are currently listed in the United States National Institute of Health database *ClinicalTrials.gov*. Only 37 of them are related to the BBB. Application of preclinical hiPSC-derived BBB models to (i) improve the prediction of drug transport across the BBB to the target location, (ii) optimize efficient drug delivery, (iii) avoid potential risks, and (iv) eliminate unsuitable drug candidates early in the discovery/development phase could streamline this process and increase awareness for BBB-related aspects for CNS drugs.

Innovative Matrices and Three-Dimensional BBB *In Vitro* Models

In recent years, there has been a shift towards the development of more complex BBB models to better mimic brain functionality and physiology. To this end, the cellular

composition and extracellular milieu of the *in vitro* models was further improved. The ECM has a significant role in influencing cellular behavior, like differentiation, proliferation and cell attachment. As of now, single proteins are typically in use to increase specific cell behavior; however, this does not represent the complex *in vivo* extracellular microenvironment. Recent advances in biomaterial engineering has enabled the development from standard two-dimensional monolayer cell culture to three-dimensional approaches of CNS models. Cell-loaded hydrogels are in focus as an ECM for three-dimensional brain models, as it possesses many aspects of the natural ECM including stiffness, enzymatic degradability, and binding ligands for cell adhesion (Katt et al., 2018; Tibbitt & Anseth, 2009). Especially for neural stem cell engineering, the understanding and the role of ECM is of growing importance (Lam et al., 2019; Murphy, Haynes, Laslett, Cameron, & O'Brien, 2020; Yang et al., 2012), which is related to the increasing interest in the development of neural transplants for therapy of neurodegenerative diseases and stroke. Neuronal progenitor cells (NPCs) and glia cells can be differentiated from hiPSCs; however, there is a lack of efficient *in vitro* models that generate functional neuronal cells. Novel hydrogels seem to be able to provide promising ECMs for neural differentiation to matured and functional cells for e.g. stroke implants (Lam, Lowry, Carmichael, & Segura, 2014; Moshayedi et al., 2016), and are therefore a current focus for biomolecular engineered stem cell transplants (Nih et al., 2017). Tissue engineered scaffolds like decellularized porcine brain tissue may also be utilized to build up a three-dimensional model of the CNS, since it consists of brain-specific matrix components, like glycosaminoglycans, collagen I, collagen III, collagen IV, collagen V, collagen VI, perlecan, as well as laminin (DeQuach, Yuan, Goldstein, & Christman, 2011). This porcine brain matrix can be used as a platform for hiPSC-derived cells of the NVU to build up a three-dimensional brain model and to support vascularization. Alternatively, it can be applied as coating reagent to enhance cell adhesion or to generate artificial hydrogel-based nanofibrous scaffolds (DeQuach et al., 2011). Despite of the great potential of such natural brain-specific tissue scaffolds, they are still from animal origin, which might pose a problem of species specificity. In this regard, it was shown that the usage of human-specific laminin led to better astroglia differentiation compared to the murine protein (Delsing, Kallur, Zetterberg, Hicks, & Synnergren, 2019), also the integrity of hiPSC-derived BCECs was even improved by human laminin compared to BCECs differentiated on (mouse-derived) Matrigel (Aoki, Yamashita, Hashita, Iwao, & Matsunaga, 2020). Cho et al. established a promising electrospun nanofibrous scaffold based on human brain ECM derived from decellularized human brain tissue to enhance the differentiation of hiPSCs into functional, myelin-expressing oligodendrocytes (Cho et al., 2019). Similar approaches might work also for the establishment of improved BBB models. To avoid possible ethical issues due to the usage of human tissue, an increasing number of studies focus on advanced self-assembling cell types to simulate *in vivo* three-dimensional tissue architecture, such as BBB spheroids, neuronal organoids and mini-brains. These approaches avoid the application of additional ECM constituents (Campisi et al., 2018; Lancaster et al., 2013; Pasca et al., 2015; Urich et al., 2013). The major advantage of these three-dimensional models over two-dimensional cocultures is the direct cell-cell contact, which is crucial for the activity of key signaling pathways. Furthermore, hiPSC-derived three-dimensional *in vitro* BBB models allow to replicate *in vivo* architecture and offer an exciting possibility to study species-specific processes in health and disease in order to develop novel assays suitable for drug discovery (Cho et al., 2017; Nzou et al., 2018).

Dynamic Flow and Microfluidic Culture Systems

BCECs, lining the lumen of capillaries and microvessels, are under constant shear stress generated by blood flow. Although it is known that the application of shear stress affects BCEC characteristics, the majority of the BBB models are represented as static models, (Cucullo, Hossain, Puvenna, Marchi, & Janigro, 2011; DeStefano, Xu, Williams, Yimam, & Searson, 2017; Faley et al., 2019; Garcia-Polite et al., 2017; Wang et al., 2017). Vascular ECs under laminar flow show elongation, polarization, and alignment in the direction of the flow (Ballermann, Dardik, Eng, & Liu, 1998; Tkachenko et al., 2013). The effects of shear stress on BCECs seem to be dependent on the BCECs origin and their tightness status. Especially, hiPSC-derived BCECs showed increased resistance to shear stress mediated elongation in comparison to immortalized BCEC lines with lower basic

tightness (DeStefano et al., 2017; Reinitz, DeStefano, Ye, Wong, & Searson, 2015; Ye et al., 2014). Despite the contradicting data on the role of shear stress and continuous supply of fresh media in different models, the influence of flow is not negligible for BCECs, but it is currently unclear how decisive this factor is for the generation of functional barriers. Different kinds of dynamic BBB models including medium flow are in use to mimic the *in vivo* situation more closer. One example is the application of spinning bioreactors to adapt and maintain mini-brains or spheroids in order to ensure an optimal nutrient distribution within the culture vessel (Qian et al., 2018; Qian et al., 2016; Yan, Song, Madinya, Ma, & Li, 2018). Thereby, the generation of large scale hiPSC-derived BBB spheroid models seems to be feasible and could be used to provide a platform for modeling human brain development and disease (Miranda et al., 2015; Qian et al., 2018; Qian et al., 2016). Engineered microvessels and chip models are another example to apply physiological sheer stress on BCECs (de Graaf et al., 2019). Hydrogel casts with a few hundred-micron range thickness allow the observation of cellular behavior in a more biomimetic environment including fabricated channels supporting fluid flow within the gel (Bertassoni et al., 2014; Lee et al., 2020; Miller et al., 2012). In engineered microfluidic models, such as three-dimensional gelatin/hydrogel channels or so-called brains-on-a-chip, hiPSC-derived BCECs represented a much more stable barrier function and a significant barrier tightness compared to static controls (Faley et al., 2019; Katt et al., 2018; Wang et al., 2017). Moreover, the addition of shear stress on hiPSC-derived BBB models increased the longevity and highlighted their potential application for studies lasting up to three weeks (Faley et al., 2019). The future developments in advanced microfluidics and their application will show (if they are able to hold their promise to recapitulate *in vivo* BBB physiology). To make them ready for industrial use, additional distinct efforts are necessary.

CONCLUSION

The decisive criterion for BBB model selection is the purpose of the study to be conducted (Bagchi et al., 2019). One could follow the credo: As easy as possible, as complex as necessary. A comparison of the currently available drug permeability datasets obtained from BBB *in vitro* models is difficult due to the diversity of the model setups applied, the characterization of variable sets of compounds targeting a variety of transport mechanisms, and the differences of the applied BCECs (Stanimirovic, Bani-Yaghoub, Perkins, & Haqqani, 2015). Moreover, complex dynamic *in vivo* processes, such as drug pharmacokinetics, brain exposure, distribution, elimination, target engagement, and also efficacy, cannot be fully replaced by *in vitro* approaches (Stanimirovic et al., 2015). We see human BBB models as an initial drug screening platform to reduce overall costs in drug development (Aday et al., 2016). Specific questions like the capacity of paracellular diffusion, directional transport across the BBB, rates of transcellular transport, efflux of substances, carrier-mediated transport, receptor-mediated transcytosis, drug metabolism/degradation by BCECs, immune cell interactions with the BBB, screening for potential BBB Trojan horses, species differences/selectivity, as well as cell-based toxicity can be answered by this technology (Stanimirovic et al., 2015). Therefore, the development, validation, and standardization of BBB models is key. HiPSC-derived BBB *in vitro* models showed high correlation to the human *in vivo* situation, but much effort has to be invested on validating these *in vitro* models in order to achieve their broad acceptance, also in industry. Additional aspects requiring critical evaluation are hiPSC-specific model variations, the long-term stability of these BBB models (Aday et al., 2016), and the integration of age-related phenotypes, since BBB models derived from pluripotent stem cells mostly represent young individuals (Lauschke, Frederiksen, & Hall, 2017). Recently, a variety of improved and complex hiPSC-derived BBB models was developed, considering relevant factors such as direct cell-cell contacts, modulation of barrier properties by specified ECM components or flow-induced shear stress, and three-dimensional structures. Nevertheless, due to cost efficiency, handling simplicity, options for automatization, time efficiency for reaching steady-state and comparative reasons, transwell-based BBB models currently seem to be the models with the most potential to be integrated into industrial testing regimes. Monolayer- or isogenic co-culture *in vitro* models of the NVU are considered the gold standard in the field of BBB research and should be incorporated into CNS drug discovery and development programs after evaluation and optimization of the desired features.

The combination of standardized *in vitro* and *in vivo* approaches will improve the translation of data and hopefully clinical success of drug development targeting CNS disease by designing safer and more efficient drug delivery systems (Bicker et al., 2014; Stanimirovic et al., 2015).

ACKNOWLEDGMENTS

We acknowledge all members of the BMBF-funded "HiPSTAR" consortium [Deutsches Zentrum für Luft- und Raumfahrt e.V. (DLR); Förderkennzeichen 01EK1608A to PD Dr. Marco Metzger, 01EK1608B to OP, 01EK1608C to Prof. Dr. Dan Rujescu] for critical discussions. We acknowledge the stipends of the University Würzburg to SO within the post-doc program SCIENTA 2020 and to SM within the PhD program of the Graduate School of Life Sciences (GSLS). This study was supported by the SET foundation (Stiftung zur Förderung der Erforschung von Ersatz- und Ergänzungsmethoden zur Einschränkung von Tierversuchen) project 060 to WN and PD Dr. Marco Metzger.

LITERATURE CITED

2020 Alzheimer's disease facts and figures. (2020). *Alzheimers Dement*. doi: 10.1002/alz.12068.

Abbott, N. J., & Friedman, A. (2012). Overview and introduction: The blood-brain barrier in health and disease. *Epilepsia*, *53*(Suppl 6), 1–6. doi: 10.1111/j.1528-1167.2012.03696.x.

Ackermann, M., Kempf, H., Hetzel, M., Hesse, C., Hashtchin, A. R., Brinkert, K., … Lachmann, N. (2018). Bioreactor-based mass production of human iPSC-derived macrophages enables immunotherapies against bacterial airway infections. *Nature Communications*, *9*(1), 5088. doi: 10.1038/s41467-018-07570-7.

Aday, S., Cecchelli, R., Hallier-Vanuxeem, D., Dehouck, M. P., & Ferreira, L. (2016). Stem cell-based human blood-brain barrier models for drug discovery and delivery. *Trends in Biotechnology*, *34*(5), 382–393. doi: 10.1016/j.tibtech.2016.01.001.

Almeida, J. F. F., dos Santos, L. R., Trancozo, M., & de Paula, F. (2018). Updated meta-analysis of BIN1, CR1, MS4A6A, CLU, and ABCA7 variants in Alzheimer's disease. *Journal of Molecular Neuroscience*, *64*(3), 471–477. doi: 10.1007/s12031-018-1045-y.

Anttila, V., Winsvold, B. S., Gormley, P., Kurth, T., Bettella, F., McMahon, G., … Consortium, I. H. G. (2013). Genome-wide meta-analysis identifies new susceptibility loci for migraine. *Nature Genetics*, *45*(8), 912–U255. doi: 10.1038/ng.2676.

Aoki, H., Yamashita, M., Hashita, T., Iwao, T., & Matsunaga, T. (2020). Laminin 221 fragment is suitable for the differentiation of human induced pluripotent stem cells into brain microvascular endothelial-like cells with robust barrier integrity. *Fluids and Barriers of the CNS*, *17*(1), 25. doi: 10.1186/s12987-020-00186-4.

Appelt-Menzel, A., Cubukova, A., Gunther, K., Edenhofer, F., Piontek, J., Krause, G., … Metzger, M. (2017). Establishment of a human blood-brain barrier co-culture model mimicking the neurovascular unit using induced pluri- and multipotent stem cells. *Stem Cell Reports*, *8*(4), 894–906. doi: 10.1016/j.stemcr.2017.02.021.

Appelt-Menzel, A., Cubukova, A., & Metzger, M. (2018). Establishment of a human blood-brain barrier co-culture model mimicking the neurovascular unit using induced pluripotent stem cells. *Current Protocols in Stem Cell Biology*, *47*(1), e62. doi: 10.1002/cpsc.62.

Bagchi, S., Chhibber, T., Lahooti, B., Verma, A., Borse, V., & Jayant, R. D. (2019). In-vitro blood-brain barrier models for drug screening and permeation studies: An overview. *Drug Design, Development and Therapy*, *13*, 3591–3605. doi: 10.2147/DDDT.S218708.

Ballermann, B. J., Dardik, A., Eng, E., & Liu, A. (1998). Shear stress and the endothelium. *Kidney International. Supplement*, *67*, S100–108. doi: 10.1046/j.1523-1755.1998.06720.x.

Banks, W. A. (2016). From blood-brain barrier to blood-brain interface: New opportunities for CNS drug delivery. *Nature Reviews Drug Discovery*, *15*(4), 275–292. doi: 10.1038/nrd.2015.21.

Barker, R. A., Parmar, M., Studer, L., & Takahashi, J. (2017). Human trials of stem cell-derived dopamine neurons for Parkinson's disease: Dawn of a new era. *Cell Stem Cell*, *21*(5), 569–573. doi: 10.1016/j.stem.2017.09.014.

Bauer, H. C., Krizbai, I. A., Bauer, H., & Traweger, A. (2014). "You Shall Not Pass"-tight junctions of the blood brain barrier. *Frontiers in Neuroscience*, *8*, 392. doi: 10.3389/fnins.2014.00392.

Berndt, P., Winkler, L., Cording, J., Breitkreuz-Korff, O., Rex, A., Dithmer, S., … Haseloff, R. F. (2019). Tight junction proteins at the blood-brain barrier: Far more than claudin-5. *Cellular and Molecular Life Sciences*, *76*(10), 1987–2002. doi: 10.1007/s00018-019-03030-7.

Bertassoni, L. E., Cecconi, M., Manoharan, V., Nikkhah, M., Hjortnaes, J., Cristino, A. L., … Khademhosseini, A. (2014). Hydrogel bioprinted microchannel networks for vascularization of tissue engineering constructs. *Lab on A Chip*, *14*(13), 2202–2211. doi: 10.1039/c4lc00030g.

Bhalerao, A., Sivandzade, F., Archie, S. R., Chowdhury, E. A., Noorani, B., & Cucullo, L. (2020). *in vitro* modeling of the neurovascular unit: Advances in the field. *Fluids and Barriers of the CNS*, *17*(1), 22. doi: 10.1186/s12987-020-00183-7.

Bicker, J., Alves, G., Fortuna, A., & Falcao, A. (2014). Blood-brain barrier models and their

relevance for a successful development of CNS drug delivery systems: A review. *European Journal of Pharmaceutics and Biopharmaceutics*, *87*(3), 409–432. doi: 10.1016/j.ejpb.2014.03.012.

Blanchard, J. W., Bula, M., Davila-Velderrain, J., Akay, L. A., Zhu, L., Frank, A., … Tsai, L. H. (2020). Reconstruction of the human blood-brain barrier *in vitro* reveals a pathogenic mechanism of APOE4 in pericytes. *Nature Medicine*, *26*(6), 952–963. doi: 10.1038/s41591-020-0886-4.

Bowman, G. L., Kaye, J. A., Moore, M., Waichunas, D., Carlson, N. E., & Quinn, J. F. (2007). Blood-brain barrier impairment in Alzheimer disease: Stability and functional significance. *Neurology*, *68*(21), 1809–1814. doi: 10.1212/01.wnl.0000262031.18018.1a.

Butt, A. M., Jones, H. C., & Abbott, N. J. (1990). Electrical resistance across the blood-brain barrier in anaesthetized rats: A developmental study. *Journal of Physiology*, *429*, 47–62. doi: 10.1113/jphysiol.1990.sp018243.

Campisi, M., Shin, Y., Osaki, T., Hajal, C., Chiono, V., & Kamm, R. D. (2018). 3D self-organized microvascular model of the human blood-brain barrier with endothelial cells, pericytes and astrocytes. *Biomaterials*, *180*, 117–129. doi: 10.1016/j.biomaterials.2018.07.014.

Canfield, S. G., Stebbins, M. J., Faubion, M. G., Gastfriend, B. D., Palecek, S. P., & Shusta, E. V. (2019). An isogenic neurovascular unit model comprised of human induced pluripotent stem cell-derived brain microvascular endothelial cells, pericytes, astrocytes, and neurons. *Fluids and Barriers of the CNS*, *16*(1), 25. doi: 10.1186/s12987-019-0145-6.

Canfield, S. G., Stebbins, M. J., Morales, B. S., Asai, S. W., Vatine, G. D., Svendsen, C. N., … Shusta, E. V. (2016). An isogenic blood-brain barrier model comprising brain endothelial cells, astrocytes and neurons derived from human induced pluripotent stem cells. *Journal of Neurochemistry*, doi: 10.1111/jnc.13923.

Castro Dias, M., Coisne, C., Baden, P., Enzmann, G., Garrett, L., Becker, L., … Engelhardt, B. (2019). Claudin-12 is not required for blood-brain barrier tight junction function. *Fluids and Barriers of the CNS*, *16*(1), 30. doi: 10.1186/s12987-019-0150-9.

Castro Dias, M., Coisne, C., Lazarevic, I., Baden, P., Hata, M., Iwamoto, N., … Engelhardt, B. (2019). Claudin-3-deficient C57BL/6J mice display intact brain barriers. *Scientific Reports*, *9*(1), 203. doi: 10.1038/s41598-018-36731-3.

Ceafalan, L. C., Fertig, T. E., Gheorghe, T. C., Hinescu, M. E., Popescu, B. O., Pahnke, J., & Gherghiceanu, M. (2019). Age-related ultrastructural changes of the basement membrane in the mouse blood-brain barrier. *Journal of Cellular and Molecular Medicine*, *23*(2), 819–827. doi: 10.1111/jcmm.13980.

Cecchelli, R., Berezowski, V., Lundquist, S., Culot, M., Renftel, M., Dehouck, M. P., & Fenart, L. (2007). Modelling of the blood-brain barrier in drug discovery and development. *Nature Reviews Drug Discovery*, *6*(8), 650–661. doi: 10.1038/nrd2368.

Challen, G. A., Sun, D., Jeong, M., Luo, M., Jelinek, J., Vasanthakumar, A., … Goodell, M. A. (2011). Dnmt3a is essential for hematopoietic stem cell differentiation. *Blood*, *118*(21), 178–178. doi: 10.1182/blood.V118.21.386.386.

Chang, Y. T., Hsu, S. W., Huang, S. H., Huang, C. W., Chang, W. N., Lien, C. Y., … Chang, C. C. (2019). ABCA7 polymorphisms correlate with memory impairment and default mode network in patients with APOEepsilon4-associated Alzheimer's disease. *Alzheimer's Research and Therapy*, *11*(1), 103. doi: 10.1186/s13195-019-0563-3.

Cho, A. N., Jin, Y., Kim, S., Kumar, S., Shin, H., Kang, H. C., & Cho, S. W. (2019). Aligned brain extracellular matrix promotes differentiation and myelination of human-induced pluripotent stem cell-derived oligodendrocytes. *ACS Applied Materials and Interfaces*, *11*(17), 15344–15353. doi: 10.1021/acsami.9b03242.

Cho, C. F., Wolfe, J. M., Fadzen, C. M., Calligaris, D., Hornburg, K., Chiocca, E. A., … Lawler, S. E. (2017). Blood-brain-barrier spheroids as an *in vitro* screening platform for brain-penetrating agents. *Nature Communications*, *8*, 15623. doi: 10.1038/ncomms15623.

Crone, C., & Olesen, S. P. (1982). Electrical resistance of brain microvascular endothelium. *Brain Research*, *241*(1), 49–55. doi: 10.1016/0006-8993(82)91227-6.

Cucullo, L., Hossain, M., Puvenna, V., Marchi, N., & Janigro, D. (2011). The role of shear stress in Blood-Brain Barrier endothelial physiology. *BMC Neuroscience*, *12*, 40. doi: 10.1186/1471-2202-12-40.

Daneman, R., & Prat, A. (2015). The blood-brain barrier. *Cold Spring Harbor Perspectives in Biology*, *7*(1), a020412. doi: 10.1101/cshperspect.a020412.

de Graaf, M. N. S., Cochrane, A., van den Hil, F. E., Buijsman, W., van der Meer, A. D., van den Berg, A., … Orlova, V. V. (2019). Scalable microphysiological system to model three-dimensional blood vessels. *APL Bioengineering*, *3*(2), 026105. doi: 10.1063/1.5090986.

de Oliveira, F. F., Chen, E. S., Smith, M. C., & Bertolucci, P. H. F. (2018). Pharmacogenetics of angiotensin-converting enzyme inhibitors in patients with Alzheimer's disease dementia. *Current Alzheimer Research*, *15*(4), 386–398. doi: 10.2174/1567205014666171016101816.

De Sousa, P. A., Steeg, R., Wachter, E., Bruce, K., King, J., Hoeve, M., … Allsopp, T. E. (2017). Rapid establishment of the European Bank for induced Pluripotent Stem Cells (EBiSC) - the hot start experience. *Stem Cell Research*, *20*, 105–114. doi: 10.1016/j.scr.2017.03.002.

Deli, M. A., Ábrahám, C. S., Kataoka, Y., & Niwa, M. (2005). Permeability studies on *in vitro* blood-brain barrier models: Physiology, pathology, and pharmacology. *Cellular and*

Molecular Neurobiology, *25*(1), 59–127. doi: 10.1007/s10571-004-1377-8.

Delsing, L., Donnes, P., Sanchez, J., Clausen, M., Voulgaris, D., Falk, A., … Synnergren, J. (2018). Barrier properties and transcriptome expression in human iPSC-derived models of the blood-brain barrier. *Stem Cells*, *36*(12), 1816–1827. doi: 10.1002/stem.2908.

Delsing, L., Kallur, T., Zetterberg, H., Hicks, R., & Synnergren, J. (2019). Enhanced xeno-free differentiation of hiPSC-derived astroglia applied in a blood-brain barrier model. *Fluids and Barriers of the CNS*, *16*(1), 27. doi: 10.1186/s12987-019-0147-4.

DeQuach, J. A., Yuan, S. H., Goldstein, L. S., & Christman, K. L. (2011). Decellularized porcine brain matrix for cell culture and tissue engineering scaffolds. *Tissue Engineering Part A*, *17*(21-22), 2583–2592. doi: 10.1089/ten.TEA.2010.0724.

Desai, B. S., Monahan, A. J., Carvey, P. M., & Hendey, B. (2007). Blood-brain barrier pathology in Alzheimer's and Parkinson's disease: Implications for drug therapy. *Cell Transplantation*, *16*(3), 285–299. doi: 10.3727/000000007783464731.

DeStefano, J. G., Jamieson, J. J., Linville, R. M., & Searson, P. C. (2018). Benchmarking *in vitro* tissue-engineered blood-brain barrier models. *Fluids and Barriers of the CNS*, *15*(1), 32. doi: 10.1186/s12987-018-0117-2.

DeStefano, J. G., Xu, Z. S., Williams, A. J., Yimam, N., & Searson, P. C. (2017). Effect of shear stress on iPSC-derived human brain microvascular endothelial cells (dhBMECs). *Fluids and Barriers of the CNS*, *14*(1), 20. doi: 10.1186/s12987-017-0068-z.

Di Marco, A., Vignone, D., Gonzalez Paz, O., Fini, I., Battista, M. R., Cellucci, A., … Munoz-Sanjuan, I. (2020). Establishment of an *in vitro* human blood-brain barrier model derived from induced pluripotent stem cells and comparison to a porcine cell-based system. *Cells*, *9*(4), 994. doi: 10.3390/cells9040994.

Dowden, H., & Munro, J. (2019). Trends in clinical success rates and therapeutic focus. *Nature Reviews Drug Discovery*, *18*(7), 495–496. doi: 10.1038/d41573-019-00074-z.

Engelhardt, B., Vajkoczy, P., & Weller, R. O. (2017). The movers and shapers in immune privilege of the CNS. *Nature Immunology*, *18*(2), 123–131. doi: 10.1038/ni.3666.

Erdo, F., Denes, L., & de Lange, E. (2017). Age-associated physiological and pathological changes at the blood-brain barrier: A review. *Journal of Cerebral Blood Flow and Metabolism*, *37*(1), 4–24. doi: 10.1177/0271678×16679420.

Erickson, M. A., & Banks, W. A. (2019). Age-associated changes in the immune system and blood-brain barrier functions. *International Journal of Molecular Sciences*, *20*(7), 1632. doi: 10.3390/ijms20071632.

Faley, S. L., Neal, E. H., Wang, J. X., Bosworth, A. M., Weber, C. M., Balotin, K. M., … Bellan, L. M. (2019). iPSC-derived brain endothelium exhibits stable, long-term barrier function in perfused hydrogel scaffolds. *Stem Cell Reports*, *12*(3), 474–487. doi: 10.1016/j.stemcr.2019.01.009.

Garcia-Polite, F., Martorell, J., Del Rey-Puech, P., Melgar-Lesmes, P., O'Brien, C. C., Roquer, J., … Balcells, M. (2017). Pulsatility and high shear stress deteriorate barrier phenotype in brain microvascular endothelium. *Journal of Cerebral Blood Flow and Metabolism*, *37*(7), 2614–2625. doi: 10.1177/0271678×16672482.

Gastfriend, B. D., Palecek, S. P., & Shusta, E. V. (2018). Modeling the blood-brain barrier: Beyond the endothelial cells. *Current Opinion in Biomedical Engineering*, *5*, 6–12. doi: 10.1016/j.cobme.2017.11.002.

Ghose, A. K., Herbertz, T., Hudkins, R. L., Dorsey, B. D., & Mallamo, J. P. (2012). Knowledge-based, central nervous system (CNS) lead selection and lead optimization for CNS drug discovery. *ACS Chemical Neuroscience*, *3*(1), 50–68. doi: 10.1021/cn200100h.

Goodall, E. F., Wang, C., Simpson, J. E., Baker, D. J., Drew, D. R., Heath, P. R., … Wharton, S. B. (2018). Age-associated changes in the blood-brain barrier: Comparative studies in human and mouse. *Neuropathology and Applied Neurobiology*, *44*(3), 328–340. doi: 10.1111/nan.12408.

Gray, M. T., & Woulfe, J. M. (2015). Striatal blood-brain barrier permeability in Parkinson's disease. *Journal of Cerebral Blood Flow and Metabolism*, *35*(5), 747–750. doi: 10.1038/jcbfm.2015.32.

Greene, C., Kealy, J., Humphries, M. M., Gong, Y., Hou, J., Hudson, N., … Campbell, M. (2018). Dose-dependent expression of claudin-5 is a modifying factor in schizophrenia. *Molecular Psychiatry*, *23*(11), 2156–2166. doi: 10.1038/mp.2017.156.

Grifno, G. N., Farrell, A. M., Linville, R. M., Arevalo, D., Kim, J. H., Gu, L., & Searson, P. C. (2019). Tissue-engineered blood-brain barrier models via directed differentiation of human induced pluripotent stem cells. *Scientific Reports*, *9*(1), 13957. doi: 10.1038/s41598-019-50193-1.

Halloin, C., Schwanke, K., Lobel, W., Franke, A., Szepes, M., Biswanath, S., … Zweigerdt, R. (2019). Continuous WNT control enables advanced hPSC cardiac processing and prognostic surface marker identification in chemically defined suspension culture. *Stem Cell Reports*, *13*(2), 366–379. doi: 10.1016/j.stemcr.2019.06.004.

Hartung, T., Bremer, S., Casati, S., Coecke, S., Corvi, R., Fortaner, S., … Zuang, V. (2004). A modular approach to the ECVAM principles on test validity. *Alternatives to Laboratory Animals*, *32*(5), 467–472. doi: 10.1177/026119290403200503.

Hawkins, B. T., & Davis, T. P. (2005). The blood-brain barrier/neurovascular unit in health and

disease. *Pharmacological Reviews*, *57*(2), 173–185. doi: 10.1124/pr.57.2.4.

Hede, E., Heegaard, C., Korbelin, J., Schwanninger, M., Moos, T., & Burkhart, A. (2019). Gene therapy to the blood-brain barrier with resulting protein secretion as a strategy for treatment of NPC2 disease. *Human Gene Therapy*, *30*(11), A100–A101.

Hollingworth, P., Harold, D., Sims, R., Gerrish, A., Lambert, J. C., Carrasquillo, M. M., … Consortium, E. (2011). Common variants at ABCA7, MS4A6A/MS4A4E, EPHA1, CD33 and CD2AP are associated with Alzheimer's disease. *Nature Genetics*, *43*(5), 429–+. doi: 10.1038/ng.803.

Hollmann, E. K., Bailey, A. K., Potharazu, A. V., Neely, M. D., Bowman, A. B., & Lippmann, E. S. (2017). Accelerated differentiation of human induced pluripotent stem cells to blood-brain barrier endothelial cells. *Fluids and Barriers of the CNS*, *14*(1), 9. doi: 10.1186/s12987-017-0059-0.

Hoshi, Y., Uchida, Y., Tachikawa, M., Inoue, T., Ohtsuki, S., & Terasaki, T. (2013). Quantitative atlas of blood-brain barrier transporters, receptors, and tight junction proteins in rats and common marmoset. *Journal of Pharmaceutical Sciences*, *102*(9), 3343–3355. doi: 10.1002/jps.23575.

Jehle, A. W., Gardai, S. J., Li, S. Z., Linsel-Nitschke, P., Morimoto, K., Janssen, W. J., … Tall, A. R. (2006). ATP-binding cassette transporter A7 enhances phagocytosis of apoptotic cells and associated ERK signaling in macrophages. *Journal of Cell Biology*, *174*(4), 547–556. doi: 10.1083/jcb.200601030.

Kaminski, W. E., Orso, E., Diederich, W., Klucken, J., Drobnik, W., & Schmitz, G. (2000). Identification of a novel human sterol-sensitive ATP-binding cassette transporter (ABCA7). *Biochemical and Biophysical Research Communications*, *273*(2), 532–538. doi: 10.1006/bbrc.2000.2954.

Karch, C. M., Jeng, A. T., Nowotny, P., Cady, J., Cruchaga, C., & Goate, A. M. (2012). Expression of novel Alzheimer's disease risk genes in control and Alzheimer's disease brains. *Plos One*, *7*(11), e50976. doi: 10.1371/journal.pone.0050976.

Katt, M. E., Linville, R. M., Mayo, L. N., Xu, Z. S., & Searson, P. C. (2018). Functional brain-specific microvessels from iPSC-derived human brain microvascular endothelial cells: The role of matrix composition on monolayer formation. *Fluids and Barriers of the CNS*, *15*(1), 7. doi: 10.1186/s12987-018-0092-7.

Katt, M. E., Xu, Z. S., Gerecht, S., & Searson, P. C. (2016). Human brain microvascular endothelial cells derived from the BC1 iPS cell line exhibit a blood-brain barrier phenotype. *Plos One*, *11*(4), e0152105. doi: 10.1371/journal.pone.0152105.

Keller, A. (2013). Breaking and building the wall: The biology of the blood-brain barrier in health and disease. *Swiss Medical Weekly*, *143*, w13892. doi: 10.4414/smw.2013.13892.

Kim, W. S., Li, H., Ruberu, K., Chan, S., Elliott, D. A., Low, J. K., … Garner, B. (2013). Deletion of Abca7 increases cerebral amyloid-beta accumulation in the J20 mouse model of Alzheimer's disease. *Journal of Neuroscience*, *33*(10), 4387–4394. doi: 10.1523/JNEUROSCI.4165-12.2013.

Kokubu, Y., Yamaguchi, T., & Kawabata, K. (2017). *in vitro* model of cerebral ischemia by using brain microvascular endothelial cells derived from human induced pluripotent stem cells. *Biochemical and Biophysical Research Communications*, *486*(2), 577–583. doi: 10.1016/j.bbrc.2017.03.092.

Kola, I., & Landis, J. (2004). Can the pharmaceutical industry reduce attrition rates? *Nature Reviews Drug Discovery*, *3*(8), 711–715. doi: 10.1038/nrd1470.

Krause, G., Winkler, L., Mueller, S. L., Haseloff, R. F., Piontek, J., & Blasig, I. E. (2008). Structure and function of claudins. *Biochimica Et Biophysica Acta*, *1778*(3), 631–645. doi: 10.1016/j.bbamem.2007.10.018.

Kropp, C., Kempf, H., Halloin, C., Robles-Diaz, D., Franke, A., Scheper, T., … Olmer, R. (2016). Impact of feeding strategies on the scalable expansion of human pluripotent stem cells in single-use stirred tank bioreactors. *Stem Cells Translational Medicine*, *5*(10), 1289–1301. doi: 10.5966/sctm.2015-0253.

Lam, D., Enright, H. A., Cadena, J., Peters, S. K. G., Sales, A. P., Osburn, J. J., … Fischer, N. O. (2019). Tissue-specific extracellular matrix accelerates the formation of neural networks and communities in a neuron-glia co-culture on a multi-electrode array. *Scientific Reports*, *9*(1), 4159. doi: 10.1038/s41598-019-40128-1.

Lam, J., Lowry, W. E., Carmichael, S. T., & Segura, T. (2014). Delivery of iPS-NPCs to the stroke cavity within a hyaluronic acid matrix promotes the differentiation of transplanted cells. *Advanced Functional Materials*, *24*(44), 7053–7062. doi: 10.1002/adfm.201401483.

Lambert, J. C., Ibrahim-Verbaas, C. A., Harold, D., Naj, A. C., Sims, R., Bellenguez, C., … Amouyel, P. (2013). Meta-analysis of 74,046 individuals identifies 11 new susceptibility loci for Alzheimer's disease. *Nature Genetics*, *45*(12), 1452–1458. doi: 10.1038/ng.2802.

Lancaster, M. A., Renner, M., Martin, C. A., Wenzel, D., Bicknell, L. S., Hurles, M. E., … Knoblich, J. A. (2013). Cerebral organoids model human brain development and microcephaly. *Nature*, *501*(7467), 373–379. doi: 10.1038/nature12517.

Lauschke, K., Frederiksen, L., & Hall, V. J. (2017). Paving the way toward complex blood-brain barrier models using pluripotent stem cells. *Stem Cells and Development*, *26*(12), 857–874. doi: 10.1089/scd.2017.0003.

Leda, A. R., Bertrand, L., Andras, I. E., El-Hage, N., Nair, M., & Toborek, M. (2019). Selective disruption of the blood-brain barrier by zika virus. *Frontiers in Microbiology*, *10*, 2158. doi: 10.3389/fmicb.2019.02158.

Lee, U. N., Day, J. H., Haack, A. J., Bretherton, R. C., Lu, W., DeForest, C. A., … Berthier, E. (2020). Layer-by-layer fabrication of 3D hydrogel structures using open microfluidics. *Lab on A Chip*, *20*(3), 525–536. doi: 10.1039/c9lc00621d.

Liebner, S., Fischmann, A., Rascher, G., Duffner, F., Grote, E. H., Kalbacher, H., & Wolburg, H. (2000). Claudin-1 and claudin-5 expression and tight junction morphology are altered in blood vessels of human glioblastoma multiforme. *Acta Neuropathologica*, *100*(3), 323–331. doi: 10.1007/s004010000180.

Lim, R. G., Quan, C., Reyes-Ortiz, A. M., Lutz, S. E., Kedaigle, A. J., Gipson, T. A., … Thompson, L. M. (2017). Huntington's disease iPSC-derived brain microvascular endothelial cells reveal WNT-mediated angiogenic and blood-brain barrier deficits. *Cell Reports*, *19*(7), 1365–1377. doi: 10.1016/j.celrep.2017.04.021.

Linville, R. M., DeStefano, J. G., Sklar, M. B., Xu, Z., Farrell, A. M., Bogorad, M. I., … Searson, P. C. (2019). Human iPSC-derived blood-brain barrier microvessels: Validation of barrier function and endothelial cell behavior. *Biomaterials*, *190-191*, 24–37. doi: 10.1016/j.biomaterials.2018.10.023.

Lippmann, E. S., Al-Ahmad, A., Azarin, S. M., Palecek, S. P., & Shusta, E. V. (2014). A retinoic acid-enhanced, multicellular human blood-brain barrier model derived from stem cell sources. *Scientific Reports*, *4*, 4160. doi: 10.1038/srep04160.

Lippmann, E. S., Al-Ahmad, A., Palecek, S. P., & Shusta, E. V. (2013). Modeling the blood-brain barrier using stem cell sources. *Fluids and Barriers of the CNS*, *10*(1), 2. doi: 10.1186/2045-8118-10-2.

Lippmann, E. S., Azarin, S. M., Kay, J. E., Nessler, R. A., Wilson, H. K., Al-Ahmad, A., … Shusta, E. V. (2012). Derivation of blood-brain barrier endothelial cells from human pluripotent stem cells. *Nature Biotechnology*, *30*(8), 783–791. doi: 10.1038/nbt.2247.

Liu, W. Y., Wang, Z. B., Zhang, L. C., Wei, X., & Li, L. (2012). Tight junction in blood-brain barrier: An overview of structure, regulation, and regulator substances. *CNS Neuroscience and Therapeutics*, *18*(8), 609–615. doi: 10.1111/j.1755-5949.2012.00340.x.

Mao, L., Jin, H., Wang, M., Hu, Y., Chen, S., He, Q., … Hu, B. (2020). Neurologic manifestations of hospitalized patients with coronavirus disease 2019 in Wuhan, China. *JAMA Neurology*, doi: 10.1001/jamaneurol.2020.1127.

McKernan, R., & Watt, F. M. (2013). What is the point of large-scale collections of human induced pluripotent stem cells? *Nature Biotechnology*, *31*(10), 875–877. doi: 10.1038/nbt.2710.

Miller, J. S., Stevens, K. R., Yang, M. T., Baker, B. M., Nguyen, D. H., Cohen, D. M., … Chen, C. S. (2012). Rapid casting of patterned vascular networks for perfusable engineered three-dimensional tissues. *Nature Materials*, *11*(9), 768–774. doi: 10.1038/nmat3357.

Minami, H., Tashiro, K., Okada, A., Hirata, N., Yamaguchi, T., Takayama, K., … Kawabata, K. (2015). Generation of brain microvascular endothelial-like cells from human induced pluripotent stem cells by co-culture with C6 glioma cells. *Plos One*, *10*(6), e0128890. doi: 10.1371/journal.pone.0128890.

Miranda, C. C., Fernandes, T. G., Pascoal, J. F., Haupt, S., Brustle, O., Cabral, J. M., & Diogo, M. M. (2015). Spatial and temporal control of cell aggregation efficiently directs human pluripotent stem cells towards neural commitment. *Biotechnology Journal*, *10*(10), 1612–1624. doi: 10.1002/biot.201400846.

Montagne, A., Barnes, S. R., Sweeney, M. D., Halliday, M. R., Sagare, A. P., Zhao, Z., … Zlokovic, B. V. (2015). Blood-brain barrier breakdown in the aging human hippocampus. *Neuron*, *85*(2), 296–302. doi: 10.1016/j.neuron.2014.12.032.

Moshayedi, P., Nih, L. R., Llorente, I. L., Berg, A. R., Cinkornpumin, J., Lowry, W. E., … Carmichael, S. T. (2016). Systematic optimization of an engineered hydrogel allows for selective control of human neural stem cell survival and differentiation after transplantation in the stroke brain. *Biomaterials*, *105*, 145–155. doi: 10.1016/j.biomaterials.2016.07.028.

Motallebnejad, P., Thomas, A., Swisher, S. L., & Azarin, S. M. (2019). An isogenic hiPSC-derived BBB-on-a-chip. *Biomicrofluidics*, *13*(6), 064119. doi: 10.1063/1.5123476.

Munji, R. N., Soung, A. L., Weiner, G. A., Sohet, F., Semple, B. D., Trivedi, A., … Daneman, R. (2019). Profiling the mouse brain endothelial transcriptome in health and disease models reveals a core blood-brain barrier dysfunction module. *Nature Neuroscience*, *22*(11), 1892–+. doi: 10.1038/s41593-019-0497-x.

Murphy, A. R., Haynes, J. M., Laslett, A. L., Cameron, N. R., & O'Brien, C. M. (2020). Three-dimensional differentiation of human pluripotent stem cell-derived neural precursor cells using tailored porous polymer scaffolds. *Acta Biomaterialia*, *101*, 102–116. doi: 10.1016/j.actbio.2019.10.017.

Neal, E. H., Marinelli, N. A., Shi, Y., McClatchey, P. M., Balotin, K. M., Gullett, D. R., … Lippmann, E. S. (2019). A simplified, fully defined differentiation scheme for producing blood-brain barrier endothelial cells from human iPSCs. *Stem Cell Reports*, *12*(6), 1380–1388. doi: 10.1016/j.stemcr.2019.05.008.

Neuhaus, W., & Noe, C. R. (2010). *Transport at the blood-brain barrier*. Wiley.

Neuwelt, E. A., Bauer, B., Fahlke, C., Fricker, G., Iadecola, C., Janigro, D., … Drewes, L. R. (2011). Engaging neuroscience to advance translational research in brain barrier biology. *Nature Reviews Neuroscience*, *12*(3), 169–182. doi: 10.1038/nrn2995.

Nih, L. R., Moshayedi, P., Llorente, I. L., Berg, A. R., Cinkornpumin, J., Lowry, W. E., … Carmichael, S. T. (2017). Engineered HA

hydrogel for stem cell transplantation in the brain: Biocompatibility data using a design of experiment approach. *Data in Brief*, *10*, 202–209. doi: 10.1016/j.dib.2016.11.069.

Nishihara, H., Soldati, S., Mossu, A., Rosito, M., Rudolph, H., Muller, W. A., … Engelhardt, B. (2020). Human CD4(+) T cell subsets differ in their abilities to cross endothelial and epithelial brain barriers *in vitro*. *Fluids and Barriers of the CNS*, *17*(1), 3. doi: 10.1186/s12987-019-0165-2.

Nzou, G., Wicks, R. T., Wicks, E. E., Seale, S. A., Sane, C. H., Chen, A., … Atala, A. J. (2018). Human cortex spheroid with a functional blood brain barrier for high-throughput neurotoxicity screening and disease modeling. *Scientific Reports*, *8*(1), 7413. doi: 10.1038/s41598-018-25603-5.

O'Shea, O., Steeg, R., Chapman, C., Mackintosh, P., & Stacey, G. N. (2020). Development and implementation of large-scale quality control for the European bank for induced Pluripotent Stem Cells. *Stem Cell Research*, *45*, 101773. doi: 10.1016/j.scr.2020.101773.

Ohshima, M., Kamei, S., Fushimi, H., Mima, S., Yamada, T., & Yamamoto, T. (2019). Prediction of drug permeability using *in vitro* blood-brain barrier models with human induced pluripotent stem cell-derived brain microvascular endothelial cells. *BioResearch Open Access*, *8*(1), 200–209. doi: 10.1089/biores.2019.0026.

Ormel, P. R., de Sa, R. V., van Bodegraven, E. J., Karst, H., Harschnitz, O., Sneeboer, M. A. M., … Pasterkamp, R. J. (2018). Microglia innately develop within cerebral organoids. *Nature Communications*, *9*, 4167. doi: 10.1038/s41467-018-06684-2.

Page, S., Raut, S., & Al-Ahmad, A. (2019). Oxygen-glucose deprivation/reoxygenation-induced barrier disruption at the human blood-brain barrier is partially mediated through the HIF-1 pathway. *NeuroMolecular Medicine*, *21*(4), 414–431. doi: 10.1007/s12017-019-08531-z.

Pamies, D., Bal-Price, A., Chesne, C., Coecke, S., Dinnyes, A., Eskes, C., … Daneshian, M. (2018). Advanced Good Cell Culture Practice for human primary, stem cell-derived and organoid models as well as microphysiological systems. *Altex*, *35*(3), 353–378. doi: 10.14573/altex.1710081.

Panza, F., Lozupone, M., Logroscino, G., & Imbimbo, B. P. (2019). A critical appraisal of amyloid-beta-targeting therapies for Alzheimer disease. *Nature Reviews Neurology*, *15*(2), 73–88. doi: 10.1038/s41582-018-0116-6.

Pardridge, W. M. (2005). The blood-brain barrier: Bottleneck in brain drug development. *NeuroRx*, *2*(1), 3–14. doi: 10.1602/neurorx.2.1.3.

Park, T. E., Mustafaoglu, N., Herland, A., Hasselkus, R., Mannix, R., FitzGerald, E. A., … Ingber, D. E. (2019). Hypoxia-enhanced Blood-Brain Barrier Chip recapitulates human barrier function and shuttling of drugs and antibodies. *Nature Communications*, *10*(1), 2621. doi: 10.1038/s41467-019-10588-0.

Pasca, A. M., Sloan, S. A., Clarke, L. E., Tian, Y., Makinson, C. D., Huber, N., … Pasca, S. P. (2015). Functional cortical neurons and astrocytes from human pluripotent stem cells in 3D culture. *Nature Methods*, *12*(7), 671–678. doi: 10.1038/nmeth.3415.

Patel, R., Page, S., & Al-Ahmad, A. J. (2017). Isogenic blood-brain barrier models based on patient-derived stem cells display inter-individual differences in cell maturation and functionality. *Journal of Neurochemistry*, *142*(1), 74–88. doi: 10.1111/jnc.14040.

Patsch, C., Challet-Meylan, L., Thoma, E. C., Urich, E., Heckel, T., O'Sullivan, J. F., … Cowan, C. A. (2015). Generation of vascular endothelial and smooth muscle cells from human pluripotent stem cells. *Nature Cell Biology*, *17*(8), 994–1003. doi: 10.1038/ncb3205.

Pfeiffer, F., Schafer, J., Lyck, R., Makrides, V., Brunner, S., Schaeren-Wiemers, N., … Engelhardt, B. (2011). Claudin-1 induced sealing of blood-brain barrier tight junctions ameliorates chronic experimental autoimmune encephalomyelitis. *Acta Neuropathologica*, *122*(5), 601–614. doi: 10.1007/s00401-011-0883-2.

Praca, C., Rosa, S. C., Sevin, E., Cecchelli, R., Dehouck, M. P., & Ferreira, L. S. (2019). Derivation of brain capillary-like endothelial cells from human pluripotent stem cell-derived endothelial progenitor cells. *Stem Cell Reports*, *13*(4), 599–611. doi: 10.1016/j.stemcr.2019.08.002.

Prieto, P., Blaauboer, B. J., de Boer, A. G., Boveri, M., Cecchelli, R., Clemedson, C., … Tahti, H. (2004). Blood-brain barrier *in vitro* models and their application in toxicology. The report and recommendations of ECVAM Workshop 49. *Alternatives to Laboratory Animals*, *32*(1), 37–50. doi: 10.1177/026119290403200107.

Prince, M., Bryce, R., Albanese, E., Wimo, A., Ribeiro, W., & Ferri, C. P. (2013). The global prevalence of dementia: A systematic review and metaanalysis. *Alzheimer's and Dementia*, *9*(1), 63–75.e62. doi: 10.1016/j.jalz.2012.11.007.

Profaci, C. P., Munji, R. N., Pulido, R. S., & Daneman, R. (2020). The blood-brain barrier in health and disease: Important unanswered questions. *Journal of Experimental Medicine*, *217*(4), e20190062. doi: 10.1084/jem.20190062.

Puelles, V. G., Lutgehetmann, M., Lindenmeyer, M. T., Sperhake, J. P., Wong, M. N., Allweiss, L., … Huber, T. B. (2020). Multiorgan and renal tropism of SARS-CoV-2. *New England Journal of Medicine*, doi: 10.1056/NEJMc2011400.

Pulgar, V. M. (2018). Transcytosis to cross the blood brain barrier, new advancements and challenges. *Frontiers in Neuroscience*, *12*, 1019. doi: 10.3389/fnins.2018.01019.

Qian, T., Maguire, S. E., Canfield, S. G., Bao, X., Olson, W. R., Shusta, E. V., & Palecek,

S. P. (2017). Directed differentiation of human pluripotent stem cells to blood-brain barrier endothelial cells. *Science Advances*, *3*(11), e1701679. doi: 10.1126/sciadv.1701679.

Qian, X., Jacob, F., Song, M. M., Nguyen, H. N., Song, H., & Ming, G. L. (2018). Generation of human brain region-specific organoids using a miniaturized spinning bioreactor. *Nature Protocols*, *13*(3), 565–580. doi: 10.1038/nprot.2017.152.

Qian, X., Nguyen, H. N., Song, M. M., Hadiono, C., Ogden, S. C., Hammack, C., … Ming, G. L. (2016). Brain-region-specific organoids using mini-bioreactors for modeling ZIKV exposure. *Cell*, *165*(5), 1238–1254. doi: 10.1016/j.cell.2016.04.032.

Raja, W. K., Mungenast, A. E., Lin, Y. T., Ko, T., Abdurrob, F., Seo, J., & Tsai, L. H. (2016). Self-Organizing 3D human neural tissue derived from induced pluripotent stem cells recapitulate Alzheimer's disease phenotypes. *Plos One*, *11*(9), e0161969. doi: 10.1371/journal.pone.0161969.

Reichel, A. (2006). The role of blood-brain barrier studies in the pharmaceutical industry. *Current Drug Metabolism*, *7*(2), 183–203. doi: 10.2174/138920006775541525.

Reinitz, A., DeStefano, J., Ye, M., Wong, A. D., & Searson, P. C. (2015). Human brain microvascular endothelial cells resist elongation due to shear stress. *Microvascular Research*, *99*, 8–18. doi: 10.1016/j.mvr.2015.02.008.

Ribecco-Lutkiewicz, M., Sodja, C., Haukenfrers, J., Haqqani, A. S., Ly, D., Zachar, P., … Bani-Yaghoub, M. (2018). A novel human induced pluripotent stem cell blood-brain barrier model: Applicability to study antibody-triggered receptor-mediated transcytosis. *Scientific Reports*, *8*(1), 1873. doi: 10.1038/s41598-018-19522-8.

Roudnicky, F., Kim, B. K., Lan, Y., Schmucki, R., Kuppers, V., Christensen, K., … Cowan, C. A. (2020). Identification of a combination of transcription factors that synergistically increases endothelial cell barrier resistance. *Scientific Reports*, *10*(1), 3886. doi: 10.1038/s41598-020-60688-x.

Roux, G. L., Jarray, R., Guyot, A. C., Pavoni, S., Costa, N., Theodoro, F., … Mabondzo, A. (2019). Proof-of-concept study of drug brain permeability between *in vivo* human brain and an *in vitro* iPSCs-human blood-brain barrier model. *Scientific Reports*, *9*(1), 16310. doi: 10.1038/s41598-019-52213-6.

Sakae, N., Liu, C. C., Shinohara, M., Frisch-Daiello, J., Ma, L., Yamazaki, Y., … Kanekiyo, T. (2016). ABCA7 Deficiency accelerates amyloid-beta generation and Alzheimer's neuronal pathology. *Journal of Neuroscience*, *36*(13), 3848–3859. doi: 10.1523/JNEUROSCI.3757-15.2016.

Savage, J. E., Jansen, P. R., Stringer, S., Watanabe, K., Bryois, J., de Leeuw, C. A., … Posthuma, D. (2018). Genome-wide association meta-analysis in 269,867 individuals identifies new genetic and functional links to intelligence. *Nature Genetics*, *50*(7), 912–+. doi: 10.1038/s41588-018-0152-6.

Schwedhelm, I., Zdzieblo, D., Appelt-Menzel, A., Berger, C., Schmitz, T., Schuldt, B., … Hansmann, J. (2019). Automated real-time monitoring of human pluripotent stem cell aggregation in stirred tank reactors. *Scientific Reports*, *9*(1), 12297. doi: 10.1038/s41598-019-48814-w.

Shawahna, R., Uchida, Y., Decleves, X., Ohtsuki, S., Yousif, S., Dauchy, S., … Scherrmann, J. M. (2011). Transcriptomic and quantitative proteomic analysis of transporters and drug metabolizing enzymes in freshly isolated human brain microvessels. *Molecular Pharmaceutics*, *8*(4), 1332–1341. doi: 10.1021/mp200129p.

Silva, M. M., Rodrigues, A. F., Correia, C., Sousa, M. F., Brito, C., Coroadinha, A. S., … Alves, P. M. (2015). Robust expansion of human pluripotent stem cells: Integration of bioprocess design with transcriptomic and metabolomic characterization. *Stem Cells Translational Medicine*, *4*(7), 731–742. doi: 10.5966/sctm.2014-0270.

Sims, R., van der Lee, S. J., Naj, A. C., Bellenguez, C., Badarinarayan, N., Jakobsdottir, J., … Schellenberg, G. D. (2017). Rare coding variants in PLCG2, ABI3, and TREM2 implicate microglial-mediated innate immunity in Alzheimer's disease. *Nature Genetics*, *49*(9), 1373–1384. doi: 10.1038/ng.3916.

Smits, L. M., Reinhardt, L., Reinhardt, P., Glatza, M., Monzel, A. S., Stanslowsky, N., … Schwamborn, J. C. (2019). Modeling Parkinson's disease in midbrain-like organoids. *NPJ Parkinson's Disease*, *5*, 5. doi: 10.1038/s41531-019-0078-4.

St George-Hyslop, P. H., Tanzi, R. E., Polinsky, R. J., Haines, J. L., Nee, L., Watkins, P. C., … et al. (1987). The genetic defect causing familial Alzheimer's disease maps on chromosome 21. *Science*, *235*(4791), 885–890. doi: 10.1126/science.2880399.

Stanimirovic, D. B., Bani-Yaghoub, M., Perkins, M., & Haqqani, A. S. (2015). Blood-brain barrier models: *in vitro* to *in vivo* translation in preclinical development of CNS-targeting biotherapeutics. *Expert Opinion on Drug Discovery*, *10*(2), 141–155. doi: 10.1517/17460441.2015.974545.

Stebbins, M. J., Gastfriend, B. D., Canfield, S. G., Lee, M. S., Richards, D., Faubion, M. G., … Shusta, E. V. (2019). Human pluripotent stem cell-derived brain pericyte-like cells induce blood-brain barrier properties. *Science Advances*, *5*(3), eaau7375. doi: 10.1126/sciadv.aau7375.

Stebbins, M. J., Wilson, H. K., Canfield, S. G., Qian, T., Palecek, S. P., & Shusta, E. V. (2016). Differentiation and characterization of human pluripotent stem cell-derived brain microvascular endothelial cells. *Methods*, *101*, 93–102. doi: 10.1016/j.ymeth.2015.10.016.

Steinberg, S., Stefansson, H., Jonsson, T., Johannsdottir, H., Ingason, A., Helgason, H., …

DemGene (2015). Loss-of-function variants in ABCA7 confer risk of Alzheimer's disease. *Nature Genetics*, *47*(5), 445–U424. doi: 10.1038/ng.3246.

Strazielle, N., & Ghersi-Egea, J. F. (2015). Efflux transporters in blood-brain interfaces of the developing brain. *Frontiers in Neuroscience*, *9*, 21. doi: 10.3389/fnins.2015.00021.

Sweeney, M. D., Sagare, A. P., & Zlokovic, B. V. (2018). Blood-brain barrier breakdown in Alzheimer disease and other neurodegenerative disorders. *Nature Reviews Neurology*, *14*(3), 133–150. doi: 10.1038/nrneurol.2017.188.

Sweeney, M. D., Zhao, Z., Montagne, A., Nelson, A. R., & Zlokovic, B. V. (2019). Blood-brain barrier: From physiology to disease and back. *Physiological Reviews*, *99*(1), 21–78. doi: 10.1152/physrev.00050.2017.

Tibbitt, M. W., & Anseth, K. S. (2009). Hydrogels as extracellular matrix mimics for 3D cell culture. *Biotechnology and Bioengineering*, *103*(4), 655–663. doi: 10.1002/bit.22361.

Tkachenko, E., Gutierrez, E., Saikin, S. K., Fogelstrand, P., Kim, C., Groisman, A., & Ginsberg, M. H. (2013). The nucleus of endothelial cell as a sensor of blood flow direction. *Biology Open*, *2*(10), 1007–1012. doi: 10.1242/bio.20134622.

Uchida, Y., Ohtsuki, S., Katsukura, Y., Ikeda, C., Suzuki, T., Kamiie, J., & Terasaki, T. (2011). Quantitative targeted absolute proteomics of human blood-brain barrier transporters and receptors. *Journal of Neurochemistry*, *117*(2), 333–345. doi: 10.1111/j.1471-4159.2011.07208.x.

Urich, E., Patsch, C., Aigner, S., Graf, M., Iacone, R., & Freskgard, P. O. (2013). Multicellular self-assembled spheroidal model of the blood brain barrier. *Scientific Reports*, *3*, 1500. doi: 10.1038/srep01500.

Vasquez, J. B., Fardo, D. W., & Estus, S. (2013). ABCA7 expression is associated with Alzheimer's disease polymorphism and disease status. *Neuroscience Letters*, *556*, 58–62. doi: 10.1016/j.neulet.2013.09.058.

Vatine, G. D., Al-Ahmad, A., Barriga, B. K., Svendsen, S., Salim, A., Garcia, L., … Svendsen, C. N. (2017). Modeling psychomotor retardation using iPSCs from MCT8-deficient patients indicates a prominent role for the blood-brain barrier. *Cell Stem Cell*, *20*(6), 831–843. doi: 10.1016/j.stem.2017.04.002.

Vatine, G. D., Barrile, R., Workman, M. J., Sances, S., Barriga, B. K., Rahnama, M., … Svendsen, C. N. (2019). Human iPSC-derived blood-brain barrier chips enable disease modeling and personalized medicine applications. *Cell Stem Cell*, *24*(6), 995–1005.e1006. doi: 10.1016/j.stem.2019.05.011.

Vijay, N., & Morris, M. E. (2014). Role of monocarboxylate transporters in drug delivery to the brain. *Current Pharmaceutical Design*, *20*(10), 1487–1498. doi: 10.2174/13816128113199990462.

Volpe, D. A. (2011). Drug-permeability and transporter assays in Caco-2 and MDCK cell lines. *Future Medicinal Chemistry*, *3*(16), 2063–2077. doi: 10.4155/fmc.11.149.

Volpe, D. A., Faustino, P. J., Ciavarella, A. B., Asafu-Adjaye, E. B., Ellison, C. D., Yu, L. X., & Hussain, A. S. (2007). Classification of drug permeability with a Caco-2 cell monolayer assay. *Clinical Research and Regulatory Affairs*, *24*(1), 39–47. doi: 10.1080/10601330701273669.

Wang, Y. I., Abaci, H. E., & Shuler, M. L. (2017). Microfluidic blood-brain barrier model provides *in vivo*-like barrier properties for drug permeability screening. *Biotechnology and Bioengineering*, *114*(1), 184–194. doi: 10.1002/bit.26045.

Waring, M. J., Arrowsmith, J., Leach, A. R., Leeson, P. D., Mandrell, S., Owen, R. M., … Weir, A. (2015). An analysis of the attrition of drug candidates from four major pharmaceutical companies. *Nature Reviews Drug Discovery*, *14*(7), 475–486. doi: 10.1038/nrd4609.

Weiss, N., Miller, F., Cazaubon, S., & Couraud, P. O. (2009). The blood-brain barrier in brain homeostasis and neurological diseases. *Biochimica Et Biophysica Acta*, *1788*(4), 842–857. doi: 10.1016/j.bbamem.2008.10.022.

Wevers, N. R., & de Vries, H. E. (2016). Morphogens and blood-brain barrier function in health and disease. *Tissue Barriers*, *4*(1), e1090524. doi: 10.1080/21688370.2015.1090524.

Wilson, H. K., Canfield, S. G., Hjortness, M. K., Palecek, S. P., & Shusta, E. V. (2015). Exploring the effects of cell seeding density on the differentiation of human pluripotent stem cells to brain microvascular endothelial cells. *Fluids and Barriers of the CNS*, *12*, 13. doi: 10.1186/s12987-015-0007-9.

Wilson, H. K., Faubion, M. G., Hjortness, M. K., Palecek, S. P., & Shusta, E. V. (2016). Cryopreservation of brain endothelial cells derived from human induced pluripotent stem cells is enhanced by rho-associated coiled coil-containing kinase inhibition. *Tissue Engineering Part C: Methods*, *22*(12), 1085–1094. doi: 10.1089/ten.TEC.2016.0345.

Wong, A. D., Ye, M., Levy, A. F., Rothstein, J. D., Bergles, D. E., & Searson, P. C. (2013). The blood-brain barrier: An engineering perspective. *Frontiers in Neuroengineering*, *6*, 7. doi: 10.3389/fneng.2013.00007.

Xiang, J., Andjelkovic, A. V., Wang, M. M., & Keep, R. F. (2017). Blood-brain barrier models derived from individual patients: A new frontier: An Editorial Highlight on 'An isogenic blood-brain barrier model comprising brain endothelial cells, astrocytes, and neurons derived from human induced pluripotent stem cells'. *Journal of Neurochemistry*, *140*(6), 843–844. doi: 10.1111/jnc.13961.

Yamashita, M., Aoki, H., Hashita, T., Iwao, T., & Matsunaga, T. (2020). Inhibition of transforming growth factor beta signaling pathway promotes differentiation of human induced pluripotent stem cell-derived brain

microvascular endothelial-like cells. *Fluids and Barriers of the CNS*, *17*(1), 36. doi: 10.1186/s12987-020-00197-1.

Yan, Y., Song, L., Madinya, J., Ma, T., & Li, Y. (2018). Derivation of cortical spheroids from human induced pluripotent stem cells in a suspension bioreactor. *Tissue Engineering Part A*, *24*(5-6), 418–431. doi: 10.1089/ten.TEA.2016.0400.

Yang, K., Lee, J. S., Kim, J., Lee, Y. B., Shin, H., Um, S. H., … Cho, S. W. (2012). Polydopamine-mediated surface modification of scaffold materials for human neural stem cell engineering. *Biomaterials*, *33*(29), 6952–6964. doi: 10.1016/j.biomaterials.2012.06.067.

Ye, M., Sanchez, H. M., Hultz, M., Yang, Z., Bogorad, M., Wong, A. D., & Searson, P. C. (2014). Brain microvascular endothelial cells resist elongation due to curvature and shear stress. *Scientific Reports*, *4*, 4681. doi: 10.1038/srep04681.

Zarbin, M., Sugino, I., & Townes-Anderson, E. (2019). Concise review: Update on retinal pigment epithelium transplantation for age-related macular degeneration. *Stem Cells Translational Medicine*, *8*(5), 466–477. doi: 10.1002/sctm.18-0282.

KEY REFERENCES

Abbott & Friedman, 2012. See above.

Gave a fundamental overview and introduction to understand the BBB in health and disease.

Lippmann et al., 2012. See above.

Published for the first time a differentiation method to generate purified BCECs from hiPSCs. These hiPSC-derived BCECs are characterized by in vivo-like properties. This work pioneered the application of patient-specific hiPSC-derived BBB models in research.

Urich et al., 2013. See above.

Investigated a three-dimensional multicellular spheroid model of the BBB, presenting for the first time a spontaneous and complex self-organization of multiple BBB cell types. Most importantly, this process was not dependent on artificial scaffolds, supporting the hypothesis that the formation and cellular architecture of the BBB is intrinsically programmed within the specific cell types.

Patel, Page, & Al-Ahmad, 2017. See above.

Established an isogenic complex BBB model derived from patient-specific hiPSCs and investigated the impact of inter-individual genetic variations on the yield and phenotype of isogenic BBB models. Differences in differentiation capacity, maturation, and barrier properties between the models derived from different hiPSC lines supported the impact of individual polymorphisms in stem cell research and for precision medicine.

Prieto et al., 2004. See above.

Within the report of the forty-ninth workshop organized by the EURL ECVAM this key reference gave fundamental recommendations on the application and validation of BBB in vitro models in toxicology screening strategies.

Reichel, 2006. See above.

Reviewed the role of BBB studies for the pharmaceutical industry in preclinical drug discovery and development. Furthermore, the specific requirements of the pharmaceutical industry for the development of effective and safe new CNS medicines were summarized.

Scaled Isolation of Mesenchymal Stem/Stromal Cell-Derived Extracellular Vesicles

Verena Börger,[1] Simon Staubach,[1] Robin Dittrich,[1] Oumaima Stambouli,[1] and Bernd Giebel[1,2]

[1]Institute for Transfusion Medicine, University Hospital Essen, University of Duisburg-Essen, Essen, Germany
[2]Corresponding author: *Bernd.Giebel@uk-essen.de*

Mesenchymal stem/stromal cells (MSCs) provide therapeutic effects in many diseases. Contrary to initial hypotheses, they act in a paracrine rather than a cellular manner. To this end, extracellular vesicles (EVs) have been found to mediate the therapeutic effects, even when harvested from MSC-conditioned cell culture supernatants. Lacking self-replicating activity and being so small that MSC-EV preparations can be sterilized by filtration, EVs provide several advantages as therapeutic agents over cellular therapeutics. At present, methods allowing EV preparation from larger volumes are scarce and regularly require special equipment. We have developed a polyethylene glycol−based precipitation protocol allowing extraction of EVs from several liters of conditioned medium. MSC-EVs prepared with this method have been successfully applied to a human graft-versus-host disease patient and to several animal models. Although the method comes with its own limitations, it is extremely helpful for the initial evaluation of EV-based therapeutic approaches. Here, we introduce the technique in detail and discuss all critical steps. © 2020 The Authors.

Basic Protocol 1: Preparation of MSC-conditioned medium for scaled MSC-EV production
Basic Protocol 2: PEG precipitation OF MSC-EV from MSC-conditioned medium

Keywords: EVs • exosomes • large-scale preparation • MSCs

How to cite this article:
Börger, V., Staubach, S., Dittrich, R., Stambouli, O., & Giebel, B. (2020). Scaled isolation of mesenchymal stem/stromal cell-derived extracellular vesicles. *Current Protocols in Stem Cell Biology*, *55,* e128. doi: 10.1002/cpsc.128

INTRODUCTION

At the turn of the millennium, mesenchymal stem/stromal cells (MSCs) were reported as multipotent cells (Pittenger et al., 1999). Considering them as an allogenic stem cell source for cell replacement strategies, several groups studied their interaction with immune cells. Quickly, it was demonstrated that MSCs were able to suppress pro-inflammatory immune responses (Bartholomew et al., 2002; Di Nicola et al., 2002). Due to their beneficial effects in various preclinical animal models, they were quickly translated into the clinic, either intended as cellular replacement or as immunomodulating

CURRENT PROTOCOLS
A Wiley Brand

Current Protocols in Stem Cell Biology e128, Volume 55
Published in Wiley Online Library (wileyonlinelibrary.com).
doi: 10.1002/cpsc.128

cells. Up to now, MSCs have been applied in more than 1000 different clinical trials for the treatment of numerous different diseases (Heldring, Mager, Wood, Le Blanc, & Andaloussi, 2015). Despite positive effects in various settings, the MSCs were barely detected in affected tissues, resulting in the hypothesis that they mainly act via their secretome rather than in a direct cellular manner (Caplan & Correa, 2011; Caplan & Dennis, 2006). Indeed, it was quickly demonstrated using the examples of an acute kidney injury model and a myocardial infarction model that MSCs exert their therapeutic effects via small extracellular vesicles (EVs), such as exosomes and microvesicles, having diameters of up to 200 nm. Indeed, an array of different head-to-head studies confirmed that preparations that are highly enriched for such vesicles exert comparable therapeutic activities as their parental MSCs (Bruno et al., 2009; Doeppner et al., 2015; He et al., 2012).

Compared to cellular transplants, EV products provide some significant advantages. Due to their small sizes, MSC-EV preparations can be processed by filtration through filters with 0.22-μm pores, which is considered as sterilization. In contrast to cells, EVs are not self-replicating and thus lack any endogenous tumor-formation potential. Furthermore, their overall handling is much easier than that of cellular products. All of these features are essential requirements for an off-the-shelf product (Lener et al., 2015).

Although we are not aware of the exact mode of action, it appears MSC-EV preparations act multimodally. Among other activities, they can modulate pro-inflammatory into regulatory immune responses, presumably an essential requirement for regenerative processes (Börger et al., 2017; Giebel & Hermann, 2019).

A bottleneck in preparing MSC-EVs for clinical applications is the fact that liters of conditioned medium (CM) need to be prepared for the treatment of an individual patient. Classically, EVs have been prepared by differential centrifugation procedures, in which the initial volume is reduced during ultracentrifugation (see Current Protocols article: Thery, Amigorena, Raposo, & Clayton, 2006). Since even the largest rotors cannot process more than 400 ml in a single, typically 2-hr run, a challenge in the field is to find other, more effective methods of volume reduction. All available methods have their own limitations, such as purity, scalability, and time/cost factor (Watson et al., 2018). Currently, tangential flow filtration (TFF) is increasingly discussed as an effective method for volume reduction (Nordin, Bostancioglu, Corso, & El Andaloussi, 2019). However, this requires specific equipment, and optimization for clinical grade production is still ongoing. Here, we present a scalable, easy-to-handle and cost-effective procedure for the preparation of EVs from larger MSC-CM volumes, which could potentially be used for the clinical-grade production of MSC-EVs (Figs. 1 and 2).

Facing the situation of a treatment-refractory graft-versus-host disease (GvHD) patient for whom no additional treatment options existed in 2011, we considered treating her with MSC-EVs and had to address the challenge of effectively extracting small EVs (<200 nm) from more than 4 L of MSC-CM. As EVs share many physical properties with viruses, especially lentiviruses (Nguyen, Booth, Gould, & Hildreth, 2003), which can effectively be prepared from larger supernatants by polyethylene glycol (PEG) precipitation, we established and optimized a PEG precipitation protocol for small EVs (Ludwig et al., 2018). Subsequently, the protocol was used to prepare MSC-EVs for the successful treatment of the GvHD patient (Kordelas et al., 2014). Notably, as demonstrated at the example of an ischemic stroke mouse model, PEG-prepared MSC-EVs showed comparable effects as their parental a MSCs (Doeppner et al., 2015).

PEG precipitation allows the scaled preparation of functional EVs

Briefly, after obtaining MSC-CM (Basic Protocol 1), the protocol (Basic Protocol 2) starts with a 2000 × *g* centrifugation step (Fig. 1). It is followed by a mid-speed centrifugation

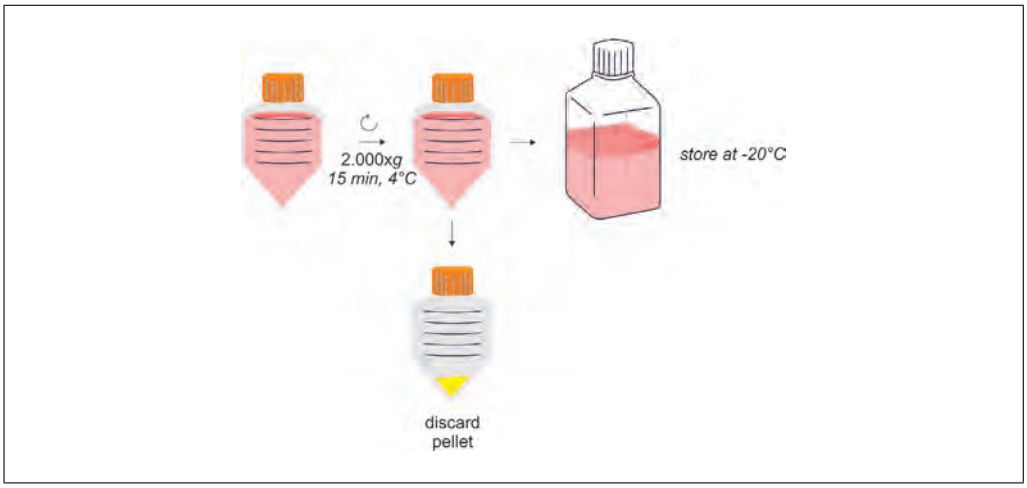

Figure 1 Harvested MSC-CM is collected and spun down for 15 min at 2000 × *g*, 4°C. Supernatant is transferred into storage containers and placed at −20°C until processing.

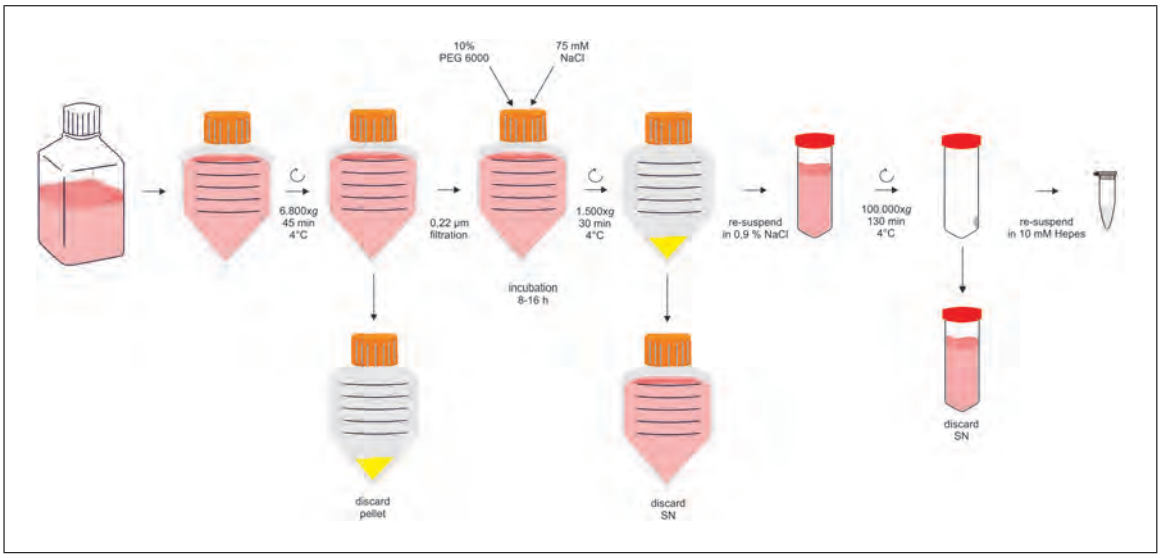

Figure 2 Harvested MSC-CM is pooled and spun down for 45 min at 6800 × *g*, 4°C. The supernatant (SN) is filtered through a 0.22-µm pore-size filter, adjusted to concentrations of 10% PEG 6000 and 75 mM NaCl, and incubated for 8-16 hr at 4°C. The suspension is centrifuged for 30 min at 1500 × *g*, 4°C. The pellet is resuspended and washed in NaCl. EVs are reprecipitated by ultracentrifugation for 130 min at 100,000 × *g*, 4°C. The obtained EV pellet is resuspended in buffer and stored at −80°C until use.

(depending on the maximum rotation speed of the rotor: 6800 to 10,000 × *g*) and a filtration step to successively remove contaminating cells, larger debris, and EVs that are larger than 200 nm (Fig. 2). Next, PEG precipitation occurs overnight, and the small EVs are pelleted at 1500 × *g*. To remove the PEG effectively, the precipitated EVs are washed with 0.9% NaCl and are pelleted again by ultracentrifugation. Thereafter, they are resuspended in the buffer of choice, e.g., HEPES or 0.9% NaCl, and stored −80°C until use (Fig. 2).

PREPARATION OF MSC-CONDITIONED MEDIUM FOR SCALED MSC-EV PRODUCTION

BASIC PROTOCOL 1

For scaled MSC-EV production, MSCs derived from bone marrow aspirates of healthy individuals are raised in 4-layered tissue culture stacks in human platelet lysate (hPL)−supplemented cultivation medium. During the expansion process, CM is harvested every 48 hr in a cumulative manner. Of note, to obtain optimal cell

expansion required for optimal MSC-EV yield, we do not remove the EVs from the hPL-supplemented cultivation medium.

NOTE: All steps should be performed under sterile conditions.

Materials

Mesenchymal stem/stromal cells (MSCs; see appropriate articles in *Current Protocols in Stem Cell Biology*)
Cultivation medium (see recipe)
1× trypsin/EDTA solution (see recipe) or other suitable enzymatic detachment reagent
Phosphate-buffered saline (PBS; Gibco, cat. no. 70013-016)
0.4% trypan blue (Sigma, cat. no. T8154)

4-layered tissue culture stack (Polystyrene Cell Factory System; ThermoFisher Scientific, cat. no. 140360)
Microscope
500-ml centrifugation tubes (Corning, cat. no. 431123)
Neubauer chamber (hemocytometer)
Medium-speed centrifuge (e.g., Avanti J26XP with rotor JS-5.3, Beckman Coulter)

Additional reagents and equipment for cell culture, including counting viable cells by trypan blue exclusion (see Current Protocols article: Phelan & May, 2015)

Cultivation of MSCs for scaled CM collection

1. Seed MSCs at a density of around 800 to 1500 MSCs/cm^2 in a 4-layered tissue culture stack containing 400 ml cultivation medium. Document the number of seeded cells.

   Proliferating MSCs, independent of their origin (including bone marrow, adipose tissue, perinatal tissue), should be raised in serum, or, if xeno-free settings are intended, in hPL-supplemented medium (10%). Because of their low protein content, which is not compatible with the PEG precipitation, chemically defined media are not applicable.

2. Examine the confluence of the cells with a microscope daily.

   Determine the approximate confluence of the cells; train participating co-workers to reach comparable outcomes.

3. Change medium when cells have reached ∼50% confluency.

   Discard the first harvest of CM. Because of low cell number, it contains only a low number of EVs.

4. Collect the CM every 48 hr from MSCs showing 50% to 90% confluency.

   MSCs normally need to be split once a week before reaching 100% confluency. Typically, collection of CM can be performed up to two times before each split.

5. For passaging, detach MSCs with suitable enzymatic detachment reagents and harvest the cells. For example, use 150 ml of 1× trypsin/EDTA for 5 min, at 37°C. Stop reaction by adding an equal volume of fresh cultivation medium; transfer to a 500-ml centrifugation tube, and spin down for 5 min at 900 × g.

   To save conditioned medium for use in Basic Protocol 2, do not stop the enzymatic reaction with CM. No enzymes should reside in the CM being used for the EV isolation, so it is critical to only use fresh cultivation medium prepared as in Reagents and Solutions for this step.

6. Resuspend pelleted cells in an appropriate volume of cultivation medium or PBS and determine the number of viable cells by trypan blue staining in a Neubauer chamber (hemocytometer; see Current Protocols article: Phelan & May, 2015).

7. Calculate the cell equivalents from which the CM was harvested:

$$n\,(t_z) = n_0 \cdot e^{k \cdot t_z}$$

$n(t_z)$: cell number during medium harvest at a time point t_z; n_0: number of originally seeded cells.

$$k = ln\left(\frac{n_1}{n_0}\right) \cdot \frac{1}{t_1}$$

n_1: cell number during passaging at time point t_1.

As an example, if 2×10^6 cells were seeded on day 0, and 4×10^7 cells are harvested on day 8 with the cells in exponential growth, the cell equivalent of day 6 CM is calculated as follows:

$$k = ln\left(\frac{4 \times 10^7}{2 \times 10^6}\right) \cdot \frac{1}{8}$$

$$k = 0.374$$

$$n\,(t_6) = 2 \times 10^6 e^{0.374 \cdot 6}$$

$$n\,(t_6) = 18.91 \times 10^6$$

Thus, at day 6, the CM can be considered to contain EVs from $\sim 1.89 \times 10^7$ cell equivalents.

Preparation of MSC-CM

8. Transfer the collected MSC-CM to a new centrifuge tube.

The size of the centrifuge tubes should be chosen based on the amount of cell culture. For small scale (up to 150 ml CM), 50-ml tubes are sufficient. For larger volumes (>150 ml) bigger tubes (e.g., 500-ml centrifugation tubes) are mandatory.

9. Centrifuge the CM 15 min at $2000 \times g$, 4°C.

10. Transfer supernatant to sterile storage containers.

The pellet contains detached cells and larger debris and should be discarded; only use the supernatant.

The supernatant can be stored either in centrifuge tubes or empty medium bottles.

11. Store CM at −20°C until further processing.

Supernatants of CM can be stored for up to several months at −20°C; however, freezing and thawing cycles should be avoided.

PEG PRECIPITATION OF MSC-EV FROM MSC-CONDITIONED MEDIUM

BASIC PROTOCOL 2

The protein content of the CM is critical; thus, only serum- or hPL-supplemented media should be used. CM is harvested in in a cumulative manner, and can be pooled after thawing.

Conditioned medium (CM; Basic Protocol 1)
3.75 M NaCl (see recipe)
50% (w/v) PEG 6000 (see recipe)
0.9% sodium chloride (B. Braun, cat. no. 151072)
Medium or buffer of choice: e.g.,10 mM HEPES buffer (see recipe)

Medium-speed centrifuge (e.g., Avanti J26XP with rotor JS-5.3, Beckman Coulter)
Rapid flow filter system (e.g., Nalgene, cat. no. 595-4520)
500-ml centrifuge tubes (Corning, cat. no. 431123)
Polycarbonate tubes for ultracentrifugation (Beckman Coulter cat. no. 355622)
Ultracentrifuge (e.g., L7-65 with rotor Ti45, Beckman Coulter)
Low-retention tubes (Kisker, cat. no. G017)

1. Thaw CM at 4°C or at room temperature.
2. Transfer CM to centrifuge tubes and—depending on the rotor—centrifuge 45 min at a minimum of 6800 × *g* and maximum of 10,000 × *g*, 4°C.

   The pellet contains larger debris and should be discarded; only use the supernatant.

   The maximum g-force that rotors can tolerate varies among available rotors. Rotors should be used that can be spun at least at 6800 × g, and if possible at 10,000 × g.
3. Perform a bottle-top filtration of the CM using 0.22-µm filters.

   Depending on the cultivation medium used, pores of the filters tend to clog.
4. Add PEG 6000 and NaCl to the filtered CM to a final concentration of 10% or 75 mM, respectively:

CM [ml]	50% PEG 6000 [ml]	3.75 M NaCl [ml]
10	2.56	0.26
40	10.26	1.03
100	25.64	2.56
400	102.56	10.26
1000	256.41	25.64
2000	512.82	51.28
4000	1025.64	102.56
10,000	2564.10	256.41

5. Incubate the suspension for 8-16 hr at 4°C (overnight).
6. Mix the suspension well before transferring to centrifuge tubes.

   Tubes from the preparation of the CM in Basic Protocol 1 can be re-used if they were kept sterile.

   Over time, the suspension will form layers. After mixing, the suspension should appear homogenous.
7. Centrifuge 30 min at 1500 × *g*, 4°C.
8. Remove and discard the supernatant carefully using a pipette; keep the white pellet.

   The supernatant should be removed from the pellet as completely as possible. With some exercise, residual supernatant also can be carefully rinsed off.
9. Resuspend the pellet in 10 ml 0.9% NaCl until the pellet is completely dispersed.

   The suspension should be clear and should show no PEG lumps.
10. Transfer the suspension to ultracentrifuge tubes.

    Ultracentrifuge tubes are available in different materials; we have experienced the best recoveries in polycarbonate tubes.
11. To transfer residual material, rinse the centrifuge tubes from the PEG precipitation with 25 ml of 0.9% NaCl.
12. Transfer each washing to the same ultracentrifuge tube as its original pellet.

13. Add 0.9% NaCl to the tubes to a final volume of 65 ml. Close the tubes with their lids.

14. Balance/tare tubes before loading tubes opposite to each other.

    For high-speed centrifugation, tubes need to be balanced according to the manufacturer's instructions. We tolerate a maximum discrepancy of 0.01 g. For odd numbers, load an empty tube with water to an equivalent weight and use it to balance the rotor.

    Mark the outer side of each tube on the lid to easily identify the pellets following centrifugation.

15. Ultracentrifuge 130 min at 100,000 × *g*, 4°C.

    Deceleration must be set without the brake. Total running time will thus increase to around 140 min.

16. Take the tubes out of the rotor and place on ice.

17. Carefully remove the supernatant with a pipette, and discard it.

    Avoid contact between the pipette and the pellet on the wall of the tube, which may be difficult to see. The mark on the lid allows localization of the pellet in case it is invisible. All of the supernatant should be removed from the pellet. The final residual amount can be carefully rinsed off; to avoid losing material, hold the pellet-containing side of the ultracentrifuge tube upwards.

18. Resuspend the pellet in an appropriate volume of the medium or buffer of choice.

    We resuspend the yield of the CM of 4 × 10^7 cells in 1 ml 10 mM HEPES buffer. For reproducibility, we recommend always resuspending the pellet in a defined volume per cell equivalent.

19. Add half of the calculated amount of buffer to the ultracentrifuge tubes, rinse the walls, and resuspend the pellet for a minimum of 4 min.

    Avoid air bubble formation during resuspension. It is best to resuspend by repetitive pipetting, keeping the tip always in the liquid.

20. Add buffer to the final volume.

21. Store small aliquots of the EV preparation in appropriate containers at −80°C.

    We have compared several commercially available tubes and currently store our samples in Kisker low-retention tubes. Other tubes can be used, but should be tested for their impact on particle recovery and EV characteristics after storage.

    Example results are shown in Table 1.

REAGENTS AND SOLUTIONS

Cultivation medium

DMEM, low-glucose (Pan Biotech, cat. no. P04-01500)
10% human platelet lysate (hPL; in house production; available also from Macopharma and PL Bioscience)
100 U/ml, penicillin-streptomycin-glutamine (Life Technologies, cat. no. 10378016)
5 IU/ml heparin (Ratiopharm, cat. no. N68743.06)
Store up to 4 weeks at 4°C

HEPES buffer, 10 mM

Add 1 ml of 1 M HEPES (Gibco, cat. no. 15630049) to 99 ml of 0.9% NaCl (B. Braun, cat. no. 151072). Sterilize by filtration using a 0.22-µm bottle-top filter. Store up to 6 months at 4°C.

Table 1 Example Results for Basic Protocol 2

Volume supernatant [ml]:	4300	Cell count:	6.45×10^8
Complete medium (after 6800-10,000 × *g* centrifugation)			
Protein concentration [ng/µl]: From BCA	5,224.69	Protein total [mg]: From BCA	22,466
Particle concentration [per ml]: From NTA	2.0×10^9	Particle total: From NTA	8.6×10^{13}
Particle size [nm]: From NTA_Average Size (×50 Value)	100.3		
EVs			
Resuspended in:	☒ 10 mM HEPES NaCl ☐ Other: _____	Volume [ml]:	16.1
Protein concentration [ng/µl]: From BCA	5518.45	Protein total [mg]: From BCA	88.85
Particle concentration [pro ml]: From NTA	2.5×10^{11}	Particle total: From NTA	4.03×10^{12}
Particle size [nm]: From NTA_Average Size (×50 Value)	116.3		
Recovery [%]: (Particle total EV/particle total CM)	4.69	Particle/mg protein:	4.5×10^{10}

NaCl, 3.75 M

Weigh 219 g sodium chloride (Sigma Aldrich, cat. no. 71376), transfer to a 1 L glass bottle, make up to 1000 ml with distillated water, and autoclave. Store up to 6 months at room temperature.

PEG 6000, 50% (w/v)

Weigh 250 g PEG 6000 (Sigma Aldrich, cat. no. 81260), transfer to a 1-L glass bottle, and make up to 500 ml with distilled water (50% w/v). Shake the bottle to mix the components, and use a magnetic stirrer until the PEG is completely dissolved, shaking from time to time. Autoclave, and store at room temperature for up to 6 months.

Trypsin/EDTA, 1×

50 ml 10× trypsin/EDTA (PAN Biotech, cat. no. P10-024100)
450 ml phosphate-buffered saline (PBS; Gibco, cat. no. 70013-016)
Store up to 4 weeks at 4°C

COMMENTARY

Background Information

The method given here is applicable for the large-scale isolation of EVs from CM of various cell types. EVs harvested with this method from MSC-conditioned media have been successfully applied to various preclinical models (Doeppner et al., 2015; Drommelschmidt et al., 2017; Gussenhoven et al., 2019; Ophelders et al., 2016; Wang et al., 2020). EVs share several features with viruses, such as their size and a comparable molecular assembly. Since viruses can be concentrated by PEG precipitation (Kanarek & Tribe, 1967; Kohno et al., 2002; Vajda, 1978), we adopted and optimized protocols originally developed for viruses to be used with EVs (Ludwig et al.,

Table 2 Troubleshooting Guide for Isolation of MSC-Derived EVs

Problem	Possible solution
Preparation of CM	
Filtration of MSC-CM causes filter clogging	Always centrifuge the CM first and filter it in a second step; alternatively, use different material for the filter membrane
PEG precipitation	
PEG incompletely dissolved	Increase the time and speed of magnetic stirring and check after autoclaving the solution for residual solids
Absence of white precipitate pellet after PEG precipitation and subsequent 1500 × *g* centrifugation step	Check for correct volumes of added reagents Check on cultivation medium used; was serum or hPL added? Incubation time of PEG precipitation should be between 8-16 hr; modified incubation times may affect the recovery
Pellet after 1500 × *g* cannot be resuspended	The precipitate from a maximum of 750 ml of CM should be applied to the 65 ml transferred to the ultracentrifuge tubes
Ultracentrifugation	
Precipitates become visible after filling ultracentrifuge tubes with samples of the resuspended PEG pellet	Check the volume equivalents of CM which was pelleted, resuspended, and transferred to the ultracentrifuge tube; do not load more than 750 ml original CM equivalents per ultracentrifuge tube Invest more effort to disperse the pellet correctly
Lack of visible EV pellet after 100,000 × *g* centrifugation	Check the seeded cell number; analyze obtained EVs with appropriate methods (like NTA or Western blot). If EVs are detectable, check the ultracentrifugation speed. It might be too low, or the run was interrupted.
High protein concentration in obtained EV preparations	Removal of residual supernatant after the 1500 × *g* step will decrease the protein concentration; EVs may not have been carefully resuspended following PEG precipitation (proteins stick to EVs)

2018). The principle of the PEG precipitation is based on replacement of water molecules that form a hydrate envelope around the EVs. Due to the hydrophobic effect, the EVs precipitate surrounded by PEG, leading to a massive volume reduction, mandatory for using subsequent ultracentrifugation-based methods. Our group established the method as a low-cost alternative to commercially available EV precipitation products.

Critical Parameters and Troubleshooting

Table 2 lists problems that may arise with the protocols in this article along with possible solutions.

For a scalable system with larger volumes (>10 L), the described method is limited. As an alternative method, TFF appears feasible. Depending on the system, TFF can be scaled to process hundreds of liters in relatively short time intervals. TFF devices from some companies are provided as automated, scalable systems, both as benchtop devices for research labs and as big machines for industry. First attempts to prepare EVs using TFF have already been published (Busatto et al., 2018; Heinemann et al., 2014). Notably, expensive hardware needs to be purchased. In contrast, for the PEG precipitation, only centrifuges are required, which should belong to each lab working with EVs.

Although the described method can be scaled for EV preparation, there are some bottlenecks to be discussed. The method needs to be considered an open system, including numerous handling steps that increase the risk of contamination. The method is only scalable to mid-range. The limiting factor is the centrifuge size. For example, only up to 5 L can be processed if only one ultracentrifuge run is going to be performed to remove residual PEG from the samples. In total, this is still 14-fold more than the amount that can be processed by conventional differential centrifugation protocols. For larger volumes, several runs need to be performed.

Time Consideration

The given method is applicable for large-scale isolation of CM from MSCs. With this approach, up to 10 L can be processed within

24 hr (including overnight incubation) on 2 subsequent days.

In detail, for the preparation of the medium in advance of the PEG precipitation, approximately 2 hr are needed, including the centrifugation and filtration of the CM. For the precipitation itself, we recommend overnight incubation. On the following day, another 5 hr need to be invested, including the 130 min for the ultracentrifugation run.

Acknowledgments

B.G. received funding from ERA-NET EuroTransBio, from the LeitmarktAgentur.NRW and European Union (European Regional Development Fund 2014–2020), and from the EU Commission for the Horizon 2020 project EVPRO [H_2O20-NMBP-TR-IND-2018]. Open access funding enabled and organized by Projekt DEAL.

We thank Michel Bremer and Tobias Tertel for assistance in figure layout and Yanis Mouloud for proofreading.

Author Contributions

Verena Börger: Conceptualization; project administration; writing-original draft; writing-review & editing. **Simon Staubach:** Conceptualization; project administration; writing-review & editing. **Robin Dittrich:** Data curation; writing-review & editing. **Oumaima Stambouli:** Writing-review & editing. **Bernd Giebel:** Methodology; supervision; writing-review & editing.

Literature Cited

Bartholomew, A., Sturgeon, C., Siatskas, M., Ferrer, K., McIntosh, K., Patil, S., … Hoffman, R. (2002). Mesenchymal stem cells suppress lymphocyte proliferation in vitro and prolong skin graft survival in vivo. *Experimental Hematology*, *30*, 42–48. doi: 10.1016/S0301-472X(01)00769-X.

Börger, V., Bremer, M., Ferrer-Tur, R., Gockeln, L., Stambouli, O., Becic, A., & Giebel, B. (2017). Mesenchymal stem/stromal cell-derived extracellular vesicles and their potential as novel immunomodulatory therapeutic agents. *International Journal of Molecular Sciences*, *18*, 1450. doi: 10.3390/ijms18071450.

Bruno, S., Grange, C., Deregibus, M. C., Calogero, R. A., Saviozzi, S., Collino, F., … Camussi, G. (2009). Mesenchymal stem cell-derived microvesicles protect against acute tubular injury. *Journal of the American Society of Nephrology*, *20*, 1053–1067. doi: 10.1681/ASN.2008070798.

Busatto, S., Vilanilam, G., Ticer, T., Lin, W. L., Dickson, D. W., Shapiro, S., … Wolfram, J. (2018). Tangential flow filtration for highly efficient concentration of extracellular vesicles from large volumes of fluid. *Cells*, *7*, 273. doi: 10.3390/cells7120273.

Caplan, A. I., & Correa, D. (2011). The MSC: An injury drugstore. *Cell Stem Cell*, *9*, 11–15. doi: 10.1016/j.stem.2011.06.008.

Caplan, A. I., & Dennis, J. E. (2006). Mesenchymal stem cells as trophic mediators. *Journal of Cellular Biochemistry*, *98*, 1076–1084. doi: 10.1002/jcb.20886.

Di Nicola, M., Carlo-Stella, C., Magni, M., Milanesi, M., Longoni, P. D., Matteucci, P., … Gianni, A. M. (2002). Human bone marrow stromal cells suppress T-lymphocyte proliferation induced by cellular or nonspecific mitogenic stimuli. *Blood*, *99*, 3838–3843. doi: 10.1182/blood.V99.10.3838.

Doeppner, T. R., Herz, J., Gorgens, A., Schlechter, J., Ludwig, A. K., Radtke, S., … Hermann, D. M. (2015). Extracellular vesicles improve post-stroke neuroregeneration and prevent postischemic immunosuppression. *Stem Cells Translational Medicine*, *4*, 1131–1143. doi: 10.5966/sctm.2015-0078.

Drommelschmidt, K., Serdar, M., Bendix, I., Herz, J., Bertling, F., Prager, S., … Felderhoff-Müser, U. (2017). Mesenchymal stem cell-derived extracellular vesicles ameliorate inflammation-induced preterm brain injury. *Brain, Behavior, and Immunity*, *60*, 220–232. doi: 10.1016/j.bbi.2016.11.011.

Giebel, B., & Hermann, D. M. (2019). Identification of the right cell sources for the production of therapeutically active extracellular vesicles in ischemic stroke. *Annals of Translational Medicine*, *7*, 188. doi: 10.21037/atm.2019.03.49.

Gussenhoven, R., Klein, L., Ophelders, D., Habets, D. H. J., Giebel, B., Kramer, B. W., … Wolfs, T. (2019). Annexin A1 as neuroprotective determinant for blood-brain barrier integrity in neonatal hypoxic-ischemic encephalopathy. *Journal of Clinical Medicine*, *8*, 137. doi: 10.3390/jcm8020137.

He, J., Wang, Y., Sun, S., Yu, M., Wang, C., Pei, X., … Zhao, W. (2012). Bone marrow stem cells−derived microvesicles protect against renal injury in the mouse remnant kidney model. *Nephrology*, *17*, 493–500. doi: 10.1111/j.1440-1797.2012.01589.x.

Heinemann, M. L., Ilmer, M., Silva, L. P., Hawke, D. H., Recio, A., Vorontsova, M. A., … Vykoukal, J. (2014). Benchtop isolation and characterization of functional exosomes by sequential filtration. *Journal of Chromatography A*, *1371*, 125–135. doi: 10.1016/j.chroma.2014.10.026.

Heldring, N., Mager, I., Wood, M. J., Le Blanc, K., & Andaloussi, S. E. (2015). Therapeutic potential of multipotent mesenchymal stromal cells and their extracellular vesicles. *Human Gene Therapy*, *26*, 506–517. doi: 10.1089/hum.2015.072.

Kanarek, A. D., & Tribe, G. W. (1967). Concentration of certain myxoviruses with polyethylene

glycol. *Nature*, *214*, 927–928. doi: 10.1038/214927a0.

Kohno, T., Mohan, S., Goto, T., Morita, C., Nakano, T., Hong, W., … Sano, K. (2002). A new improved method for the concentration of HIV-1 infective particles. *Journal of Virological Methods*, *106*, 167–173. doi: 10.1016/S0166-0934(02)00162-3.

Kordelas, L., Rebmann, V., Ludwig, A. K., Radtke, S., Ruesing, J., Doeppner, T. R., … Giebel, B. (2014). MSC-derived exosomes: A novel tool to treat therapy-refractory graft-versus-host disease. *Leukemia*, *28*, 970–973. doi: 10.1038/leu.2014.41.

Lener, T., Gimona, M., Aigner, L., Borger, V., Buzas, E., Camussi, G., … Giebel, B. (2015). Applying extracellular vesicles based therapeutics in clinical trials—an ISEV position paper. *Journal of Extracellular Vesicles*, *4*, 30087. doi: 10.3402/jev.v4.30087.

Ludwig, A. K., De Miroschedji, K., Doeppner, T. R., Borger, V., Ruesing, J., Rebmann, V., … Giebel, B. (2018). Precipitation with polyethylene glycol followed by washing and pelleting by ultracentrifugation enriches extracellular vesicles from tissue culture supernatants in small and large scales. *Journal of Extracellular Vesicles*, *7*, 1528109. doi: 10.1080/20013078.2018.1528109.

Nguyen, D. G., Booth, A., Gould, S. J., & Hildreth, J. E. (2003). Evidence that HIV budding in primary macrophages occurs through the exosome release pathway. *Journal of Biological Chemistry*, *278*, 52347–52354. doi: 10.1074/jbc.M309009200.

Nordin, J. Z., Bostancioglu, R. B., Corso, G., & El Andaloussi, S. (2019). Tangential flow filtration with or without subsequent bind-elute size exclusion chromatography for purification of extracellular vesicles. *Methods in Molecular Biology*, *1953*, 287–299. doi: 10.1007/978-1-4939-9145-7_18.

Ophelders, D. R., Wolfs, T. G., Jellema, R. K., Zwanenburg, A., Andriessen, P., Delhaas, T., … Kramer, B. W. (2016). Mesenchymal stromal cell-derived extracellular vesicles protect the fetal brain after hypoxia-ischemia. *Stem Cells Translational Medicine*, *5*, 754–763. doi: 10.5966/sctm.2015-0197.

Pittenger, M. F., Mackay, A. M., Beck, S. C., Jaiswal, R. K., Douglas, R., Mosca, J. D., … Marshak, D. R. (1999). Multilineage potential of adult human mesenchymal stem cells. *Science*, *284*, 143–147. doi: 10.1126/science.284.5411.143.

Phelan, K. & May, K. M. (2015). Basic techniques in mammalian cell tissue culture. *Current Protocols in Cell Biology*, *66*, 1.1.1–1.1.22. doi: 10.1002/0471143030.cb0101s66.

Thery, C., Amigorena, S., Raposo, G., & Clayton, A. (2006). Isolation and characterization of exosomes from cell culture supernatants and biological fluids. *Current Protocols in Cell Biology*, *30*, 3.22.1–3.22.29. doi: 10.1002/0471143030.cb0322s30.

Vajda, B. P. (1978). Concentration and purification of viruses and bacteriophages with polyethylene glycol. *Folia Microbiologica*, *23*, 88–96. doi: 10.1007/BF02876605.

Wang, C., Börger, V., Sardari, M., Murke, F., Skuljec, J., Pul, R., … Hermann, D. M. (2020). Mesenchymal stromal cell-derived small extracellular vesicles induce ischemic neuroprotection by modulating leukocytes and specifically neutrophils. *Stroke*, *51*(6), 1825–1834. doi: 10.1161/STROKEAHA.119.028012.

Watson, D. C., Yung, B. C., Bergamaschi, C., Chowdhury, B., Bear, J., Stellas, D., … Pavlakis, G. N. (2018). Scalable, cGMP-compatible purification of extracellular vesicles carrying bioactive human heterodimeric IL-15/lactadherin complexes. *Journal of Extracellular Vesicles*, *7*, 1442088. doi: 10.1080/20013078.2018.1442088.